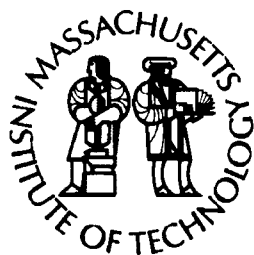
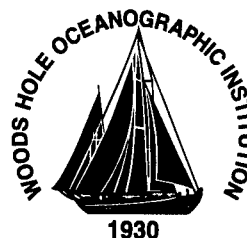


**Massachusetts Institute of Technology
Woods Hole Oceanographic Institution**



**Joint Program
in Oceanography/
Applied Ocean Science
and Engineering**



DOCTORAL DISSERTATION

*Organic Phosphorus in Marine Sediments:
Chemical Structure, Diagenetic Alteration, and
Mechanisms of Preservation*

by

Kirsten Lynn Laarkamp

September 2000

DISTRIBUTION STATEMENT A
Approved for Public Release
Distribution Unlimited

DTIC QUALITY INSPECTED 4

20001129 045

MIT/WHOI

00-24

**Organic Phosphorus in Marine Sediments:
Chemical Structure, Diagenetic Alteration, and Mechanisms of Preservation**

by

Kirsten Lynn Laarkamp

Massachusetts Institute of Technology
Cambridge, Massachusetts 02139

and

Woods Hole Oceanographic Institution
Woods Hole, Massachusetts 02543

September 2000

DOCTORAL DISSERTATION

Funding was provided by grants from the American Chemical Society Petroleum Research Fund and by National Science Foundation grant OCE-9216553. In addition, work was funded by Office of Naval Research Grant N00014-95-1-0478 and NSF grant OCE-9417097.

Reproduction in whole or in part is permitted for any purpose of the United States Government. This thesis should be cited as: Kirsten Lynn Laarkamp, 2000. Organic Phosphorus in Marine Sediments: Chemical Structure, Diagenetic Alteration, and Mechanisms of Preservation. Ph.D. Thesis. MIT/WHOI, 00-24.

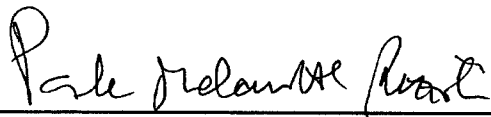
Approved for publication; distribution unlimited.

Approved for Distribution:



Robert S. Detrick, Chair

Department of Geology and Geophysics



Paola Malanotte-Rizzoli
MIT Director of Joint Program



John W. Farrington
WHOI Dean of Graduate Studies

Organic Phosphorus in Marine Sediments: Chemical Structure, Diagenetic Alteration, and Mechanisms of Preservation

by

Kirsten Lynn Laarkamp

B.S., Geosciences

The Pennsylvania State University, 1993

Submitted in partial fulfillment of the requirements for the degree of
Doctor of Philosophy

at the

MASSACHUSETTS INSTITUTE OF TECHNOLOGY

and the

WOODS HOLE OCEANOGRAPHIC INSTITUTION

September 2000

© 2000 Kirsten Lynn Laarkamp. All rights reserved.

The author hereby grants to MIT and WHOI permission to reproduce paper and
electronic copies of this thesis in whole or in part and to distribute them publicly.

Signature of Author Kirsten L. Laarkamp
Joint Program in Oceanography, Massachusetts Institute of Technology and
Woods Hole Oceanographic Institution, August 4, 2000

Certified by Kathleen C. Ruttenberg
Kathleen C. Ruttenberg
Associate Scientist, Department of Marine Chemistry and Geochemistry
Thesis Supervisor

Accepted by Timothy L. Grove
Timothy L. Grove
Chair, Joint Committee for Marine Geology and Geophysics
Massachusetts Institute of Technology and Woods Hole Oceanographic Institution

Organic Phosphorus in Marine Sediments: Chemical Structure, Diagenetic Alteration, and Mechanisms of Preservation

by

Kirsten Lynn Laarkamp

Submitted to the MIT/WHOI Joint Program in Oceanography
on August 4, 2000, in partial fulfillment of the
requirements for the degree of Doctor of Philosophy

Abstract

Phosphorus, an essential nutrient, is removed from the oceans only through burial with marine sediments. Organic phosphorus (P_{org}) constitutes an important fraction (*ca.* 25%) of total-P in marine sediments. However, given the inherent lability of primary P_{org} biochemicals, it is a puzzle that any P_{org} is preserved in marine sediments. The goal of this thesis was to address this apparent paradox by linking bulk and molecular-level P_{org} information.

A newly-developed sequential extraction method, which isolates sedimentary P_{org} reservoirs based on solubility, was used in concert with ^{31}P nuclear magnetic resonance spectroscopy (^{31}P -NMR) to quantify P_{org} functional group concentrations. The coupled extraction/ ^{31}P -NMR method was applied to three sediment cores from the Santa Barbara Basin, and the first-ever high-resolution depth profiles of molecular-level P_{org} distribution during diagenesis were generated.

These depth profiles were used to consider regulation of P_{org} distribution by biomass abundance, chemical structure, and physical protection mechanisms. Biomass cannot account for more than a few percent of sedimentary P_{org} . No evidence for direct structural control on remineralization of P_{org} was found. Instead, sorptive protection appears to be an important mechanism for P_{org} preservation, and structure may act as a secondary control due to preferential sorption of specific P_{org} compound classes.

Curriculum Vitae

Kirsten Lynn Laarkamp

Birth: November 30, 1971, Philadelphia, PA

Education:

The Pennsylvania State University

B.S. in Geosciences, May 1993

Minor in Marine Science

Professional Activities:

1996 - 1997 Student Representative, MIT/Woods Hole Joint Program

1995 - present Member of American Geophysical Union

1992 - 1995 Member of Geological Society of America

Awards and Honors:

1993 Office of Naval Research Graduate Fellowship

1993 The Pennsylvania State University
Honess Award: Outstanding Geosciences Graduate

1992 The Pennsylvania State University
Drake Memorial Scholarship

1989 The Pennsylvania State University
Dean's Freshman Scholarship

Experience:

1991-1993 Undergraduate Research Assistant, Pennsylvania State University

- inorganic and organic carbon analyses

1993 - 1996 Graduate Research Assistant, MIT/Woods Hole Oceanographic
Institution Joint Program in Oceanography

- organic carbon isotopic analyses
- core sampling and carbonate analyses
- stable isotope analysis of foraminifera
- ^{14}C analysis by accelerator mass spectrometer

1996 - present Graduate Research Assistant (Thesis work)

- isolation of organic fractions from sediment samples
- ^{31}P nuclear magnetic resonance spectroscopy
- organic and inorganic phosphorus analyses

Publications

- Laarkamp, K.L. and K.C. Ruttenberg (2000) Structural Controls on Reactivity of Sedimentary Organic Phosphorus: Linking Bulk Concentration Profiles to Molecular-Level Information. Paper presented at the Ocean Sciences Meeting, San Antonio, Texas.
- Curry W. B., Marchitto T. M., McManus J. F., Oppo D. W., and Laarkamp K. L. (submitted to *Paleoceanography*) Millennial-scale changes in ventilation of the thermocline, intermediate, and deep waters of the glacial North Atlantic.
- Arthur M. A., Dean W. E., and Laarkamp K. (1998) Organic carbon accumulation and preservation in surface sediments on the Peru Margin. *Chemical Geology* 152(3-4), 273-286.
- Laarkamp, K.L. and M.E. Raymo (1995) Carbon isotopic composition of particulate organic material from the interior of the equatorial Pacific Ocean. Paper presented at the 5th International Conference on Paleocyanography, Halifax, Nova Scotia, Canada.
- Arthur, M.A., K. Laarkamp, W.E. Dean, C.R. Glenn, and R.A. Jahnke (1993) The modern Peru margin: organic carbon sedimentation and preservation patterns. *Geological Society of America Abstracts with Programs* 25, 239.

Acknowledgements

I would like to gratefully acknowledge financial support from a number of sources. My first three years in the Joint Program were funded by a fellowship from the Office of Naval Research. The WHOI education office provided funding for the balance of my graduate studies. A course at Bridgewater State College, providing a much-needed grounding in basic biochemistry, was made possible by the WHOI endowed “Ditty Bag” fund. Travel to conferences was supplemented by the Frank W. Tchitcherine Student Opportunity Fund.

Most of the work presented here was funded by grants from the American Chemical Society Petroleum Research Fund (#32186-G2 and 35930-AC2 to K. Ruttenberg) and by NSF grant OCE-9216553 (to K. Ruttenberg and J. Whelan). In addition, work in our lab on dissolved organic P in the water column, funded by ONR grant N00014-95-1-0478 to K. Ruttenberg, contributed valuable insights for this project on sediment organic P. The 1996 cruise to the Santa Barbara Basin was funded by a NSF grant OCE-9417097 to J.M. Bernhard and S.S. Bowser, and space for K. Ruttenberg on the 1995 Santa Barbara Basin cruise was made available by A. Van Geen from the Lamont Doherty Earth Observatory.

My thesis advisor, Kathleen Ruttenberg, set a high standard for careful and thorough work both in the lab and the thought process of research. Her attention to detail has contributed a great deal to this thesis, and her encouragement along the way has been appreciated. In particular, this project (or at least my involvement in it) would not have been possible if it weren't for her willingness to take on a student who decided to change research areas so late in the program. The other members of my thesis committee (Bill Curry, Tim Eglinton, Phil Gschwend, John Hayes, Jean Whelan) have offered support and spirited discussion and, separately and collectively, have been an invaluable resource. I thank them for their many contributions to the work presented here.

The work presented here was helped immeasurably by the contributions of the Ruttenberg lab group. Many thanks to the research assistants (Eileen Monaghan, Nicole Colasacco), high school helpers (So Young Jordan Morris, Anastasia Prapas, Kate Doyle—my Coffee O' connection) and fellow students (Christie Haupt, Nicole Keon) who kept the lab full of music and conversation and helped with everything from simple lab tasks to interpreting data. Nanako Ogawa helped with some of the bulk Asphila analyses. The results presented in Appendix C-1 are largely thanks to the efforts of Amy Kinner, a 1998 summer student fellow at WHOI, whose experiments were crucial to evaluating the utility of differential hydrolysis for phosphonate quantification.

As I charged headlong into the field of organic geochemistry, there were a lot of people who made the going a bit easier and kept me from doing anything to injure myself or my samples. Jean Whelan gave very generously of her time and expertise to provide a solid foundation in organic chemistry, and was a constant source of advice (chemical and otherwise) and encouragement, for which I will always be grateful. During the initial extraction tests, I was fortunate to have assistance with things large and small from Lorraine Eglinton, Bob Nelson, and Bryan Benitez-Nelson. Pat Hatcher (Ohio State University) was a resource for all things humic and Mark Nanny (Oklahoma State University) provided insights and expertise about ^{31}P -NMR analyses. ^{210}Pb analyses were run in the lab of Bill Martin, Fred Sayles and Ken Buesseler.

During the final phases of this project, I have often joked that my degree should be jointly conferred by the University of South Carolina. Certainly, there are a lot of people based at that institution that have contributed immeasurably to this work. Many thanks to Joan Bernhard, who allowed me to tag along on one of her Santa Barbara Basin cruises, and also provided a place to stay and a cheerful taxi service during my visit to South Carolina. Most of the solution-state NMR data presented in this thesis were collected by Perry Pellechia and Helga Cohen from the NMR facility operated by the U.S.C. Department of Chemistry and Biochemistry. In particular, I am grateful for Perry's helpful NMR advice, his constant willingness to squeeze in "just a few more samples" and the tremendous amount of help he and Helga gave me during my visit to Columbia for the NMR standardization tests presented in Chapter 2. My initial contact with the USC-NMR facility was through P.V. Sundareshwar, who also provided some valuable insights from his work in ^{31}P -NMR. Miguel Goñi, from the U.S.C. Department of Geological Sciences provided the surface area measurements presented in Chapter 4, and also a place to stay during a visit to South Carolina.

Although the NMR samples presented in this study were run elsewhere, Carl Johnson here at WHOI worked extensively with me to try to get similar results at the WHOI-NMR facility. When it was clear that a new instrument was in order, the good folks at Bruker Instruments (Tony Bielecki, Connie Johnson, and Sophie Kazanis) and Varian Inc. (Steve Cheatham and Bill Kenney) provided useful information about the new instrument, and about NMR in general, and ran test samples for us. Specifically, the solid-state NMR data in Chapter 4 were collected by Tony Bielecki and the lipid NMR spectra in Chapter 3 were collected by Steve Cheatham.

Throughout my Joint Program experience, my officemates have blended helpful advice and much-needed levity with a good dose of patience for my sporadic bouts of organization (or lack thereof). Thanks to Dana Stuart (who moved offices with me so

many times I lost count), Carolyn Gramling (who never seemed to mind when the tide of my belongings crept out each time she got on the bus back to MIT) and Christie Haupt (who has seen me through the last days of my own thesis as she tried to write hers).

I have been blessed to live with a great group of people who (oddly enough) seemed to appreciate my quirky sense of humor. Thanks to Dana Stuart and Lihini Aluwihare (long live the house of Tall, Dark and Handsome!), who kept me laughing and gave me a deep appreciation for the value of costume parties. Thanks also to Mak Saito and Ann Pearson, who have been cheerful companions for the last few months, and always seemed to know when I needed to be dragged home from the lab. Special thanks to Ann for bringing me the “comfy” chair for the times when I couldn’t be dragged out of the office (and to Doug Quintiliani for helping us get it here!).

When no one else quite understood why I had turned into a cave dweller, the members of the thesis support group (TSG) were always standing by with encouragement, sympathy and a cold beer. Many thanks to Liz Kujawinski, Eli Hestermann, Brenda Jensen, Nicole Poulton, Sheri White, Mak Saito, Albert Fisher, and Joe Warren. I couldn’t have asked for a better bunch to share the trials and tribulations of the “home stretch”.

Straddling the fence between departments can be a challenge, administrative and otherwise. I am grateful to the staff of both the G&G and MC&G departments for always making me feel welcome, whatever my “department du jour” happened to be. Special thanks to Pam Foster in the G&G office and Sheila Clifford, Joanna Ireland and Susan Casso in the MC&G department for their help. Similarly, the Education office has always been a home for me, no matter what department I affiliated myself with. Special thanks to Julia Westwater for handling the mound of paperwork, the daily crises and for lending a friendly ear, and to Stella Callagee who always knew of a fund to pay for anything.

I would like to thank two people who encouraged my interest in science and set me a on the course that has brought me here to Woods Hole. Thanks to Eugene Bouley, from McCall Jr. High School in Winchester, MA who first taught me what now seems obvious- geology is fun! Thanks also to Mike Arthur, my senior thesis advisor at Penn State who taught me that if geology is good, oceanography is better.

Words cannot express my gratitude for the love and support I have had from Stefan Hussenoeder. There were many times when that light he was shining at the end of the tunnel was the only thing that kept me hanging on.

Through my years here my family has been a huge source of support and encouragement, and I thank them all (even when they seemed baffled by what I could possibly be working on for so LONG).

Dedication

This thesis is dedicated to my mother,
my first teacher and biggest supporter.

Contents

List of Figures	15
List of Tables	19
Chapter 1 Introduction	21
1.1 The Role of Organic Phosphorus in the Marine P Cycle	21
1.2 The Paradox Of Sedimentary Organic P Preservation	23
1.3 Contribution of This Thesis	24
1.4 Thesis Organization	26
Chapter 2 Methods for Extraction and Structural Analysis of Organic Phosphorus	28
2.1 Introduction.....	28
2.1.1 Marine Sedimentary Organic P: The Bulk Approach.....	29
2.1.2 Marine Sedimentary Organic P: The Molecular-Level Approach.....	30
2.1.3 Bridging The Gap: The Approach of This Study.....	30
2.2 ³¹ P-NMR Spectroscopic Analysis of Sediment Extracts	31
2.2.1 Previous Studies	32
2.2.2 Theoretical Background.....	34
2.2.3 Chemical Shift.....	36
2.2.3.1 The Effect of pH on Chemical Shift.....	43
2.2.4 Improving the Signal-to-Noise Ratio	44
2.2.5 Quantification of Functional Groups Using ³¹ P-NMR Data	45
2.2.6 Solid State NMR Analyses	48
2.3 Analysis of Phosphorus Concentration	49
2.3.1 Cleaning and Materials	49
2.3.2 Soluble Reactive Phosphorus: Extracts.....	50
2.3.3 Total Dissolved Phosphorus: Extracts.....	50
2.3.4 The Aspila Method: Sediments and Sediment Residues	52
2.3.4.1 The Acid Hydrolysis Experiment.....	53
2.3.5 Reproducibility of P Concentration Results.....	55

2.4 Sequential Extraction	56
2.4.1 Definition Of Organic Reservoirs	57
2.4.1.1 Solvent Extraction Step (Extracts 1, 2): Simple Biochemicals	57
2.4.1.2 Base Extraction Steps (Extracts 3-6): Humic Compounds	59
2.4.1.3 Insoluble Residue: Kerogen	59
2.4.2 Lipid Extraction Procedure.....	60
2.4.2.1 Lipid Extraction Protocol Tests.....	62
2.4.2.2 Partitioning Experiment.....	64
2.4.3 Base Extraction Procedure.....	66
2.4.3.1 Filtration of Extracts	66
2.4.3.2 The Iron Problem: Minimizing Paramagnetic Effects on NMR Spectra.....	67
2.4.3.2.1 <i>Chelex</i>	67
2.4.3.2.1 <i>EDTA</i>	68
2.4.3.2.1 <i>Citrate Dithionite Bicarbonate (CDB)</i>	69
2.4.3.3 $MgCl_2$	69
2.4.3.4 HCl	69
2.4.3.5 $NaOH$ Extraction	72
2.4.3.2.1 <i>Solid:Solution Ratio</i>	73
2.4.3.6 Separation Of Humic And Fulvic Acids	74
2.4.3.2.1 <i>Modification for Analysis of Isolated Humic Acids</i>	75
2.4.3.7 The Origin Of Orthophosphate In The Base Extractable Reservoir	76
2.4.3.2.1 <i>Base Hydrolysis Experiment</i>	76
2.4.3.8 Evidence for Metal Binding of Orthophosphate in the Humic Extract	80
2.4.4 Reproducibility of Sediment Extractions	84
2.5 Conclusion	85

Chapter 3 Contribution of Biomass to the Organic P Reservoir in Central Santa Barbara Basin Sediments 106

3.1 Introduction.....	106
3.2 Biomass Estimated by Quantification of P_{org} Compounds	110
3.2.1 Biomass Determined from Phospholipid Concentration	110
3.2.2 Biomass Determined from ATP concentration.....	111
3.3 Study Site: The Central Santa Barbara Basin	112

3.4 Methods	113
3.4.1 Sediment Collection and Core Sectioning	113
3.4.2 Measurement of Phospholipid Concentration.....	113
3.4.3 Measurement of ATP Concentration.....	114
3.5 Conversion Factors.....	115
3.5.1 Bulk Density, Cell P_{org} and C Content, Cell Numbers	115
3.5.2 Phospholipid and ATP Intracellular Concentrations	116
3.6 Results	118
3.6.1 P Biochemical Concentration Profiles	118
3.6.2 Biomass profiles inferred from ATP and Lipid P concentration	118
3.6.3 Direct Comparison of ATP and Lipid P Data	119
3.7 Discussion	120
3.7.1 Is the Lipid P Reservoir Derived Entirely from Living Biomass?.....	120
3.7.2 What Is the Nature of the “Residual” Lipid P?.....	124
3.7.3 The Contribution of Biomass to the Total Organic P Reservoir	125
3.8 Conclusion	127

Chapter 4 Chemical Structure and Diagenetic Modification of Organic P in Marine Sediments 134

4.1 Introduction.....	134
4.1.1 What Controls The Distribution And Composition Of P_{org} In Marine Sediments?.....	135
4.1.1.1 Chemical Structure	136
4.1.1.2 Physical Protection	136
4.1.1.3 Analytical Artifact: Overestimation of P_{org} ?	138
4.1.2 Depositional Environment: The Importance of Bottom-Water Oxygen Concentration	138
4.1.3 Approach of this Study	140
4.2 Study Site: Santa Barbara Basin	142
4.3 Methods	145
4.3.1 Sample Collection and Sub-sampling	145
4.3.2 Sample Handling.....	146
4.3.3 Extraction of Soluble P Reservoirs	146
4.3.4 P Analyses	147
4.3.5 ^{31}P -NMR Analyses	147
4.3.6 ^{210}Pb	148
4.3.7 Surface Area.....	148

4.4 Results	149
4.4.1 Unsupported ^{210}Pb	149
4.4.2 Bulk Sediment P	150
4.4.3 Soluble P Reservoirs	154
4.4.3.1 Simple Biochemicals: Lipid P and Water-soluble P	154
4.4.3.2 Other Soluble P Reservoirs	156
4.4.3.3 Citrate Dithionite Bicarbonate (CDB)	156
4.4.3.4 Acid Pre-extract	157
4.4.3.5 Base Extract	157
4.4.4 Insoluble Residue	157
4.4.5 ^{31}P -NMR Analysis Of Sediment Base Extracts.....	158
4.4.5.1 Phosphonate	160
4.4.5.2 Orthophosphate	161
4.4.5.3 Monoester.....	162
4.4.5.4 Diester	162
4.4.5.5 Polyphosphates.....	162
4.4.6 Mineral Surface Area.....	163
4.5 Discussion	165
4.5.1 The Importance of Chemical Structure for P_{org} Preservation	165
4.5.2 Simple Biochemicals: Lipid and Aqueous P Reservoirs	166
4.5.3 Mechanisms for Incorporation of Monoester and Diester P into the Humic Fraction	167
4.5.4 Metal-Bound P and Analytical Artifacts.....	173
4.5.5 Transfer of P Into the Insoluble Sediment Residue	177
4.5.6 Sorption to Mineral Surfaces	178
4.5.7 Depositional Conditions: The Importance of Bottom Water Oxygen Concentration	179
4.5.8 Polyphosphates: Indicators of Luxury P Consumption	180
4.6 Conclusions.....	182
 Chapter 5 Conclusions	 206
5.1 Results of This Study	206
5.2 Directions for Future Research	209

Summary of Appendices.....	211
Appendix A: Laboratory Procedures for Sediment	
Extraction	212
Appendix A-1: Solvent Extraction Protocol	212
Appendix A-2: Base Extraction Protocol.....	218
Appendix B: Additional Sediment Extraction Data.....	226
Appendix B-1 Base Extraction Data for Santa Barbara Basin Core J	226
Appendix B-2 Data from Peru Margin Cores.....	232
Appendix C: Alternative Methods for Analysis of P_{org}.....	238
Appendix C-1 Quantification of Phosphonates by Differential Hydrolysis	238
Appendix C-2 Structural Characterization of Phospholipids by High-Performance Liquid Chromatography (HPLC)	247
Appendix C-3 Kerogen Isolation from the Insoluble Sediment Residue.....	252
Appendix C-4 Analysis of P _{org} Structure using Pyrolysis-Gas Chromatography with a Flame Photometric Detector (Py-GC-FPD)	259
References	266

List of Figures

Figure 2-1. Schematic of the NMR pulse sequence used in this study	87
Figure 2-2. A spectrum of P standards run in 0.5 M NaOH, showing the chemical shift regions corresponding to different P functional groups.....	88
Figure 2-3. A typical spectrum of a sediment base extract, showing the chemical shift regions corresponding to different P functional groups.....	89
Figure 2-4. The effect of pH on the chemical shift of orthophosphate.....	90
Figure 2-5. Recovery of P standards using modifications to the Solórzano and Sharp (1980) method of TDP analysis.....	91
Figure 2-6. The sequential extraction procedure used for separation of organic P reservoirs.....	92
Figure 2-7. Total P extracted in 0.5 M NaOH solutions containing different concentrations of EDTA	93
Figure 2-8. NMR spectra of base extracts of sediment samples pre-treated with CDB and extracted with a mixed solution of base and EDTA	94
Figure 2-9. Difference in P solubilized during base extraction of sediments prepared with and without acid pre-extraction	95
Figure 2-10. NMR spectra of base extracts of sediments prepared with and without acid pre-extraction	96
Figure 2-11. Total P extracted by successive 0.5 M NaOH treatments.....	97
Figure 2-12. NMR spectra of the first two successive base extracts	98
Figure 2-13. Hydrolysis of nucleotides and other P compounds in 0.5 M NaOH during two months of storage.....	99
Figure 2-14. Hydrolysis of glucose-6-phosphate in 0.5 M NaOH	100
Figure 2-15 Phosphocreatine stability in 0.5 M NaOH	101
Figure 2-16. Hydrolysis of RNA in 0.5 M NaOH	102
Figure 2-17. ³¹ P-NMR spectra of the total base extract, and the fulvic and humic acid fractions, from surface sediments (0-0.3 cm) of the central Santa Barbara Basin	103

Figure 2-18. ^{31}P -NMR spectra of the total base extract, and the fulvic and humic acid fractions, from deep sediments (38-40 cm) of the central Santa Barbara Basin	104
Figure 2-19. ^{31}P -NMR spectra of the fulvic acid fraction of a base extract from deep sediments (38-40 cm) of the central Santa Barbara Basin, with and without dialysis	105
Figure 3-1. Profiles of lipid P, ATP, and water-soluble P concentrations in core SBB9610 J	129
Figure 3-2. Profiles of bacterial cell numbers calculated from lipid P and ATP sediment concentrations.....	130
Figure 3-3. Comparison of lipid P and ATP measured in the same sediment intervals with the range of ATP:Lipid P ratios estimated from the literature.....	131
Figure 3-4. Same as Figure 3-3, but the lines representing cellular ATP:lipid P ratios have been shifted up along the y-axis to indicate a non-biomass, "background" concentration of residual lipid P.	132
Figure 3-5. ^{31}P -NMR spectra of lipid extracts from Santa Barbara Basin sediments from the sediment-water interface (0-0.3 cm) and at depth (38-40 cm).....	133
Figure 4-1. Map of the Santa Barbara Basin, showing the location of the three cores used in this study	184
Figure 4-2. Pore water profiles of soluble reactive P (e.g., orthophosphate) and ammonia in cores A and C	185
Figure 4-3. Comparison of excess ^{210}Pb measured in cores A and C with depth profiles of ^{210}Pb from parallel cores	186
Figure 4-4. Total P (TP), total inorganic P (TIP), and total organic P (TOP) concentrations determined for the three Santa Barbara Basin cores using the Aspila et al. (1976) method.	187
Figure 4-5. Total dissolved P concentration in lipid (left) and aqueous (right) reservoirs extracted from the three Santa Barbara Basin cores	188
Figure 4-6. Depth profiles of total P in cores A and C extracted from sediments with citrate dithionite bicarbonate (CDB)	189
Figure 4-7. Depth profiles of total P in cores A and C extracted in 0.1 M HCl.....	190
Figure 4-8. Depth profiles of total P in cores A and C extracted in 0.5 M NaOH	191
Figure 4-9. Total P in the insoluble sediment residue after sequential extraction of cores A and C	192

Figure 4-10. Organic P in the insoluble sediment residue after sequential extraction of cores A and C	193
Figure 4-11. ^{31}P -NMR spectra of base extracts from margin core SB11/95 A	194
Figure 4-12. ^{31}P -NMR spectra of base extracts from central basin core SB11/95 C.....	195
Figure 4-13. ^{31}P -NMR spectra of base extracts from central basin core J	196
Figure 4-14. Concentration of base-extractable phosphonates in cores A and C.....	197
Figure 4-15. Concentration of base-extractable orthophosphate in cores A and C.....	198
Figure 4-16. Concentration of base-extractable monoester P in cores A and C.....	199
Figure 4-17. Concentration of base-extractable diester P in cores A and C	200
Figure 4-18. Concentration of base-extractable polyphosphates in cores A and C.....	201
Figure 4-19. A model for binding of P into the humic fraction of sedimentary organic matter via a metal bridge	202
Figure 4-20. A model for binding of P into the humic fraction of sedimentary organic matter via covalent bonding to the humic matrix	203
Figure 4-21. Comparison of base-extractable inorganic P and organic P in cores A and C, determined by NMR and wet chemical methods	204
Figure 4-22. Solid state ^{31}P -NMR spectrum of the insoluble sediment residue at depth in core J.....	205
Figure B-1. Depth profiles of total P in core J extracted in 0.1 M HCl.....	229
Figure B-2. Depth profiles of total P in core J extracted in 0.5 M NaOH + 0.01 M EDTA.....	229
Figure B-3. Total P in the insoluble sediment residue after sequential extraction of core J.....	230
Figure B-4. Organic P in the insoluble sediment residue after sequential extraction of core J.....	230
Figure B-5. Map of the Peru Margin, showing the locations of cores BC091 and GGC143	235
Figure B-6. Depth profiles of TOP in sediments from two sites on the Peru Margin	236
Figure B-7. Partitioning of P_{org} in different organic compound classes vs. depth in cores BC091 and GGC143.....	237

Figure C-1. Relative percent error for replicate standards as a function of heating time	242
Figure C-2. Major classes of phospholipids separated by the described HPLC method	250
Figure C-3 HPLC separation of major membrane phospholipids	251
Figure C-4. Profiles of insoluble organic P in sediments and organic P isolated by the kerogen isolation procedure	255
Figure C-5. P extracted in 20% HCl treatment used for kerogen isolation.....	256
Figure C-6. Chromatograms obtained by Py-GC-FPD analysis of kerogen samples from the Mississippi Delta and the Peru Margin	260
Figure C-7. Schematic diagram of a flame photometric detector (FPD)	263
Figure C-8. Emission spectra of HPO and S ₂ species (Dressler, 1986).	264

List of Tables

Table 1-1. Estimates of global reactive-P burial	22
Table 2-1. Chemical shift of compounds measured in CDCl_3	38
Table 2-2. Chemical shift of compounds measured in 0.5 M NaOH	40
Table 2-3. Relative peak response for different organic P functional groups	47
Table 2-4. Hydrolysis of P compounds in 1 M HCl.	54
Table 2-5. Organic P reservoirs separated by the sequential extraction	58
Table 2-6. Partitioning of compounds between solvent and aqueous phases following lipid extraction.	65
Table 2-7. Comparison of P extracted with and without pre-extraction of samples with dilute acid	71
Table 2-8. Relative abundance of organic P functional groups solubilized by repeated extraction of a sediment sample with 0.5 M NaOH	74
Table 2-9. Results of the base hydrolysis experiment	78
Table 2-10. A comparison of inorganic and organic P in base extracts from core SBB9610 J, determined by ^{31}P -NMR and wet chemical analyses	81
Table 2-11. Total P in the fulvic acid fraction of the base extract from deep (38-40 cm) sediments of the Santa Barbara Basin before and after dialysis	83
Table 2-12. Reproducibility of sediment extractions.....	84
Table 3-1. The abundance of P biochemicals in bacterial biomass.....	107
Table 3-2. Literature values of ATP and phospholipid cell content used to estimate the expected ATP:lipid P ratio in living biomass.....	117
Table 3-3. Reasonable ratios for ATP:Lipid P in sediment biomass based on literature values for intracellular concentrations of ATP and lipid	120
Table 3-4. Calculated concentrations of biomass and “residual” lipid P fractions in sub-surface sediments (38-40cm).....	123
Table 3-5. Estimates of the total sedimentary P_{org} reservoir accounted for by living biomass	126
Table 4-1. Locations of cores used for this study.	144

Table 4-2. Solid-phase concentration of total, inorganic, and organic P for margin core A, determined by the Aspila method	151
Table 4-3. Solid-phase concentration of total, inorganic, and organic P for deep basin core C, determined by the Aspila method.....	152
Table 4-4. Solid-phase concentration of total, inorganic, and organic P for deep basin core J, determined by the Aspila method.....	153
Table 4-5. Total P in extracts from margin core A	155
Table 4-6. Total P in extracts from central basin core C	155
Table 4-7. Concentration of P functional groups base extracts from margin core A, determined by ^{31}P -NMR.....	159
Table 4-8. Concentration of P functional groups base extracts from in central basin core C , determined by ^{31}P -NMR.....	160
Table 4-9. Concentration of P functional groups base extracts from in central basin core J , determined by ^{31}P -NMR.....	160
Table 4-10. Surface area determined for surface sediments of the three Santa Barbara Basin cores.....	164
Table 4-11. The abundance of P biochemicals in bacterial biomass compared to the distribution of functional groups in base extracts of sediments from cores A and C.....	169
Table 4-12. A comparison of inorganic and organic P in base extracts from central basin cores J and C, and margin core A, determined by ^{31}P -NMR and wet chemical analyses.....	175
Table C-1. Hydrolysis of standard compounds using the modified Bartlett (1959) method	243
Table C-2. Comparison of the phosphonate concentration in living cells, lipid and base extracts of Santa Barbara Basin sediments, and the detection limits for the Aalbers and Bieber “difference method” approach.....	245

Chapter 1

Introduction

1.1 The Role of Organic Phosphorus in the Marine P Cycle

Changes in the oceanic nutrient inventory exert an important control on the primary productivity potential of surface waters, and can drive changes in atmospheric CO₂ levels (Broecker, 1982; McElroy, 1983). It is generally accepted that P, an essential nutrient, limits marine productivity on geological timescales (Holland, 1978; Broecker & Peng, 1982; Smith, 1984; Codispoti, 1989). It can also limit productivity in the present-day ocean (Fisher *et al.*, 1992; Smith & Hitchcock, 1994; Cotner *et al.*, 1997; Karl & Tien, 1997; Monaghan & Ruttenberg, 1999). Estimated residence times for P in the ocean of 16,000 years (Ruttenberg, 1993) and 10,000 years (Colman & Holland, 2000) suggest that changes in the whole-ocean nutrient budget on glacial-interglacial timescales are possible.

To estimate the productivity potential of modern and ancient oceans, it is therefore essential to understand the processes controlling the water column concentration of P. Over long time-scales, the seawater concentration of P depends on the balance between riverine input and removal to sediments (Froelich *et al.*, 1982; Ruttenberg, 1993). This balance has been evaluated by quantifying the flux of bioavailable P to the ocean (Froelich, 1988; Filippelli & Delaney, 1994; Colman & Holland, 2000) and reconciling this input with the P burial flux. Burial with sediments is the sole means of P removal from the ocean (Froelich *et al.*, 1982; Ruttenberg, 1993; Delaney, 1998; Colman & Holland, 2000).

Biogenic fluxes of P are the main mode of P delivery to marine sediments (Froelich *et al.*, 1982), and organic phosphorus (P_{org}) has been reported to constitute a

significant fraction (*ca.* 25%) of the total P buried in marine sediments. P_{org} is therefore an important component of the total marine P budget (Froelich *et al.*, 1982; Ruttenberg, 1990; Ruttenberg, 2000). Estimated burial fluxes for reactive-P pools in marine sediments are shown in Table 1-1. The fact that organic P constitutes such an important fraction of the total burial flux of reactive-P indicates that changes in the efficiency of organic P remineralization can exert a strong influence on the efflux of P from sediments. Regeneration of nutrients from coastal marine sediments can supply a significant fraction of the nutrients required for primary productivity in the overlying water column (Callender & Hammond, 1982; Maher & DeVries, 1994). Predictions of phosphate efflux to bottom waters can be made only with a mechanistic understanding of the diagenetic pathways for P_{org} degradation and remobilization of this limiting nutrient.

Table 1-1. Estimates of global reactive-P burial (after Ruttenberg, 1993).

<u>Reservoir</u>	Phosphorus Burial Flux
	<u>(10^{10} mol/yr)</u>
Organic P	4.1
Iron-P	4.0
Authigenic-P	9.1
Loosely sorbed-P	1.3
Total reactive-P	18.5

1.2 The Paradox Of Sedimentary Organic P Preservation

The known primary P_{org} chemicals delivered to marine sediments are derived mainly from planktonic and bacterial biomass. This suite of compounds, composed mainly of nucleic acids, phospholipids, and metabolic intermediates such as ATP, is considered biochemically labile, with highly energetic bonds and structures susceptible to attack by widely-distributed enzymes (e.g., White *et al.*, 1977; Paul *et al.*, 1987; Westheimer, 1987). Accordingly, no substantial preservation of organic P in marine sediments is expected.

Consistent with this prediction, the size of the bulk P_{org} pool in marine sediments typically decreases with depth, indicating remineralization during the initial stages of early diagenesis (e.g., Krom & Berner, 1981; Ruttenberg & Berner, 1993; Reimers *et al.*, 1996). However, concentrations of P_{org} stabilize at some asymptotic value deeper in sediments as remineralization of P_{org} slows to undetectable levels. Consequently, measurable quantities of P_{org} , as determined by wet chemical methods, are found in deeply buried sediments (Filippelli & Delaney, 1994; Delaney & Anderson, 1997) and in ancient shales (e.g., Sandstrom, 1982; Ingall *et al.*, 1993).

The underlying motivation for the work presented in this thesis was to address the apparent conflict between the biochemical lability of P_{org} and its preservation in sediments. This paradox can be resolved by one or more of the following explanations, considered in more detail in Chapters 3 and 4: (i) P compounds from live sedimentary biological communities contribute substantially to the inventory quantified as “sedimentary organic P”, (ii) P_{org} compounds with intrinsically resistant structural features are preferentially preserved, (iii) physical protection of otherwise chemically labile P_{org} compounds causes them to be preserved, or (iv) the concentration of P_{org} in sediments is overestimated as a result of analytical artifacts. The results detailed in Chapters 3 and 4 suggest that physical protection is more important than chemical structure as a mechanism for P_{org} preservation, although structure may play a secondary

role. Analytical artifacts associated with commonly-used P_{org} quantification methods have likely led to overestimation of the size of the sedimentary P_{org} reservoir.

1.3 Contribution of This Thesis

Most previous studies of P_{org} in marine sediments have adopted a one-sided approach, focusing either on bulk parameters such as total sediment P_{org} concentration and organic C:P ratios (e.g., Morse & Cook, 1978; Filipek & Owen, 1981; Krom & Berner, 1981; Froelich *et al.*, 1982; Ruttenberg, 1990; Reimers *et al.*, 1996; Ruttenberg & Gofii, 1997) or on simple biochemicals such as ATP and phospholipids (e.g., White *et al.*, 1979b; 1979c; Harvey *et al.*, 1984; Meyer-Reil, 1984; Craven *et al.*, 1986; Balkwill *et al.*, 1988; Mancuso *et al.*, 1990; Karl, 1993). Alone, each of these approaches provides useful information but leaves important gaps in our understanding of the composition of the total P_{org} pool and of the processes that control the diagenetic modification and ultimate preservation of P_{org} .

The intention of this thesis was to combine these approaches, using molecular-level structural information as a tool to understand the observed trends in bulk parameters such as total P_{org} concentration. The initial rapid remineralization of P_{org} is usually attributed to destruction of compounds that are more easily degraded by virtue of their inherently labile chemical structures (Krom & Berner, 1981; Ingall & Van Cappellen, 1990), and by inference the deeply buried P_{org} is assumed to be more refractory. Bulk P_{org} concentrations alone, however, do not provide a means for explicitly testing these inferences. In fact, a mechanistic understanding of P_{org} degradation can only be achieved by examining the molecular-level composition of the P_{org} pool. Analytically, this has been difficult because few methods are available for studying P_{org} on the molecular level.

A sequential extraction method was developed to separate organic P into operationally defined reservoirs on the basis of solubility. This extraction technique serves two main functions: (i) to maximize solubilization of P_{org} , making possible a more

detailed structural analysis, and (ii) to minimize the impact of simple P biochemicals derived from intact cells on the depth trends of diagenetically vulnerable P_{org} . In this thesis, "diagenetically vulnerable organic matter" refers to the entire pool of organic matter that is not associated with live cells. Molecular-level changes that accompany diagenesis were inferred for lipid and base extracts by contrasting ^{31}P -NMR spectra from different sediment horizons. ^{31}P nuclear magnetic resonance spectroscopy (^{31}P -NMR) is a non-destructive method that provides unique information about the electronic environment surrounding P nuclei and thus the structure of phosphorus compounds in natural samples. Because abundances of P in lipid samples are often low, most of the ^{31}P -NMR data presented in this thesis were restricted to the base-extractable P reservoir.

Bulk P_{org} concentrations, P abundance in soluble reservoirs, and structural information from ^{31}P -NMR were examined in tandem in depth profiles from the Santa Barbara Basin. ^{31}P -NMR data for marine sediments that have been presented to date include only single depth intervals (Ingall *et al.*, 1990) or use solid state NMR (Berner *et al.*, 1993), which provides much less structural information than solution NMR. Downcore analyses of P_{org} structure (presented here) are required to determine whether particular linkages are preserved during early diagenesis. The complementary molecular-level and bulk data provided by this study allow a more comprehensive examination of the structure and early diagenetic modification of P_{org} than has been possible in any previous studies.

The Santa Barbara Basin was chosen as the primary study site for this examination of P_{org} structure for a number of reasons. Coastal sites are important in the total burial of organic material (Berner, 1982) and phosphorus (Ruttenberg, 1993; Ruttenberg & Berner, 1993) in oceanic sediments. High productivity, a relatively short water column, and high sedimentation rates in the Santa Barbara Basin contribute to the high organic carbon content of basin sediments (*ca.* 4%), a prerequisite for this initial detailed examination of P_{org} . Due to their high organic content and excellent stratigraphic

resolution, sediments from the Santa Barbara Basin have been the focus of a large number of studies of pore water, and organic and inorganic solid phase chemistry (see review by Schimmelmann & Lange, 1996). This additional data provides a useful context for understanding P_{org} structure and preservation mechanisms in the Santa Barbara Basin. Martens and Klump (1984) showed in another high-organic-matter sedimentary environment (Cape Lookout Bight) that most organic remineralization occurs in the upper 25 cm of sediments. The three cores examined for this study focus on this metabolically active surface sediment layer.

1.4 Thesis Organization

The first goal of this thesis was to develop analytical methods for the separation and quantification of organic P reservoirs, and for structural characterization of organic P. In Chapter 2, the development of these methods is described. A sequential extraction procedure is presented, along with a discussion of the tests used to optimize the extraction method and an evaluation of the reproducibility of results. Quantification of organic and inorganic P by a standard wet chemical technique (the Aspila *et al.* (1976) method) is evaluated by comparison with ^{31}P -NMR results. This comparison indicates that a fraction of P_{org} measured in deep sediments and ancient shales by the commonly used Aspila method may not be organic, but rather a result of an analytical artifact.

The remainder of the thesis is divided into two chapters, each of which focuses on different possible explanations for the observed depth trends in P_{org} concentration. In Chapter 3, the assumption that phospholipids are immediately degraded upon cell death is challenged. The results in this chapter, based on a comparison of the concentrations of ATP and lipid-P in sediments, indicated that a fraction of lipid-P is unaccounted for by biomass. Diagenetic changes in the sedimentary P_{org} reservoir can be inferred from depth trends in P_{org} abundance and composition only if the pool of diagenetically vulnerable

organic matter can be distinguished from the biochemicals derived from intact, living cells. With this in mind, the importance of biomass in driving bulk P_{org} trends was also examined in Chapter 3.

In Chapter 4, P_{org} concentration and chemical structure were determined in depth profiles of three cores from Santa Barbara Basin. These data were used to evaluate the relative importance of chemical structure and physical protection for preservation of organic P. Depth profiles of P functional groups show that, contrary to conventional wisdom, phosphonates (compounds with direct C-P linkage) are not more resistant to degradation than other P_{org} compounds. The high abundance of monoester P suggests that interaction of the charged phosphate end-group, which characterizes phosphomonoesters, with mineral surfaces, metals, and large organic molecules may be important in dictating the ultimate fate of P compounds. Thus, while direct structural control of the extent and/or rate of P_{org} degradation is not suggested by these data, P_{org} structure can be quite important in determining the interaction of P compounds with mineral surfaces or protective macromolecules. Differences in P_{org} concentration between cores from the central basin and the basin slope suggest that the concentration of oxygen in bottom waters plays an important role in P_{org} preservation.

The information gained by taking a combined bulk and molecular-level approach to P_{org} composition provides the means to evaluate controls on remineralization of P_{org} . The methods detailed in this thesis provide a new approach for studies of the marine organic P cycle and the data presented here allow insights into the depositional environmental controls on P_{org} structure and preservation.

Chapter 2

Methods for Extraction and Structural Analysis of Organic Phosphorus

Measure what is measurable, and make measurable what is not so.

- Galileo Galilei

2.1 Introduction

Organic phosphorus (P_{org}) constitutes a significant fraction (*ca.* 25%) of the total P buried in marine sediments and is therefore an important component of the total marine P budget (Froelich *et al.*, 1982; Ruttenberg, 1990). Despite this importance, the chemical form of P_{org} in marine sediments has remained virtually uncharacterized due to analytical difficulties in obtaining molecular-level information about sedimentary P_{org} . Previous studies of P_{org} in marine sediments have generally adopted a one-sided approach: either focusing on the size of the total P_{org} pool and bulk organic C:P ratios in sediments (e.g., Morse & Cook, 1978; Filipek & Owen, 1981; Krom & Berner, 1981; Froelich *et al.*, 1982; Ruttenberg, 1990; Reimers *et al.*, 1996; Ruttenberg & Goñi, 1997) or quantifying simple biochemicals such as ATP and phospholipids (e.g., White *et al.*, 1979b; 1979c; Harvey *et al.*, 1984; Meyer-Reil, 1984; Craven *et al.*, 1986; Balkwill *et al.*, 1988; Mancuso *et al.*, 1990; Karl, 1993). Alone, each of these approaches provides useful information but leaves important gaps in our understanding of the composition of the total P_{org} pool and of the processes that control the diagenetic modification and ultimate preservation of P_{org} .

2.1.1 Marine Sedimentary Organic P: The Bulk Approach

Most organic P studies to date have made inferences about the composition of sedimentary P_{org} and its alteration during diagenesis based on measurements of total P_{org} concentration and/or bulk organic C:P ratios (see references listed above). These studies have shown that, typically, the size of the bulk P_{org} pool in marine sediments decreases substantially with depth, indicating partial remineralization during early diagenesis. Further, the generally observed increase in organic C:P ratios with depth indicates that, on average, organic P compounds are more labile than the bulk organic matter pool. This initial rapid remineralization of P_{org} is usually attributed to destruction of more labile components (Krom & Berner, 1981; Ingall & Van Cappellen, 1990) and by inference the deeply buried P_{org} is assumed to be more refractory. However, no molecular information has been available to support this assertion.

Persistence of P_{org} at depth in sediments (Filippelli & Delaney, 1994; Delaney & Anderson, 1997) and in ancient shales (e.g., Sandstrom, 1982; Ingall *et al.*, 1993) indicates that some P_{org} escapes remineralization. The fact that any P_{org} is preserved in marine sediments has long been a puzzle, however, given the highly labile nature of primary P_{org} biochemicals. Preservation may occur by one or more of the following mechanisms: (i) concentration of P_{org} compounds that are inherently refractory due to specific structural features, (ii) transformation reactions during diagenesis that convert labile compounds to more refractory compounds, or (iii) preservation of inherently labile P_{org} compounds by some mechanism of physical protection. To differentiate between these mechanisms, it is necessary to quantify changes in the abundance of particular P_{org} compound classes with depth by coupling detailed structural information with observed trends in bulk parameters.

2.1.2 Marine Sedimentary Organic P: The Molecular-Level Approach

Changes with depth in marine sediments have been quantified for a limited number of P compounds such as phospholipids (e.g., White *et al.*, 1979b; Harvey *et al.*, 1984; Balkwill *et al.*, 1988; Mancuso *et al.*, 1990; White, 1993) and ATP (e.g., Meyer-Reil, 1984; Bossard & Karl, 1986; Craven *et al.*, 1986; Balkwill *et al.*, 1988; Karl, 1993). Generally, these measurements are used to estimate intact, live biomass in sediments. Cell numbers are calculated based on the measured abundance of P biochemicals in sediments and estimates of the concentrations of these biochemicals in intact cells. The assumption inherent in this approach is that these P biochemicals are immediately degraded when the cells die. This assumption of instantaneous degradation of labile P biochemicals will be discussed in Chapter 3. These reactive biochemicals make up only a small fraction of the total organic P pool in sediments. Therefore, from the perspective of understanding molecular changes in sedimentary P_{org} , quantification of these compounds provides little information about the diagenetic alteration of the total P_{org} reservoir.

Molecular-level characterization of the bulk P_{org} reservoir has proven difficult because the polar, high molecular weight P compounds are not generally amenable to conventional organic geochemical techniques such as gas chromatography (GC) and GC/mass spectrometry. Pyrolysis and derivatization, two approaches that make organic compounds more amenable to GC analysis, result in degradation of simple P standard compounds (See Appendix C-4). ^{31}P -NMR, the structural tool used in this study, is currently the only non-destructive technique that provides detailed structural information about the complex sedimentary P_{org} reservoir.

2.1.3 Bridging The Gap: The Approach of This Study

The approach of this thesis was to combine the bulk and molecular-level approaches just described, using molecular-level structural information as a tool to

understand the observed trends in bulk parameters such as total P_{org} concentration and organic C:P ratios. This link is crucial to understanding the evolution of the total P_{org} pool during diagenesis, and to identifying the mechanisms that dictate P_{org} preservation. A sequential extraction was used to separate organic matter into operationally defined reservoirs on the basis of solubility. Bulk chemical parameters were measured to identify general trends in the abundance and composition of P_{org} during diagenesis. Molecular-level changes that accompany diagenesis were inferred for each soluble reservoir by contrasting ^{31}P -NMR spectra from different sediment horizons. This specific structural information was used to evaluate mechanistic explanations for the observed bulk trends.

The focus of this chapter is a description of the methods used for a combined bulk and molecular-level approach. An introduction to analysis by ^{31}P -NMR is provided, followed by a discussion of interpretation of the NMR results. The methods used to quantify organic and inorganic P are described. Finally, a sequential extraction procedure is presented, along with a discussion of the tests used to optimize the extraction method and an evaluation of the reproducibility of results. In summary, using complementary molecular-level and bulk information provides a more complete picture of the composition and diagenetic alteration of sedimentary P_{org} than can be obtained using either approach alone. This added information provides the means to evaluate controls on the remineralization of P_{org} and, specifically, to directly test the hypothesis that structure governs the preservation of P_{org} .

2.2 ^{31}P -NMR Spectroscopic Analysis of Sediment Extracts

^{31}P nuclear magnetic resonance spectroscopy (^{31}P -NMR) is a non-destructive method that provides unique information about the structure of phosphorus compounds in natural samples. Several other methods for structural analysis were explored (see Appendix C), but none were amenable to study of the bulk P_{org} pool. In the past few

decades, NMR has been used increasingly to characterize geochemical samples (e.g., Hayes *et al.*, 1989; Preston, 1996, and references therein). This is largely a result of the development of instruments with higher magnet strength and field stability over long run times, allowing analysis of samples with low natural abundances. In this section, I present a brief review of studies that have utilized ^{31}P -NMR, followed by the theoretical background necessary to understand the data collected in this study. Finally, I discuss application of ^{31}P -NMR to extracts from marine sediments. The theoretical background and discussion of spectra that follow are largely restricted to solution state data, because that constitutes the bulk of the data presented. Solid state NMR provides less structural resolution, and was used to examine only the insoluble sediment residue in a limited number of samples. Special considerations for application of solid state NMR are presented in Section 2.2.6.

2.2.1 Previous Studies

Most ^{31}P -NMR studies of geochemical samples have examined P in terrestrial soils, with the first application of ^{31}P -NMR to base extracts of soils published by Newman and Tate (1980). The main focus of most of these soil studies has been to characterize structural differences in P under varying conditions of temperature and soil moisture (Ogner, 1983; Hawkes *et al.*, 1984; Condrón *et al.*, 1985; Adams & Byrne, 1989; Condrón *et al.*, 1990; Bedrock *et al.*, 1994; Bishop *et al.*, 1994; Bedrock *et al.*, 1995). In a more limited number of studies, the speciation of P was examined in more nutrient-rich compost and sewage sludge (Preston *et al.*, 1986; Hinedi *et al.*, 1988; Hinedi *et al.*, 1989), bacteria (Doi *et al.*, 1989) and algae (Sianoudis *et al.*, 1986; Feuillade *et al.*, 1995). Degradation of monoesters and diesters in soils has also been monitored by examining changes in ^{31}P -NMR spectra upon exposure to specific enzymes (Bishop *et al.*, 1994) or addition of sewage sludge to soils (Hinedi *et al.*, 1988). In general, these studies suggest that diesters are remineralized more rapidly than monoesters in soils.

^{31}P -NMR has been used to characterize the structure of organic P in the marine environment in only a limited number of studies. Recently, Clark *et al.* (1998; 1999) used solid state ^{31}P -NMR to detect phosphoester and phosphonate linkages in the high molecular weight fraction of water column dissolved organic matter, showing that the relative abundance of phosphonates is high (25%) compared to their biomass abundance (3%). The few studies of P structure in sediments are generally based on analysis of single sediment horizons at each site (Uhlmann & Bauer, 1988; Ingall *et al.*, 1990; Carman & Jonsson, 1991; Ingall, 1991; Hupfer *et al.*, 1995a; Hupfer *et al.*, 1995b). Such studies cannot be used to examine modification of P_{org} during diagenesis. However, the dominant forms of P_{org} identified in these studies were monoesters and diesters with small contributions by phosphonates. In one study (Berner *et al.*, 1993), bulk sediments from three depths in a core were examined using solid state ^{31}P -NMR. The presence of phosphonates in bulk sediment samples was used to argue for their selective preservation during diagenesis. By examining higher resolution depth trends in P_{org} structure, inferred from contrasting NMR spectra from different sediment horizons, the work presented in this thesis provides these much needed insights into the diagenetic modification of P_{org} . The use of solution ^{31}P -NMR in this thesis provides more detailed structural information and more robust quantification of specific functional groups, allowing the hypothesis of selective phosphonate preservation to be more thoroughly tested.

Most ^{31}P -NMR analyses are performed using solutions (e.g., soil extracts). Solution NMR is generally preferred because solid state NMR provides less structural resolution due to extensive line broadening, and relative abundances of functional groups are less easily quantified. The sequential extraction used in this study was designed to maximize solubilization of P_{org} , and lipid and base extracts were analyzed by solution ^{31}P -NMR. Solid state ^{31}P -NMR was used as a complementary method for characterizing the P_{org} that was otherwise insoluble and thus analytically inaccessible.

2.2.2 Theoretical Background

The brief background given here is intended to provide context for the data presented in this thesis. More detailed explanations of NMR theory and its applications to geochemical studies can be found in Wilson (1987; 1991) and Sanders and Hunter (1993). Bloch decay, the simplest type of high resolution NMR experiment, is used to quantify the abundance of different functional groups. The functional group information obtained by Bloch decay experiments will be the sole focus of this discussion and of the NMR data presented in this study.

Nuclear magnetic resonance is related to an intrinsic property of the nucleus called spin. When the spins of protons and neutrons are not paired, the overall spin of the charged nucleus generates a magnetic dipole along the spin axis (often compared to a bar magnet). ^{31}P nuclei have no unpaired protons and 1 unpaired neutron, to give a net spin of $1/2$. When nuclei are placed in a stationary magnetic field (B_0), their spins align either with or against the field. The Boltzmann equation predicts the ratio of the number of nuclei aligned against the field (high-energy state, N_e) to the number of nuclei aligned with the field (low energy state, N_g):

$$\frac{N_e}{N_g} = e^{-\Delta E/kT} \quad (2-1)$$

where k is the Boltzmann factor (1.38×10^{-23} J/K), ΔE is the energy difference between spin states, and T is the temperature in degrees Kelvin. Under equilibrium conditions, there are generally slightly more nuclei at the lower energy level. A nucleus in the lower energy state can undergo a transition to the higher energy state by absorption of a photon with energy that exactly matches ΔE . The energy of the photon is related to its frequency ν :

$$\Delta E = h\nu \quad (2-2)$$

where h is Planck's constant, 6.63×10^{-34} J-sec. In NMR spectroscopy, ν is referred to as the resonance, or Larmor, frequency and is in the radio frequency (RF) range. This energy is provided by a second, oscillating magnetic field (B_1). The NMR signal arises from the difference between energy absorbed by nuclei making the low-to-high transition, and the energy emitted by nuclei making the high-to-low transition. Thus, the signal is proportional to the population difference between states, which is increased at higher magnet strength (larger B_0) and lower temperature. The frequency at which energy is absorbed by nuclei is characteristic of the nucleus itself (e.g., ^{31}P , ^1H , ^{13}C) and its electronic environment, thus providing the information on chemical structure presented here.

Figure 2-1 shows an example of a pulse sequence, which illustrates the parameters employed in this study. During the NMR experiment, a short pulse of RF radiation establishes resonance with nuclei in the sample. The result is to tilt the net magnetization vector (initially oriented along the Z-axis) 45° into the XY plane. The angle of this tilt, called the flip angle, is determined by the duration of the pulse. As the nuclei precess about the Z-axis, the XY component of magnetization is detected by the spectrometer. As the nuclei relax, the net magnetization decays back toward the Z axis, and the resulting signal of net magnetization in the XY plane tapers off in the characteristic free induction decay (FID) recorded in the time domain (Figure 2-1). This signal can be described as a series of sine waves, each with a frequency equal to the Larmor frequency of nuclei in the sample. The pulse sequence is repeated for thousands of scans, and the sum of the FID signals is transformed from the time domain into the frequency domain using a fast Fourier transform (FFT). The result is a plot of signal intensity versus frequency, the familiar NMR spectrum.

All the solution ^{31}P -NMR spectra presented here were run on a Varian 500 MHz (11.7 Tesla) spectrometer with a broad band probe. Spectra were collected on a 100 parts per million (ppm) spectral window centered at 0 ppm, using a 45° flip angle, 0.6 second

acquisition time and a relaxation delay of 1.5 seconds. The choice of spectral window indicates that only compounds with a chemical shift between -50 and +50 ppm will be detected. The amount of time required for each scan is dependent upon the range of frequencies to be scanned, so the spectral window has been chosen to encompass only the range of values expected for naturally-occurring P compounds.

2.2.3 Chemical Shift

The absolute values of the frequencies measured are dependent on the configuration of a particular spectrometer. For comparison of samples run on different instruments, values are typically reported as chemical shifts (δ) in units of parts per million (ppm) relative to a standard, as shown in the equation below. Again, ν is defined as the resonance, or Larmor, frequency.

$$\delta = \left(\frac{\nu_{ref} - \nu}{\nu_{ref}} \right) \times 10^6 \quad (\text{ppm}) \quad (2-3)$$

^{31}P chemical shifts are reported relative to an external standard of phosphoric acid, which is assigned a chemical shift of 0 ppm. The structural information derived from NMR spectroscopic analysis reflects differences in the electronic environment of each nucleus. The spinning nucleus is partially shielded from the applied magnetic field by the surrounding atoms in the molecule. This shielding alters the effective magnetic field experienced by the nucleus, and thus affects the frequency of the applied field needed to induce resonance. The chemical shift therefore reflects differences in the electronic shielding of nuclei from the applied magnetic field. The magnitude of the shielding effect depends on the electron density near the nucleus, and thus is affected by bond geometry, the electronegativity of the chemical groups attached to the P nucleus, and the relative amount of pi bonding. This means that the chemical shift is diagnostic of the type of P linkages present in the sample. For example, the only structural difference between

orthophosphate and a phosphomonoester is the ester-linked carbon skeleton attached to the P nucleus in the phosphomonoester (see structures in Figures 2-2 and 2-3). Since the attached carbon skeleton acts as an electron-donating group, the chemical shift of monoester P is shifted downfield (toward more negative chemical shift values) compared to orthophosphate.

Commercially available standard compounds were analyzed in aqueous or chloroform solutions to determine their chemical shifts. The insolubility of most P compounds in non-polar solvents limited the number of compounds run in chloroform (Table 2-1). Table 2-2 shows the chemical shifts for a broader suite of compounds in a solution of 0.5 M NaOH. The position of spectral absorbance lines can be solvent dependent, so comparisons of chemical shifts can only be made between standards (or samples) run in the same solvent. All standards were run at concentrations of approximately 10 mM to minimize run time. Changes in concentration did not affect chemical shift. For example, standards run at concentrations of 10, 5, and 0.5 mM did not differ in chemical shift by more than 0.2 ppm. Figure 2-2 shows a mixture of P standards run in 0.5 M NaOH and Figure 2-3 shows a typical spectrum of a sediment base extract, with each functional group region labeled. Each of the major chemical shift regions found in typical spectra of sediment base extracts (Figure 2-3) is discussed below. The broad peaks observed in samples compared to standards reflect the detection of several discrete resonance frequencies in natural samples, indicating similar but chemically distinct structures. Peak broadening may also arise due to the presence of paramagnetic metals and other matrix effects in the sediment extracts that are absent in a mixture of pure standards.

The peaks in sample spectra are nonetheless much sharper than the peaks generally observed in ^1H or ^{13}C NMR spectra of sediment and soil extracts. This is likely a result of the fact most naturally-occurring P compounds contain a phosphate group as their basic building block. Since the P nucleus is surrounded by four oxygens, the

Table 2-1. Chemical shift of compounds measured in CDCl₃.

Compound	Chemical Shift (ppm)	Chemical Structure
<u>Diester</u>		
Phosphatidyl choline	-0.4	<chem>CCOP(=O)(OC(=O)R1)OC(=O)R2[N+](C)(C)C</chem>
Phosphatidyl ethanolamine	0.6	<chem>CCOP(=O)(OC(=O)R1)OC(=O)R2N</chem>
Sphingomyelin	0.3	<chem>CCOP(=O)(OC(=O)R)N[C@@H](CCCCCCCCCCCCCCCC)C[C@H](O)C[C@H](N)COP(=O)(OC(=O)R3)OC(=O)R4</chem>
Cardiolipin	2.4	<chem>CCOP(=O)(OC(=O)R1)OC(=O)R2COP(=O)(OC(=O)R3)OC(=O)R4</chem>
<u>Monoester</u>		
Phosphatidic acid	3.4	<chem>CCOP(=O)(OC(=O)R1)OC(=O)R2</chem>

immediate chemical environment surrounding the P nucleus does not vary widely. Proton decoupling employed during these experiments eliminated peak splitting. The sharpness of the peaks in the ^{31}P -NMR spectra presented here is also indirect evidence for the lack of paramagnetic metals in the solution, which would tend to suppress the signal and broaden the individual peaks (see discussion in Section 2.4.3.2).

The structure of most common P biochemicals is based on esterification of a phosphate group to a carbon skeleton. Phosphonates, an exception to this rule, are a minor class of biochemicals that have been identified in bacteria, ciliates, and higher organisms (Kittredge & Roberts, 1969; Quin & Shelburne, 1969; Alhadeff & Daves Jr., 1970), as well as in marine sediments (Ingall *et al.*, 1990) and the high-molecular-weight fraction of dissolved organic matter in the oceans (Clark *et al.*, 1998; Clark *et al.*, 1999). Instead of a phosphate ester with a C-O-P linkage, these compounds have a direct bond between P and the carbon skeleton. The two phosphonate standards we tested have chemical shifts of 14.7 and 20.2 ppm. The range of phosphonate chemical shifts previously published in the literature is 18-22 ppm (Newman & Tate, 1980; Hawkes *et al.*, 1984; Bedrock *et al.*, 1994). To quantify changes in functional group abundance, the phosphonate region was defined from 14 to 25 ppm.

In repeated runs ($n=6$), the chemical shift of orthophosphate standards varied between 5.9 and 6.1 ppm. The chemical shift of the peak identified as orthophosphate in base extracts of sediment samples ranged from 6.3 to 6.7 ppm. This difference in chemical shift in natural samples may arise from association of P with the humic matrix and with paramagnetic cations (see discussion in Section 2.4.3.2). Because of the potential for sediment extract matrix effects, as well as the fact that different compounds within a compound class can have very similar chemical shifts, interpretation of the data will be limited to differences within regions, but will not include identification of specific compounds based on chemical shift.

Table 2-2. Chemical shift of compounds measured in 0.5 M NaOH. All solutions had a pH of approximately 13.4, eliminating pH-dependent changes in chemical shift. All chemical shifts are referenced to an external standard of 85% H₃PO₄ at 0 ppm. Listed are the chemical shifts for individual compounds (plain text), as well as the range of values measured for each compound class (boldface).

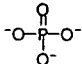
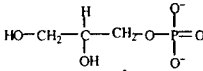
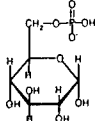
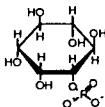
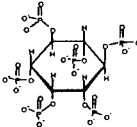
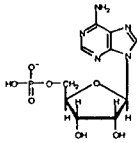
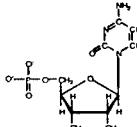
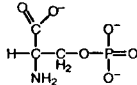
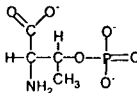
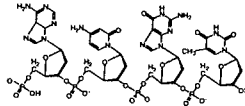
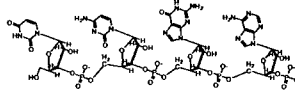
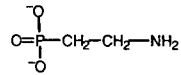
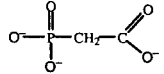
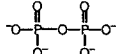
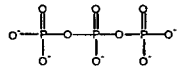
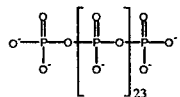
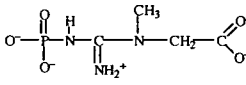
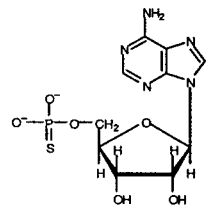
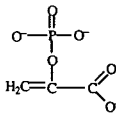
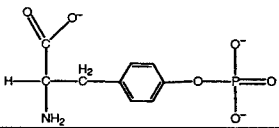
Compound	Chemical Shift (ppm)	Chemical Structure
Orthophosphate	5.9 to 6.1	
Monoester	4.0 to 5.9	
<u>Phosphosugar</u>		
glycerol-2-phosphate	4.7-5.1	
glucose-6-phosphate	4.8; 5.4	
<u>Inositol</u>		
inositol-2-monophosphate	5.4	
phytic acid	4.5 to 5.9	
<u>Nucleotide</u>		
adenosine-5'-monophosphate	4.7	
cytosine-5'-monophosphate	4.6	
<u>Phosphoprotein</u>		
phosphoserine	4.7	
phosphothreonine	4.0	

Table 2.2 (cont'd.)

Diester	- 0.1 to - 0.5	
<u>Nucleic Acids</u>		
deoxyribonucleic acid	- 0.1 to - 0.5	
*ribonucleic acid	*4.2 to 4.8	
Phosphonate	14.7 to 20.3	
2-aminoethylphosphonic acid	20.3	
phosphonoacetic acid	14.7	
Polyphosphate		
End Groups	- 4.0 to -5.0	
Middle Groups	- 18.8 to -22.9	
pyrophosphate	- 5.0	
tripolyphosphate	- 4.3	
	- 18.8	
polyphosphate (n=25)	- 4.0	
	- 19.3 to - 22.9	
Other		
phosphocreatine	- 1.3	
adenosine-5'-thiomonophosphate	- 43.6	
phospho(enol)pyruvate	0.26	
phosphotyrosine	1.0	

* as discussed in the section on the base hydrolysis experiment (Section 2.4.3.2.1), RNA is immediately hydrolyzed to its constituent monoesters upon solution in base. The chemical shifts observed are consistent with this hydrolysis.

Phosphomonoesters (referred to hereafter simply as monoesters) include phosphosugars, phosphoproteins, nucleotides, and inositols. In soil extracts, the chemical shift region from 4 to 6 ppm is thought to be dominated by these compounds (White & Miller, 1976; Newman & Tate, 1980; Hawkes *et al.*, 1984; Condon *et al.*, 1985; van Wazer & Ditchfield, 1987; Adams & Byrne, 1989). A suite of monoester standards was analyzed (Tables 2-1 and 2-2), ranging in chemical shift from 4.0 to 5.9 ppm. For quantification purposes, the monoester region is defined as the region between 3.5 and 6 ppm.

Phosphodiester (or, simply, diester) include phospholipids and nucleic acids. Their lower chemical shift values compared to monoesters reflect increased shielding of the P nuclei by the presence of additional ester linkages. DNA and RNA were the only diesters run as chemical shift standards in alkaline solution, because phospholipid standards were insoluble in base. RNA degraded into monoester nucleotides (see Section 2.4.3.2.1), leaving DNA as the only diester with a measurable chemical shift (-0.1 to -0.5 ppm).

Polyphosphates are detected in two different chemical shift regions, as shown in Figures 2-2 and 2-3. The end groups have a chemical shift of -3 to -5 ppm and the middle groups have a chemical shift of -17 to -23 ppm. This difference has been exploited in some studies to estimate the chain length of polyphosphates by examining the ratio in the abundance of end groups to middle groups (e.g. Gard *et al.*, 1992a; Gard *et al.*, 1992b).

Even after extensive tests of available standards (Tables 2-1 and 2-2), there were peaks in some chemical shift regions that could not be confidently assigned to a particular functional group. Unidentified peaks at 1.5 and 3 ppm have been observed in studies of terrestrial soils (Hawkes *et al.*, 1984; Adams & Byrne, 1989). Compounds with chemical shifts in the range from 1.5 to 3 ppm include phosphate triesters and imidophosphates (compounds with an N-P bond) (van Wazer & Ditchfield, 1987)

Peaks between 25 and 30 ppm may be additional phosphonate resonances or other compounds with direct C-P linkage such as phosphine oxides (R_3PO) or phosphinic acids ($R_2PO(OH)$), which have resonances between 22 and 40 ppm. Alternatively, these peaks may represent thiophosphates (compounds with a P-S bond, chemical shift = 24 to 45 ppm), which may be found in sediments both as naturally occurring compounds and as anthropogenic contaminants. For example, parathion and diazinon are widely used thiophosphate insecticides (Eto, 1974). Finally, small peaks in the region from 8 to 12 ppm are observed in some sample spectra (not shown in Figure 2-3). Such peaks have been assigned to aromatic diesters in a previous study (Bedrock *et al.*, 1994).

2.2.3.1 The Effect of pH on Chemical Shift

pH can have a dramatic effect on the chemical shift of individual peaks because protonation of the phosphate oxygens alters the electronic environment of the nucleus. An example of this effect is shown in Figure 2-4. The orthophosphate peak is shifted upfield (toward higher chemical shift values) with increasing pH. Changes in chemical shift are particularly dramatic near the pK_a values for phosphoric acid. This pH effect is important because it can result in different chemical shift values for the same compound in different samples, but also because the chemical shifts of orthophosphate and phosphate monoesters are coincident at pH 11-12. The pH effect is minimal above pH 13.4, which corresponds to a 0.5 M NaOH solution. For the pH range above 13.3 (inset of Figure 2-4), pH changes could not be measured using a standard pH electrode and all of the chemical shift measurements shown have been assigned a pH of 13.4. However, these measurements represent a range of NaOH concentration up to 20 times higher (or roughly equivalent to the maximum concentration in samples used for this study). At pH 13.4 or above (corresponding to 0.5 M NaOH, the minimum concentration used in these samples), there is very little variation in chemical shift. Changes in other P compounds

showed varying degrees of pH dependence, but none changed significantly in the pH range above 13.4. The pH of all base extracts used in this study was 13.4 or higher.

2.2.4 Improving the Signal-to-Noise Ratio

The concentration of P in natural samples is low, but various methods exist to maximize the NMR signal. At a given magnetic field strength, the most straightforward way to enhance the signal-to-noise ratio (S/N) is to concentrate extracts, thus increasing the number of nuclei in the sample tube. In practice, the concentration of P in sediment extracts is limited by the quantity of sediment available and by the solubility of dissolved constituents in a given sample volume. However, even with limitations in sample concentration, a number of tools can be used for signal enhancement.

The advent of fast Fourier transform (FFT) techniques, replacing the single pulse experiment, has been one of the most important advances in NMR spectroscopy. For each experiment, the pulse sequence is repeated for many (in this study, 30,000-70,000) scans and the resulting signals are added and transformed from the time domain into the frequency domain via an FFT. While the signal increases linearly with this addition, the noise level increases as a square root function. Thus, the signal-to-noise ratio increases in proportion with the square root of the number of spectra averaged.

Spin-spin coupling with other nuclei influences the field (B_0) and causes peak splitting. For example, the signal from identical P nuclei can split into several peaks because the spin of neighboring protons can either enhance or oppose the local magnetic field. Proton decoupling can eliminate this phenomenon. A saturation pulse of white noise in the RF range of proton resonance is applied to the sample, increasing the rate of proton transitions so that a given P nucleus experiences only one average magnetic field. A potential drawback of this approach is nuclear Overhauser effects (NOE) that can arise when decoupling enhances the signal in a non-uniform way. In this study, NOE effects were suppressed by using broadband decoupling through WALTZ (Shaka *et al.*, 1983)

modulation, a technique that achieves proton decoupling with very little power. By minimizing the input of power to the sample, WALTZ modulation effectively avoids problems associated with heating the sample, including thermal degradation and loss of spectral resolution due to heat gradients in the sample tube.

Spectral processing techniques such as line broadening can be used to further enhance the signal to noise ratio. Line broadening is a mathematical technique that exploits the fact that while the signal decays over time, the noise level remains approximately constant. The FID is multiplied by a decaying exponential, giving more weight to the data collected when the signal is strongest. This increased signal is gained at the expense of frequency resolution, because frequency information is lost by forcing the signal to decay more quickly. The line-broadening factor is chosen to maximize the enhancement of S/N without degrading the natural resolution. In this study, we applied 10 Hz of line broadening to all samples. By dividing this frequency by 202.466 MHz (the operating frequency of the spectrometer), this value can be converted into a chemical shift δ value of 0.05 ppm. This is less than the minimum natural variation in chemical shift of most peaks in these spectra. The line broadening applied to these samples is therefore unlikely to cause sufficient broadening to degrade the natural resolution.

2.2.5 Quantification of Functional Groups Using ^{31}P -NMR Data

To quantify P compound types using ^{31}P -NMR, two criteria must be satisfied: (i) all of the P in the sample is detected, and (ii) the relative peak area response is the same for different P functional groups. Tate and Newman (1982) found that the values for total P determined by perchloric acid digestion and ^{31}P -NMR analyses of a soil base extract were in agreement, showing that ^{31}P -NMR detects all P in the extract. A direct way to confirm this agreement is by using an internal standard. The difficulty in this approach is finding a standard that is not present in natural samples, but has a chemical shift in the region of interest (-50 to 50 ppm). A number of samples were run with a capillary insert

of AMPS (adenosine-5'-thiomonophosphate, chemical shift = 43 ppm), a thiol analog of the nucleotide AMP. However, over time it was observed that this compound degraded, producing orthophosphate. Therefore, no direct comparison between total P determined by NMR and wet chemical measurements was possible. The absolute concentration of P functional groups in this study is calculated by multiplying the total P concentration (measured by the wet chemical technique described in Section 2.3.3) by the fraction of P in each functional group region determined by integrating peak areas on the spectra.

One of the advantages of using solution NMR spectroscopy is that peak area in the spectrum is proportional to the number of nuclei, or chemical linkages, of a given type in the sample. However, it is important to be cautious in interpreting quantitative results because peak area can also be affected by coupling effects and differences in the relaxation times for different nuclei. As discussed earlier, broadband WALTZ decoupling was used in this study to suppress nuclear Overhauser effects that can artificially enhance the peak area for particular functional groups. If the relaxation time allowed by the pulse sequence is shorter than the relaxation time of some nuclei, they will not fully return to their low energy state before the next pulse. As a consequence, not as many nuclei will be flipped into the high-energy state by the next pulse and the signal will decrease. The result is to bias the spectrum, with relative signal enhancement for functional groups that have shorter relaxation times. In this study, there was a delay of 2.1 seconds (0.6 sec. acquisition time, 1.5 sec. relaxation delay, shown in Figure 2-1) between pulses. There have been few studies of relaxation parameters in ^{31}P -NMR, although data from Newman and Tate (1980) suggest that the major compounds found in soil extracts have relaxation times shorter than 3 seconds. The 2.1 second delay was chosen for this study after weighing the importance of allowing maximum relaxation of the nuclei and obtaining a large number of scans to enhance the total signal. As shown below, this reduced relaxation time does not result in excessive biasing of the relative peak sizes in the ^{31}P -NMR spectra.

The relative peak area response for different standard compounds of known concentration was calculated to determine the error in P abundance estimated from the NMR spectra. For each standard compound tested, the peak area was divided by P content in mmol to give a response factor. The response factor for each compound was then divided by the response factor for orthophosphate, giving the peak area response relative to orthophosphate (Table 2-3). Orthophosphate was chosen as the “reference peak” because it is abundant in the spectra of all base extracts. A relative response of 1 for each compound would indicate that the relationship between P abundance and peak area is identical for all compounds. The relative responses calculated at different P concentrations, demonstrated that the most uniform peak area response (the values closest to 1 for all compounds) occurs at lower P abundance (Table 2-3).

The peak response at 0.5 mmol P per compound ranges from 0.93 to 1.08, for a total variation of 0.15, or 15%. Since this concentration (0.5 mmol P) is most similar to the concentration of the base extracts examined in this study (0.02-0.1 mmol P), 15% is

Table 2-3. Relative peak response for different organic P functional groups, obtained by analyzing standard compounds. The integrated area for each peak is divided by its concentration, and this value is compared to the concentration-normalized orthophosphate peak area, as described in the text. The most uniform response occurs at lower P concentration. Uncertainty estimates indicate the standard deviation of replicate measurements (n=4) or the total range of variation (n=2).

Compound	Peak Area Response Relative to Orthophosphate		
	<u>0.5 mmol</u>	<u>5 mmol</u>	<u>10 mmol</u>
2-AEP	1.08 (n=1)	1.08±0.11 (n=2)	1.20±0.09 (n=4)
phosphonoacetic acid	1.03±0.12 (n=2)	1.01±0.11 (n=2)	1.15±0.07 (n=4)
phosphoserine	0.93±0.06 (n=2)	0.91±0.13 (n=2)	1.05 (n=1)
phosphocreatine	1.03±0.08 (n=2)	1.22±0.01 (n=2)	1.21 (n=1)

used as an estimate of the possible variation in peak response that can be expected. Therefore, only differences larger than 15% will be considered significant in evaluating concentration changes in different P functional groups.

2.2.6 Solid State NMR Analyses

Solid state NMR techniques are often used to analyze geochemical samples (e.g., analysis of humic acids by ^{13}C -NMR). In contrast with solution NMR samples, the concentration of the nucleus of interest in solid samples is not constrained by limited solubility. Therefore, higher sample concentrations can often be used in solid samples, reducing the required acquisition time. In spite of the larger number of nuclei that can be detected in a solid sample, the spectral resolution is much poorer. The primary reason for better resolution of structure using solution NMR is that inhomogeneities in the sample are averaged out by spinning the sample tube and by random tumbling of molecules within the liquid. The result is that all nuclei in a particular electronic environment experience the same average magnetic field. This is not the case for solid samples, where molecules are locked into a fixed lattice and the magnetic field experienced by each nucleus is modified by the molecules around it through dipole-dipole interactions. The magnitude of these interactions depends on the angle of the molecule with respect to the magnetic field. At a specified angle (54.7° , called the magic angle), this dipole interaction approaches zero. If every molecule could be oriented at this angle, the spectrum would have line widths comparable to solution spectra. This is not possible, but some of the dipole interaction can be eliminated by using the magic angle spinning (or MAS) technique, where the sample is spun rapidly at the magic angle relative to the magnetic field. The MAS technique was used for the solid state spectra presented in this study.

2.3 Analysis of Phosphorus Concentration

For the wet chemical analyses described here, the distinction between organic and inorganic P is made according to conventions in the literature. Briefly, inorganic P for all extracts and solid phase samples is operationally defined as P that is extractable in 1 M HCl and reacts with colorimetric molybdate reagents. Total P is determined by extraction of an ashed split (either of solutions or solids). In all cases, organic P is calculated as the difference between inorganic and total P. Total and inorganic P were measured on splits of the unextracted sediment samples and the sediment residues after solvent and base extraction. These data and the P concentration measured in each extract were used to assess the efficiency of each extraction, loss of P, and transformation during chemical treatments (e.g., hydrolysis of organic P).

2.3.1 Cleaning and Materials

The standard cleaning procedure for all supplies used in sample handling and extraction, unless otherwise noted, was to soak overnight in Liqui-Nox™ phosphate-free soap, rinse copiously with tap water, soak for 48 hours in 10% HCl and rinse 6 times with milli-Q H₂O. Glassware was allowed to dry, then combusted for two hours at 500°C. Volumetric glassware and Teflon centrifuge tubes were soaked overnight in soap, rinsed copiously with tap water and dried, soaked for 48 hours in NoChromix™ acid solution, and rinsed 6 times with milli-Q H₂O. Glassware was rinsed two times with methanol and two times with dichloromethane immediately before use. All organic solvents used were GC² purity and all chemicals were reagent grade quality or better. Sample blanks were run through the full sequential extraction procedure to evaluate glassware, filter and other procedural blanks. For purposes of evaluating the loss of sample on filters during base extraction, filters were combusted and analyzed for total P. Therefore, blank values for the Gelman 10 µm polypropylene and 0.45 µm GH Polypro filters were determined by

combusting and extracting the filters. The P contents of the combined filters (1 of each), with and without acid cleaning, were 0.010 and 0.013 μmol , respectively. Based on these totals, it was determined that acid cleaning of filters was unnecessary.

2.3.2 Soluble Reactive Phosphorus: Extracts

Inorganic P was quantified in the acid extract and the base extract as soluble reactive phosphorus (SRP). A split of each extract was adjusted to pH 1, which is necessary for color development. The solutions were reacted and measured using the phosphomolybdate blue method of Koroleff (1976). Absorbance was measured spectrophotometrically at 880 nm in a 1 cm cell. In the range from 0 to 20 μM , absorbance is linearly proportional to concentration. Samples with high P concentration were diluted to within this concentration range. Orthophosphate standards with concentrations of 0, 5, 10, 15, and 20 μM were analyzed at the beginning and the end of each sample run, and these standard values were used to calculate the relationship between absorbance and concentration. The relative percent error between duplicate measurements was calculated as follows:

$$\text{Relative \%error} = \frac{[\text{SRP}]_1 - [\text{SRP}]_2}{\text{mean } [\text{SRP}]} \times 100 \quad (2-4)$$

When the relative percent error was greater than 2%, samples were re-run until the standard deviation of replicate measurements was less than 2%.

2.3.3 Total Dissolved Phosphorus: Extracts

Total dissolved phosphorus (TDP) analyses using the method of Solórzano and Sharp (1980) result in efficient recovery of P from seawater samples (Monaghan & Ruttenberg, 1999). However, P is under-recovered when this method is used for non-

seawater samples, such as the sediment extracts analyzed in this study. As modified by Monaghan and Ruttenberg (1999), 0.2 mL of 0.17 M MgSO_4 was added to a 20 cc borosilicate vial, followed by 10 mL of sample (in this case, orthophosphate standards). Samples were dried and then combusted for two hours at 500°C. A 3 mL aliquot of 0.75 M HCl was added to each vial, and samples were heated for 20 minutes at 80°C. After cooling, 7 mL of milli-Q H_2O was added to each vial and samples were heated for 10 minutes at 80°C. We determined the percent of total P recovered for orthophosphate standards prepared using variations of this procedure (Figure 2-5a). In all cases, samples were acidified to pH 1 before drying. The fact that significantly more P ($98.5 \pm 0.7\%$) is recovered from standards made in artificial seawater (ASW: 0.43 M NaCl and 0.03 M MgSO_4 Strickland & Parsons, 1972) suggests that higher salt content is necessary to prevent P loss. To mimic the composition of seawater samples, a concentrated salt solution (or “brine”) was added before drying to give a final salt concentration equivalent to ASW, as suggested by Monaghan and Ruttenberg (1999). With this brine addition, P recovery from 0.1 M HCl standard solutions was indistinguishable from those in ASW (Figure 2-5a). This TDP method was used for initial sample tests. However, additional problems were encountered when this method was used for analysis of citrate dithionite bicarbonate, MgCl_2 , and base extracts due to the high dissolved solids in these solutions. After combustion, heating in 0.75 M HCl and then in milli-Q H_2O , as described above, did not completely dissolve the sample. The suspended solids resulted in erroneously high P concentration estimates. When the solutions were filtered after the hydrolysis step, P was under-recovered.

Using a modification of the standard Aspila (1976) method used for solid samples, problems with the dissolution of the sample matrix were avoided, and orthophosphate and tripolyphosphate standards were recovered quantitatively (Figure 2-5b). The higher acid concentration and longer extraction time used in this method resulted in more efficient dissolution of P than modifications of the Solórzano and Sharp

method. Only two modifications were necessary to apply the Aspila method to solutions rather than solid samples: (i) acidification of the solutions to pH 1, (ii) and drying the solutions at 80°C before combustion. As modified for the sediment extracts, 0.2 mL of 50% (w/v) $\text{Mg}(\text{NO}_3)_2$ was added to a 20 mL borosilicate vial, followed by 5 mL of sample solution and 12 M HCl to adjust the pH. Samples were dried and combusted for 2 hours at 550°C, extracted for 16 hours in 1M HCl, and filtered through a 0.4 μm polypropylene filter. Unlike the modifications of the Solórzano and Sharp method described above, addition of a brine solution to these samples resulted in lower P recovery (Figure 2-5b). The salt content of the 50% (w/v) $\text{Mg}(\text{NO}_3)_2$ added to samples is sufficient to prevent P volatilization, and additional salts resulted in solids that were not completely dissolved during HCl extraction, scavenging P from solution. All TDP measurements of sediment extracts from Santa Barbara Basin samples were made using the “modified Aspila” method.

2.3.4 The Aspila Method: Sediments and Sediment Residues

Solid-phase P was analyzed using the Aspila (1976) method with minor modifications for smaller sample size. For total P measurement, an aliquot (0.04 g) of sediment was weighed into a 20 cc borosilicate vial and 0.2 mL of 50% (w/v) $\text{Mg}(\text{NO}_3)_2$ was added. Samples were dried and ashed at 550°C for two hours to degrade organic P to inorganic P. The ashed residue and a separate split of unashed sediment were each extracted in 5 mL of 1 M HCl. After shaking at room temperature for 16 hours on a shaker table at 250 rpm, each supernatant was passed through a 0.45 μm polypropylene filter. A split of each extract was adjusted to pH 1 and analyzed colorimetrically using the phosphomolybdate blue method of Koroleff (1976). Organic P was calculated as the difference between total P and inorganic P.

This method of estimation has several potential sources of error. Since P_{org} is determined by taking the difference between two (often similar) values, the uncertainty in

calculated P_{org} is often high. Inorganic P may be underestimated if it is not extracted by 1 M HCl or is not reactive with the colorimetric reagents (e.g., polyphosphates). The ashing process may mobilize some inorganic P phases that are not detected by acid extraction alone (Hartmann *et al.*, 1976; Froelich *et al.*, 1982; Mach *et al.*, 1987). In addition, chemical species that interfere with SRP measurement (e.g., sulfide) may be oxidized by the ashing process and not interfere in the total P measurement. Thus, there exist a number of ways that inorganic P can be underestimated by the difference method. Alternatively, inorganic P could be overestimated if organic P compounds are hydrolyzed by acid extraction.

2.3.4.1 The Acid Hydrolysis Experiment

An acid hydrolysis experiment, modeled after the study of Monaghan and Ruttenberg (1999), was used to quantify degradation of organic and inorganic P compounds during extraction and subsequent storage in 1 M HCl. Each compound was dissolved to a concentration of *ca.* 100 μ M P in a solution of 1.0 M HCl. The solutions were shaken at 250 rpm for 16 hours and then analyzed for SRP. Solutions were stored refrigerated (4°C) and analyzed for SRP again after 5 days, the maximum time that elapsed between extraction of the Aspila split for inorganic P and SRP determination. In addition to the data shown (Table 2-4), it is presumed that phosphocreatine is extensively hydrolyzed, based on data for hydrolysis in 0.1 M HCl (Monaghan & Ruttenberg, 1999) and upon acidification of a basic solution to pH 1 (Section 2.4.3.2.1).

To quantify inorganic P accurately, the acid extraction must not only efficiently dissolve inorganic P phases to liberate orthophosphate, but must also decompose polyphosphates into orthophosphate. Based on SRP measurements of polyphosphate solutions made after 16 hours, hydrolysis of polyphosphate is not complete immediately upon extraction. Up to 4 days of acid hydrolysis is needed for complete hydrolysis to orthophosphate. During this same time interval, there was no significant hydrolysis of the

Table 2-4. Hydrolysis of P compounds in 1 M HCl.

Compound	Total P (μM)	* Initial Hydrolysis		After refrigerated storage for 4-5 days	
		[SRP (μM)]	% hydrolyzed	[SRP] (μM)	% hydrolyzed
<u>Inorganic P</u>					
tripolyphosphate	98.8	9.1 ± 0.1	9.2	98.5 ± 0.8	99.7
pyrophosphate	106.2	7.8 ± 0.3	7.4	105.9 ± 0.7	99.7
polyphosphate (n=25)	101.6	10.6 ± 0.1	10.5	98.8 ± 0.4	97.2
<u>Organic P</u>					
ribonucleic acid	111.7	1.0 ± 0.0	0.9	2.3 ± 0.0	2.0
deoxyribonucleic acid	99.7	0.5 ± 0.0	0.5	1.4 ± 0.2	1.4
adenosine-5'- monophosphate	113.4	0.0 ± 0.0	0.0	0.1 ± 0.0	0.1
phosphoserine	112.2	2.9 ± 0.1	2.6	3.2 ± 0.1	2.9
phytic acid	102.0	2.1 ± 0.0	2.0	2.0 ± 0.0	2.0

* After 16 hours of hydrolysis at room temperature with continuous agitation (250 rpm).

organic P compounds we tested. Ingall and Van Capellan (1990) demonstrated that only a few percent of the P in fresh zooplankton and seaweed samples were analyzed as inorganic P using the Aspila method. It should be noted that before acid extraction, the zooplankton and seaweed were washed in water to remove water-soluble P (Ingall & Van Cappellen, 1990), so the amount of P solubilized in acid is probably a minimum estimate. Together these data indicate that the Aspila method hydrolyses polyphosphates and does not significantly hydrolyze organic P compounds during inorganic P extraction. In Section 2.4.3.8, a comparison between inorganic and organic P distributions determined by the Aspila method and using ^{31}P -NMR will be used to further evaluate the Aspila method.

2.3.5 Reproducibility of P Concentration Results

The reproducibility of P concentration data for each reservoir depends on: (i) replication of P measurements, and (ii) replication of the extraction process. Both of these components were evaluated. For all extractions and P concentration analyses, relative percent error (see Equation 2-4) was the criteria used to describe reproducibility. The concentration range for duplicate analyses ($n=2$) is simply the arithmetical difference between the two measurements, and provides a conservative estimate of error. For $n>2$, it is possible to calculate a standard deviation over all measured concentrations, and the standard deviation is substituted for the concentration range in the numerator of Equation 2-4. The discussion that follows applies to reproducibility of P concentration analyses. The reproducibility of sediment extractions, and of functional group quantification using ^{31}P -NMR analysis, is discussed elsewhere (Sections 2.4.4 and 2.2.5, respectively).

SRP and TDP were each analyzed in duplicate. When necessary, SRP measurements were repeated until the relative percent error was less than 2%. For TDP analyses, duplicate vials were processed and the P concentration for each vial was determined to within 2% error. Using these data, the relative percent error for TDP analysis of each of the soluble reservoirs was determined. For the CDB, acid, and base extracts, the relative percent error of TDP measurements was less than 2%. The relative percent error between duplicate TDP analyses of total lipid extracts was between 0 and 6%, with a mean error of 1.6%. The error for TDP measurement in the aqueous extracts was somewhat higher (0.5 to 20%; mean error = 9.6%) because the P concentrations were much lower, so small measurement error resulted in a high percent error.

The hydrolysis data presented in Section 2.4.3.2.1 were used to make a more rigorous assessment of the day-to-day reproducibility of P measurements. In most of the organic P standard solutions, there was no measurable hydrolysis (and therefore a constant SRP concentration) over a 60 day period. The range of SRP measured in these solutions was used to assess measurement reproducibility between sample runs. In all

solutions where hydrolysis was negligible, the standard deviation of P concentration over the 60 day time-course of the experiment (12 solutions measured, between 7 and 11 analyses per solution) was less than 0.1 μM P. The error estimated here is probably larger than the true variability of P concentrations measured in sediment extracts for the following reason. The solutions analyzed for the hydrolysis experiment had very low SRP concentrations, and the associated errors were undoubtedly larger than for the high-P-concentration sediment extracts. The P concentration values presented in this thesis are reported to the nearest 0.1 μM P. In addition, the full range of P concentration values measured in replicate analyses of each sample are indicated in both the Tables and Figures.

2.4 Sequential Extraction

A sequential extraction separates solid-phase chemical species on the basis of their solubility in a sequence of different solvents. In this study, a sequential extraction was developed to isolate reservoirs of organic P from marine sediments. Changes with depth in the concentration of P_{org} within these operationally defined reservoirs, indicated which reservoirs are most vulnerable to diagenetic mineralization, and changes in molecular structure were examined using ^{31}P -NMR. The objective of the sequential extraction was twofold: (i) to maximize solubilization of P for analysis by ^{31}P -NMR, and (ii) to separate P into biogeochemically meaningful reservoirs. In this section, the sequence of extractants is described and the rationale for each extraction step is discussed. A schematic of the sequential extraction procedure is shown in Figure 2-6. Detailed analytical protocols for each of the extractions can be found in Appendix A.

2.4.1 Definition Of Organic Reservoirs

Remineralization of organic matter in the water column and in sediments is extremely efficient, such that greater than 99% is ultimately degraded (e.g., Emerson & Hedges, 1988; Berner, 1989). The dominant form of organic matter preserved in sedimentary rocks is amorphous, insoluble organic matter referred to as kerogen. The “classical” pathway for formation of kerogen is by degradation of natural biopolymers (e.g., polysaccharides, proteins) into monomers and subsequent condensation of these monomers into “geopolymers” (Tissot & Welte, 1984). More recently, it has been suggested that at least some fraction of kerogen originates not from geopolymerization, but from selective preservation of intact, or slightly modified, biopolymers (Tegelaar *et al.*, 1989; De Leeuw & Largeau, 1993). In either case, the starting product is composed primarily of simple biochemicals and the residuum is a complex mixture of amorphous, insoluble macromolecules. The model for the laboratory separation of organic P described here was this early diagenetic transformation of organic matter from simple biochemicals to insoluble organic matter. The three main reservoirs of organic matter isolated were (i) simple biochemicals including water-soluble organic P compounds and phospholipids, isolated by extraction with water and organic solvents, (ii) humic compounds, thought to be a precursor in kerogen formation (Nissenbaum & Kaplan, 1972; Nissenbaum, 1974; Welte, 1974; Huc & Durand, 1977), which are isolated by extraction in aqueous alkali solution, and (iii) insoluble organic matter, or kerogen. Each of these reservoirs is described in greater detail below. Table 2-5 indicates the compounds targeted for isolation in each of these extraction steps.

2.4.1.1 Solvent Extraction Step (Extracts 1, 2): Simple Biochemicals

Organic matter in its primary form (i.e., biomass) is composed largely of structurally identifiable compounds, such as sugars, lipids and proteins. In organic rich

Table 2-5. Organic P reservoirs separated by the sequential extraction. Numbers refer to the fractions defined in the sequential extraction scheme in Figure 2-6.

#	<u>Reservoir</u>	<u>Target Compounds</u>	<u>Method of Analysis</u>
1	Water-Soluble P	Nucleic Acids Nucleotides Phosphosugars	P _{org} concentration
2	Chloroform-Extractable P	Phospholipids	Solution ³¹ P-NMR P _{org} concentration
6	Base-Extractable P	Humic-Associated P	Solution ³¹ P-NMR P _{org} concentration
	Insoluble Residue	Kerogen-Bound P	Solid state ³¹ P-NMR P _{org} concentration

sediments such as those used in this study, bacterial biomass can contribute substantial amounts of organic matter, particularly in surface sediments. Any examination of diagenetic trends in organic matter composition requires careful attention to the contribution to depth trends by intact biomass components. Here, the distinction between simple biochemicals derived from intact biomass and more complex, or humic, compounds is based on differences in chemical solubility. Solvent extraction prior to the base extraction diminished the overlap between primary biochemicals and humic compounds. This operationally-defined separation is not absolute, but it minimizes solubilization of compounds from fresh organic tissues during alkali extraction, which has long been a concern in studies of soil humic compounds (Stevenson, 1994). The contribution of biomass to the lipid-P and total-organic-P reservoirs is discussed in Chapter 3.

2.4.1.2 Base Extraction Steps (Extracts 3-6): Humic Compounds

The rationale for including the citrate dithionite bicarbonate (CDB), MgCl_2 , and 0.1 M HCl extractions as part of the full base extraction procedure is discussed in Section 2.4.3. It is unlikely that substantial quantities of organic P are solubilized in these extracts (# 3, 4, 5), because easily-solubilized organic matter is removed prior to these steps by the aqueous/organic solvent extraction. Further, Ruttenger (1990; 1992) showed that CDB extracts less P from fresh plankton than distilled water and Jensen and Thamdrup (1993) found that solutions of NaCl and NaOH solubilized significantly more P from pure cultures of blue-green algae (*Synecococcus sp.*) and diatoms (*Skeletonema costatum*) than was solubilized by a solution of bicarbonate dithionite. Measurements of P in acid extracts from central Santa Barbara Basin sediments indicate that at least 97% of the P extracted by 0.1 M HCl is inorganic (detected as SRP).

As defined in the soil literature (e.g., Hayes *et al.*, 1989; Stevenson, 1994), humic acids are compounds that are soluble in alkaline solution but insoluble at $\text{pH} < 2$. Fulvic acids are soluble in both acidic and basic solutions. Together, the humic acid and fulvic acid fractions are referred to simply as humic compounds. P bound to humic compounds accounts for most of the organic phosphorus in unconsolidated sediments and, similarly, humic compounds constitute a large fraction of the total organic matter (Baker, 1977; Nissenbaum, 1979). As defined here, humic compounds are insoluble in organic solvents, but soluble in an aqueous solution of 0.5 M NaOH.

2.4.1.3 Insoluble Residue: Kerogen

Operationally, kerogen is often defined as the fraction of organic matter that is insoluble in organic solvents and non-oxidizing acids. Kerogen is defined here, following the definition of Larter and Douglas (1980), as the fraction of organic matter that is insoluble both in organic solvents and aqueous alkali solution. The insoluble organic

matter isolated from unconsolidated sediments is generally referred to as “proto-kerogen” (Whelan & Thompson-Rizer, 1993), although the continuum of chemical and physical properties does not allow a clear dividing line to be drawn between proto-kerogen and kerogen (Whelan & Thompson-Rizer, 1993). As such, the simpler term kerogen will be used here to refer to the insoluble organic matter fraction in unconsolidated sediments. As discussed in Appendix C, the kerogen isolation procedure tested on Santa Barbara Basin sediments resulted in excessive loss of P. Therefore, no kerogen isolates were used in this study. Discussion of P in the insoluble fraction will include kerogen-associated P as well as any residual P associated with the mineral matrix.

2.4.2 Lipid Extraction Procedure

The first step in the sequential extraction solubilizes unbound polar lipids in organic solvents. The method used here is based on the Bligh and Dyer (1959) procedure, an accepted technique for isolation of lipids and other biochemicals from cell suspensions. The Bligh-Dyer solvent mixture is a single phase of water: methanol: chloroform (0.8:2:1) that efficiently extracts polar lipids, including phospholipids. Since polar lipids were the compounds of primary interest in this reservoir, the Bligh and Dyer procedure was chosen in lieu of other solvent extraction methods developed for studies of the non-polar lipid fractions. For this study, two major modifications were made to the Bligh-Dyer method. First, sediments were extracted by sonicating the sediment-solvent mixture in a centrifuge tube rather than by manual shaking in a separatory funnel. Exhaustive extraction was accomplished by successive treatments with fresh solvent until the extract was pale yellow in color. The second modification is the insertion of a single extraction with 2-propanol prior to extraction with the Bligh-Dyer solvent mixture. This extra step is intended to deactivate lipases, as suggested by the observations of Nichols *et al.* (1987) (also see Section 2.4.2.1), and thus prevents degradation of phospholipids during the extraction process.

Before extraction, sediments were freeze-dried, ground and sieved to $<125\ \mu\text{m}$. Dry sediment was weighed into 50 mL centrifuge tubes and 40 mL of 2-propanol was added to each sample. Sediments were suspended by stirring with a stainless steel spatula, then sonicated for 10 minutes using a Tekmar sonic disrupter probe. After sonication, samples were centrifuged for 10 minutes at $900 \times g$ and the supernatant was decanted into a 500 mL separatory funnel. Bligh and Dyer extractant (40 mL) was added to each sample and the sediment was resuspended, sonicated, and centrifuged as above. This procedure was repeated with fresh solvent until the extract was pale yellow in color (generally 5-7 extraction steps).

After the supernatants from all extraction steps (including the initial extraction with 2-propanol) were combined in the separatory funnel, the mixture was partitioned into solvent and aqueous phases by addition of chloroform and water to form a final ratio of water:propanol/methanol:chloroform (1.8:2:2). The mixture was shaken and the solvent and aqueous layers were allowed to separate overnight (~10 hours). Inorganic P and other water-soluble compounds partition into the aqueous phase, while phospholipids partition into the chloroform phase. To achieve complete partitioning, the upper (aqueous) layer was rinsed consecutively with three 20 mL aliquots of chloroform and the lower (chloroform) layer was back-extracted with 3 consecutive rinses of milli-Q H_2O . These rinses were combined with the chloroform and aqueous extracts, respectively, before they were concentrated.

Organic solvent- and water-soluble compounds are often separated using a Folch extraction (Folch *et al.*, 1957), a procedure identical to that described above except that a solution of 0.88% KCl in water is used instead of pure water. The Folch procedure was not used in this study, largely due to concerns about NMR analysis of concentrated aqueous extracts with very high salt concentrations. However, the concentration of P in all aqueous extracts was too low for NMR analysis. Based on the partitioning of P compounds between organic and aqueous phases tested here, water alone was effective in

ensuring separation of phospholipids from other P biochemicals. However, in future work, it is recommended that the Folch extraction be adopted to allow a more straightforward comparison with the aqueous and chloroform extracts isolated in other studies.

The chloroform extract was concentrated to a volume of a few mL using a rotary evaporator, filtered through a 0.45 μ m PTFE filter, and brought to a final volume of 10 mL. An aliquot was removed for analysis of total P. SRP concentration was not determined for this fraction because orthophosphate is efficiently partitioned from the lipid phase (see Section 2.4.2.2). The remaining lipid sample was evaporated to dryness under a stream of nitrogen, then dissolved in 4 mL CDCl₃ for ³¹P-NMR analysis. The P concentration of individual lipid extracts was generally too low for detection by ³¹P-NMR, and extracts from adjacent intervals were often pooled for NMR analysis. Lipid extracts were stored in a -30°C freezer for 1-2 weeks during TDP analysis and preparation for ³¹P-NMR. If stored longer, samples were kept in a dewar with LN₂ to minimize degradation.

The aqueous extract was concentrated for 2 hours on rotary evaporator, then frozen and lyophilized. The dried extract was rehydrated in a small volume of milli-Q H₂O, filtered through a 0.4 μ m polycarbonate membrane filter, and brought to a final volume of 10 mL with milli-Q H₂O. Solids retained on the filter were returned to the bulk sediment and therefore included in subsequent extraction steps. The solvent-extracted residue was freeze-dried and then lightly crushed with a mortar and pestle. A split was retained for elemental analysis, and the remainder was transferred to a polypropylene bottle in preparation for base extraction (Section 2.4.3).

2.4.2.1 Lipid Extraction Protocol Tests

Two modifications to the lipid extraction protocol of Bligh and Dyer, intended to minimize artifacts during lipid preparation, were tested: (i) inserting a 2-propanol

extraction before extraction with the prescribed Bligh-Dyer solvent mixture, and (ii) replacing milli-Q H₂O in the Bligh-Dyer solvent mixture with a 50 mM phosphate buffer. For both of the tests, duplicate sediment samples were solvent extracted under each set of extraction conditions. The lipid extracts were compared, and degradation of phospholipids was inferred from increased concentrations of free fatty acids and decreased concentrations of polar lipids.

One quarter of each total lipid extract was separated into fractions by column chromatography. Samples were loaded onto a column of 5% deactivated silica gel (100-200 mesh) and fractions were eluted sequentially with (1) chloroform ("neutral lipids"), (2) acetone ("glycolipids"), and (3) methanol ("polar lipids"). Free fatty acids were quantified by GC analysis of fraction 1. Polar lipids were transesterified with acidic methanol to form fatty acid methyl esters (FAMES), and analyzed by GC. Prior to injection on the GC column, all samples were silylated and a C₂₁ fatty acid was added as a quantification standard.

White *et al.* (1979c) proposed a modification of the Bligh and Dyer method wherein a 50 mM phosphate buffer is used in place of water in the extraction mixture. The rationale for this modification is that an excess of available orthophosphate deactivates phospholipases and thus hinders degradation during extraction and storage of lipid extracts. For this study, it was not possible to adopt this modification because addition of P at a concentration several orders of magnitude higher than natural sediment concentrations would preclude P quantification in the remaining reservoirs. However, we evaluated whether addition of a P buffer to the extractant affected degradation and recovery of polar lipids. The concentration of free fatty acids in samples extracted with P buffer (152 ng/g sediment) was slightly higher than the concentration in samples prepared without P buffer (140±2 ng/g sediment), indicating that cleaving of fatty acids from lipids was not elevated in non-P buffer samples. Similarly, the concentration of FAMES derived from polar lipids was not markedly different in P buffer (155 ng/g sediment) and

non-P buffer samples (148 ± 1 ng/g sediment). Based on these data, we believe that foregoing the use of P buffer in the solvent extractant did not result in phospholipid degradation.

Based on empirical observations, it has been suggested that by pre-extracting sediments with 2-propanol before extraction with the Bligh-Dyer solvent mixture, lysing of phospholipids is reduced (Nichols *et al.*, 1987). The free fatty acid concentration of lipid extracts prepared only with the Bligh-Dyer solvent mixture (160 ± 16 ng/g sediment) was twice as high as in samples that were first extracted with 2-propanol (80 ± 4 ng/g sediment). The increased abundance of free fatty acids does not demonstrate unequivocally that phospholipid degradation is enhanced in the samples prepared without 2-propanol. Alternatively, the increased free fatty acid concentrations could indicate lysing of fatty acids from non-P-containing lipids, or an increased efficiency in extraction of free fatty acids from the sediments. However, the 2-propanol treatment was a simple modification requiring little additional extraction time. To minimize the potential for phospholipid degradation, the extraction with 2-propanol was inserted as part of the standard protocol used in this study (Figure 2-6).

2.4.2.2 Partitioning Experiment

By manipulating the proportions of water, methanol, and chloroform, lipids and water-soluble P compounds were partitioned into two phases. We tested the efficiency of this separation using commercially available standards representative of a variety of P compound classes (nucleic acids, phosphosugars, inorganic P, polyphosphates, phosphonates, and phospholipids). For each test, the compound was dissolved in Bligh-Dyer solvent extract at a P concentration of $17.5 \mu\text{M}$. The extract was then partitioned into aqueous and solvent phases by adding chloroform and water to achieve a final ratio of water:methanol:chloroform (1.8:2:2). The layers were allowed to separate overnight and then each layer was back-extracted as described previously to assure complete

separation of the compounds. Without these rinses, partitioning of inorganic P was not complete (87% in the aqueous phase, 13% in the chloroform phase). The extracts were concentrated and the total volume of each extract was brought up to 10 mL in a volumetric flask. Two 0.5 mL aliquots of each extract were added to 20mL borosilicate vials for TDP analysis. The amount of P in each phase was calculated as a percentage of total P (Table 2-6). Inorganic phosphate species (orthophosphate and polyphosphate) as well as nucleic acids, nucleotides, simple phosphonates, and phosphosugars are partitioned into the aqueous phase, while phospholipids are partitioned into the chloroform phase.

Table 2-6. Partitioning of compounds between solvent and aqueous phases following lipid extraction.

Compound Class	Compound Tested	% P in Chloroform Phase	% P in Aqueous Phase
Inorganic P	Orthophosphate	2.6	97.4
	Tripolyphosphate	1.0	99.0
Nucleic Acid	DNA	0.2	99.8
Nucleotide	ATP	1.3	98.7
Phosphonate	2-aminoethylphosphonic acid	2.6	97.4
Phosphosugar	Glucose-6-phosphate	0.5	99.5
Phospholipid	Phosphatidyl Choline	99.5	0.5

2.4.3 Base Extraction Procedure

The base extraction procedure was designed to maximize solubilization of P_{org} while minimizing structural alteration. To optimize the procedure for maximum extraction efficiency and to achieve the best ^{31}P -NMR results, several modifications of the method were tested. The finalized procedure is shown in Figure 2-6. Details of the procedure and the method tests are described below.

2.4.3.1 Filtration of Extracts

Tests with organic-rich sediments from Peru Margin sediments demonstrated that during base extraction, large losses of P occurred due to trapping of particles on filters. Modifications were made to minimize this loss. For all steps of the base extraction (CDB, MgCl_2 , HCl, NaOH), a single filtration setup was used, consisting of a 10 μm polypropylene “pre-filter” in line with a 0.45 μm GH Polypro filter, which is composed of polypropylene treated to render it hydrophilic. These filters were chosen based on their resistance to the chemicals used in all steps of the base extraction, low P blank, and their “flat” membrane design, allowing maximum recovery of sediment from the filter surface. Following each extraction, samples were centrifuged (10 minutes, 2000 x g), then filtered under a vacuum pressure of 12 psi. When the entire extract had been filtered, the filter was transferred to a small plastic beaker and suspended in the extractant to be used in the next step (e.g., suspended in MgCl_2 following CDB filtration). The filter was gently scraped to suspend the particles, and this slurry was returned to the sample. The volume was then adjusted to give the final solid:solution ratio used for that extractant. By following this procedure, the entire sediment sample was extracted during each step. Filtration units were rinsed with milli-Q H_2O after each extractant to minimize carryover of the supernatant. When all extraction steps were complete, the filters were scraped and then sonicated in a small volume (~10 mL) of milli-Q H_2O . Recovered particles were

added to the sediment residue before lyophilization. Filters were analyzed for total P to quantify loss.

2.4.3.2 The Iron Problem: Minimizing Paramagnetic Effects on NMR Spectra

In this study, most of the organic matter solubilized is in the base-extractable fraction. Therefore, it is crucial to maximize the structural information obtained from this reservoir. The surface sediments of the Santa Barbara Basin have very high iron content (3% by weight: Schmidt & Reimers, 1991). Paramagnetic metals such as Fe and Mn in NMR samples cause line broadening and reduced signal to noise, affecting peak width and visibility (Vassallo *et al.*, 1987; Hutson *et al.*, 1992). These problems arise both as a result of interaction of unpaired electrons with the magnetic field (causing line broadening) and due to abbreviated relaxation times (shortened such that they are not detected during data acquisition). For analysis of extracts from these sediments, several approaches were tested to either remove iron or to suppress its interference during ^{31}P -NMR analysis: (i) base extracts were treated with a chelating resin prior to NMR analysis, (ii) EDTA was added to the base extractant, and (iii) sediments were extracted with citrate dithionite bicarbonate (CDB) prior to base extraction. Each of these approaches is described below. The most effective method of iron treatment was extraction with CDB before base extraction.

2.4.3.2.1 Chelex

Chelating resins such as ChelexTM 100 (Sigma) have been used both to enhance extraction of organic matter and to reduce the metal content of solutions prior to NMR analysis (e.g., Gressel *et al.*, 1996). The weakly acidic Chelex resin contains iminodiacetate groups that bind polyvalent cations, effectively scavenging them from solution. To evaluate the effectiveness of this Fe removal method, a base extract was

analyzed by ^{31}P -NMR before and after Chelex treatment. The sample was not pre-concentrated as described in the standard protocol (Appendix B). Therefore, due to low P concentration and paramagnetic effects, only the dominant orthophosphate peak was detected by ^{31}P -NMR analysis of the untreated sample. No direct test was made to measure the efficiency of iron removal by the Chelex resin. However, no P was detected by ^{31}P -NMR analysis of the Chelex-treated sample, indicating that orthophosphate had been stripped from the sample. Based on this loss of P from the sample, Chelex treatment was deemed inappropriate for Fe removal from extracts. The mechanism for this P loss may be metal bridging between the resin and organic P or inorganic P, or direct sorption of P-containing organic compounds to the resin.

2.4.3.2.2 EDTA

The amount of P solubilized by base extraction was increased by adding ethylenediaminetetraacetic acid (EDTA) to the alkaline solution, with maximum P recovery obtained using 0.01 M EDTA (Figure 2-7). Further, it has been suggested that EDTA, by chelating paramagnetic cations, suppresses their undesirable effect on NMR spectra (Hupfer *et al.*, 1995b). However, there are several problems with adding EDTA to the base extractant. First, the considerable amounts of added C and N preclude determination of C:N:P ratios in the base extractable reservoir. Second, precipitation of EDTA during SRP analyses, presumably due to its lower solubility in acidic solution, resulted in erroneous measured phosphate concentrations (described in Section 2.4.3.6). Finally, a comparison of ^{31}P -NMR spectra from samples prepared using EDTA in the base extractant and samples pre-treated with CDB clearly demonstrates that CDB is a more effective approach. This comparison was based on a ^{31}P -NMR analysis of identical sediment samples prepared two ways: (i) sediments treated with CDB before base extraction, (ii) no CDB treatment, but 0.01 M EDTA added to the base extractant to suppress the iron paramagnetic problem. The spectra obtained for these two samples are

shown in Figure 2-8. The CDB treated sample gives a far superior spectrum, with much higher signal-to-noise ratio and less peak-broadening.

2.4.3.2.3 Citrate Dithionite Bicarbonate (CDB)

Extracting sediments with a solution of citrate dithionite bicarbonate (CDB) is an effective method of solubilizing easily reducible or reactive Fe, and liberating the associated P (Ruttenberg, 1992). The dithionite reduces Fe^{3+} in the sediments, and citrate chelates the iron so that it remains in solution. Following the procedure of Ruttenberg (1992), a solid:solution ratio of 1g:100 mL was used. Dithionite was added to the dry sediment, then a solution of sodium citrate and sodium bicarbonate, adjusted to pH 7.6, was added. After venting the evolved gas, samples were shaken for 8 hours at 250 rpm. Following extraction, samples were centrifuged at $2000 \times g$ for 10 minutes, then filtered as described above.

2.4.3.3 MgCl_2

Extraction with 1M MgCl_2 acts as a “rinse”, removing residual CDB and iron from the previous step. In addition, P that was reversibly adsorbed to the sediment matrix after solubilization by CDB is effectively extracted, driven by formation of the stable MgPO_4^- complex and/or by mass action displacement of PO_4^{3-} by Cl^- (Ruttenberg, 1992). MgCl_2 was added in a solid:solution ratio of 1 g:50 mL, shaken for 2 hours, then centrifuged and filtered as above.

2.4.3.4 HCl

Many of the humic compounds in soils are insoluble as a result of complexes formed with Ca and other cations, primarily by exchange with carboxylic acids and other

acidic groups (Hayes *et al.*, 1989). Leaching soils with dilute HCl prior to alkaline extraction breaks up these salts and results in more efficient extraction of organic matter. The standard base extraction protocol used in this study included pre-extraction of sediments with 0.1 N HCl at a solid:solution ratio of 1 g:13.3 mL. Samples were shaken for 1 hour at 250 rpm and then centrifuged and filtered as above.

Our empirical observations demonstrate that solubilization of both organic and inorganic P in base was enhanced when sediments were first extracted with acid (Figure 2-9). While acid pre-treatment is part of the approved extraction method of the International Humic Substances Society, alteration of the chemical structure of P_{org} (e.g., by acid hydrolysis), was still a concern. Analysis of organic P standards in a solution of 0.1 M HCl indicates that even reactive biochemical intermediates are hydrolyzed less than 5% during the one hour interval used for this extraction (Monaghan & Ruttenberg, 1999). Nonetheless, a comparison of ^{31}P -NMR spectra was used to confirm that hydrolysis did not alter P_{org} structure. Acid-treated sediment extracts were prepared in duplicate by extracting 15 g of solvent-extracted sediment according to the procedure described in Appendix B. For untreated samples, duplicate samples of 15 g solvent-extracted Santa Barbara Basin surface sediment were extracted with CDB and MgCl_2 , then immediately base extracted (omitting only the acid-pre-extraction step). Surface sediments were used for this test because they presumably contain the freshest, and thus the most potentially acid-labile, organic matter.

Figure 2-10 shows ^{31}P -NMR spectra for acid treated and untreated samples. The spectra have been scaled so that the large monoester peaks are roughly the same size, allowing all peaks to be visually compared. None of the peaks detected in the untreated sample are absent in the acid treated sample. For each functional group, the amount of P extracted in the acid-treated sample is greater, although the extent of this increase ranges from 38% to almost 400% , as shown in Table 2-7. Based on these results, there is no compelling reason to omit the acid step. The most compelling reason to include this step

is that by including acid treatment, the total P solubilized is increased by 61% and total P in the first extraction step is increased by 186%. Maximum solubilization is desired because the only tool available for analysis of the sediment residue is solid state ^{31}P -NMR, with considerably diminished resolution compared to solution NMR. The enhanced extraction of P in the first base extraction step is particularly crucial because it is the only extract analyzed by ^{31}P -NMR, as discussed below (Section 2.4.3.5.1).

Adams and Byrne (1989) noted a relative increase in the amount of orthophosphate extracted compared to monoester and diester P when acid pre-extraction was used, and cited this increase as evidence for hydrolysis. The results presented here (Figure 2-9) demonstrate that extraction of both organic and inorganic P is enhanced in acid-treated samples, although the effect is more pronounced for orthophosphate (Table 2-7). This explains the increase in relative abundance of orthophosphate without the need to invoke hydrolysis as an explanation. Additionally, the hydrolysis experiments of Monaghan and Ruttenberg (1999) indicate that little hydrolysis of organic P takes place during the limited acid exposure (1 hour) used in our procedure.

Finally, solubilization of P_{org} in the acid extract, even without hydrolysis, would effectively remove it from the pool analyzed by ^{31}P -NMR. Our data show that at least 97% of the P extracted by 0.1 M HCl is inorganic (detected as SRP). The errors

Table 2-7. Comparison of P extracted with and without pre-extraction of samples with dilute acid. The extent to which extraction is enhanced differs for each functional group, but in all cases more P is extracted after acid pre-treatment.

	Phosphonate	Orthophosphate	Monoester	Diester	Polyphosphate
Untreated	1.1 ± 0.2	3.8 ± 0.6	5.2 ± 0.8	0.7 ± 0.1	0.3 ± 0.04
Acid treated	1.5 ± 0.2	19 ± 2.9	8.4 ± 1.2	2.1 ± 0.3	1.0 ± 0.1
% increase	36	396	63	222	250

associated with the difference method do not allow a reliable determination of organic P in this extract. However, based on a maximum estimate of 3% organic P, the acid extract could contain at most only 1 to 9% of the total P measured in the base extracts. Even if this amount of P_{org} was lost from the base extract due to acid treatment, it still does not equal the amount of P_{org} gained by the increased extraction efficiency in acid-treated samples.

2.4.3.5 NaOH Extraction

Sediments were extracted with 0.5 M NaOH at a solid:solution ratio of 1 g:6.67 mL to solubilize humic substances. Immediately prior to extraction, the base solution was sparged with N_2 to remove oxygen and thus prevent formation of peroxides and hydroxyl radicals that attack organic matter (P. Hatcher, personal communication). All extractions were performed at room temperature, and samples were extracted and stored in polypropylene bottles to avoid etching of silica from glass vessels. After the base solution was added, the headspace of each sample bottle was flushed with N_2 . The bottles were sealed and shaken for 12 hours at 250 rpm, then centrifuged for 10 minutes at 2000 x g, filtered (as described above), and brought to a known volume with milli-Q H_2O . An aliquot of the extract was removed for elemental analysis, and the remaining extract was concentrated by lyophilization, then dissolved to a final volume of 4 mL (1 mL D_2O , 1 mL 2M NaOH, 2 mL mQ- H_2O) for ^{31}P -NMR analysis. The extraction process was repeated for a total of five base extraction steps. Extracts 2 through 5 were each brought to a known volume with milli-Q H_2O and stored refrigerated until elemental analyses were completed (generally 1-6 weeks), then stored in a -30°C freezer.

When all extractions were complete, the sediment residue was transferred quantitatively to a 50 mL centrifuge tube. The solid residue from the filters was added to each sample as described previously, and the samples were lyophilized. After freeze-

drying, the base extracted residue was lightly crushed with a mortar and pestle, then transferred to a vial and stored for elemental analyses and solid state ^{31}P -NMR analysis.

2.4.3.5.1 *Solid:Solution Ratio*

The efficiency of an extraction is dependent upon the choice of solid:solution ratio. In particular, a high solid:solution ratio can result in incomplete dissolution of a target phase (e.g., Ruttenberg, 1990; Ruttenberg, 1992). Ideally, complete dissolution of humic substances could be achieved in a single extraction step. However, it was important to consider P concentration and total volume when preparing base extracts. The quantity of dissolved solids limits the amount of extract that can be concentrated into the small volume used for ^{31}P -NMR analysis. In practice, 100 mL of 0.5 M NaOH extract can be concentrated to the 4 mL final sample volume. To maintain a constant solid:solution ratio, this 100 mL volume was used for the largest sediment samples extracted in this study (15g), to give a ratio of 1:6.7 (g/mL). Comparable ratios of 1:2 to 1:5 are often used for extracting humic substances from soils (Stevenson, 1994). For comparison, a solid:solution ratio of 1:100 is used in the SEDEX method (Ruttenberg, 1990; Ruttenberg, 1992), a highly standardized method for sequential extraction of sedimentary P. To insure that extraction of base-soluble P was exhaustive, successive base extraction steps were performed for each sample. The number of extraction steps needed was determined by measuring P in each extract.

The amount of P recovered decreases with each successive extraction step (Figure 2-11). Beyond extraction step 5, a negligible amount of P is extracted. Therefore, 5 extraction steps are included in the standard base extraction procedure (Appendix B). Analysis by ^{31}P -NMR requires high P concentration. Therefore, only extract 1 is analyzed for each sample. The structural composition of extracts 1 (66% of total extractable P) and 2 (17% of total extractable P) were compared to determine whether structurally distinct organic P was extracted in successive steps (Figure 2-12). Visually, there are no clear

differences in the spectra other than the lower signal to noise ratio of extract 2, due to lower P concentration. To examine these data more quantitatively, the relative amount of each organic P functional group was determined by integration of peak areas. Table 2-8 shows the percentage of the total organic P attributed to phosphonates, monoesters and diesters. The relative abundance of these three functional groups does not differ between the two extracts. The small increase in concentration gained by pooling extracts 1 and 2 is not sufficient to offset the accompanying problems in sample handling (e.g., higher salt content), and there is no indication that any bias in structural analysis occurs as a result of analyzing extract 1 alone. It is not feasible to structurally analyze the remaining 17% of total extractable P contained in extracts 3-5 using ^{31}P -NMR. Therefore, only extract 1 was used for all ^{31}P -NMR analyses in this study.

Table 2-8. Relative abundance of organic P functional groups solubilized by repeated extraction of a sediment sample with 0.5 M NaOH. Percentages were determined by ^{31}P -NMR, based on peak areas within the characteristic chemical shift region of each functional group.

	% of total organic P signal		
	Phosphonate	Monoester	Diester
Extract 1	12	70	18
Extract 2	14	67	19

2.4.3.6 Separation Of Humic And Fulvic Acids

The operationally-defined separation of fulvic acids (FA) and humic acids (HA) was achieved by acidification of the base extract, thus precipitating the HA fraction (e.g., Stevenson, 1994). To quantify SRP, an aliquot of base extract was transferred to a 50 mL centrifuge tube, 1 M HCl was added to adjust the solution to pH 1, and the solution was brought to a final volume of 50 mL by adding 0.1 M HCl. The extracts were then

centrifuged for 10 min at 3500 rpm and filtered through a 0.4 μm GH Polypro syringe filter.

For SRP analysis of extracts prepared with EDTA (Core SBB9610 J), HA/FA separation and SRP determination was completed within 1 day. After filtration, additional precipitation occurred if extracts were allowed to stand for more than a few hours (i.e., overnight). The white precipitate was presumably excess EDTA insoluble in the acidic solution. Once this additional precipitation occurred, samples had to be re-filtered before analysis or particulates result in erroneously high absorbance readings. However, this additional filtration resulted in artificially low SRP numbers because P was sequestered in the solid material. Organic P concentrations calculated based on these low SRP numbers were clearly in error as a result. By expediting the handling of FA extracts, this problem was eliminated. No such separation difficulty was encountered for base extracts that did not contain EDTA (Cores SB11/95 A and SB11/95 C).

2.4.3.6.1 Modification for Analysis of Isolated Humic Acids

For selected samples, separated humic acids were analyzed by ^{31}P -NMR, and P concentration in the humic acids was determined independently (rather than as the difference between TDP in FA and the total base extract). In Santa Barbara Basin sediments, the fulvic acids generally contain 4-5 times as much total P as the humic acid fraction. Therefore, it was important to avoid contamination of the HA with residual solution. Samples were acidified and centrifuged as above, then filtered through a 0.4 μm polycarbonate membrane filter assembled in a Swinnex holder so that solids trapped on the filter could be recovered. The HA pellet was then successively resuspended and centrifuged with three 5 mL aliquots of 0.1 M HCl. These rinses were filtered and combined with the FA extract. The pelleted material and the material trapped on the filter were pooled to yield the purified HA sample.

2.4.3.7 The Origin Of Orthophosphate In The Base Extractable Reservoir

Orthophosphate is the most abundant P species in all of the base extracts analyzed for this study. Hydrolysis of ester linkages in alkaline solution has been suggested as the source of much of the orthophosphate detected in base extracts from soils and sediments (Newman & Tate, 1980; Tate & Newman, 1982; Hawkes *et al.*, 1984; Ingall *et al.*, 1990). A hydrolysis experiment performed to determine the extent of degradation of organic P compounds during solubilization and long-term storage in the base solution used for humic extraction (0.5 N NaOH) indicated that no significant hydrolysis occurred (discussed below). Thus, we postulate that the orthophosphate found in base extracts is actually bound to macromolecular humic compounds (e.g., by metal bridges), a mechanism for immobilization of orthophosphate that has been widely described in the soil science and limnological literature (e.g., Levesque & Schnitzer, 1967; Koenings & Hooper, 1976; Francko & Heath, 1982; Gerke, 1992; Jones *et al.*, 1993; Frossard *et al.*, 1995).

2.4.3.7.1 Base Hydrolysis Experiment

Hydrolysis of P compounds in a solution of 0.5 M NaOH was monitored by measuring the accumulation of soluble reactive P (SRP) in the solution during a 2 month time course. Like the acid hydrolysis experiment described previously, this experiment was modeled after the study of Monaghan and Ruttenberg (1999). SRP data were supplemented by analyses of standard solutions using ^{31}P -NMR, a more direct method for evaluating changes in P structure in alkaline solution.

Standards representing a range of P compound classes were dissolved in 0.5 M NaOH to a concentration of *ca.* 100 μM P. TDP in each solution was calculated based on information provided by the vendor, and TDP was also measured directly using the procedure described in Section 2.3.3. SRP measured by the phosphomolybdate method of

Koroleff (1976) necessitates acidification of samples to pH 1. Thus, hydrolysis measured by quantifying liberated SRP is a maximum estimate, incorporating both acid and alkaline hydrolysis. To minimize the extent of acid hydrolysis, samples were acidified immediately prior to SRP determination.

SRP was measured on a split of each sample immediately after it was brought into solution. Base solutions were stored refrigerated and splits were taken at subsequent intervals (days to months) for SRP analysis. Table 2-9 shows the concentration of SRP measured immediately upon solubilization and after 60-70 days of storage. SRP measured in each solution over the full time course of the experiment is shown in Figures 2-13, 2-14a, 2-15a, and 2-16a. Even after 60-70 days of storage, most compounds were hydrolyzed by less than a few percent (Table 2-9, Figure 2-13). As mentioned above, the SRP data collected for this test are maximum estimates in that they include hydrolysis by three processes: (i) base hydrolysis, (ii) (acid) hydrolysis during pH adjustment, and (iii) (acid) hydrolysis by the color development reagents.

Limited hydrolysis of P_{org} compounds under acidic conditions is expected (Monaghan & Ruttenberg, 1999). Glucose-6-phosphate and phosphocreatine were the only compounds tested for which the SRP results indicate substantial hydrolysis (Table 2-9). For these compounds, ^{31}P -NMR was used to evaluate the extent of base hydrolysis alone.

Liberated SRP in the glucose-6-phosphate solution increased steadily over the time course of the experiment (Figure 2-14a), with 63% of total P measurable as SRP by day 69. The apparent decrease in hydrolysis rate indicated by the change in slope in Figure 2-14a is likely due to the decreased rate of hydrolysis once the sample was refrigerated. The initial measurement of less than 1 μM SRP indicates that acidification and reagent effects are not important in the observed hydrolysis of this compound. The ^{31}P -NMR data support the assertion that base hydrolysis alone causes the observed increase in SRP. Figure 2-14b and c show, respectively, the ^{31}P -NMR spectra of

Table 2-9. Results of the base hydrolysis experiment. The only compound that shows substantial accumulation of SRP is glucose-6-phosphate, and only after prolonged storage under alkaline conditions. Although high SRP concentrations were measured in the phosphocreatine solution, ³¹P-NMR data indicate that there is no alkaline hydrolysis of phosphocreatine (see text).

Compound	Total P * (μM)	Initial Hydrolysis		After refrigerated (4°C) storage for 60-70 days	
		[SRP (μM)]	% hydrolyzed	[SRP] (μM)	% hydrolyzed
<u>Inositol</u>					
phytic acid	106.0	2.1 ± 0.0	2.0	2.2 ± 0.0	2.1
<u>Nucleic Acid</u>					
ribonucleic acid	100.9	0.2 ± 0.0	0.2	1.4 ± 0.1	1.4
<u>Nucleotide</u>					
adenosine-5'-monophosphate	101.4	0.0 ± 0.0	0.0	0.4 ± 0.0	0.4
adenosine-5'-diphosphate	98.9	0.2 ± 0.0	0.2	0.4 ± 0.0	0.4
adenosine-5'-triphosphate	102.3	0.8 ± 0.0	0.8	1.0 ± 0.1	1.0
cytosine-5'-monophosphate	101.1	0.0 ± 0.0	0.0	0.4 ± 0.0	0.4
cytosine-5'-diphosphate	102.6	1.2 ± 0.0	1.1	1.2 ± 0.0	1.2
cytosine-5'-triphosphate	101.2	1.2 ± 0.0	1.2	1.2 ± 0.0	1.2
<u>Phosphonate</u>					
2-aminoethylphosphonic acid	99.1	0.2 ± 0.0	0.2	0.2 ± 0.0	0.2
<u>Phosphoprotein</u>					
phosphoserine	100.4	2.6 ± 0.0	2.6	2.8 ± 0.0	2.8
<u>Phosphosugar</u>					
glucose-6-phosphate	98.5	0.7 ± 0.1	0.7	61.8 ± 1.1	62.7
<u>Polyphosphate</u>					
tripolyphosphate	131.6	1.9 ± 0.3	1.5	1.8 ± 0.1	1.4
pyrophosphate	97.9	0.6 ± 0.1	0.6	0.4 ± 0.0	0.4
polyphosphate (n=25)	84.4	2.4 ± 0.0	2.9	2.8 ± 0.1	3.4
<u>Reactive Biochemical Intermediates</u>					
phospho(enol)pyruvate	100.6	0.9 ± 0.0	0.9	0.9 ± 0.0	0.9
phosphocreatine	99.2	52.2 ± 1.1	52.6	39.4 ± 0.4	39.7

* Total P was measured by the modified Aspila method described in Section 2.3.3.

glucose-6-phosphate in 0.5 M NaOH measured immediately upon solubilization and after 165 days of storage. Initially, there was no measurable orthophosphate. After 165 days of hydrolysis, there was a prominent orthophosphate peak and the remaining sugar phosphate was a complex mixture of structures, as indicated by the peaks centered between 4.8 and 5.4 ppm.

The SRP data indicate that phosphocreatine hydrolysis was immediate, with 52% of total P measured as SRP within the two hours elapsed between solubilization and measurement (Figure 2-15a). Unlike the data for glucose-6-phosphate, SRP was high (40-80% of total P) at each time point, and did not increase systematically with time. The fact that no increase in hydrolysis was observed even after two months of storage suggests that base hydrolysis was not responsible for the observed degradation. The SRP data are consistent with acid hydrolysis of phosphocreatine, which was also observed by Monaghan and Ruttenberg (1999). However, to insure that base hydrolysis was not simply masked by the extensive acid hydrolysis during SRP measurement, we analyzed a base solution of phosphocreatine by ^{31}P -NMR (Figure 2-15b, c). If hydrolysis occurred under alkaline conditions, there would be an orthophosphate peak at ~ 6 ppm in addition to the peak at -1.3 ppm. No orthophosphate peak is observed, either at the initial time point or after 165 days of storage, indicating that the measured liberation of SRP was entirely a result of acid hydrolysis. Finally, ^{31}P -NMR reveals a detail of hydrolysis that is not apparent from the SRP data alone. Measurement of SRP in the RNA standard solution indicates less than 1.5% hydrolysis after 60 days of storage (Figure 2-16a). However, RNA is not unaffected by base treatment. As shown in Figure 2-16b, P in the RNA solution exists largely as monoesters with a range of chemical shifts consistent with individual nucleotides, indicated by the shaded bar. The RNA standard was run with a capillary insert of H_3PO_4 as a chemical shift reference, concealing peaks in the diester region (2 to -3 ppm). However, integration of peak areas indicates that approximately half of the total P is detected in the monoester region. Thus, although the nucleotides are

quite stable to base hydrolysis (Table 2-9), much of the RNA present in alkaline solution is immediately (within a few hours) dissociated into its constituent nucleotides. Other standard compounds were analyzed during ^{31}P -NMR trials (see Table 2-2), but no hydrolysis effect was observed for any other compound.

To summarize the hydrolysis data, negligible hydrolysis to orthophosphate was observed for all compounds other than glucose-6-phosphate. RNA in alkaline solution is degraded into its constituent nucleotides, as demonstrated by ^{31}P -NMR data. Phosphocreatine degradation by base hydrolysis could not be distinguished from acid hydrolysis using SRP data, but ^{31}P -NMR revealed that phosphocreatine is stable under alkaline conditions. Based on these data, it is unlikely that the orthophosphate observed in the base spectra was a result of alkaline hydrolysis of organic P compounds. Glucose-6-phosphate alone liberated considerable SRP during two months of storage, but this compound is expected to be a minor P constituent in biomass (Neidhardt, 1987), and thus in sediments.

2.4.3.8 Evidence for Metal Binding of Orthophosphate in the Humic Extract

Lacking any evidence for significant hydrolysis of P_{org} in 0.5 M NaOH, an alternative explanation is needed for the high concentration of orthophosphate in the base extracts. A plausible explanation is that orthophosphate is bound to the humic compounds in these extracts through metal bridging. It is well known that humic substances contain substantial concentrations of metals (Nissenbaum & Swaine, 1976) and that metals can scavenge phosphate. Several lines of evidence suggest that metal binding may be responsible for the abundance of orthophosphate in the base-extractable fraction.

As described in Section 2.3, organic P is determined operationally as the difference between inorganic and total P. A comparison of the relative proportions of inorganic and organic P determined by ^{31}P -NMR and the wet chemical difference method reveals a discrepancy in the results (Table 2-10). In the surface sediments of the central

basin, results obtained using these two methods agree quite well. In deeper sediments, the values obtained by the wet chemical method and ^{31}P -NMR analyses are strikingly different. While the wet chemical method suggests that only 40% of total P is inorganic, ^{31}P -NMR reveals that 75% of total P can be attributed to orthophosphate and polyphosphates. The fact that the methods are in agreement for central basin surface sediments suggests that some process alters the association of P, increasing the fraction of the inorganic P that is not accessible to wet chemical analysis as diagenesis progresses.

Table 2-10. A comparison of inorganic and organic P in base extracts from core SBB9610 J, determined by ^{31}P -NMR and wet chemical analyses. The NMR inorganic and organic values represent, respectively, the sum of orthophosphate and polyphosphate peaks, and the sum of the phosphonate, monoester, and diester peaks. Errors reported for wet chemical analysis indicate the range of concentrations determined in duplicate analyses. Errors reported for ^{31}P -NMR indicate the 15% estimated uncertainty in functional group quantification by this method (Section 2.2.5).

	Inorganic P ($\mu\text{mol /g sediment}$)	Organic P ($\mu\text{mol /g sediment}$)
SBB9610 Core J		
Surface (0-0.3 cm)		
^{31}P -NMR	32.9 ± 4.9 (70%)	14.0 ± 2.1 (30%)
Wet Chemical Analysis	34.0 ± 0.1 (72%)	12.9 ± 0.4 (28%)
Deep (38-40 cm)		
^{31}P -NMR	4.9 ± 0.7 (75%)	1.6 ± 0.24 (25%)
Wet Chemical Analysis	2.6 ± 0.2 (40%)	3.9 ± 1.15 (60%)

Examination of the humic acid fraction of the base extracts by ^{31}P -NMR provides further evidence for diagenetic accumulation of orthophosphate in a fraction that is inaccessible to wet chemical detection. Based on the accepted operational definition, humic acids are precipitated when the base extract is acidified. Inorganic P determined by the wet chemical method includes only P soluble in acid. Consequently, all P in the

humic acid fraction is by definition organic. This operational definition does not always accurately reflect the form of humic-bound P, a fact revealed by ^{31}P -NMR analysis of the humic acid fraction. In Santa Barbara Basin surface sediments, all orthophosphate in the total base extract is found in the FA fraction, with only ester linkages detected in the HA fraction (Figure 2-17). However, there is substantial orthophosphate in both the HA and FA fractions of deeper sediments (Figure 2-18). Orthophosphate has also been observed in soil HA (Ogner, 1983; Bedrock *et al.*, 1994), although it was attributed to either incomplete dialysis or hydrolysis of esters in the base extract. However, while orthophosphate constitutes a rather small fraction of the total P signal in the soil studies, it accounts for 60% of the total P signal in the deep sediment humic acid. We have demonstrated that hydrolysis is probably not a quantitatively important source of orthophosphate in these extracts. Incomplete dialysis could not account for such a large signal. Incorporation of orthophosphate into the HA fraction during early diagenesis is the most reasonable explanation for the data, and can explain at least part of the discrepancy between the wet chemical and NMR estimations of inorganic P content.

A likely mechanism for this incorporation is metal bridging between humic compounds and orthophosphate. Metals can be complexed by oxygen-containing functional groups (e.g., carboxylic acids, phenols) found in humic and fulvic acids. Indeed, Schnitzer (1969) suggested that metal-humic complexes are an important intermediate in soil cycling of P. During diagenesis, metals dissolved from mineral phases can become incorporated into humic compounds (Nissenbaum & Swaine, 1976). Metal-P association need not be restricted to the HA fraction. Dialysis of the FA fraction demonstrates that 79% of the total P, and 66% of orthophosphate, is associated with compounds larger than 500 Daltons (Table 2-11). As demonstrated by Figure 2-19, orthophosphate is the dominant P species in the fulvic acid fraction, even after dialysis. Metal bridging may cause orthophosphate that would otherwise be soluble in acid to be non-reactive with the molybdate reagents used to measure SRP. The fact that a Chelex

resin efficiently removed orthophosphate from a base extract (Section 2.4.3.2.1) is indirect evidence for metal-P association in these sediments. While the sediment treatment with CDB extracted metals from mineral phases, metals would be retained in the humic matrix if it was a stronger chelator than citrate.

The identification of orthophosphate by ^{31}P -NMR is unequivocal, while the wet chemical method relies on an operational separation of inorganic and organic P. Metal bridging between humic compounds and orthophosphate provides a mechanism to explain the discrepancy between inorganic P measured by wet chemical and NMR techniques. The increase in this discrepancy with depth in the sediments suggests that

Table 2-11. Total P contained in the fulvic acid fraction of the base extract from deep (38-40 cm) sediments of the Santa Barbara Basin. Dialysis (500 Dalton nominal cutoff) results in incomplete removal of orthophosphate from the sample, indicating that orthophosphate is bound to high molecular weight organic matter .

	<u>$\mu\text{mol P/g sediment}$</u>		<u>% lost by dialysis</u>	<u>% in the >500 Dalton Fraction</u>
	<u>Not Dialyzed</u>	<u>Dialyzed</u>		
Total P	5.2	4.1	21 %	79%
Orthophosphate	4.4	2.9	34 %	66%

metal-bound orthophosphate accumulates in the humic matrix during diagenesis. These data suggest that metallohumic complexes could constitute an important sedimentary sink for orthophosphate. The amount of preserved organic P in marine sediments and ancient shales has been determined exclusively by wet chemical techniques in all studies to date. Comparison of wet chemical and NMR results indicate that at least a fraction of the organic P measured by wet chemical techniques may not be organic at all.

2.4.4 Reproducibility of Sediment Extractions

In addition to evaluating the variation in P concentration measured in a single extract, the amount of P extracted from replicate sediment samples was measured. For some extraction steps, several tests were done, and each of these is listed separately in Table 2-12. The variation in lipid P and water-soluble P arises from differences in the efficiency of P extraction from sediments and from differences in the partitioning of P between lipid and aqueous phases. The total amount of P extracted by the solvent mixture (lipid + aqueous) varied by 3.3% over triplicate samples. However, the variation in P content of lipid and aqueous extracts is higher, indicating that much of the variation between replicate samples results from partitioning and not from the extraction itself.

Table 2-12. Reproducibility of sediment extractions. The relative percent error of P concentration determined in the extracts is shown, along with the number of samples used for each comparison. For extraction steps where multiple tests were conducted, each is listed separately.

<u>Reservoir</u>	<u>Relative % Error</u>	<u>Number of replicates</u>
Solvent Extract (Chloroform+Aqueous)	3.3 %	n = 3
Chloroform Extract	5.1 %	n = 3
Aqueous Extract	33.2 %	n = 3
CDB	1.7 %	n = 4
	3.5 %	n = 4
0.1 M HCl	8.7 %	n = 4
	0.1 %	n = 2
0.5 M NaOH (Extract 1)	5.5 %	n = 4
	6.0 %	n = 2
0.5 M NaOH (Total Extract)	4.2 %	n = 2

The variation in P extracted by 0.5 NaOH was calculated two ways (Table 2-12). Reproducibility based only on P concentration in the first base extraction step is important because this extract alone was used for NMR analysis. However, the sum of P in all five extraction steps was used to quantify P in the base reservoir. The variation in total base-extractable P is somewhat lower than the variation between single base extractions, indicating that small variations in extraction efficiency are averaged out over several extraction steps.

Although we also recognize that sediment sub-sampling is a potential source of error due to natural heterogeneities in sediments deposited on the sea floor, the sample set is limited based on availability of sufficient quantity of sediment to exceed detection limit. The number of samples analyzed is further limited by the labor-intensive sample extraction procedure.

2.5 Conclusions

The analytical approach of this thesis was developed to bridge the gap in our current understanding of the structure and diagenetic modification of sedimentary P_{org} . New insights are achieved by combining a broad view of changes in total P_{org} concentration with molecular information about the structure of P_{org} in operationally defined reservoirs.

The primary tool used to characterize P_{org} structure is solution ^{31}P -NMR, a non-destructive technique that yields information about the relative abundance of different P functional groups in sediment extracts. Tests with standard compounds demonstrate that ^{31}P -NMR can be used to obtain quantitative information about P_{org} structure. Through a series of exhaustive tests, a sequential extraction was optimized to maximize solubilization of P_{org} for analysis by ^{31}P -NMR and to separate P_{org} into meaningful

biogeochemical reservoirs on the basis of solubility. Extraction procedures were adjusted to maximize P solubility, and to minimize structural alteration and degradation.

Organic and inorganic P are defined according to the operationally-defined conventions in the literature. The results of an acid hydrolysis experiment support the robustness of these definitions. However, a comparison of inorganic P estimated by wet chemical and ^{31}P -NMR techniques indicate that there is a pool of orthophosphate that is not accurately quantified as inorganic P when the traditional operational definition is used. This non-reactive orthophosphate may be bound to humic compounds via metal bridges.

In summary, the methods developed here allow examination of depth trends in total P_{org} as well as specific P_{org} functional groups, an approach that can provide much-needed insights into the diagenetic modification of P_{org} . The sequential extraction separates total P_{org} into reservoirs, enabling an examination of the relative susceptibility of each pool to diagenetic modification. The specific structural information within these separated reservoirs, obtained by ^{31}P -NMR, can be used to resolve questions about mechanistic controls on P_{org} preservation.

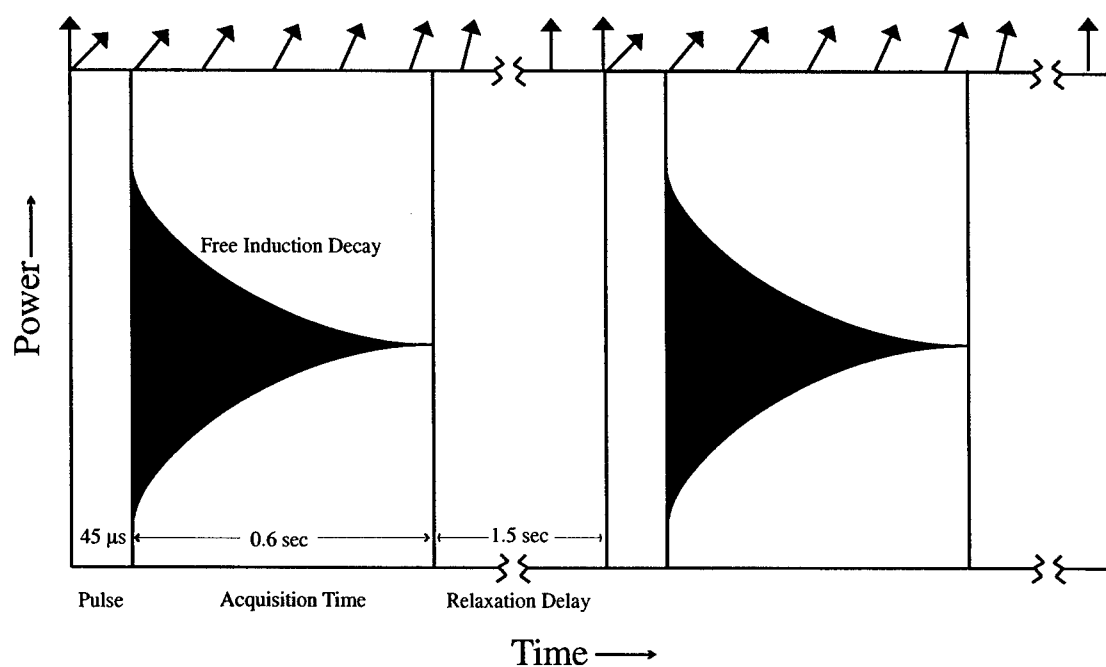


Figure 2-1. Schematic of the NMR pulse sequence used in this study, (modified from Rzepa, 1994). Intervals shown on the time axis are not to scale. The pulse rotates the net magnetization vector (indicated by arrows shown at the top of the diagram) 45° toward the XY plane. During acquisition and relaxation delay, the magnetization vector decays back to its initial orientation along the Z axis. The sequence is repeated for thousands of scans and the free induction decay (FID) signals are averaged, then transformed from the time domain into the frequency domain.

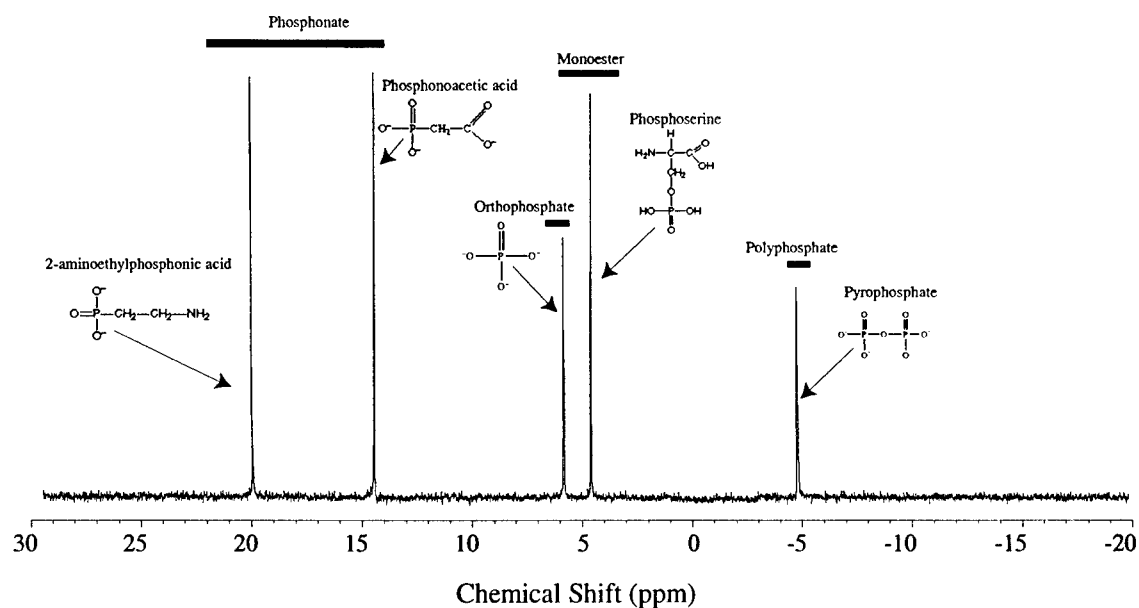


Figure 2-2. A spectrum of P standards run in 0.5 M NaOH, showing the chemical shift regions corresponding to different P functional groups.

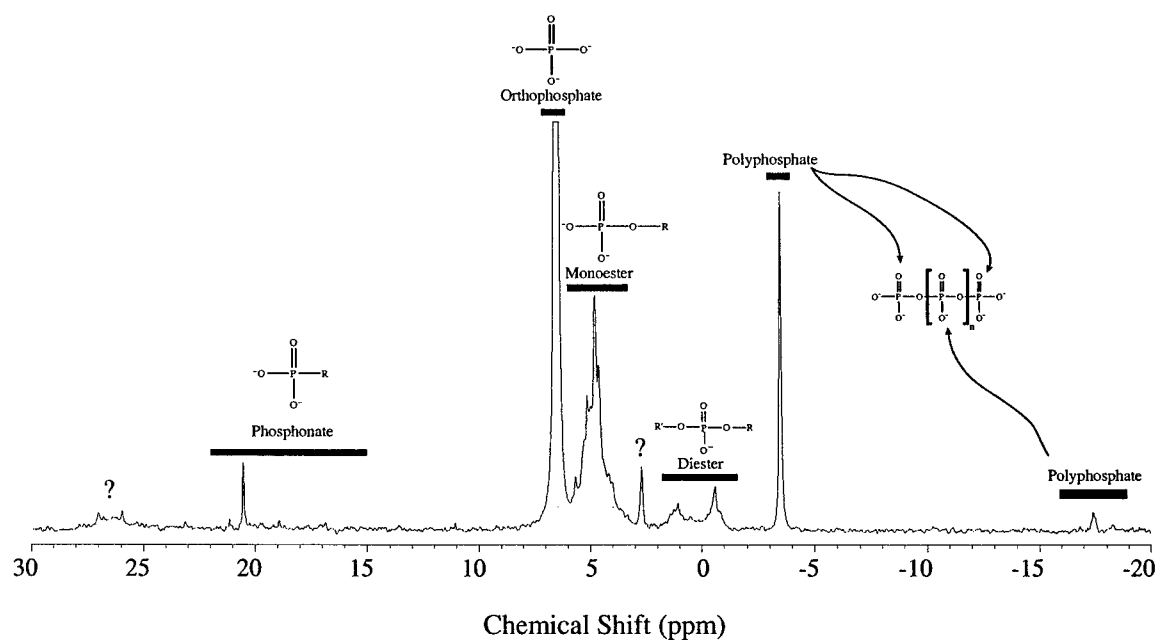


Figure 2-3. A typical spectrum of a sediment base extract, showing the chemical shift regions corresponding to different P functional groups. The general structure of each functional group is shown. Polyphosphate peaks are found in two chemical shift regions, representing middle groups and end groups on the polyphosphate chain. For the three peaks indicated by question marks (discussed in the text), no standard compounds were found that corresponded to these chemical shifts. Orthophosphate generally comprises ~70% of the total P signal, and in all spectra this peak has been truncated to make the other peaks visible in more detail.

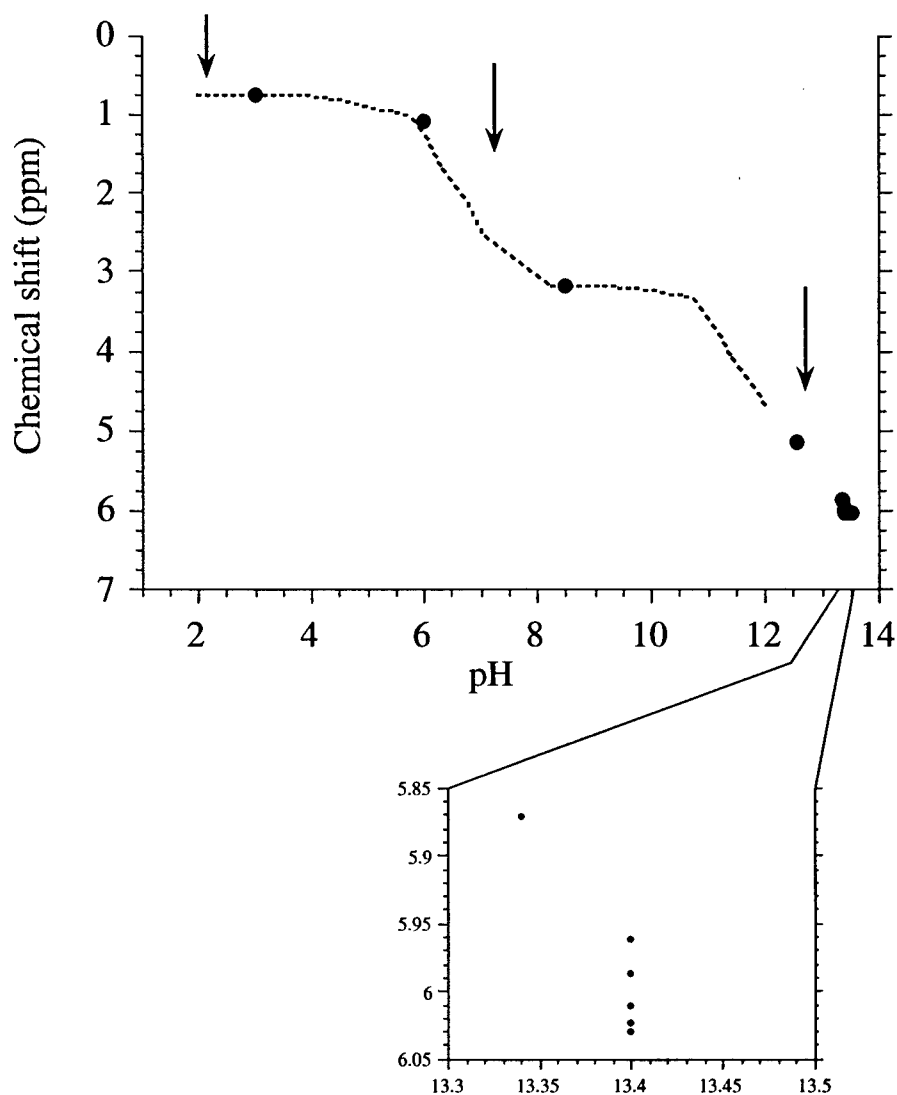


Figure 2-4. The effect of pH on the chemical shift of orthophosphate. The three arrows correspond to the three pK_a values for phosphoric acid, where the most dramatic changes in chemical shift are observed. The filled circles indicate measurements made in this study. The dashed line is based on data from Vogel (1984) Above pH 13.3, chemical shift variations are small.

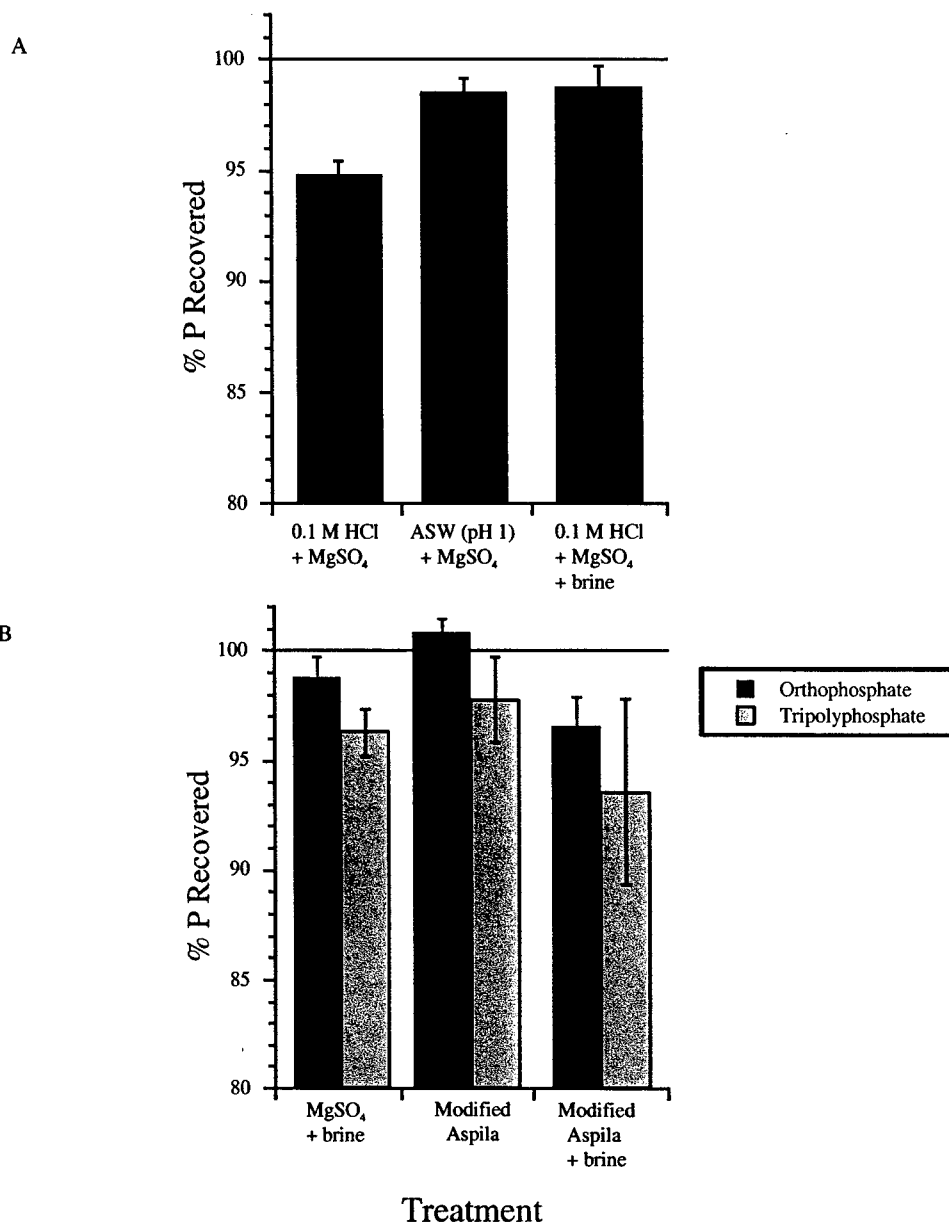


Figure 2-5. Recovery of P standards using modifications to the Solórzano and Sharp (1980) method of TDP analysis (discussed in the text). (A) The amount of salt in solution must be sufficiently high to prevent volatile loss. (B) Samples prepared using a modified Aspila (1976) procedure (see text) had higher orthophosphate and polyphosphate recovery than any modifications of the Solórzano and Sharp method tested here. The modified Aspila method described in the text was used for TDP analysis of all extracts.

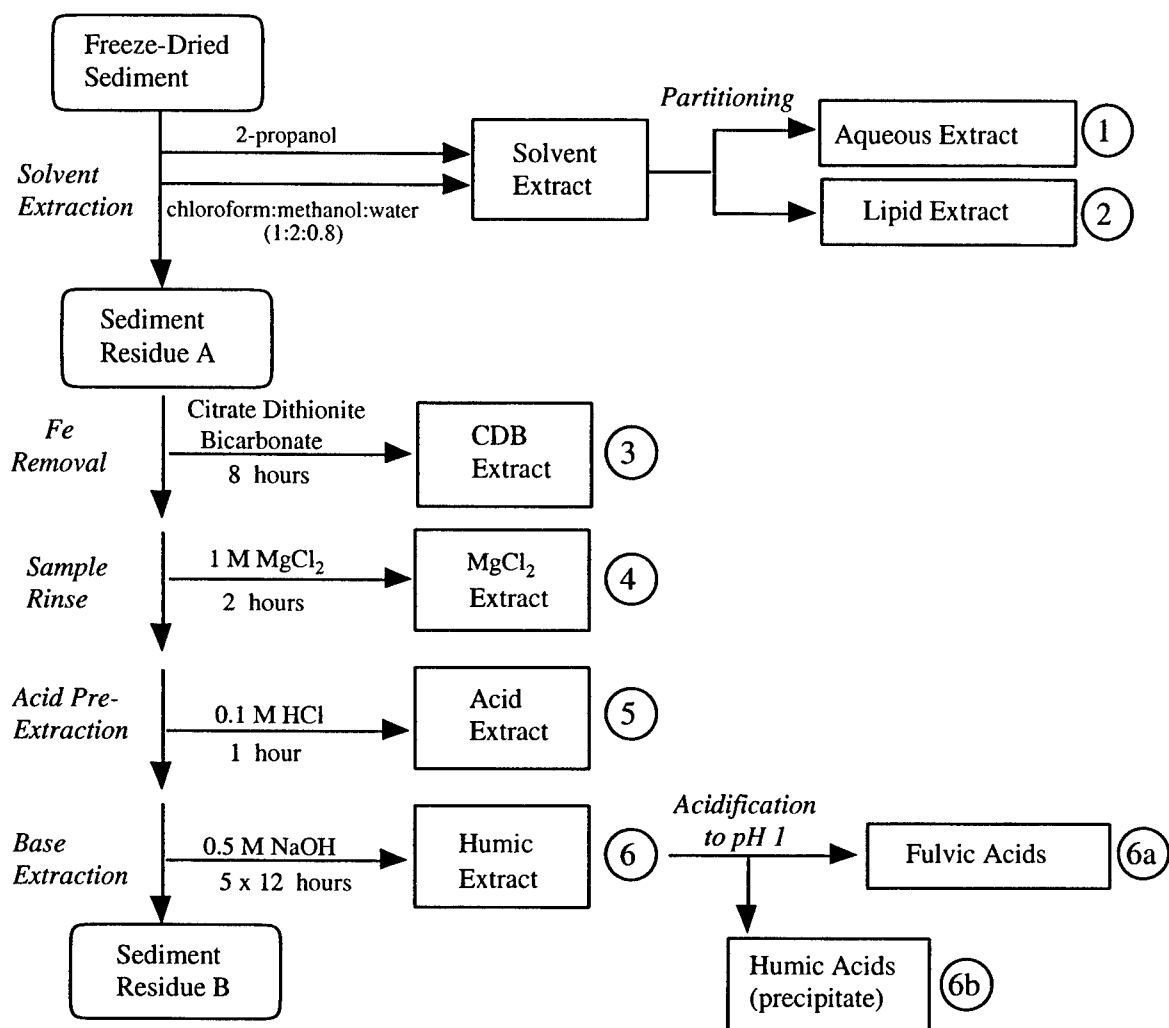


Figure 2-6. The sequential extraction procedure used for separation of organic P reservoirs. Details of the procedure, and tests used for its optimization, are described in the text.

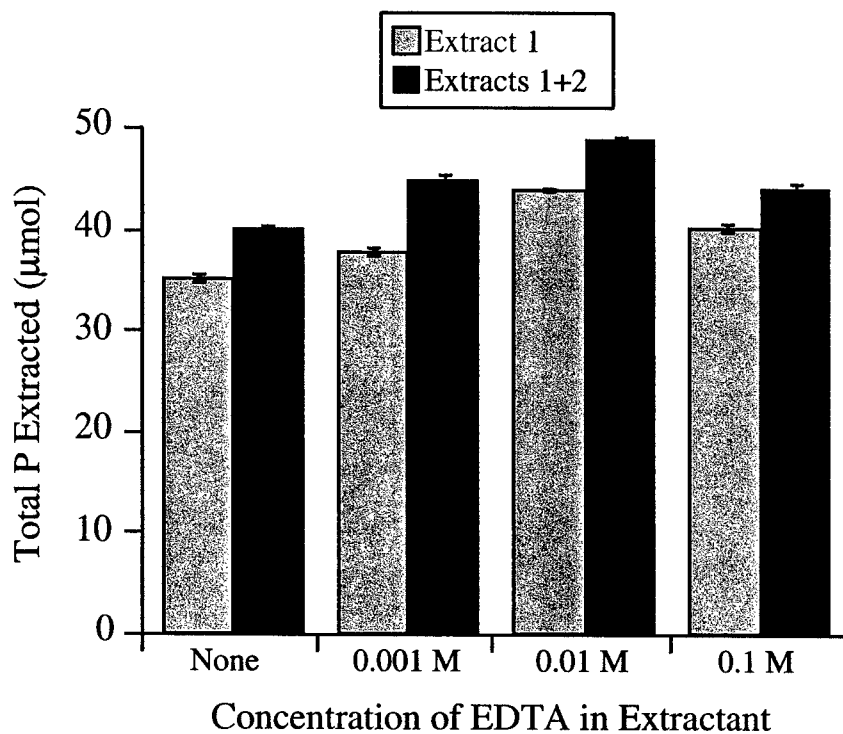


Figure 2-7. Total P extracted in 0.5 M NaOH solutions containing different concentrations of EDTA. For each treatment, the amount of P extracted only in the first extraction (gray bars) and the cumulative amount extracted in the first two extraction steps (black bars) is shown. Addition of EDTA to the base extractant results in a small increase in the amount of P extracted. Maximum P recovery is obtained at 0.01 M EDTA concentration.

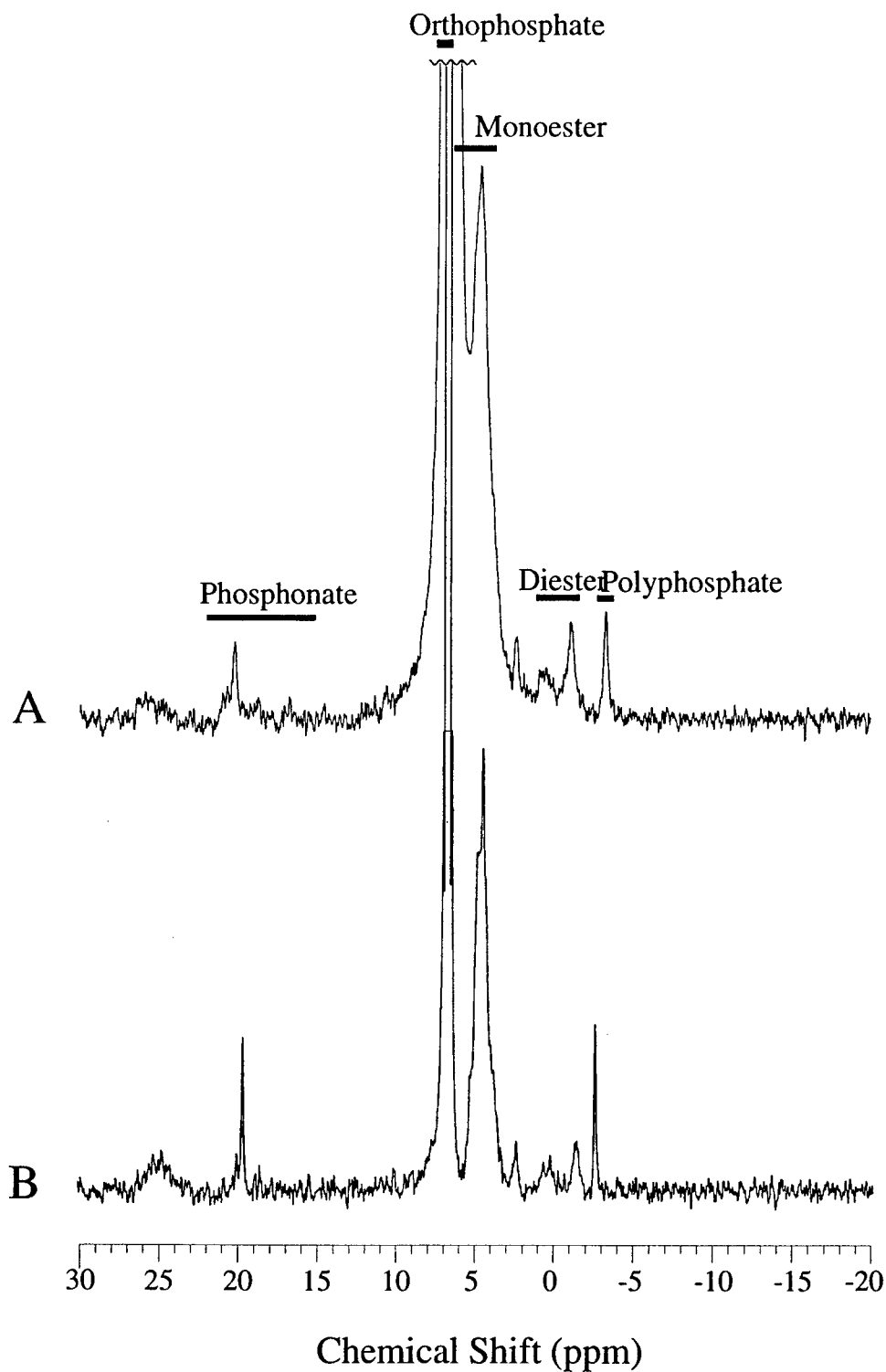


Figure 2-8. NMR spectra of base extracts of identical sediment samples (a) with 0.01 M EDTA added to the base extractant, and (b) after the sediment was pre-treated with CDB and MgCl_2 as described by Ruttenberg (1992).

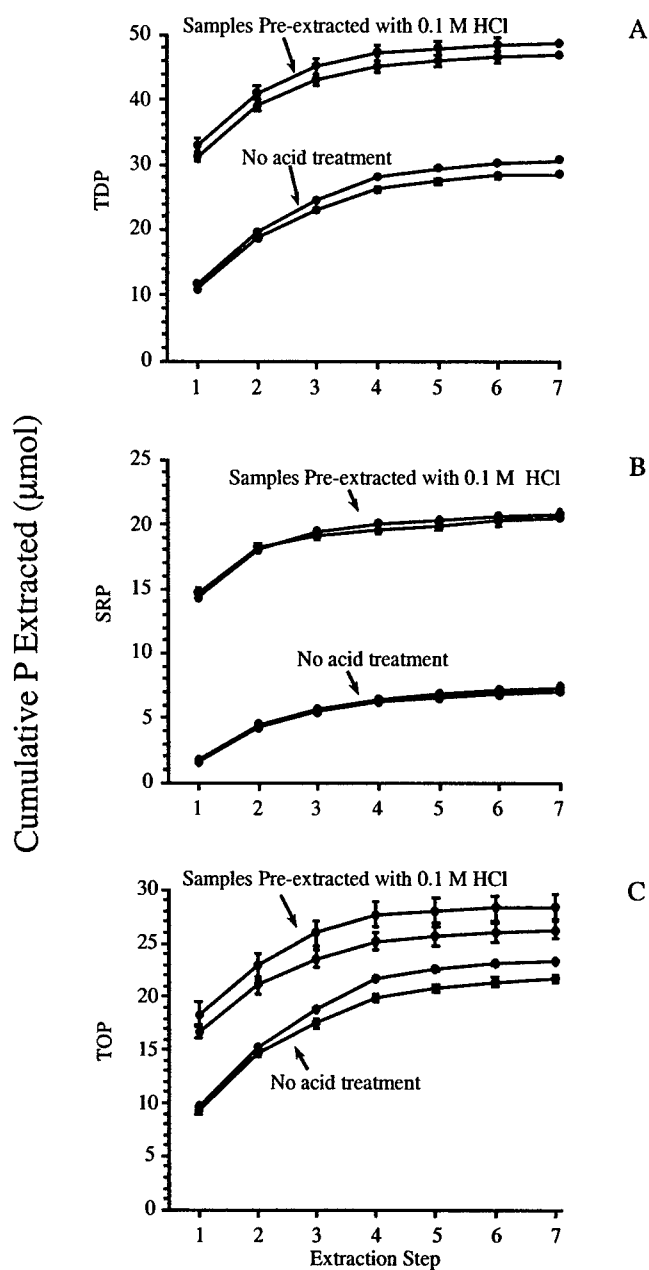


Figure 2-9. Difference in P solubilized during base extraction of sediments prepared with and without acid pre-extraction. Duplicate extractions were performed for each treatment. (A) Total P, (B) inorganic P, and (C) organic P were measured as described in the text. Error bars represent replicate P analyses of each extract. SRP is much higher in the acid-treated samples, resulting in larger error bars for TOP (calculated by difference).

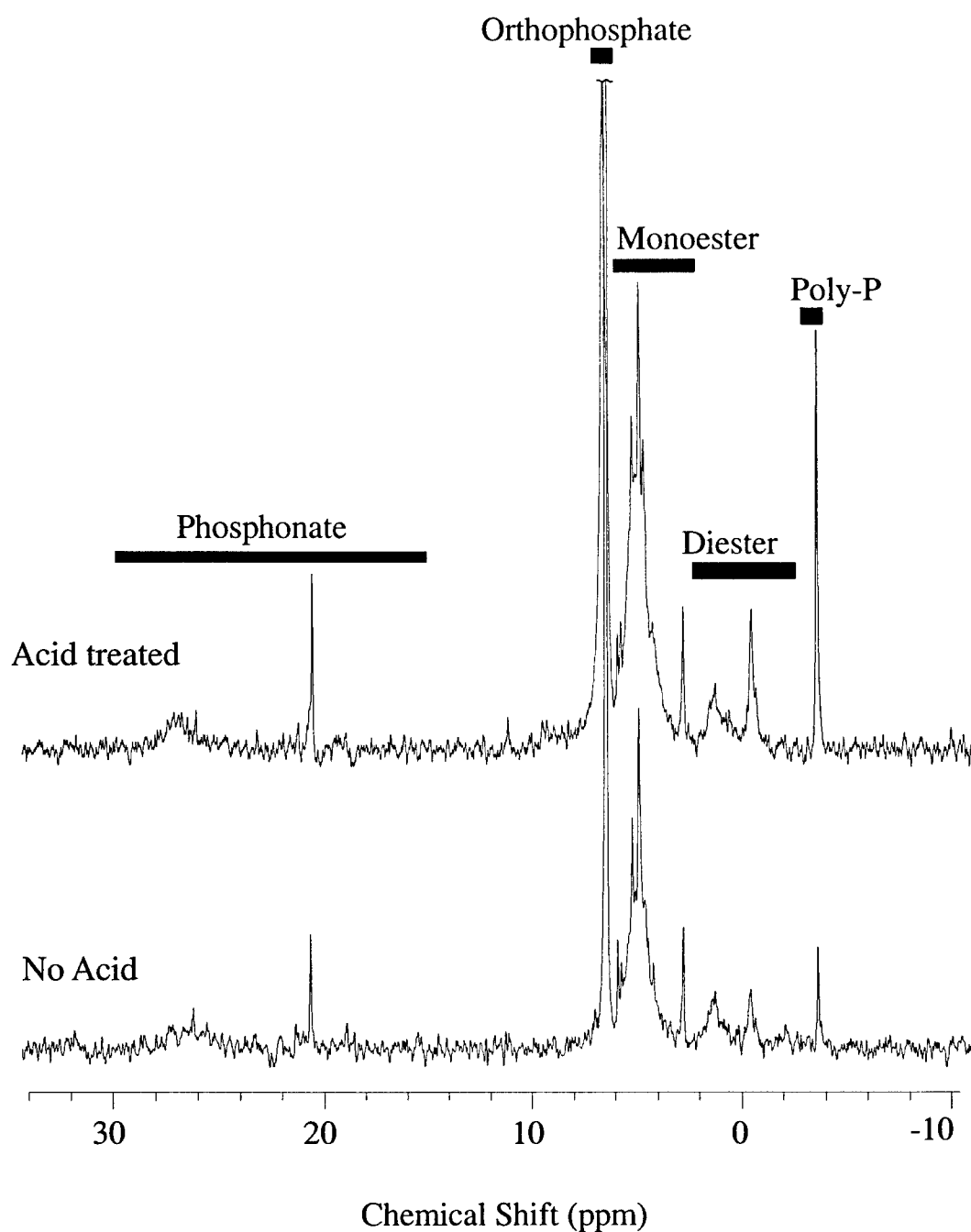


Figure 2-10. NMR spectra of base extracts of sediments prepared with and without acid pre-extraction. The concentration of P is significantly higher in the acid pre-treated sample, particularly in the orthophosphate, polyphosphate and diester regions. However, the fact that no peaks observed in the untreated sample are absent in the acid treated sample suggests that acid treatment does not cause hydrolysis of P.

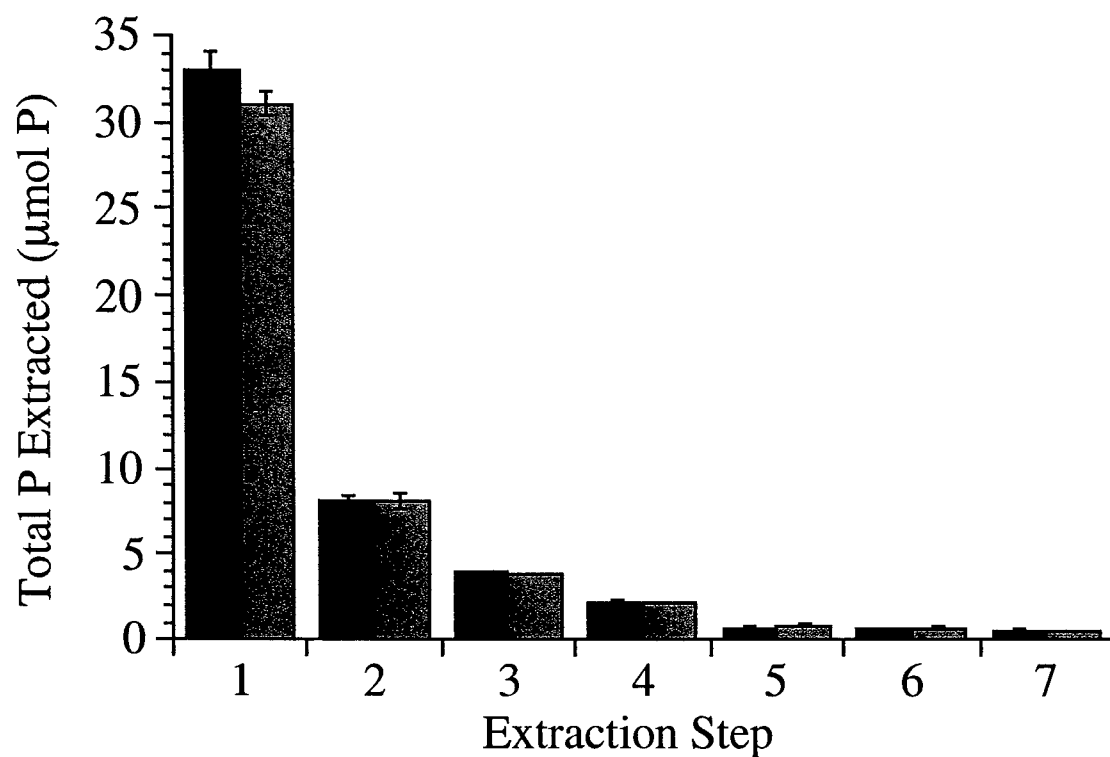


Figure 2-11. Total P extracted by successive 0.5 M NaOH treatments. Black and gray bars represent replicate sediment extractions. Error bars indicate the range of P concentration measured for each extract. Most of the base soluble P is extracted in step 1, with progressively less P in each of the subsequent steps. The standard extraction procedure adopted for this study includes 5 base extraction steps. Only extract 1 is analyzed by ^{31}P -NMR.

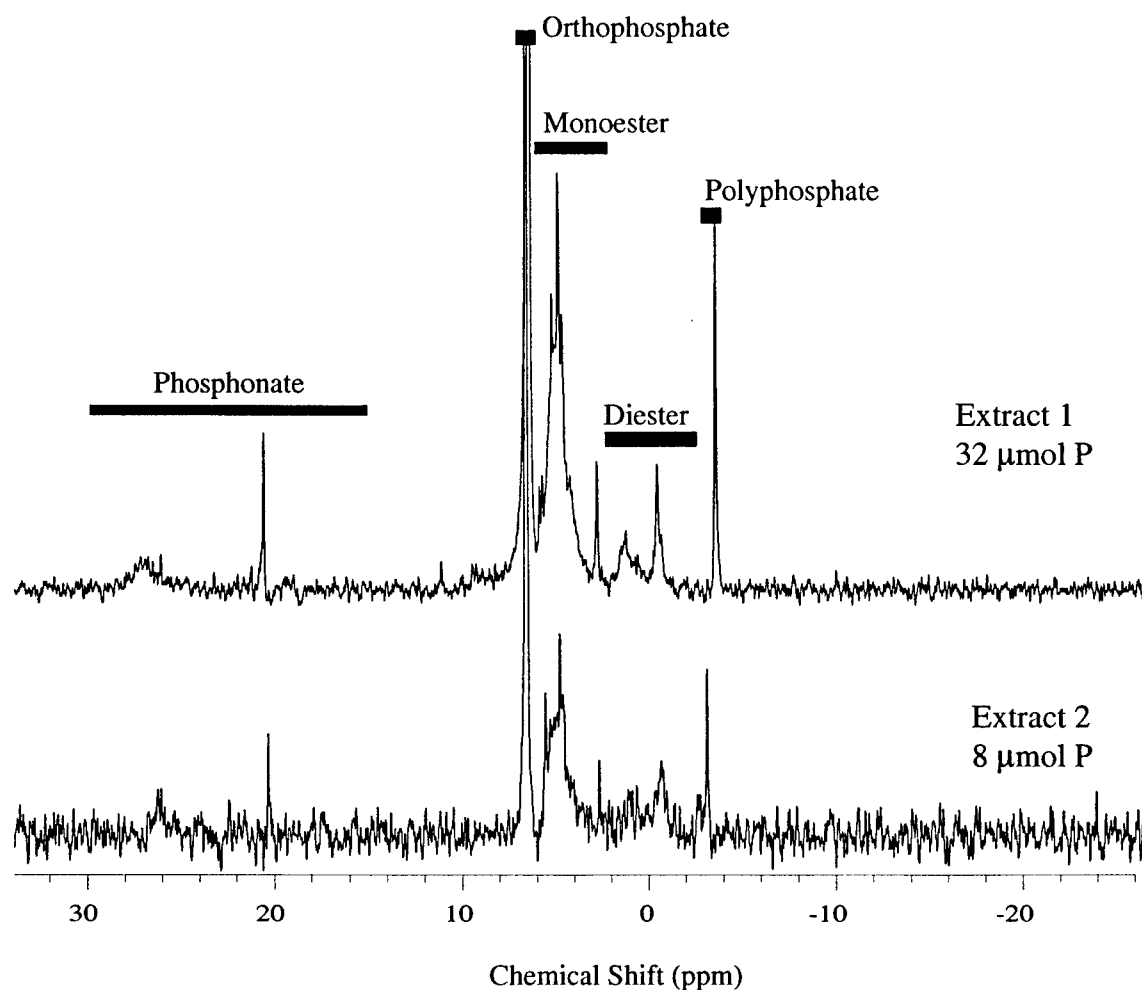


Figure 2-12. NMR spectra of the first two successive base extracts (concentration of all P extracts shown in previous figure). P concentration in extract 1 is much higher than in extract 2, but the structural features are similar, suggesting that extract 1 is structurally representative of the total base soluble pool. Together, extracts 1 and 2 comprise 83% of the total base extractable P.

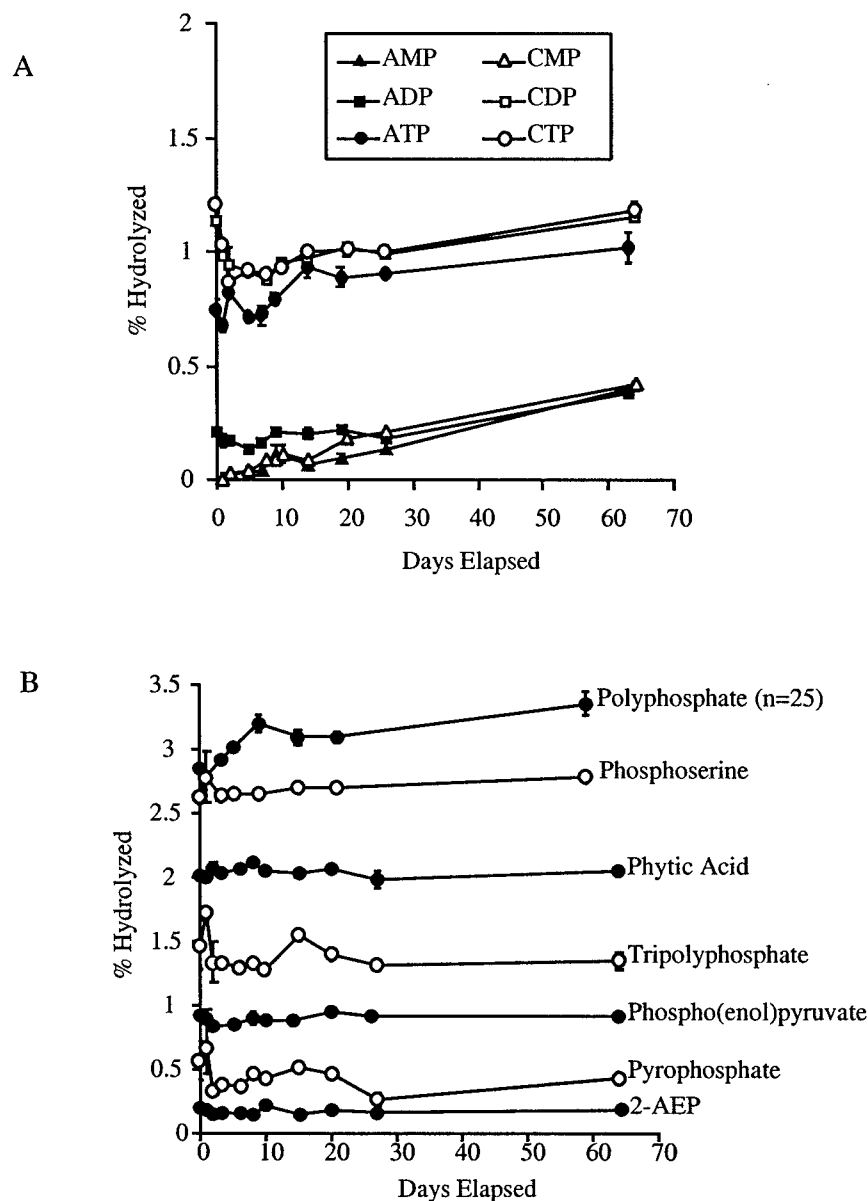


Figure 2-13. Hydrolysis of (A) nucleotides, and (B) other P compounds in 0.5 M NaOH during two months of storage. Data are expressed as the percent of total P measured as soluble reactive P (SRP) at each time point. All compounds shown were hydrolyzed by less than 3.5%, even after 60-70 days of storage. Measured SRP may indicate acid hydrolysis due to pH adjustment and the acidic reagents used for SRP detection (see text). Error bars represent the range of SRP values from duplicate analyses.

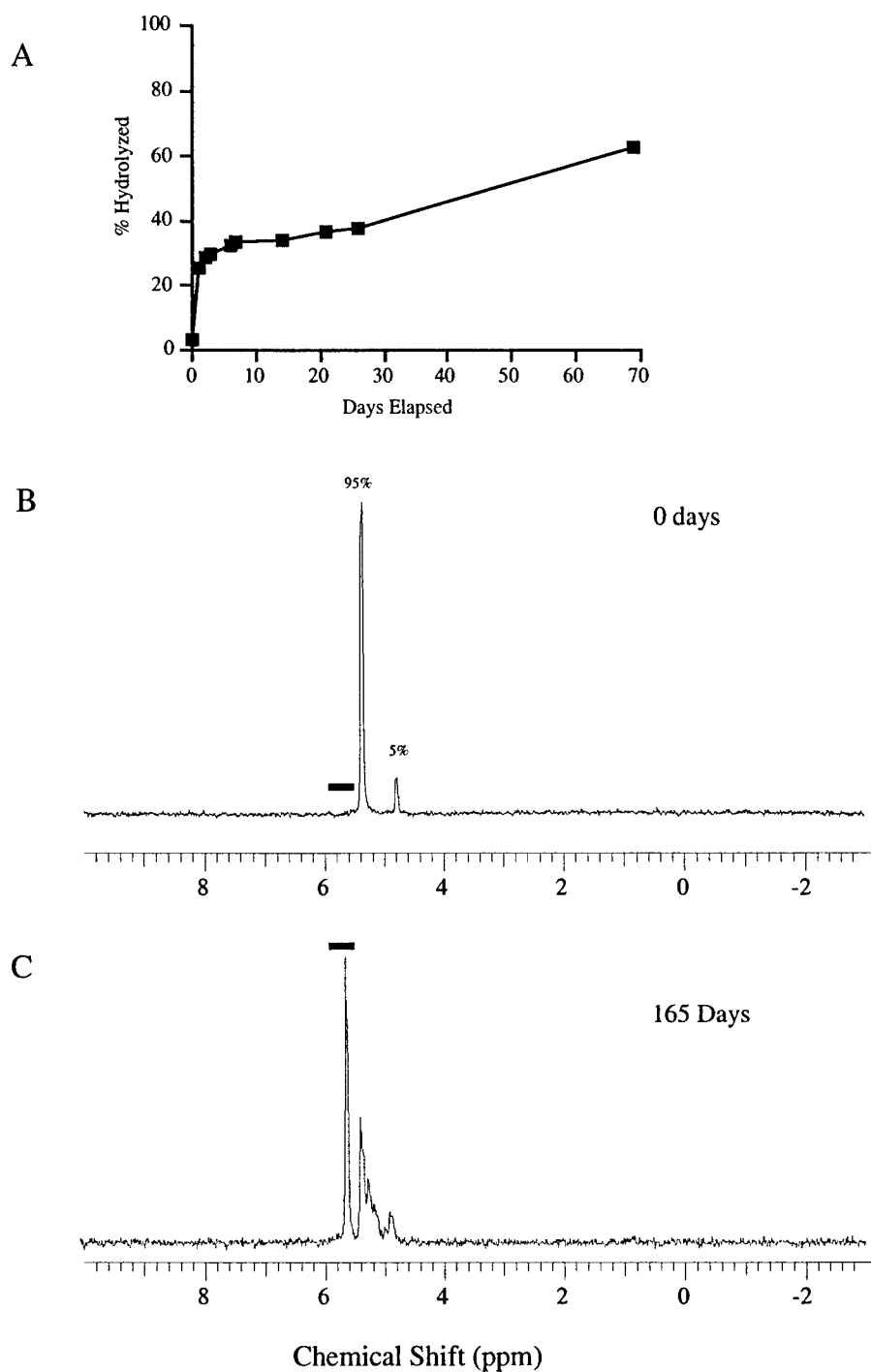


Figure 2-14. Hydrolysis of glucose-6-phosphate in 0.5 M NaOH, demonstrated (A) by measurement of SRP concentration in the solution, (B) by ^{31}P -NMR analysis of the solution immediately after solubilization, and (C) by ^{31}P -NMR analysis after 165 days of storage. The shaded bars on the spectra indicate the chemical shift region characteristic of orthophosphate, produced by hydrolysis of the phosphosugar. Error bars in panel A, representing the range of SRP values from replicate analyses, are smaller than the symbol size for each data point.

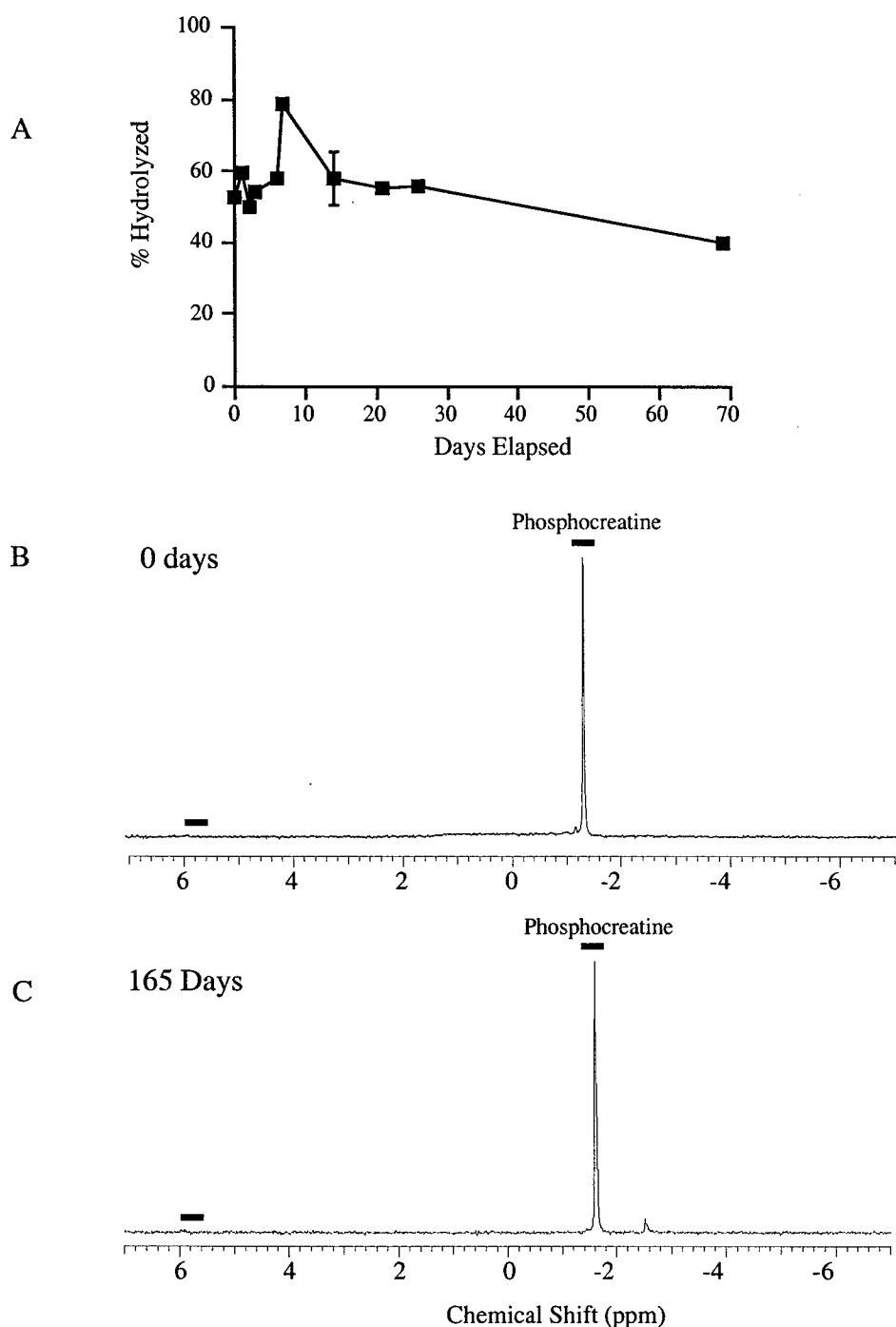


Figure 2-15 Phosphocreatine stability in 0.5 M NaOH. Evidence for extensive hydrolysis based on the SRP data (A) is not supported by the NMR data. There is no peak in the chemical shift region of orthophosphate (shaded bars) either immediately after solubilization (B), or after 165 days of storage (C). The small peak at -2.5 ppm may be a degradation product, but represents less than 8% of the total P signal. High SRP concentrations are likely a result of acidification of the sample for P analysis (see text). Error bars in panel A represent the range of SRP values from replicate analyses.

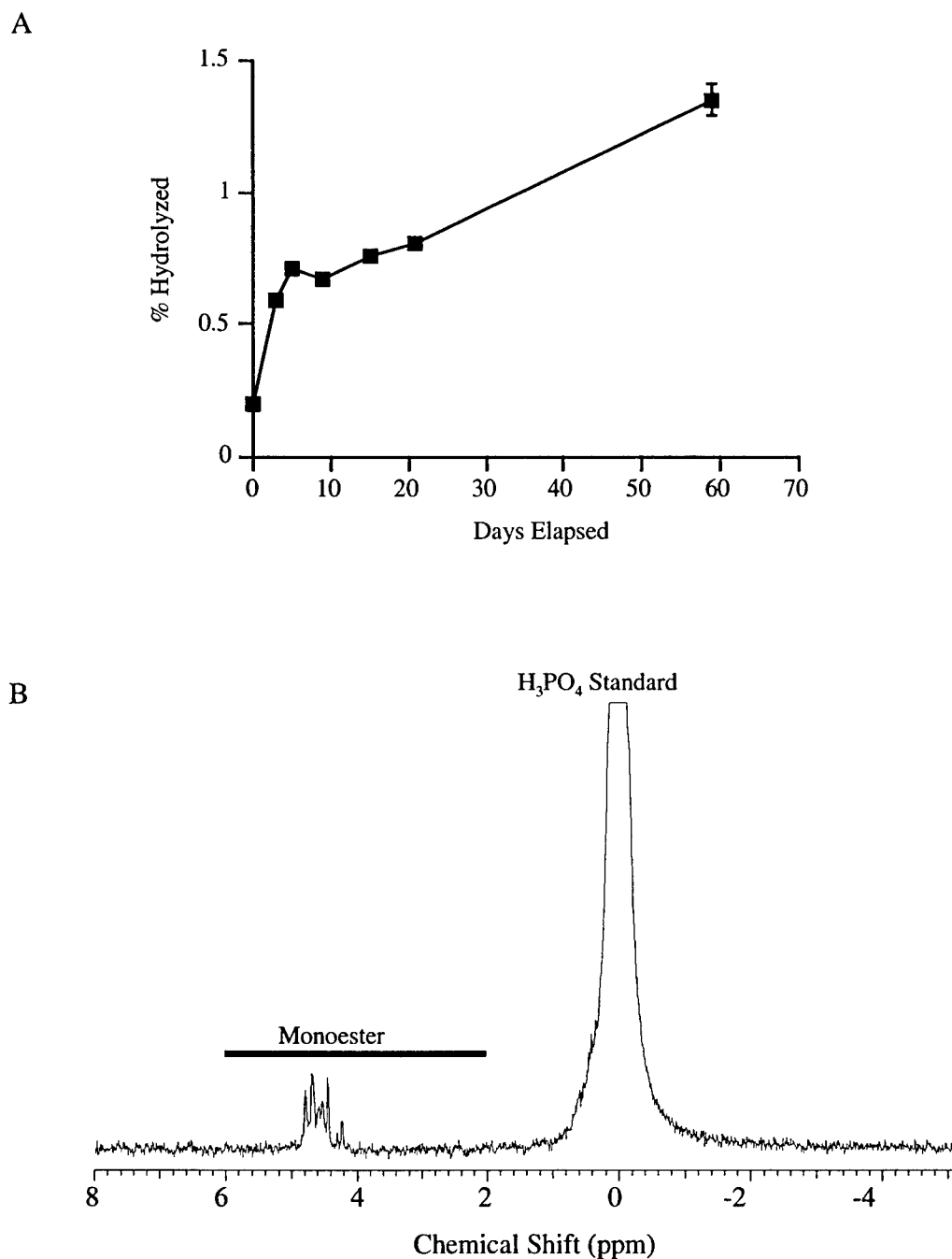


Figure 2-16. Hydrolysis of RNA in 0.5 M NaOH based on (a) SRP concentration (error bars represent the range of SRP values from replicate analyses), and (b) ^{31}P -NMR spectrum. Little SRP accumulates in solution, but NMR shows that much of the compound is immediately degraded into its constituent nucleotides. The H_3PO_4 standard (capillary insert) conceals the diester region, but relative peak areas indicate that approximately half the standard is intact (diester region 2 to -3 ppm) and the remainder is in monoester form.

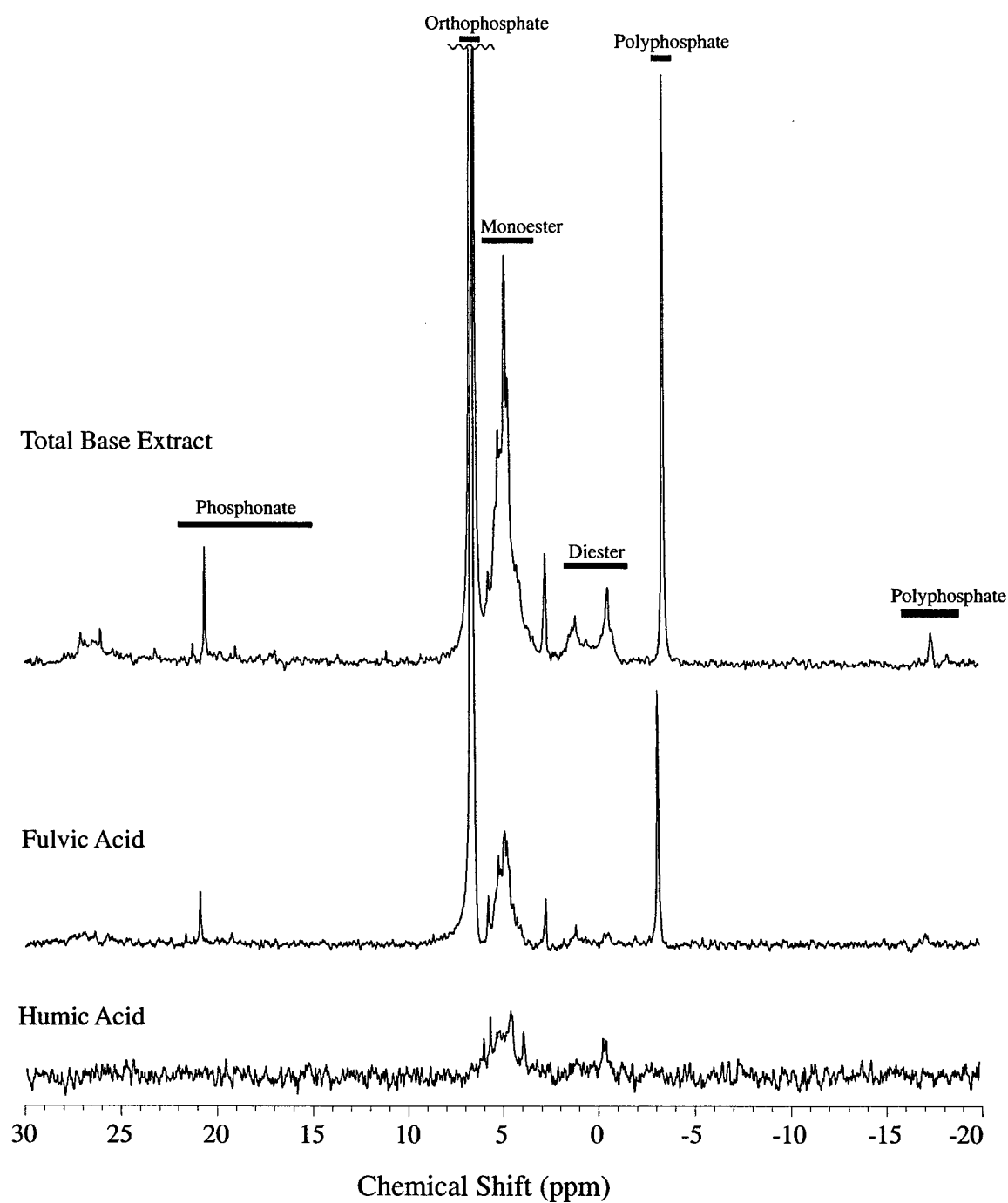


Figure 2-17. ^{31}P -NMR spectra of the total base extract, and the fulvic and humic acid fractions, from surface sediments (0-0.3 cm) of the central Santa Barbara Basin. Most of the P and all of the orthophosphate is in the fulvic acid fraction. Only monoesters and diesters are detected in the humic acid fraction.

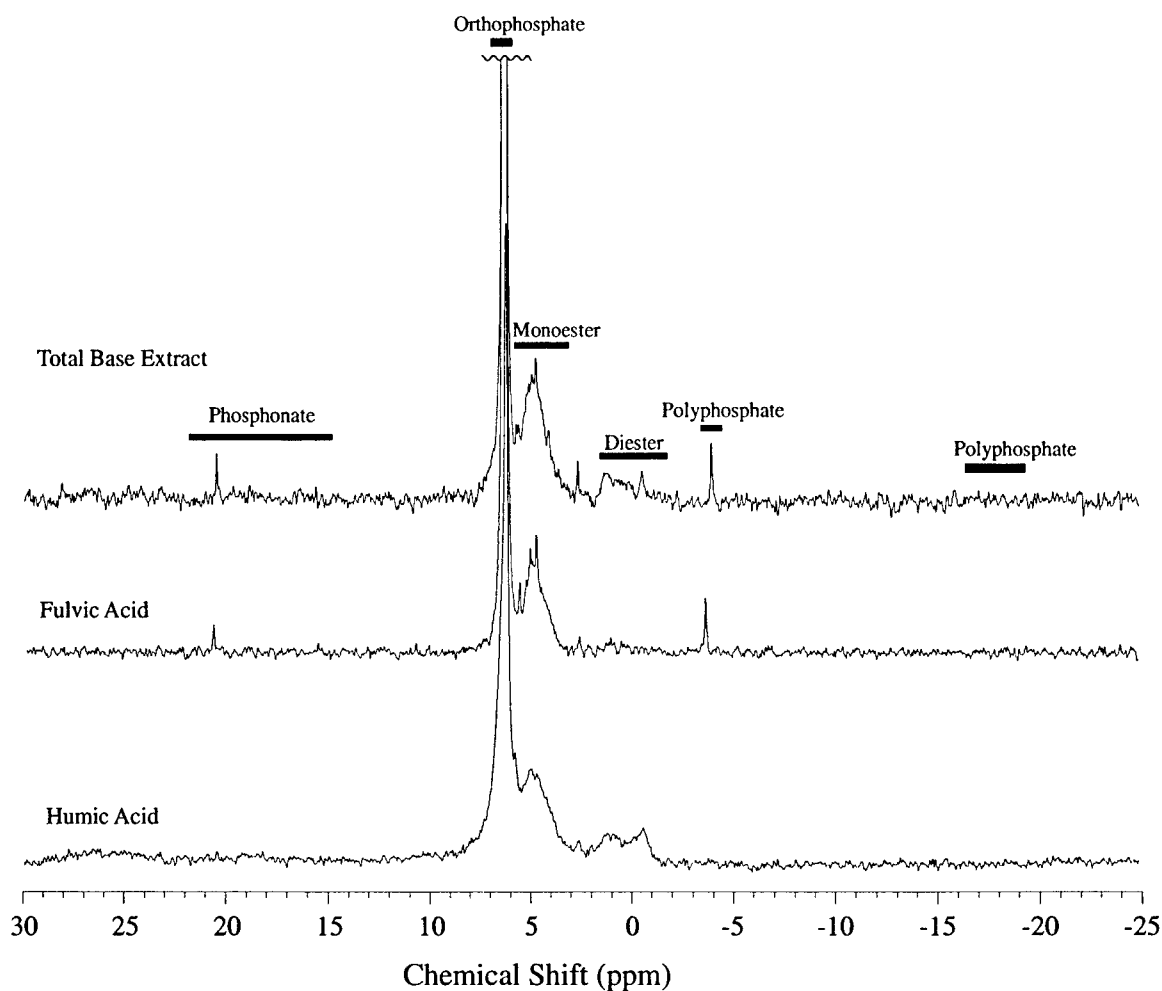


Figure 2-18. ^{31}P -NMR spectra of the total base extract, and the fulvic and humic acid fractions, from deep sediments (38-40 cm) of the central Santa Barbara Basin. Orthophosphate is the most abundant P species in all spectra (including the humic acids). No polyphosphate or phosphonate P is detected in the humic acid fraction.

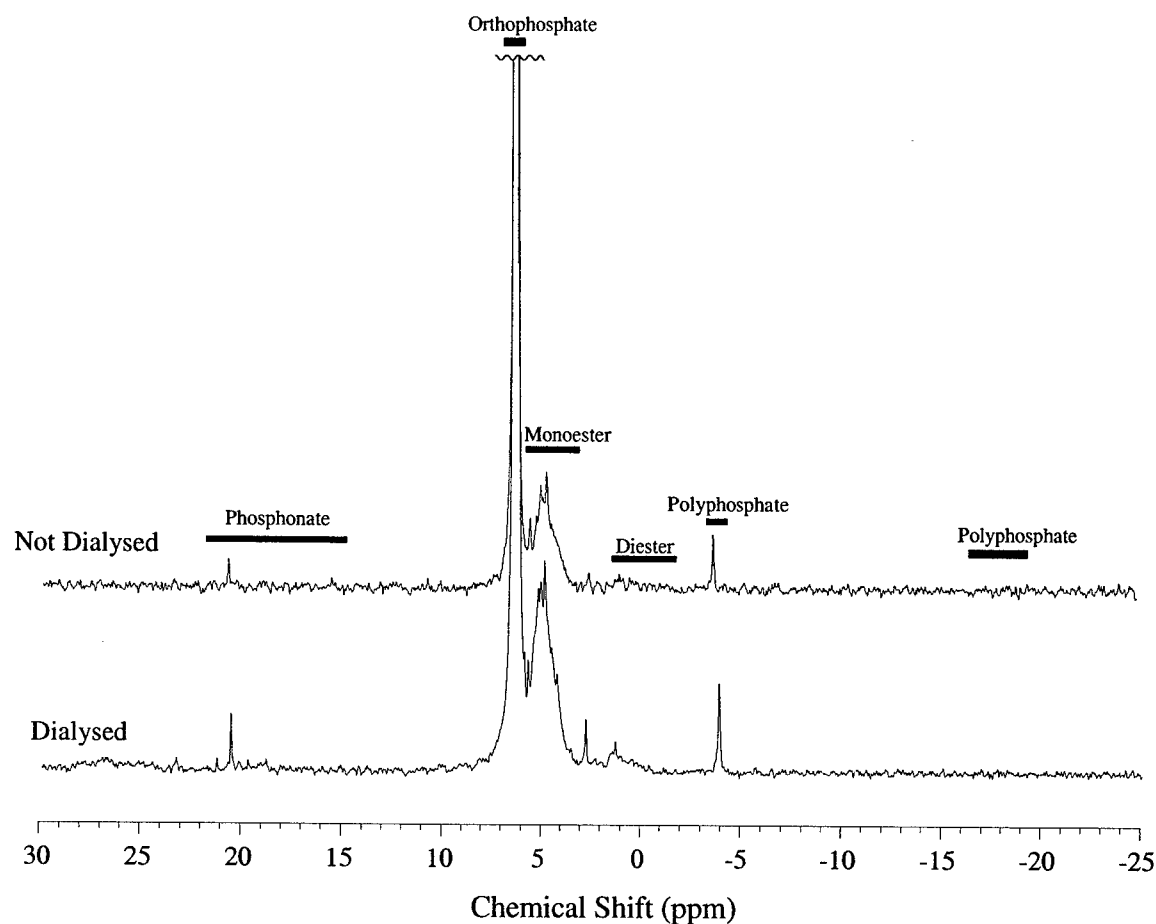


Figure 2-19. ^{31}P -NMR spectra of the fulvic acid fraction of a base extract from deep sediments (38-40 cm) of the central Santa Barbara Basin, with and without dialysis. The nominal molecular weight cutoff for dialysis was 500 Daltons. All of the peaks are enhanced in the dialyzed sample because the lower salt content allowed more sample to be concentrated in the same volume of NMR tube (therefore increasing P concentration). Orthophosphate is the most abundant functional group, even in the dialyzed sample, indicating that it is associated with compounds of greater than 500 Daltons molecular weight.

Chapter 3

Contribution of Biomass to the Organic P Reservoir in Central Santa Barbara Basin Sediments

*The significant chemicals of living tissue are rickety and
unstable, which is exactly what is needed for life.*

-Isaac Asimov

3.1 Introduction

Diagenetic changes in the sedimentary P_{org} reservoir can be inferred from depth trends in P_{org} abundance and composition only if the pool of diagenetically vulnerable organic matter can be distinguished from the biochemicals derived from resident biological populations in the sediments. The outer membrane acts as a protective barrier for living cells, preventing degradation of intracellular P biochemicals. Once a cell dies, its contents are subject to decomposition. Throughout this chapter, the expression “diagenetically vulnerable” indicates organic matter that is not associated with living biomass, and thus is not protected from remineralization by virtue of cell physiology. Diagenetically vulnerable organic matter may, however, be protected from degradation by inherent chemical resistance or by physical protection mechanisms (discussed in Chapter 4). Therefore, for the purpose of discussion, all sedimentary organic matter (excluding the living biological community) is included as part of the diagenetically

vulnerable pool, regardless of whether it is labile (easily degraded) or refractory (resistant) with respect to degradation in the sediments.

The primary source of P in marine sediments is the pool of P biochemicals derived from planktonic and bacterial biomass. The biochemical composition of cells is generally reported in terms of the fractional contribution of particular compounds to the total carbon content or total dry weight of a cell. To examine cellular P distribution, the fractional contribution to total cell P concentration was calculated from the percent cell dry weight and P content of each compound (Table 3-1). This compilation of data, derived from cultured bacteria, only includes compounds that contribute significantly to total cell dry weight, thereby omitting potentially important P compounds such as phosphosugars, phosphoproteins, and polyphosphates. Nevertheless, these data allow some insight into the composition of the primary compounds that contribute to sedimentary P_{org}.

Table 3-1. The abundance of P biochemicals in bacterial biomass, calculated based on data from Neidhardt (1987). This data compilation does not include phosphosugars, phosphoproteins or polyphosphates.

	% cell dry weight	% cell P *
ATP	1	6
DNA	3	13
Phospholipid	10	19
RNA	14	63

*% cell P is calculated assuming that all cellular P is accounted for by these compounds. The total cellular P from each compound is calculated by dividing the total weight of the compound in a cell (from % cell dry weight) by the molecular weight of the compound, and multiplying by the number of P atoms per mole of compound.

Nucleic acids (DNA, RNA) constitute the largest fraction of P in a living cell, with smaller contributions by phospholipids and ATP. A common characteristic of all of these P biochemicals is that they are considered very labile and therefore are not expected to persist in sediments upon cell death. While enzymes capable of degrading each of these compounds are ubiquitous in cells, the efficiency of degradation for different P_{org} fractions in natural sediments is not known. In particular, cell culture studies, which have been the basis for assuming essentially instantaneous degradation of P biochemicals upon cell death, do not include potentially important mechanisms for preservation of P_{org} biochemicals in sediments. Sorption to mineral surfaces and incorporation into macromolecular organic matrices are two possible mechanisms for enhancing P_{org} preservation.

The persistence of P_{org} in marine sediments and ancient shales (e.g. Ingall *et al.*, 1993; Filippelli & Delaney, 1994; Delaney & Anderson, 1997) has long been a puzzle, given that the primary sources of P_{org} (planktonic and bacterial biomass) are composed largely of compounds thought to be rapidly degraded upon cell death (Table 3-1). The intrinsic lability of P_{org} and the observed persistence of P_{org} in deep sediments and ancient shales can be reconciled if: (i) sedimentary P_{org} represents live biomass, (ii) P_{org} biochemicals are not entirely degraded upon cell death, either because of physical protection or inherent structural features, and/or (iii) P_{org} biochemicals are transformed into more refractory P_{org} compounds during diagenesis. The first two of these possible explanations for persistence of sedimentary P_{org} are considered in this chapter, while the chemical structure and diagenetic alteration of sedimentary P_{org} are discussed in Chapter 4.

Frequently, a substantial fraction of sedimentary organic matter is accounted for by intact, living biomass (e.g., Cranwell, 1984). The known primary (i.e., biochemical) forms of P_{org} are considered so labile in marine sediments (White *et al.*, 1977; Paul *et al.*, 1987; Westheimer, 1987) that P biochemicals such as phospholipids and ATP are often

used as chemical assays for sedimentary biomass abundance (e.g. Holm-Hansen & Booth, 1966; Karl & Holm-Hansen, 1976; White *et al.*, 1979c; Findlay & Dobbs, 1993). The assumption implicit in use of ATP and phospholipids as proxies for sedimentary biomass is that these compounds are degraded immediately upon cell death. There are large uncertainties in these and other methods of biomass estimation, however. As a result of these uncertainties, it is difficult to differentiate between the depth profiles of diagenetically vulnerable organic matter and living biomass in sediments. Generally, both bacterial abundance and organic matter concentration are highest at the sediment-water interface and show an exponential decrease with depth in sediments, with the decrease in cell numbers reflecting the decrease in availability of organic matter and terminal electron acceptors (e.g., Dale, 1974; Kemp, 1987; Cragg *et al.*, 1992; Deming & Baross, 1993). It is therefore unclear, when looking at a P_{org} depth profile, to what extent living biomass and diagenetically vulnerable organic matter contribute to the overall profile shape.

This chapter focuses on the contribution of biomass to the composition of the sedimentary P_{org} reservoir by addressing the following questions: (i) is extractable lipid P accounted for by living biomass alone? (i.e., can instantaneous degradation after cell death be assumed?), and (ii) what fraction of the total sedimentary P_{org} reservoir can be attributed to biomass? Biomass was determined by measuring both lipid P and ATP concentrations in sediments from the central Santa Barbara Basin. A comparison of these two methods indicates that a fraction of the lipid P pool at this site is not accounted for by biomass. The fraction of the lipid P reservoir that is in excess of biomass, as determined by ATP, appears to be resistant to remineralization over the timescale represented by the sediment core. We consider whether this “resistant” lipid P is composed of compounds that are inherently resistant to degradation. Phosphonolipids, thought to be chemically resistant by virtue of their direct C-P bond, are a prime candidate for a resistant lipid P compound. However, no evidence for preferential preservation of phosphonolipids was

found. Together, the ATP and lipid P data indicate that most of the total sedimentary P_{org} pool in these sediments, as well as a fraction of lipid P, is composed of diagenetically vulnerable P_{org} , rather than live biomass.

3.2 Biomass Estimated by Quantification of P_{org} Compounds

ATP and phospholipids were quantified in this study to estimate total biomass abundance and its contribution to the sedimentary P_{org} reservoir. To accurately estimate biomass based on the concentration of a particular biochemical in sediments, two criteria must be satisfied: (i) the concentration of the compound in living cells is predictable, and (ii) the compound is completely degraded when a cell dies. The extent to which ATP and phospholipids adhere to these criteria is discussed below.

3.2.1 Biomass Determined from Phospholipid Concentration

The abundance of phospholipids in sediments, estimated either by quantifying fatty acids in the polar lipid fraction (e.g., Baird & White, 1985; Nichols *et al.*, 1987; Balkwill *et al.*, 1988; Findlay & Dobbs, 1993), or by measuring lipid phosphate concentration (e.g., White *et al.*, 1979b; 1979c; Gehron & White, 1983) has been used extensively as a proxy for the abundance of bacterial biomass. Phospholipids are membrane constituents of all organisms but do not accumulate as storage products (e.g., Kates, 1964; Hawthorne & Ansell, 1982), and predictable phospholipid content has been demonstrated under a range of growing conditions (White *et al.*, 1977; 1979b; 1979c).

The relatively rapid turnover of phospholipids observed in laboratory sediment studies (King *et al.*, 1977; White *et al.*, 1979c) suggests that sedimentary phospholipid concentration is directly proportional to biomass abundance. However, these laboratory degradation studies do not demonstrate complete remineralization of phospholipids, because turnover time for the total lipid P pool is calculated based on degradation of only

a fraction of the phospholipids. Thus, these data alone do not preclude the existence of a resistant lipid P fraction. In addition, bacterial abundance calculated from lipid P concentration can exceed bacterial cell numbers determined by direct cell counts (Harvey *et al.*, 1984; 1986), indicating that the extractable sedimentary lipid P pool can include compounds other than phospholipids from the intact bacterial membranes of live cells. If a diagenetically-resistant lipid P fraction persists in sediments, biomass determined by quantifying lipid P will be overestimated.

3.2.2 Biomass Determined from ATP concentration

Adenosine-5'-triphosphate (ATP) is another biochemical that is frequently used to estimate biomass abundance (e.g., Holm-Hansen & Booth, 1966; Hodson *et al.*, 1976; Karl & Holm-Hansen, 1976; Karl, 1993). ATP, an intermediate in the intracellular transfer of P and energy, is crucial to cell function. The turnover of ATP in a typical cell is rapid, and a molecule of ATP will generally be consumed within a minute following its formation (Chapman & Atkinson, 1977). Similarly, since ATP is rapidly dissipated after metabolic death (Holm-Hansen & Booth, 1966; King & White, 1977), the ATP concentration in sediments is a robust indicator of the total ATP content of living biomass.

A difficulty encountered when using ATP to estimate biomass abundance is the variable intracellular concentration of ATP, a response to changes in cell physiology (Goldenbaum *et al.*, 1975; Bobbie *et al.*, 1978; Davis & White, 1980). Nevertheless, the good correlation between sediment ATP concentration and direct cell counts (Webster *et al.*, 1985) indicates that sedimentary ATP concentration is a reliable proxy for biomass abundance.

3.3 Study Site: The Central Santa Barbara Basin

The concentrations of lipid P and ATP were measured in a sediment core from the central Santa Barbara Basin (Core SBB9610: 34°17.25'N; 120°02.2'W, 576 m water depth). The study site underlies highly productive coastal waters, resulting in high sedimentation rates (~0.8 cm/y: Reimers *et al.*, 1990) and relatively high (~4% by weight) total organic carbon content. Low oxygen concentrations in bottom water, due to a combination of restricted circulation and high organic matter flux, inhibit colonization by benthic macrofauna. Filaments of *Beggiatoa spp.*, which are autotrophic, sulfur-oxidizing bacteria, bind together detrital minerals and organic matter to form an interfacial bacterial mat that further prevents physical disruption of the sediment surface (DeBoer, 1981). As a consequence, sediments are finely laminated, maintaining millimeter-scale gradients in sediment chemistry.

ATP and phospholipids, the two compounds examined here, are present in all living cells and thus are non-specific measures of total biomass (e.g., Holm-Hansen, 1969; Goldenbaum *et al.*, 1975). In these sediments, as in many pelagic sediments, bacteria account for only part of the total cellular biomass in surface sediments. The fresh organic matter provided by the interfacial bacterial mat can be an important food source for benthic grazers (Stein, 1984; Baird & Thistle, 1986), and benthic foraminifera, dominated by *Nonionella stella*, are abundant in the surface sediments (Bernhard & Reimers, 1991; Bernhard *et al.*, 2000). In addition, there are smaller numbers of protozoa and nematodes (Bernhard *et al.*, 2000). In deep ocean benthic communities, the meiofauna and non-bacterial microfauna are generally limited to the upper few centimeters of sediments (Burnett, 1977), while bacteria can have a deeper distribution (Rittenberg, 1940). A similar pattern is observed in the Santa Barbara Basin, where foraminifera are observed only to depths of 3 to 4 centimeters (Bernhard & Reimers, 1991), but bacteria have been observed to depths of 70 meters (Cragg *et al.*, 1995). Based on an increasing number of observations of deep bacterial biomass at depths of hundreds

of meters in marine sediments (e.g., Cragg *et al.*, 1990; Cragg *et al.*, 1992; Getliff *et al.*, 1992; Parkes *et al.*, 1994), it is likely that bacteria exist at depths greater than 70 meters in the Santa Barbara Basin, as well.

3.4 Methods

3.4.1 Sediment Collection and Core Sectioning

Sediments were collected in October, 1996 aboard the R/V Sproul (Scripps Institute of Oceanography) using a Soutar box corer. A 50 cm sub-core was sectioned at high resolution (0.6 cm intervals) under an inert (N₂) atmosphere at *in situ* temperatures. In addition, a bulk surface sample (0-0.3 cm) was collected, providing enough material for ³¹P-NMR analysis of the surface sediment lipid extract. Splits were immediately preserved for subsequent ATP analysis, and the remaining sediment was stored frozen (-30°C). Upon return to WHOI, frozen samples were weighed, and then freeze dried in the collection tubes. After freeze drying, the dry weight was recorded, and the salt-corrected dry weight was calculated by assuming an average pore water salinity of 34.2‰ (Sholkovitz & Gieskes, 1971), and using the equation:

$$\text{Salt - Corrected Dry Weight} = \text{Dry Weight} - \left[(\text{Wet Weight} - \text{Dry weight}) * \frac{34.2}{1000} \right] \quad (3-1)$$

3.4.2 Measurement of Phospholipid Concentration

Phospholipids were extracted from freeze-dried sediment samples using the modified Bligh and Dyer (1959) method described in Chapter 2. Quantitative (105±5%) recovery of phospholipids from sediments using the Bligh and Dyer method has been demonstrated (White *et al.*, 1979c). Briefly, sediments were extracted first with 2-

propanol, then exhaustively extracted by successive treatments with a single phase of chloroform: methanol: water (1:2:0.8). The total extract was partitioned into chloroform and aqueous phases, with phospholipids partitioned quantitatively into the chloroform extract. The chloroform extract was concentrated by rotary evaporation. The aqueous extract was lyophilized, then re-hydrated in milli-Q H₂O. For each extract, duplicate aliquots were combusted, hydrolyzed in 1 M HCl, and total P was determined spectrophotometrically. Results of duplicate analyses of phosphate concentration in the lipid fraction agreed to within 1.6% (range: 0 to 6%), and in the aqueous fraction duplicate analyses agreed to within 9.7% (range: 0.8 to 24%). Errors in the aqueous fraction were amplified due to the low absolute phosphate concentrations typical for this fraction.

3.4.3 Measurement of ATP Concentration

Immediately after sectioning the core, sediment splits were preserved for subsequent ATP analysis by the luciferin-luciferase photometric method (Holm-Hansen & Booth, 1966; Morrison *et al.*, 1977; Karl & Holm-Hansen, 1978; Webster *et al.*, 1984). Following this method, 0.1 cm³ of sediment was suspended in a vial with 1.025 ml of phosphate-citrate buffer and heated at 100°C for 10 minutes. Samples were allowed to cool, then transferred to microcentrifuge tubes and stored at -30°C until analysis.

ATP concentration was measured using an EG&G Berthold Lumat LB 9501 luminometer. Samples were thawed (but kept cold) and centrifuged for 1.5 minutes at 5000 g. A split of the sample (250 µL) was added to the reaction vessel, and 250 µL of firefly extract (FLE-50, Sigma) was automatically injected by the luminometer. Each sample vial was run in duplicate and ATP concentration was calculated from a standard curve. The series of standards ranged in concentration from 0.1 to 1000 ng ATP/ml. Samples ranged in concentration from 1 to 402 ng ATP/mL. The relative percent error between duplicate analyses was between 2 and 26%, with an average error of 11%.

3.5 Conversion Factors

To compare the ATP and lipid P concentration data, and to calculate biomass abundance using these proxies, it was necessary to make assumptions about cell composition and cell dry weight. Balkwill *et al.*, (1988) presented a review of published values for such conversion factors. The conversion factors adopted for this study are described below.

3.5.1 Bulk Density, Cell P_{org} and C Content, Cell Numbers

The P biochemical concentrations determined directly in this study were μmol lipid P per gram sediment and μmol ATP per cm^3 sediment. To convert between grams and cm^3 of sediment, the bulk density (g/cm^3) of each sediment interval was calculated by dividing the salt-corrected dry weight by the original sediment volume (before drying). Sediments were packed into 50 mL collection tubes during core sectioning, so all sediment weights were divided by 50 cm^3 to calculate bulk density. To calculate total carbon and P_{org} per cell, it was assumed that cells are 3% P by dry weight (e.g., Neidhardt, 1987) and that each cell contains 20 fg C (Lee & Fuhrman, 1987). Cell numbers were calculated assuming 5.9×10^{12} cells per gram dry weight of cellular biomass (White *et al.*, 1979a; Balkwill *et al.*, 1988).

There is inherent uncertainty in the estimation of cell dry weight and carbon content. Much of this uncertainty arises from assumptions about cell size and geometry. The assumption made here is that the cells are relatively small, uniform spheres. Such an assumption is reasonable at depth in these sediments (below 3-4 cm), but is less robust near the sediment-water interface, where large-celled, non-spherical *Beggiatoa* contribute a substantial fraction of the total biomass. There is also a large uncertainty in the calculated cell abundance near the sediment-water interface because of the presence of non-bacterial sediment biomass (e.g., benthic foraminifera). Therefore, the bacterial

numbers calculated here are presented only as a model for comparison of the ATP and lipid P data. Although the cell numbers calculated at depth in the sediments are likely to closely reflect actual bacterial abundance, the bacterial cell counts estimated for surface sediments are likely overestimates, since no correction was made for larger cell sizes and non-bacterial sources of cellular ATP and lipid P.

3.5.2 Phospholipid and ATP Intracellular Concentrations

To calculate phospholipid abundance based on lipid P concentration, an average phospholipid molecular weight of 748 was assumed, corresponding to a simple membrane glycerophospholipid with two C₁₆ fatty acids (Harvey *et al.*, 1984). Although cellular phospholipid content between 3 and 9% of cell dry weight has been observed (Osborne *et al.*, 1974), a phospholipid content of 3% (Harvey *et al.*, 1984) to 3.5 % (White *et al.*, 1979c) is generally assumed. The slightly higher value of 3.5% was adopted as a best estimate of cellular concentration (Table 3-2). The full range from 3 to 9% was used to calculate possible ATP:lipid P intracellular ratios.

The large number of published values for concentrations of intracellular ATP are quite variable. Expressed as a ratio of total cellular carbon to ATP (g C:g ATP), the range of reported values is from 43 to 9500 (Karl, 1980). However, most of the reported ratios are between 100 and 300, with more extreme values generally reported for stressed, and often nutrient-starved cultures (Karl, 1980). Such nutrient-starved conditions are not found in the surface sediments of the Santa Barbara Basin. A C:ATP ratio of 250 is often assumed (Holm-Hansen, 1973; Webster *et al.*, 1985), based on extensive monoculture studies. For example, in culture studies of marine algae (Holm-Hansen, 1970) and marine bacteria (Hamilton & Holm-Hansen, 1967), cellular C:ATP ratios of 287 and 250, respectively, were observed in a wide number of species. The canonical value of 250 was adopted here as a best estimate of cellular concentration. The maximum and minimum

end-member estimates of C:ATP considered here are 500 and 43, representing the range of reported values for prokaryotes grown under nutrient-replete conditions (Karl, 1980).

As mentioned above, cell carbon content has an associated uncertainty because it relies on an assumed cell size. Since the range of intracellular ATP concentrations considered here is calculated based on a C:ATP ratio, this imposes a similar uncertainty of the intracellular ATP concentration estimate. However, our assumptions are supported by the direct measurements of intracellular ATP concentration reported by Webster *et al.* (1985). Their measured value of 1.7 ng ATP per 10^7 cells, or 3.3×10^{-13} μmol ATP per cell, is often cited as the “canonical” value and is in excellent agreement with the range of intracellular ATP concentrations considered here (Table 3-2).

Table 3-2. Literature values of ATP and phospholipid cell content used to estimate the expected ATP: lipid P ratio in living biomass. The concentrations shown in the top row (boldface) are widely accepted average intracellular concentrations for these biochemicals and are therefore our best estimate for cell composition in these sediments.

	Total C: ATP Ratio (wt/wt)	ATP ^c (μmol /cell)	Phospholipid as % cell dry weight	Lipid P ^f (μmol /cell)
Best estimate	250 ^a	1.58x 10⁻¹³	3.5 % ^d	7.93 x 10⁻¹²
Minimum	500 ^b	7.89×10^{-14}	3 % ^e	6.80×10^{-12}
Maximum	43 ^b	9.17×10^{-13}	9 % ^e	2.04×10^{-11}

a: (Hamilton & Holm-Hansen, 1967; Webster *et al.*, 1985)

b: (Karl, 1980)

c: $\text{ATP } (\mu\text{mol} / \text{cell}) = [(20 \text{ fg C/cell}) * (\text{g ATP/g C}) * (1 \text{ mol ATP}/507 \text{ g ATP}) * (1 \mu\text{mol}/10^9 \text{ fmol})]$

d: (White *et al.*, 1979c)

e: (Osborne *et al.*, 1974)

f: $\text{Lipid P } (\mu\text{mol} / \text{cell}) = (\text{g phospholipid} / 100 \text{ gdw biomass}) * (\text{gdw biomass} / 5.9 \times 10^{12} \text{ cells}) * (1 \text{ mol phospholipid} / 748 \text{ g}) * (10^6 \mu\text{mol} / 1 \text{ mol})$

3.6 Results

3.6.1 P Biochemical Concentration Profiles

Downcore profiles of lipid P, ATP, and water-soluble P concentration in core SBB9610 are shown in Figure 3-1. The concentration axes have been scaled so that the core-top values coincide, allowing a comparison of the three depth trends. Both lipid P and ATP concentrations decrease dramatically with depth, although the decrease in ATP is more pronounced. The two profiles share common features such as the small subsurface maximum at approximately 3 cm depth, and both ATP and lipid P approach a constant value with depth.

The concentrations of water-soluble P are intermediate between those of ATP and lipid P, and decrease similarly with depth. As described in Chapter 2, the solubilization of P compounds in the solvent extract, and subsequent partitioning of P compounds between chloroform and aqueous phases, results in efficient partitioning of non-lipid P compounds into the aqueous phase. These water-soluble compounds are presumed to derive dominantly from the intracellular material that is released into solution by cell lysis as a consequence of solvent extraction. Thus, the measured P concentration in the aqueous extract is likely to reflect the concentration of polar biochemicals such as nucleic acids, nucleotides, phosphosugars and other simple P biochemicals. However, these data should be interpreted cautiously because adsorption to sediments can result in inefficient extraction of compounds such as nucleic acids (Craven & Karl, 1984), and the extraction efficiency of the above-listed compounds by this method has not been explicitly tested.

3.6.2 Biomass profiles inferred from ATP and Lipid P concentration

Figure 3-2 shows depth profiles of bacterial cell abundance in Core SBB9610 calculated from lipid P and ATP concentrations. Cell numbers are calculated assuming

the “best estimates” of ATP and lipid P cell concentration given in Table 3-2, and using the following equations:

$$\text{Lipid P estimate: } \frac{\text{cells}}{\text{cm}^3} = \left(\frac{\mu\text{mol lipid P}}{\text{g sed}} \right) \times \left(\frac{1 \text{ cell}}{7.93 \times 10^{-12} \mu\text{mol lipid P}} \right) \times \left(\frac{\text{g sed}}{\text{cm}^3} \right) \quad (3-2)$$

$$\text{ATP estimate: } \frac{\text{cells}}{\text{cm}^3} = \left(\frac{\mu\text{mol ATP}}{\text{cm}^3} \right) \times \left(\frac{1 \text{ cell}}{1.58 \times 10^{-13} \mu\text{mol ATP}} \right) \quad (3-3)$$

Presenting the data in terms of bacterial cell numbers is a simplification because, as discussed earlier, the fraction of biomass accounted for by foraminifera and other benthic organisms, and the composition of their cellular biomass, is not well known.

Compared to the lipid P data, the number of cells calculated using ATP concentration is slightly higher at the sediment-water interface, but much lower at depth. While the number of cells calculated from the lipid P data decreases by a factor of 5 in the upper 40 cm of this core, the ATP-based cell numbers decrease by more than two orders of magnitude.

3.6.3 Direct Comparison of ATP and Lipid P Data

For all intervals where both lipid P and ATP concentrations were measured, the data were plotted for direct comparison (Figure 3-3). Since this direct comparison can be made only for sediment intervals where both ATP and lipid P were analyzed, the data presented in Figure 3-3 represents only a subset of the data presented in Figure 3-1. To interpret changes in the ATP:lipid P ratio, it is useful to recall that both drop off sharply with depth and therefore low concentrations of lipid P and ATP represent data from deeper in the core. When total lipid P concentration is plotted versus ATP concentration in the sediments, the expected relationship for a purely biomass signal would be a straight line, with the slope defined by the cellular ratio of ATP to phospholipid. That is not the case for these data, where there is no consistent linear relationship. The three lines shown

in Figure 3-3 represent the range of possible ATP:lipid molar ratios based on values published in the literature (Table 3-3). The two end-member ratios represent minimum and maximum extremes in ATP and phospholipid intracellular concentration. In the sediment intervals near the top of the core (0 to 3 cm), the ATP:lipid P ratios are consistent with the calculated range of cell composition. These surface sediments include the interfacial bacterial mat and are expected to have very high biomass abundance. In contrast with the surface sediments, the amount of lipid P in the deeper intervals of the core is always higher than the concentration predicted from ATP concentration, and exceeds the range of accepted cellular ATP: lipid P ratios (Figure 3-3).

Table 3-3. Intracellular concentrations of ATP and lipid P used to calculate reasonable ratios for ATP: Lipid P in sediment biomass. Each of the values is taken from the published concentration given in Table 3-2. The ratio of 1:50 is calculated from the best estimates for concentration of both ATP and lipid P. The other 2 ratios are end-member estimates for maximum ATP/minimum lipid P (1:7) and minimum ATP/maximum lipid P (1:258).

	ATP:Lipid P Molar Ratio		
	<u>1:7</u>	<u>1:50</u>	<u>1: 258</u>
ATP ($\mu\text{mol /cell}$)	9.17×10^{-13}	1.58×10^{-13}	7.89×10^{-14}
Lipid P ($\mu\text{mol /cell}$)	6.80×10^{-12}	7.93×10^{-12}	2.04×10^{-11}

3.7 Discussion

3.7.1 Is the Lipid P Reservoir Derived Entirely from Living Biomass?

There are several lines of evidence to suggest that some fraction of the sedimentary lipid P reservoir is not associated with living biomass. The fact that the ATP concentration in these sediments decreases much more rapidly with depth than the lipid P

concentration indicates that different processes are driving these depth profiles. Using the reasoning that a more pronounced decline with depth indicates more rapid degradation, these depth profiles indicate that ATP is degraded more quickly than either the water-soluble P or lipid-P reservoirs extracted from these sediments. Rapid degradation of ATP relative to other biochemicals is expected based on the high free energy liberated by hydrolysis of its phosphoanhydride bonds. The fact that the profile of water-soluble P is intermediate between the ATP and lipid P profiles supports the idea that lipid P is more resistant to degradation after cell death than water-soluble P biochemicals such as DNA, RNA, and phosphosugars.

The higher relative concentrations of lipid P in deep intervals of the core indicate a much higher bacterial cell count than is indicated by the ATP data. The number of bacteria calculated from ATP concentration (10^8 cells/cm³ sediment) is more consistent with counts of the number of dividing cells (10^8 cells/cm³ sediment) at similar sediment depths (30 cm) at this site (Cragg *et al.*, 1995) and with the cell numbers of 10^8 - 10^9 per cm³ generally observed in shallow marine sediments (Dale, 1974; Deming & Colwell, 1982; Harvey *et al.*, 1984).

Differences in the ATP and lipid P profiles may partly reflect changes in cell physiology of the sediment biota. The fact that the ATP:lipid P ratio for the core-top interval falls between the "best estimate" and the maximum ATP end-member ratio is not surprising for this environment. Fresh organic matter is delivered to the grazing population, and the abundance of sulfide and nitrate (from the underlying sediments and overlying water, respectively) stimulate the growth of sulfur-oxidizing *Beggiatoa*, forming a bacterial mat at the sediment-water interface. The resulting levels of metabolic activity are considerably higher than in more typical marine sediments with no interfacial bacterial mat, and this elevated metabolic activity tends to increase cellular concentrations of ATP (Davis & White, 1980). However, the measured concentrations of

phospholipid at depth in the core (below ~4 cm) cannot be explained by biomass, given the ATP concentration and any reasonable estimate of ATP:lipid P ratio (Figure 3-3).

There is a significant fraction of sedimentary lipid P that is unaccounted for by living biomass. This observation is consistent with the results of Harvey *et al.*, (1984), who found that the measured concentrations of lipid P and polar lipid fatty acids were too high to be accounted for by the bacterial population in a number of sediment types (turbidite, carbonate, hemipelagic) in the deep Venezuela Basin. The Santa Barbara Basin data support their cautionary note that phospholipid-based estimates of biomass can be erroneously high. To estimate the fraction of total lipid P in the “residual”, or non-biomass, fraction, lipid P derived from living biomass was calculated for the deepest sediment interval (38-40 cm) using the ATP:lipid P ratios in Table 3-3. The calculated values are shown in Table 3-4. In the end-member case where the concentration of ATP in cells is very high (ATP:lipid P = 1:7), almost none of the lipid P is associated with biomass. However, even when the other end-member is considered, with very high cell phospholipid content and very low ATP (ATP:lipid P = 1:258), less than half of the total lipid P in the deeper sediments can be accounted for by living biomass. The fraction of total lipid P unaccounted for by biomass is similarly high for the entire core below 4 cm depth. Only for values calculated using the extreme end-member ratio of 1:258 does any interval contain more than half of the total lipid P as biomass (Table 3-4). However, even in this extreme case, there is a minimum of 36% of total lipid P in the residual fraction. The observation that such a large fraction of lipid P persists in sediments after cell death is at odds with the assumption that all phospholipids are immediately degraded upon cell death.

If we assume that this residual lipid P represents a non-biomass “background” concentration in the sediments, and that the remaining lipid P concentration profile is driven by changes in biomass abundance, the data can be plotted as shown in Figure 3-4. In both panels shown in Figure 3-4, the slopes of the end-member ATP:lipid P ratios are

identical to those in the previous figure. However, the lines have been shifted up from the origin, such that the y-intercepts reflect different values for the non-biomass “background” lipid P concentration. In the top panel, the y-intercept corresponds to a residual lipid P concentration of 0.07 $\mu\text{mol/g}$, the concentration calculated for the deepest sediment interval (see Table 3-4). In the bottom panel, the end-member ratio lines have been shifted up to achieve the best fit to the data. In this case, residual lipid P is 0.14 $\mu\text{mol/g}$, corresponding to the y-intercept of the plotted sediment data. In both cases, subtracting the “background” from the total lipid P concentration improves the agreement between the theoretical and the measured ratio of ATP:lipid P. When the residual P concentration calculated for the bottom of the core is assumed (Figure 3-4a), there is still an excess of lipid P in some sediment intervals compared to even the most lipid-rich end-member. A reasonable interpretation for these data is that the concentration of residual lipid P changes with depth. Because the data are better fit when a higher “background” lipid P concentration is assumed (Figure 3-4b) the residual lipid P concentration in the sediment intervals presented in Figure 3-4 is probably closer to 0.14 $\mu\text{mol/g}$ than to the

Table 3-4. Calculated concentrations of biomass and “residual” lipid P fractions in sub-surface sediments (38-40cm). The amount of lipid P accounted for by biomass is calculated using the estimates of cellular ATP:lipid P ratio from Table 3-3. Residual lipid P is calculated by subtracting biomass P from the total lipid P concentration for this sediment interval (0.07 $\mu\text{mol/g}$). Values shown in parentheses for the residual as a percent of lipid P indicate the range calculated for all sediment intervals below 4 cm.

ATP: Lipid P	Lipid P in Biomass ($\mu\text{mol/g}$)	Residual Lipid P ($\mu\text{mol/g}$)	Residual as % Total Lipid P
1:7	0.0007	0.0693	99 (98-100)
1:50	0.0050	0.0650	93 (88-96)
1:258	0.0258	0.0442	63 (36-82)

core-bottom residual lipid P concentration of 0.07 $\mu\text{mol/g}$. Therefore, while the data suggest that a large fraction of the lipid P in these sediments is not associated with biomass, it is likely that both biomass abundance and the size of the residual lipid P pool change with depth.

3.7.2 What Is the Nature of the “Residual” Lipid P?

A potential explanation for the persistence of lipid P in these sediments is that some fraction of the total phospholipid pool is inherently resistant to degradation due to its chemical structure. Phosphonolipids, phospholipids with a phosphonate linkage, have been considered a likely candidate for a stable phospholipid fraction. Phosphonates are a minor class of P biochemicals that contain a direct C-P bond, which is not as sensitive to hydrolysis as the C-O-P bond found in most P biochemicals (Aalbers & Bieber, 1968). This structural feature could potentially lead to enhanced preservation of phosphonolipids in sediments (Ingall *et al.*, 1990; Berner *et al.*, 1993).

^{31}P -NMR is currently the only technique capable of resolving the abundance of phosphonates in natural sediment samples (Glonek *et al.*, 1970). Differential hydrolysis, the only other method that has been proposed for phosphonate quantification (Aalbers & Bieber, 1968), is not sensitive enough for analysis of sediment extracts (see Appendix C-1). The abundance of phosphonates was measured in lipid extracts from sediments at the sediment-water interface (0-0.3 cm) and at depth (38-40 cm). The fraction of the total P signal accounted for by phosphonates was multiplied by the total lipid P concentration in each extract to give the absolute phosphonolipid concentration for the two intervals. The prominent diester peak in both lipid spectra is consistent with domination of this fraction by simple membrane phospholipids (Figure 3-5). Phosphonates comprise a small fraction (<10%) of total lipid P in surficial sediments, but are below detection limits at depth (Figure 3-5), indicating degradation at the same or more rapid rates than diester phospholipids. From the top to the bottom of the core, the lipid P concentration decreases

by a factor of 15. If phosphonolipids represented a stable residual pool of lipid P, the relative importance of the phosphonate peak should increase with depth. On the contrary, at the current resolution of the two spectra, phosphonates comprise less of the total lipid pool at depth than in the surface sediments. The apparent absence of phosphonolipids at depth suggests that residual lipid P is not a stable component by virtue of a resistant chemical structure. What then, is the explanation for persistence of a pool of lipid P that equals or exceeds the biomass contribution in deeper sediments?

Lipid P may be protected from degradation by physical association, either with mineral surfaces or with a resistant organic matrix, such as humic acids. Harvey *et al.*, (1984; 1986) suggested sorption of membrane lipids to an organic matrix as a preservation mechanism to explain the observed excess of phospholipid above that predicted from independent biomass estimates (similar to the results of this study). However, even if some lipid P is physically associated with humic compounds, laboratory experiments by Brannon and Sommers (1985) suggest that phospholipids that are not chemically bound but only mixed with model humic compounds are enzymatically degraded as quickly as free phospholipids. It is not clear if simply mixing humic compounds with lipids adequately simulates the protection which might occur in natural systems, and protection by an organic matrix is an avenue for further investigation. Alternatively, it is possible that lipid P is sorbed to mineral surfaces rather than to organic matter.

3.7.3 The Contribution of Biomass to the Total Organic P Reservoir

A fraction of the P_{org} in sediments represents cellular biomass, particularly at sites characterized by high bacterial abundance, such as the deep Santa Barbara Basin. So far, we have focussed on the relative importance of biomass in the lipid P fraction. To evaluate diagenetically-driven depth trends in total P_{org} , it is important to estimate the contribution of biomass to the total P_{org} reservoir. The sediment concentration profiles of

ATP and lipid P indicate that a significant fraction of lipid P is not derived from living biomass. However, using both the lipid P and ATP concentration data, the fraction of the total P_{org} in these sediments that can be attributed to living biomass can be constrained.

A maximum concentration for biomass P_{org} can be calculated for these sediments if we assume that all of the measured lipid P is derived from intact membranes (almost certainly an over-estimate). Phospholipids account for approximately 20% of cellular P (Neidhardt, 1987). Therefore, the total concentration of sedimentary biomass P_{org} is calculated by multiplying lipid P by 5. These calculated values for surface sediments (0-0.3 cm) and at depth (38-40 cm) are shown in Table 3-5. At maximum, biomass P can account for 6-33% of the total P_{org} in this core, with the highest biomass contribution in surface sediments.

A second estimate of total biomass P was calculated based on sediment ATP concentration. Total biomass dry weight was calculated assuming 0.08 fg ATP/cell (20 fg C/cell: (Lee & Fuhrman, 1987); C:ATP = 250: Holm-Hansen, 1973; Webster *et al.*, 1985). Total biomass P was calculated, again for surface sediments and at depth, assuming that cells are 3% P by dry weight (Neidhardt, 1987; Table 3-5). The percent of P_{org} contributed by biomass in surface sediments exceeds the total sediment organic P concentration measured on the bulk sediments. The simplest explanation for this over-

Table 3-5. Estimates of the total sedimentary P_{org} reservoir accounted for by living biomass, using estimated biomass calculated from sediment concentrations of lipid P and ATP. For both ATP and lipid P estimates, biomass P is calculated using the best estimate of cellular concentration of these biochemicals (Table 3-2). Calculated biomass abundance is expressed both as the absolute concentration of P_{org} and as a percentage of total sediment P_{org} .

Depth	Total P_{org} ($\mu\text{mol/g}$)	Lipid P Estimate			ATP Estimate		
		Lipid P ($\mu\text{mol/g}$)	Biomass P ($\mu\text{mol/g}$)	% total P_{org} as biomass	ATP ($\mu\text{mol/g}$)	Biomass P ($\mu\text{mol/g}$)	% total P_{org} as biomass
0- 0.3 cm	18.28	1.2	6.0	33%	0.068	43.1	236%
38- 40 cm	5.46	0.07	0.35	6%	0.0001	0.06	1%

estimate is that the ATP concentration in biomass at the sediment-water interface is higher than has been assumed here. As mentioned previously, elevated metabolic rates tend to increase the concentration of ATP per cell. The fact that the ratio of ATP:lipid P in the surface interval is much higher than in the rest of the core supports this idea. At depth, the estimate of biomass P based on ATP concentration is about 1% of total sediment organic P. Thus, live cells contribute very little of the total organic P at depth in the sediments, with a maximum estimate of 6% (from lipid P) and a minimum estimate of 1% (from ATP). Biomass estimates calculated using the ATP data are likely to be more accurate than the lipid P estimates, given that there is strong evidence for a non-biomass lipid P fraction in these sediments. However, under extreme circumstances such as those in the bacterial-mat-dominated surface sediments of the Santa Barbara Basin, ATP-based biomass estimates may also prove unreliable. Even when lipid P concentrations, which contain a non-biomass “background”, are used to calculate the biomass contribution to sedimentary P_{org} , it is clear that most of the P_{org} in these sediments is not associated with living biomass. The fraction of total P_{org} contributed by living biomass decreases with depth, but even in surface sediments, biomass is likely to represent less than 10% of total sedimentary P_{org} .

3.8 Conclusions

Phosphorus-containing biochemicals constitute the primary source of P to marine sediments. Thus, to understand which P_{org} compounds are preferentially preserved or diagenetically altered by examining depth trends in sediments, it is important to quantify the living biomass component of P_{org} in marine sediments. Both ATP and lipid P have been used as proxies for sediment bacterial biomass. Measurements of the sediment concentrations of ATP and lipid P indicate that a significant fraction of lipid P is not associated with living biomass. Biomass abundances estimated from sediment lipid P

concentrations at this site are therefore likely to be too high. This result concurs with other studies that suggest viable, intact cells cannot explain the entire pool of sedimentary lipid P.

There is no evidence for preferential preservation of phosphonolipids, previously considered a resistant class of phospholipids, during diagenesis. In the absence of a mechanism for preservation due to inherent chemical structure, it is likely that some physical protection mechanism (association with either mineral surfaces or with an organic matrix) is responsible for the persistence of lipid P in sediments after cell death.

The results of this study indicate that instantaneous degradation of all simple P_{org} compounds after cell death cannot be assumed. While ATP is attributed entirely to biomass, a fraction of the extractable lipid P pool in Santa Barbara Basin sediments is not associated with live cells. As a result, estimates of biomass abundance based on lipid P concentration are likely to be too high. Below 4 cm, biomass is an insignificant factor in determining P_{org} concentration and depth distribution. Differences in the depth distributions of P_{org} biochemicals in marine sediments, such as those observed here, provide important insights into P_{org} preservation mechanisms and indicate that a closer examination of physical protection mechanisms for these compounds is warranted.

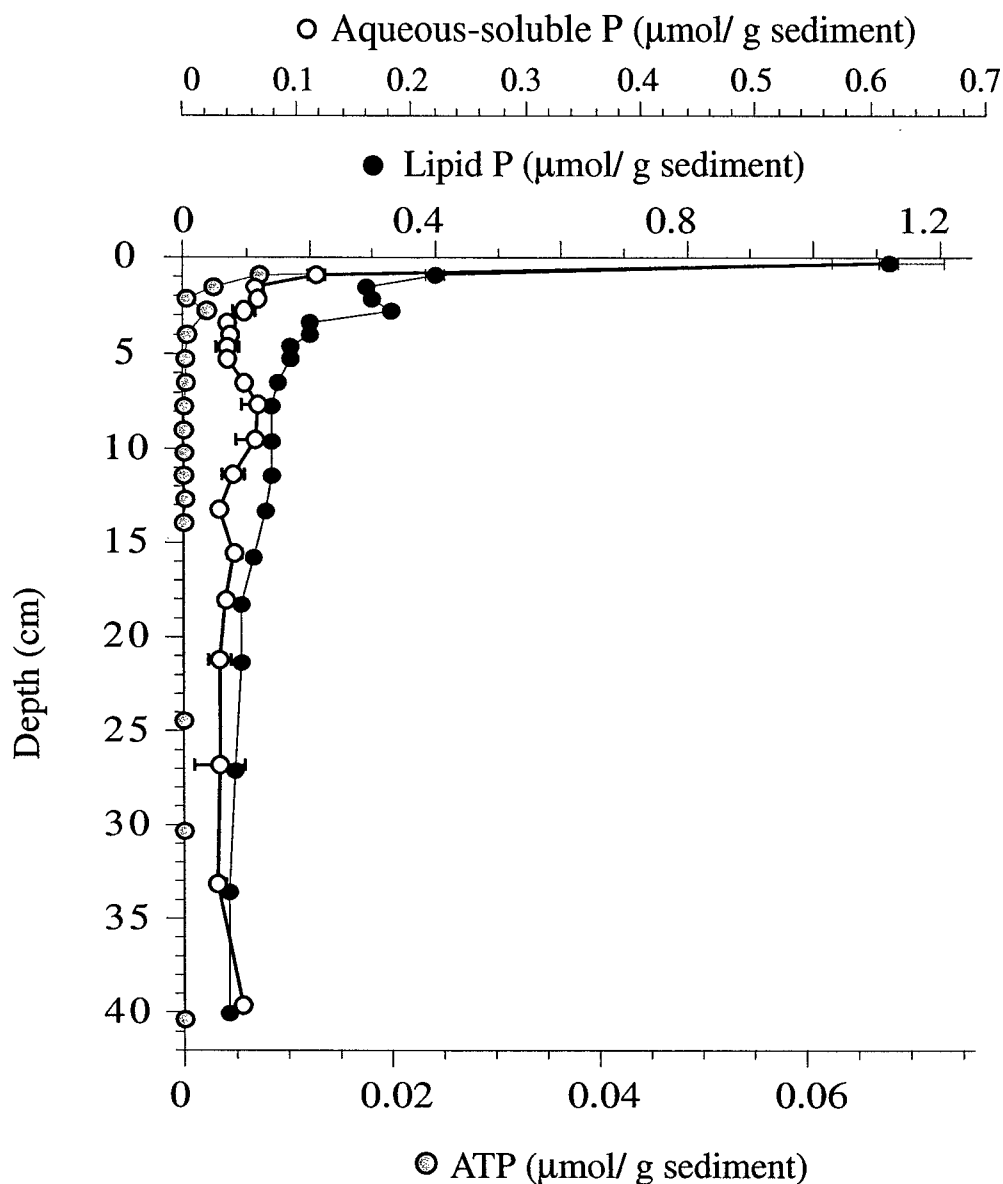


Figure 3-1. Profiles of lipid P, ATP, and water-soluble P concentrations in core SBB9610 J. The concentration axes have been scaled so that the concentrations in the top interval (0-0.6 cm) coincide, allowing the relative decrease with depth to be visually compared. ATP concentration drops off most sharply with depth, leaving a residual lipid P fraction that is not accounted for by biomass. The depth profile of aqueous P concentration is intermediate between the ATP and lipid P concentration profiles. Error bars (most smaller than the symbol size) indicate the range of concentrations measured in duplicate analyses.

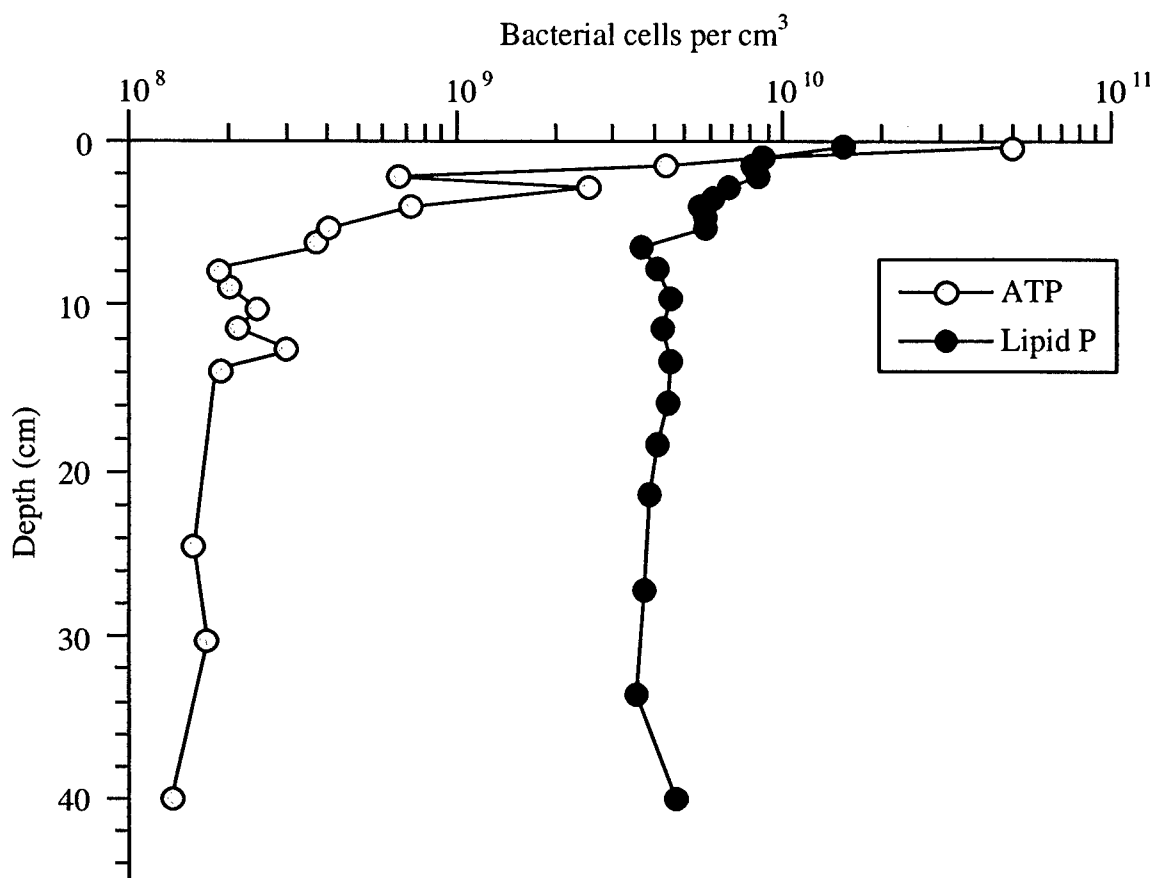


Figure 3-2. Profiles of bacterial cell numbers calculated from lipid P and ATP sediment concentrations. The number of cells estimated from ATP concentration is higher than the lipid P estimate in surface sediments, but more than an order of magnitude lower in deeper sediments. The assumed cellular concentration of each biochemical used to calculate cell numbers is the “best estimate” value from Table 3-2.

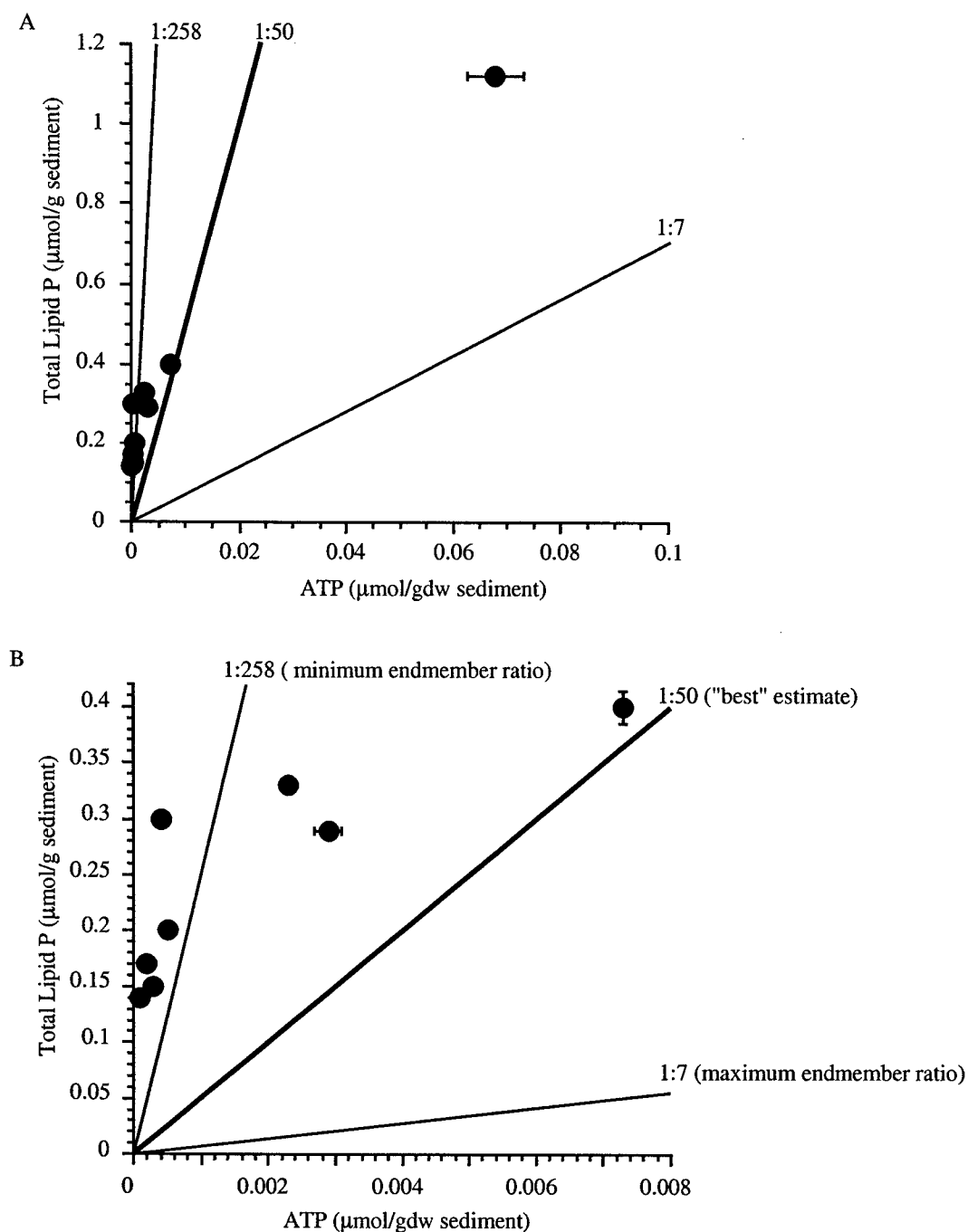


Figure 3-3. Comparison of lipid P and ATP measured in the same sediment intervals. The top panel (A) shows all of the data. In the bottom panel (B), the surface interval (0-0.6 cm) has been omitted and the expanded axes show more detail for the other intervals. The three lines represent a range of ATP: Lipid P ratios estimated from the literature (Table 3-3). In the deeper sediments (with lower ATP and lipid P concentration), the measured lipid P concentration is consistently higher than can be explained using even the most lipid-rich and ATP-poor end-member estimate of biomass composition.

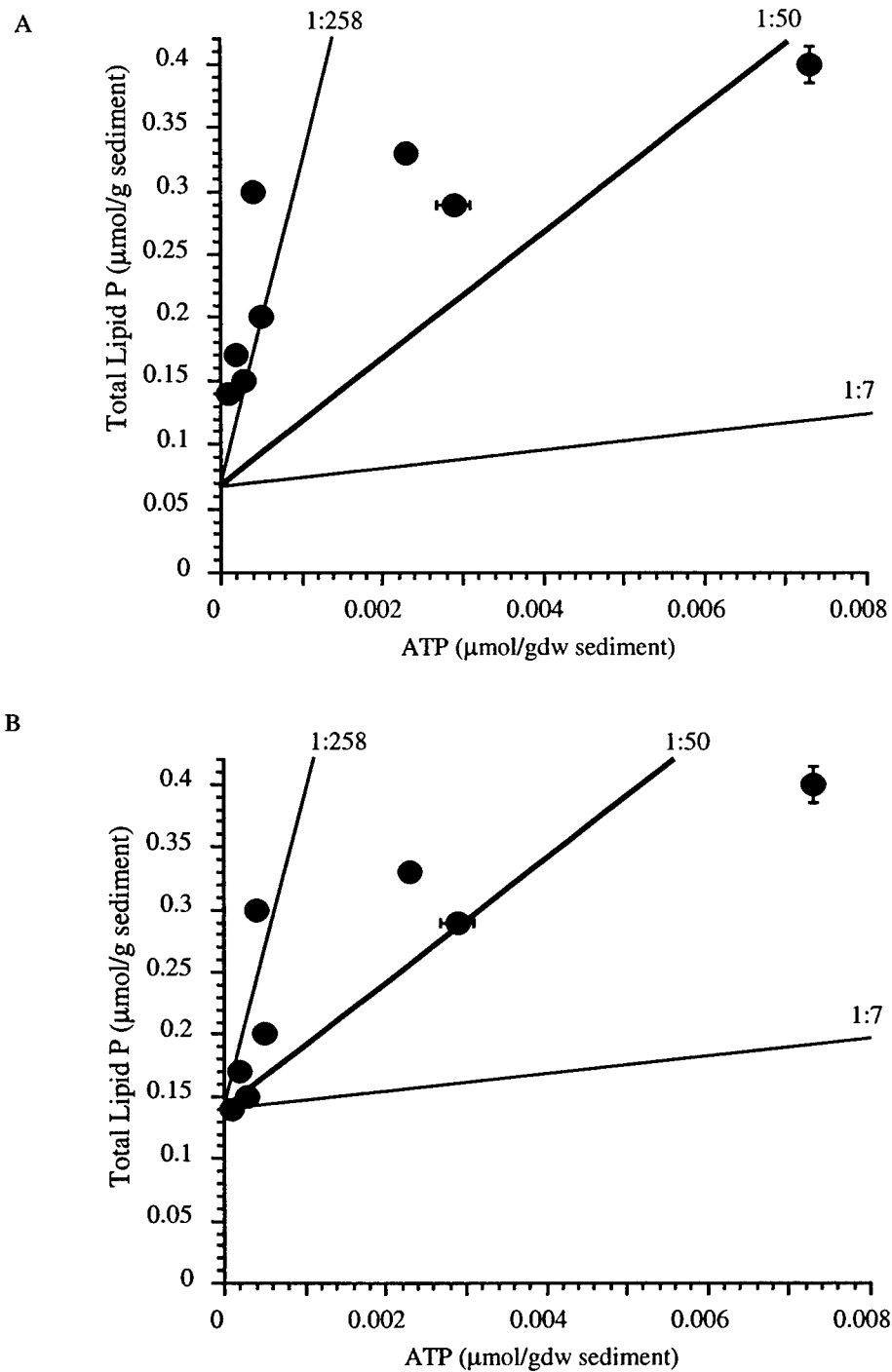


Figure 3-4. Same as Figure 3-3, but the lines representing cellular ATP:lipid P ratios have been shifted up along the y-axis by (A) 0.07 μmol lipid P and (B) 0.14 μmol lipid P. The positive y-intercept is interpreted as a non-biomass, “background” concentration of residual lipid P.

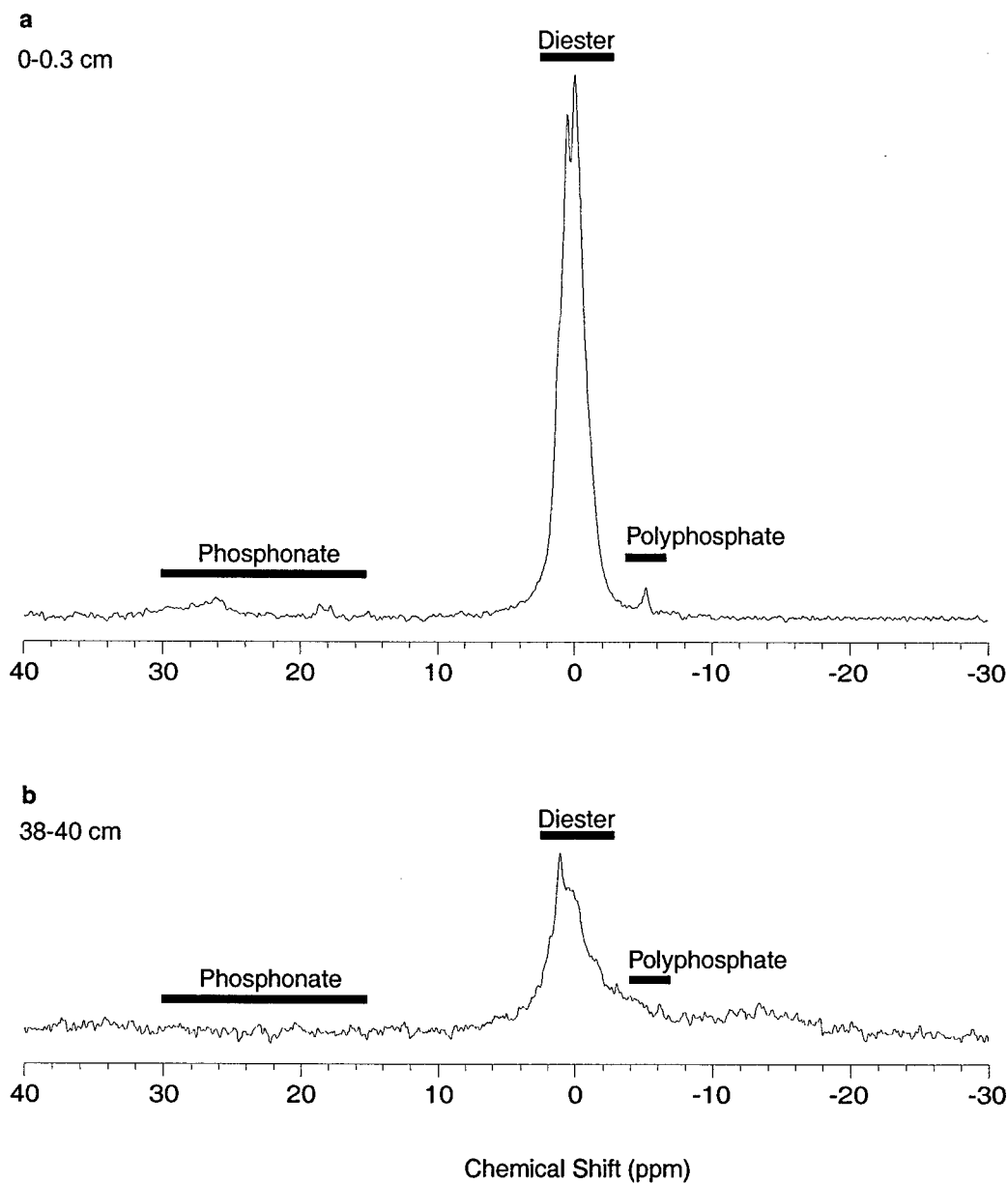


Figure 3-5. ^{31}P -NMR spectra of lipid extracts from Santa Barbara Basin sediments from the sediment-water interface (0-0.3 cm) and at depth (38-40 cm). Spectra were acquired with a 100 ppm spectral window centered at 0 ppm, using a 45° flip angle, 0.4 second acquisition time and a delay of 1 second. The lock solvent was *d*-chloroform (CDCl_3). Broad band decoupling was used to suppress nuclear overhauser effects. 25 Hz line-broadening was applied to both spectra. The solvent extract from the deep interval contains less total P than the surface interval sample (3.4 compared to 13.2 μmol total P), and a longer run time was used (surface interval: 55,000 scans; deeper interval: 67,500 scans). The region indicated by each horizontal bar on the spectra represents a functional group and encompasses chemical shifts diagnostic of many individual compounds. Phosphonates are a minor component (<10% of total P) in the surface sediment extract, but are below the detection limit in the deep sample

Chapter 4

Chemical Structure and Diagenetic Modification of Organic P in Marine Sediments

*"Every generation thinks it has the answers, and
every generation is humbled by nature."*

- Phillip Lubin

4.1 Introduction

It is generally accepted that P, an essential nutrient, limits marine productivity on geological timescales (Holland, 1978; Broecker & Peng, 1982; Smith, 1984; Codispoti, 1989). P can limit productivity in the present-day ocean (Fisher *et al.*, 1992; Smith & Hitchcock, 1994; Cotner *et al.*, 1997; Karl & Tien, 1997; Monaghan & Ruttenberg, 1999) as well. Therefore, to predict the productivity potential of modern and ancient oceans, it is essential to understand the processes controlling the input and removal of P. Burial of phosphorus in marine sediments is the ultimate mechanism of P removal from the oceans (Ruttenberg, 1993). Organic phosphorus (P_{org}) represents a significant portion (*ca.* 25%) of the total P buried in marine sediments and is therefore an important component of the total marine P budget (Froelich *et al.*, 1982; Ruttenberg, 1990). Since efflux from sediments can be a substantial source of phosphate to bottom waters (Colman & Holland, 2000), establishing the processes that control degradation of P_{org} compounds is key to understanding controls on P-return to the water column where it can again fuel biological production.

Despite its importance to the total marine P budget, the chemical form of P_{org} in marine sediments is virtually uncharacterized, and little is known about the processes that control remineralization of sedimentary P_{org} . The known primary (i.e., biological) forms of P_{org} are considered biochemically labile, with highly energetic bonds and enzyme-susceptible structures (e.g., White *et al.*, 1977; Paul *et al.*, 1987; Westheimer, 1987). Given this initial lability, the observation that some fraction of P_{org} persists in deeply buried sediments (Filippelli & Delaney, 1994; Delaney & Anderson, 1997) and in ancient shales (Ingall *et al.*, 1993) is surprising. Possible explanations for the persistence of P_{org} in marine sediments are discussed below.

4.1.1 What Controls The Distribution And Composition Of P_{org} In Marine Sediments?

Persistence of some fraction of P_{org} in deeply buried sediments and ancient shales suggests that at least one, and possibly all, of the following must be true: (i) measured P_{org} represents simple biochemicals from intact, live cells that are remineralized when cells die, (ii) some fraction of P_{org} is preserved because it is inherently refractory due to specific structural features, (iii) transformation reactions during diagenesis convert initially labile P_{org} compounds into more refractory compounds, (iv) P_{org} compounds are preserved via some mechanism of physical protection, (v) analytical artifacts result in an overestimation of the quantity of P_{org} that survives diagenesis. The importance of biomass in the sedimentary P_{org} reservoir (possibility (i)) was discussed in Chapter 3. The results of Chapter 3 indicate that below the sediment-water interface (where the bacterial mat contributes a large fraction of total organic matter), biomass only contributes a small fraction (<10%) of the total sedimentary P_{org} pool in the central Santa Barbara Basin, and cannot substantially drive observed P_{org} depth trends. Since this environment represents an extreme in high bacterial abundance and the contribution of biomass to total P_{org} below the sediment-water interface is still small, this result can be

reasonably extrapolated to other marine sedimentary environments. Each of the other explanations listed above will now be discussed in more detail.

4.1.1.1 Chemical Structure

An important focus of this chapter is to determine the extent to which chemical structure controls susceptibility to microbial degradation. Intuitively, it is reasonable that the structure of an organic compound should control its rate of degradation. The chemical structure of each molecule will dictate which enzymes are required to cleave its chemical bonds, and molecular conformation may prevent or enhance compound degradation due to steric effects. However, the relative importance of chemical structure compared to other controls on organic matter preservation, such as physical protection mechanisms and depositional environment, is not clear.

The initial rapid remineralization of P_{org} in marine sediments is usually attributed to destruction of more chemically labile components (Krom & Berner, 1981; Ingall & Van Cappellen, 1990), and by inference the deeply buried P_{org} is assumed to be more refractory. Analytically, this hypothesis has been difficult to test because few methods are available for studying P_{org} at the molecular level. P_{org} compounds present at depth in sediments may represent refractory compounds directly inherited from source materials or, alternatively, they may represent the diagenetically altered products of initially labile compounds.

4.1.1.2 Physical Protection

Preservation of intrinsically reactive organic compounds may be enhanced by physical protection mechanisms, including sorption to mineral surfaces or sequestering within a matrix of macromolecular, resistant organic material. For example, based on the observation that mineral surface area and total organic carbon are linearly correlated, it

has been suggested that sorption onto sediment surfaces enhances preservation of organic matter (e.g., Keil *et al.*, 1994a; Mayer, 1994b). The mechanism for enhanced organic matter preservation in high-surface-area sediments is not known, although several plausible explanations have been suggested: (1) Mayer (1994a; 1994b) observed that much of the organic matter associated with sediment particles is sorbed in small mesopores (<10 nm wide), which would effectively prevent enzymatic access to these molecules. (2) Sorption of organic matter to mineral surfaces should favor condensation reactions by increasing the local concentration of organic molecules. The resulting larger, more refractory molecules are likely to be more resistant to remineralization (Hedges, 1988). (3) Hydraulically, organic matter tends to be deposited in the same low-energy regimes where high surface area (small grain sized) particles are deposited (e.g., Tyson, 1987). (4) The decreased pore spaces between the grains in high surface area sediments restricts circulation of pore water fluids, leading to a buildup of inhibitory metabolites and preventing replenishment of terminal electron acceptors (Tissot & Welte, 1984).

Physical protection of organic compounds need not be limited to sorption by mineral surfaces. Harvey *et al.* (1984; 1986) suggested sorption to an organic matrix as a mechanism for preservation of membrane phospholipids in marine sediments. Emerson and Hedges (1988) pointed out that any organic molecule, no matter what its structure, may be preserved if it is contained within a protective organic matrix. Much like organic matter contained within mesopores, organic matter that is sequestered within a humic matrix may be protected from degradation by steric inhibition of enzymes.

It is important to recognize that the influence of chemical structure and physical protection can be interrelated. There are structural features of particular compounds that make them more prone to sorption, either to organic matter or to mineral surfaces. For example, large geomacromolecules are expected to have a greater affinity for mineral surfaces than simpler organic compounds (Theng, 1979), which may enhance the

protective influence of mineral surfaces. Further, it may be analytically difficult to distinguish between structural and physical protection mechanisms because it is difficult to discern compounds that have been physically sequestered versus those that are chemically bound within a humic matrix.

4.1.1.3 Analytical Artifact: Overestimation of P_{org} ?

In Chapter 2, the fraction of inorganic P in base extracts determined by indirect (wet chemical difference method) and direct (spectroscopic) techniques was compared. These data suggest that a fraction of P_{org} measured by the wet chemical technique is actually orthophosphate. The formation of metal bridges between orthophosphate and humic compounds, described extensively in the limnological and soil science literature (e.g., Levesque & Schnitzer, 1967; Koenings & Hooper, 1976; Francko & Heath, 1982; Gerke, 1992; Jones *et al.*, 1993; Frossard *et al.*, 1995), may result in inaccessibility of orthophosphate to simple acid extraction, and overestimation of the organic P pool. Such an analytical artifact could potentially lead to a large overestimation of the total organic P buried and ultimately preserved in marine sediments.

4.1.2 Depositional Environment: The Importance of Bottom-Water Oxygen Concentration

The relative importance of chemical structure, physical protection, and analytical artifacts on the observed depth distribution of sedimentary P_{org} may be modulated by differences in depositional conditions, such as the concentration of oxygen in bottom waters. Organic matter concentrations (e.g., Demaison & Moore, 1980) and burial efficiency (e.g. Canfield, 1993) tend to be elevated in sediments located in anoxic basins and other regions of low oxygen concentration. In fact, the only sediments with organic

matter loadings higher than predicted from sediment surface areas are from deposits that underlie waters with very low oxygen concentrations (Mayer, 1994a).

When compared to other degradation pathways, aerobic degradation yields the most energy per unit of organic material decomposed. While it has been proposed that intrinsic rates of oxic and anoxic degradation are not significantly different (e.g., Lee, 1992), degradation pathways are likely to differ, reflecting different bacterial communities and available oxidants. In addition to the direct control of oxygen in degradation, the absence of oxygen in bottom waters inhibits colonization of the sediments by burrowing macrofauna. The resulting buildup of inhibitory metabolites and decrease in availability of terminal electron acceptors tends to depress rates of organic matter degradation.

There is a second effect of low oxygen conditions that is potentially important for degradation of P_{org} compounds. It has long been recognized that when waters overlying the sediments are oxic, phosphorus is bound in the sediments, and that P is released under reducing conditions. There is disagreement, however, as to whether the mechanism for this P release is physicochemical (Mortimer, 1941; Bostrom & Pettersson, 1982; Doremus & Clesceri, 1982) or due to bacterial activity (Gächter *et al.*, 1988; Hupfer & Uhlmann, 1991; Gächter & Meyer, 1993). In oxic sediments, P can be sorbed to the surfaces of ferric iron minerals. Under reducing conditions, these minerals reductively dissolve and P is released into pore waters, where it can diffuse out of the sediments. If this sorbed P is in organic form, redox conditions have a direct influence on the fate of organic P. If the released P is inorganic, buildup of orthophosphate in sediment pore waters can reduce the activity of enzymes such as phosphatases, reducing the efficiency of P_{org} degradation. The role of oxygen in preservation of phospholipids has been suggested previously (Harvey *et al.*, 1984; 1986). In addition, Ingall and Jahnke (1994) observed increased preservation of P in bioturbated vs. laminated shales. The absence of bioturbation is used as an indication that low oxygen conditions

prevented colonization of surface sediments by macrofauna that mix sediments. The implication of these results is that P is more efficiently removed from sediments under low-oxygen conditions, suggesting that redox conditions are important for the ultimate preservation of P in sedimentary rocks.

It is difficult to examine the influence of bottom water oxygen alone on the quantity or structural characteristics of P_{org} compounds. Many other parameters such as organic matter rain rate, extent of sediment mixing, and differences in the sediment bacterial community are correlated with changes in oxygen concentration. The sediment cores chosen for this study were intended to provide a comparison of P_{org} concentration and composition under different depositional conditions. To provide this contrast, it is not necessary that only oxygen concentration vary between these two sites. Throughout this chapter, these different parameters will be referred to collectively as the “effects of oxygen”. Although the contrast between cores will be discussed in terms of bottom water oxygen concentration, it is understood that any differences observed between cores are likely to depend on these other variables, as well.

4.1.3 Approach of this Study

To develop a mechanistic framework for understanding controls on the ultimate burial and preservation of sedimentary P_{org} , the relative importance of chemical structure, physical protection and depositional environment, as well as potential analytical artifacts, are considered in this chapter. The hypothesis that the structure of P_{org} compounds controls susceptibility to microbial degradation can only be tested by examining the molecular-level composition of the P_{org} pool. Simultaneous examination of changes with depth in total P_{org} , the size of P_{org} reservoirs, and the concentration of specific P functional groups was used to assess the molecular-level changes in P_{org} that drive bulk trends. The sequential extraction method described in Chapter 2 was used to separate P reservoirs based on their chemical solubility, and solution ^{31}P -NMR was used

to quantify the abundance of specific functional groups in base-soluble (humic-associated) P_{org} . The concentrations of P in aqueous and most lipid P extracts were too low for NMR analysis, and most of the information about specific functional groups is therefore restricted to the base-soluble fraction. ^{31}P -NMR data have been used previously to identify phosphomonoester, phosphodiester and phosphonate linkages in marine sediments (Ingall *et al.*, 1990). However, because Ingall *et al.* (1990) analyzed single depth intervals, they could not comment on the relative abundance of these functional groups with depth. Berner *et al.* (1993) examined P structure in three sediment horizons using solid state ^{31}P -NMR, which allowed only differentiation between phosphonate and non-phosphonate P compounds. In both of the above studies, observations of measurable phosphonate concentrations in marine sediments were used to argue for their preferential preservation during diagenesis.

Preferential preservation of compounds that are thought to be inherently structurally resistant, such as phosphonates, would suggest that chemical structure plays an important role in P_{org} preservation. However, the results of this study, which include high-resolution depth profiles of the molecular-level distribution of sedimentary P_{org} compounds, indicate that there is no preferential preservation of phosphonates in marine sediments. This suggests either that structure is not a primary control, or that phosphonates are not resistant compounds. The lack of evidence for direct structural control on P_{org} preservation shifts the focus to the most likely alternative mechanism, sorption of P_{org} compounds on mineral surfaces or in an organic matrix. Protective sorption can result in the preservation of compounds that would normally be subject to microbial attack (Emerson & Hedges, 1988; Keil *et al.*, 1994a; Keil *et al.*, 1994b; Mayer, 1994b).

A comparison of total inorganic P determined by ^{31}P -NMR and wet chemical methods in Santa Barbara Basin cores is used to evaluate the potential analytical artifact in P_{org} quantification suggested by the data in Chapter 2. The data from two sediment

cores, in addition to the core discussed in Chapter 2, consistently demonstrate that the amount of organic P estimated by wet chemical techniques (such as the commonly-used Aspila *et al.* (1976) method) can be erroneously high. These data suggest that burial rates for organic P in marine sediments must be re-evaluated. Further, the P_{org} overestimation artifact, and its potential impact on P_{org} burial rates, has broader implications for the global marine P budget.

4.2 Study Site: Santa Barbara Basin

Santa Barbara Basin is the northernmost of the shallow California Borderland basins. A sill in the western portion of the basin at 470 m water depth restricts the exchange of bottom waters with water outside of the basin and dictates that deep basin water can only be replaced by Pacific Intermediate water within the oxygen minimum zone (Thornton, 1984). High organic matter flux further depletes deep water oxygen such that dissolved oxygen at water depths greater than 550 m is often less than 0.1 ml/l (Emery & Hulsemann, 1962) and dissolved sulfide in bottom water ranges from 5-15 nM (Kuwabara *et al.*, 1999). Deep basin water can be replaced by turbidity flows (Sholkovitz & Soutar, 1975) or by flushing, associated with periods of intensified upwelling (Sholkovitz & Gieskes, 1971).

A characteristic feature of the central basin sediments is varves, consisting of alternating light and dark bands in the laminated sediments deposited in annual couplets of approximately 0.4 cm thickness. The sediments are compacted over time to form millimeter-scale varves that extend meters deep in the sediment column. The origin of these sediment couplets is a subject of considerable debate. The dominant source of sediment input changes seasonally, with terrigenous sediment delivery most important in winter (dark bands), and delivery of planktonic debris during the warmer months (light bands). Changes in the composition and the porosity of the two sediment layers can be

attributed to these changes in input (Hulsemann & Emery, 1961; Emery & Hulsemann, 1962; Thunell *et al.*, 1995). The response of the interfacial bacterial mat to changes in organic matter supply can further enhance differences in sediment structure (Soutar & Crill, 1977). Alternatively (or in addition), annual cycles of bottom water oxygen replenishment and depletion can lead to changes in the bacterial mat growth and thereby affect sediment properties (Reimers *et al.*, 1990).

Three cores from the Santa Barbara Basin were analyzed: two from the central basin, and one from the basin margin (Figure 4-1). The extraction of lipid P from all three cores was identical. However, because core J was analyzed prior to full optimization of the base extraction protocol, base extract data from core J are not strictly comparable to the other two cores (described below). Therefore, most of the comparison in this chapter will be based on the two SB 11/95 cores, A and C. However, comparison of the bulk sediment data and of the lipid P and water-soluble P concentrations in cores C and J are used to evaluate temporal and spatial variability in the central basin, since the two cores were collected at different times and different locations within the central basin (Table 4-1).

Because the coring sites for SB11/95 cores A and C were in close proximity, they have comparable 'input' terms (e.g., organic matter rain rates, terrestrial organic matter contribution, sedimentation rate). The principal difference between them is bottom water oxygen content, with the deep basin (core C) characterized by anoxic bottom water and varved sediments, whereas the basin margin site (core A) is suboxic and bioturbated to a depth of 5-10 cm. Analyses of the stable carbon isotopic composition of sedimentary organic matter indicate that the dominant source of organic matter to the basin is marine, with a more minor contribution by river-borne terrestrial organic matter (Schimmelmann & Tegner, 1991).

The varved sediments of the central Santa Barbara Basin provide an ideal setting for the study of diagenetic changes in P_{org} structure. To infer diagenetic changes based

Table 4-1. Location of cores used for this study.

Core Designation	Date Collected	Latitude	Longitude	Water Depth	Core Type
SBB 9610, Core J	October 2, 1996	34°17.25' N	120°02.2' W	576 m	Box Core
SB 11/95, Core A	November 30, 1995	34°18.57' N	119°54.18' W	431 m	Multi-Core
SB 11/95, Core C	December 1, 1995	34°13.85' N	120°02.89' W	590 m	Multi-Core

on depth profiles in sediments, steady-state deposition must be assumed. Such an assumption is robust in the central Santa Barbara Basin, given the physically undisturbed sediments and relatively uniform seasonal depositional cycles (Hulsemann & Emery, 1961). The repeating couplets that characterize these sediments imply regularity in the input of sediments to this location. Pore water profiles show uniformly increasing concentrations of ammonia with depth (Figure 4-2), which indicate progressive remineralization of organic matter during sediment burial, and further support the assumption of steady-state conditions. For the margin core, bioturbation is restricted to the upper 5-10 cm. Although this makes the assumption of steady state less robust in the surface intervals, steady state can be assumed for the sediments below the zone of bioturbation. A comparison of P_{org} concentration and molecular-level structure between the two sites in the Santa Barbara Basin is used to evaluate the importance of bottom water oxygen concentration on the sedimentary P_{org} reservoir. One factor that might compromise the assumption of steady-state is the possibility of secular changes in P and/or sediment input over the time-span represented by these cores. For simplicity, the possibility of such secular changes has not been explicitly considered in this study.

4.3 Methods

4.3.1 Sample Collection and Sub-sampling

Samples were collected during two cruises to the Santa Barbara Basin. Sampling locations are shown in Figure 4-1. The three cores used in this study are listed in Table 4-1, along with their locations and date of collection. All cores were collected with a visually undisturbed sediment-water interface and greater than 10 cm overlying water. Each core was sectioned at *in situ* temperatures in a glove bag under an inert (N_2) atmosphere, and overlying water was siphoned off within the glove bag immediately prior to sectioning to minimize contact with air. After sectioning (and, for cores A and C, after pore water removal), all samples were capped tightly, removed from the glove bag, and frozen for shipment back to WHOI. Sediments remained frozen (-30°C) until they were freeze-dried for analysis.

Multi-cores from two sites (SB11/95, Cores A and C) were collected aboard the R/V Pt. Sur, operated by Moss Landing Marine Laboratories. Core A was collected from the basin margin on November 30, 1995, and core C was collected from the central basin in December 1, 1995. The top 3.5 cm of these cores were sectioned at 0.35 cm intervals. Deeper intervals were sectioned at 0.6 cm intervals. After sectioning, samples from both SB 11/95 cores were centrifuged and pore water was collected under N_2 . These two multi-cores will be referred to hereafter simply as core A and core C.

A Soutar box core was collected from the central basin in October 1996 aboard the R/V Sproul, operated by Scripps Institute of Oceanography. The core was sampled with a 50 cm (4 inch ID) PVC acid-cleaned subcore. This core will be referred to hereafter as core J. The entire core was sectioned at 0.6 cm intervals. In addition, after all subcores were placed, the remaining surface sediment of the box core ($\sim 0\text{--}0.3$ cm, mainly interfacial bacterial mat) was collected in an acid-cleaned bottle and frozen. This additional material provided enough surface sediment for analysis by ^{31}P -NMR.

4.3.2 Sample Handling

Upon return to WHOI, frozen samples were weighed, and then freeze dried in the collection tubes. For core J (pore water not removed), the dry weight was recorded after freeze drying, and the salt-corrected dry weight was calculated by assuming an average pore water salinity of 34.2‰ (Sholkovitz & Gieskes, 1971), and using the equation:

$$\text{Salt - Corrected Dry Weight} = \text{DryWeight} - \left[(\text{Wet Weight} - \text{Dry weight}) * \frac{34.2}{1000} \right] \quad (4-1)$$

For each sediment interval, an aliquot of freeze-dried, untreated sediment (approximately 0.3 g per sample) was retained for surface area estimation. The remaining split of each sample was crushed lightly with an agate mortar and pestle. The sediment was ground just enough to pass through a sieve with a mesh size of 125 µm. Excessive grinding was avoided to prevent creation of artificial surface area. Splits of the ground samples were retained for ²¹⁰Pb and elemental analyses, and the remaining sediment was weighed into 50 mL glass centrifuge tubes to begin the sequential extraction procedure.

4.3.3 Extraction of Soluble P Reservoirs

Sediments from cores A and C, as well as the surface (0-0.3 cm) and deepest (38-40 cm) intervals of core J, were extracted using the full sequential extraction procedure described in Chapter 2 and detailed in Appendix A. The lipid P and water-soluble P fractions of all sediment intervals in cores A, C, and J were extracted using the procedures described in Chapter 2.

4.3.4 P Analyses

All of the procedures used for analysis of P in extracts and solid samples have been described in Chapter 2. The Aspila *et al.* (1976) method was used to quantify total P and inorganic P in sediments, and organic P was calculated by difference. Sediment P was measured before and after sequential extraction. All sediment extracts were analyzed for total dissolved P (TDP) using a modified Aspila-TDP method. A select number of acid and base extracts from cores A and C were analyzed for soluble reactive P (SRP), and total organic P (TOP) was calculated by difference.

4.3.5 ^{31}P -NMR Analyses

The parameters used for ^{31}P -NMR analyses are discussed in Chapter 2, and are briefly outlined here. All solution ^{31}P -NMR spectra were run on a Varian 500 MHz (11.7 T) nuclear magnetic resonance spectrometer with a broad band probe. Spectra were collected on a 100 ppm spectral window centered at 0 ppm, using a 45° flip angle, 0.6 second acquisition time and a relaxation delay of 1.5 seconds. Broad band decoupling with WALTZ modulation was used to suppress nuclear overhauser effects. ^{31}P chemical shifts are reported relative to an external standard of phosphoric acid, which is assigned a chemical shift of 0 ppm.

Samples were prepared with 25% D_2O as a lock solvent, and all extracts had a pH greater than 13.4, so that chemical shift variations imposed by changes in pH were negligible (see Chapter 2). Between 35,000 and 80,000 scans were collected for each sample, the signal was averaged, and 10 Hz of line-broadening was applied.

The peak areas in solution NMR spectra are proportional to the number of nuclei, or chemical linkages, of a given type in the extracts. The absolute concentration of P functional groups in each base extract was calculated by multiplying total base-extractable P, determined directly by the wet chemical Aspila-TDP method, by the

fraction of P in each functional group region, determined by integrating peak areas on the spectra.

4.3.6 ^{210}Pb

An age model for cores A and C was developed using depth profiles of unsupported (or “excess”) ^{210}Pb . Zheng (1999) measured detailed downcore profiles of excess ^{210}Pb for multicores recovered in the same deployments as cores A and C. For this study, excess ^{210}Pb was measured in selected intervals from cores A and C and these data were compared to Zheng’s results.

Freeze-dried, ground ($<125\ \mu\text{m}$) sediments were weighed into jars and analyzed with a planar gamma ray detector. Supported ^{210}Pb was determined by counting the ^{214}Pb γ -rays (295.2 and 352 KeV) and total ^{210}Pb was determined by counting the 46.5 KeV γ -ray. Unsupported ^{210}Pb was calculated by subtracting supported ^{210}Pb from total ^{210}Pb . Peak counts were corrected for background blanks and counting efficiency was determined using pitchblende standards. Total ^{210}Pb measurements were corrected for self-absorbance by measuring gamma ray emission from a Ra-U source through the sample (source placed on top of the sample jar) to the detector.

4.3.7 Surface Area

Mineral surface area measurements were performed on a Coulter SA-3100 Surface Area and Pore Size Analyzer using a five-point BET (Brunauer-Emmett-Teller adsorption isotherm) method. No pretreatment was used to remove organic matter before surface area determinations. Before analysis, salts were removed by washing the sediments with 10% acetone in water (Mayer, 1999), and then lyophilized. Samples were degassed prior to analysis. A sediment standard run between samples had a measured surface area within 2% of the expected value.

4.4 Results

4.4.1 Unsupported ^{210}Pb

Excess ^{210}Pb concentrations measured in core A are slightly higher than those measured by Zheng (1999) in a parallel core collected in the same multi-core deployment (Figure 4-3). This difference may indicate better recovery of the core-top in core A compared to the parallel core used by Zheng. An alternative explanation is that lateral heterogeneity in sediment deposition resulted in sediment focussing at core A. However, this would have increased the overall sedimentation rate (not observed) instead of uniformly increasing excess ^{210}Pb concentration. Although only four intervals were analyzed, the slopes of the natural log $[\text{xs-}^{210}\text{Pb}]$ vs. depth relationships (used to calculate sedimentation rate) for the two data sets are in excellent agreement. For core C, the agreement of data from this study with the more complete data set by Zheng from a parallel core (same multi-core deployment) was sufficient (Figure 4-3) to warrant using Zheng's data to calculate the sedimentation rate and develop an age model for the core.

The sedimentation rate can be calculated using the slope of the best-fit regression of natural log $[\text{xs-}^{210}\text{Pb}]$ vs. depth and the equation:

$$\text{Sedimentation rate (cm/y)} = \frac{\lambda}{\text{slope}} \quad (4-2)$$

where λ is the decay rate of ^{210}Pb (0.0311/y).

The sedimentation rate determined for core A is 0.3 cm/y and for core C is 0.55 cm/y. These sedimentation rates are similar to previously measured rates of 0.4 cm/y (Koide *et al.*, 1972), and are consistent with observations that accumulation rates in slope cores (such as core A) tend to be somewhat lower than in central basin cores (Huh *et al.*, 1987). In margin core A, the change in slope of the natural log $[\text{xs-}^{210}\text{Pb}]$ vs. depth at about 10 cm is evidence for mixing of the near-surface sediments. No such change in

slope is seen in core C, indicating that it is essentially totally unmixed, which is consistent with the presence of varves and reflects inhibition of burrowing macrofauna in the anoxic central basin. Sediment mixing in core A will tend to result in higher ^{210}Pb concentration in deeper sediments. As a simplification, mixing of ^{210}Pb has not been taken into account in the age model. Therefore, the age of sediments in core A may be slightly underestimated.

4.4.2 Bulk Sediment P

Total, inorganic and organic P concentration in sediments from the three Santa Barbara Basin cores are shown in Figure 4-4, and listed in Tables 4-2, 4-3, and 4-4. In all three cores, organic and inorganic P concentrations decrease rapidly from maxima at the sediment surface to fairly constant values with depth. Organic P in each core represents approximately 20-30% of total P, which is typical for marine sediments. P concentrations in the two central basin cores (core J, core C) are slightly higher than in the margin core (core A). Within the central basin, P concentrations in core J are higher than those in core C.

While the difference in core-top P concentration between core A and core C is mostly due to P_{org} (21 $\mu\text{mol/g}$ sediment for core C, 11 $\mu\text{mol/g}$ sediment for core A), the difference between the two central basin cores is mainly due to differences in core-top TIP (55 $\mu\text{mol/g}$ sediment for core C, 72 $\mu\text{mol/g}$ sediment for core J). To compare the asymptotic values for P concentration at depth in each core, the mean and standard deviation of all TP, TIP, and TOP concentrations below 5 cm depth were calculated for each core. At depth, the three cores have similar TP concentrations (Core A: 38.3 ± 1.6 $\mu\text{mol/g}$; Core C: 38.7 ± 2.5 $\mu\text{mol/g}$; Core J: 38.5 ± 1.9 $\mu\text{mol/g}$) and a similar fraction of organic and inorganic P. The distribution of P between organic and inorganic P phases is

Table 4-2. Solid-phase concentration of total, inorganic, and organic P for margin core A, determined by the Aspila method. Errors indicate the range of P concentration measured in duplicate analyses. The depth interval indicates the mid-depth for a homogenized interval.

Depth (cm)	$\mu\text{mol TP /g sed}$			$\mu\text{mol TIP /g sed}$			$\mu\text{mol TOP /g sed}$		
0.18	58.9	±	0.4	48.0	±	0.1	10.9	±	0.5
0.53	50.7	±	0.6	40.4	±	0.1	10.2	±	0.6
0.88	48.7	±	0.4	39.3	±	0.9	9.4	±	1.0
1.23	47.2	±	0.1	37.8	±	0.9	9.3	±	0.9
1.58	43.4	±	0.9	35.6	±	0.0	7.9	±	0.9
1.93	45.6	±	1.3	37.0	±	0.2	8.6	±	1.3
2.28	43.2	±	0.3	34.5	±	0.1	8.7	±	0.4
2.63	42.5	±	0.2	34.1	±	0.1	8.4	±	0.2
2.98	41.4	±	0.0	33.8	±	0.5	7.6	±	0.5
3.34	40.9	±	0.6	33.4	±	0.1	7.5	±	0.6
3.82	40.8	±	0.3	33.2	±	1.0	7.6	±	1.1
4.43	40.0	±	0.2	32.6	±	1.0	7.4	±	1.1
5.04	40.3	±	0.7	33.4	±	0.3	6.9	±	0.7
5.65	41.2	±	0.1	32.6	±	0.1	8.6	±	0.2
6.26	39.5	±	0.3	32.6	±	0.7	6.9	±	0.8
6.88	39.7	±	0.9	32.9	±	0.6	6.8	±	1.1
7.49	39.6	±	0.1	32.6	±	0.6	7.0	±	0.6
8.10	40.0	±	0.4	32.9	±	0.0	7.1	±	0.4
8.71	39.4	±	0.5	31.2	±	1.2	8.3	±	1.3
9.32	39.5	±	0.2	32.1	±	0.3	7.4	±	0.4
9.94	40.2	±	0.5	31.9	±	1.2	8.4	±	1.3
10.55	39.8	±	1.1	32.0	±	0.3	7.9	±	1.1
11.16	39.0	±	0.6	32.2	±	0.4	6.9	±	0.7
11.77	39.1	±	0.5	31.7	±	0.5	7.5	±	0.7
12.38	38.2	±	0.6	31.6	±	0.6	6.7	±	0.8
13.00	38.9	±	0.3	30.8	±	0.5	8.1	±	0.6
18.61	37.1	±	0.4	30.9	±	0.1	6.2	±	0.4
19.22	37.5	±	0.7	31.5	±	0.3	6.0	±	0.8
22.03	34.3	±	0.1	28.8	±	0.1	5.5	±	0.1
24.83	36.6	±	1.6	30.5	±	0.1	6.1	±	1.6
25.44	37.0	±	0.6	30.7	±	1.2	6.3	±	1.3

Table 4-3. Solid-phase concentration of total, inorganic, and organic P for deep basin core C, determined by the Aspila method. Errors indicate the range of P concentration measured in duplicate analyses. The depth interval indicates the mid-depth for a homogenized interval.

Depth(cm)	$\mu\text{mol TP/g sed}$			$\mu\text{mol TIP/g sed}$			$\mu\text{mol TOP/g sed}$		
0.18	75.6	±	2.6	54.5	±	0.7	21.1	±	2.7
0.53	55.4	±	0.5	38.5	±	1.0	17.0	±	1.1
0.88	46.2	±	0.1	32.0	±	0.4	14.2	±	0.4
1.23	42.9	±	0.0	30.1	±	0.0	12.8	±	0.0
1.58	45.0	±	2.8	31.5	±	0.8	13.5	±	2.9
1.93	47.6	±	0.3	32.2	±	0.8	15.4	±	0.8
2.28	43.0	±	1.2	31.4	±	1.0	11.6	±	1.5
2.63	42.2	±	0.1	30.6	±	1.1	11.6	±	1.1
2.98	42.4	±	2.7	28.8	±	0.9	13.6	±	2.9
3.34	43.3	±	1.4	29.9	±	0.8	13.4	±	1.6
3.82	42.4	±	2.2	29.6	±	1.8	12.8	±	2.8
4.43	43.7	±	0.4	29.6	±	0.3	14.1	±	0.5
5.04	43.1	±	0.5	28.5	±	0.2	14.5	±	0.5
5.65	44.2	±	0.0	30.5	±	0.9	13.7	±	0.9
6.26	42.2	±	0.7	30.5	±	0.5	11.7	±	0.9
6.88	42.3	±	1.8	30.2	±	0.5	12.1	±	1.8
7.49	37.5	±	1.5	28.6	±	0.1	8.9	±	1.5
8.10	38.3	±	0.2	28.6	±	0.7	9.7	±	0.7
8.71	36.8	±	0.5	27.8	±	1.2	9.1	±	1.3
9.32	36.3	±	3.6	28.0	±	0.2	8.3	±	3.6
9.94	38.8	±	1.9	27.4	±	0.6	11.4	±	2.0
10.55	36.7	±	0.5	28.2	±	1.1	8.6	±	1.2
11.16	38.0	±	2.8	28.1	±	1.2	10.0	±	3.0
11.77	36.6	±	0.0	28.1	±	0.7	8.5	±	0.7
12.38	37.6	±	3.2	27.0	±	0.5	10.6	±	3.2
13.00	37.4	±	0.7	26.7	±	1.5	10.7	±	1.7
18.61	36.9	±	0.4	28.8	±	0.4	8.1	±	0.6
19.22	37.9	±	2.0	29.1	±	0.4	8.8	±	2.0
24.83	37.5	±	0.5	29.1	±	0.3	8.5	±	0.6
25.44	38.8	±	1.3	28.5	±	0.5	10.3	±	1.4
28.25	34.3	±	1.0	27.8	±	0.4	6.4	±	1.1
31.055	40.1	±	1.5	29.2	±	0.0	10.9	±	1.5
31.667	41.0	±	0.2	29.9	±	0.1	11.1	±	0.2

Table 4-4. Solid-phase concentration of total, inorganic, and organic P for deep basin core J, determined by the Aspila method . Errors are relative percent error for duplicate measurements. The depth interval indicates the mid-depth for a homogenized interval. Concentrations are presented based on the calculated salt-free sediment weight, since pore waters were not separated from this core at the time of collection.

<u>Depth(cm)</u>	<u>μmol TP /g sed</u>			<u>μmol TIP /g sed</u>			<u>μmol TOP /g sed</u>		
0.31	90.4	±	0.4	72.2	±	0.3	18.3	±	0.5
0.93	48.7	±	0.0	35.1	±	0.0	13.6	±	0.0
1.55	43.9	±	0.1	36.6	±	1.3	7.3	±	1.3
2.17	38.2	±	0.5	31.7	±	0.0	6.5	±	0.5
2.79	40.0	±	0.1	30.9	±	0.2	9.2	±	0.2
3.41	40.7	±	0.2	30.8	±	0.1	9.9	±	0.3
4.03	38.9	±	0.1	31.7	±	0.5	7.3	±	0.5
4.65	38.4	±	0.5	32.6	±	0.0	5.7	±	0.5
5.27	41.5	±	0.1	32.3	±	0.3	9.2	±	0.3
6.51	40.6	±	0.3	35.1	±	0.6	5.5	±	0.7
7.75	38.5	±	0.2	33.3	±	0.3	5.2	±	0.3
9.61	36.5	±	0.2	29.7	±	0.2	6.8	±	0.3
11.47	38.8	±	0.5	29.8	±	0.0	9.0	±	0.5
13.33	38.4	±	0.4	30.5	±	0.6	7.9	±	0.7
15.81	40.3	±	0.1	32.5	±	0.4	7.8	±	0.4
18.29	37.6	±	0.0	34.3	±	1.2	3.3	±	1.2
21.39	40.1	±	0.3	32.4	±	0.3	7.7	±	0.4
27.11	36.0	±	0.4	31.4	±	0.4	4.7	±	0.5
33.59	38.8	±	0.4	30.3	±	0.1	8.5	±	0.4
40.07	35.2	±	0.6	29.7	±	0.5	5.5	±	0.8

also similar in the three cores. The TIP concentration in each core (Core A: 31.7 ± 1.1 $\mu\text{mol/g}$; Core C: 28.6 ± 1.1 $\mu\text{mol/g}$; Core J: 31.8 ± 1.8 $\mu\text{mol/g}$) represents ~70-75% of total P, and the remaining 20-25% of total P is organic (Core A: 7.1 ± 0.9 $\mu\text{mol/g}$; Core C: 10.1 ± 1.9 $\mu\text{mol/g}$; Core J: 6.8 ± 1.9 $\mu\text{mol/g}$).

4.4.3 Soluble P Reservoirs

Due to the labor-intensive nature of the sequential extraction procedure described in Chapter 2, limited sediment intervals were analyzed in detail. Therefore, the data shown in Tables 4-5 and 4-6 represent P concentration in extracted reservoirs for only selected horizons from cores A and C. These intervals were chosen, based on the changes with depth in total P_{org} concentration in each core, with a maximum density of sampling in shallow sediment intervals where the most rapid P degradation occurs. Concentration profiles for each of the P reservoirs are shown in Figures 4-5 through 4-8. The depth profiles for each reservoir are discussed below.

4.4.3.1 Simple Biochemicals: Lipid P and Water-soluble P

The lipid P concentration profiles for the three cores (Figure 4-5) are similar in that P concentration decreases rapidly with depth, and lipid P in all three cores accounts for only a few percent of total organic P. In the central basin cores, the lipid P concentration in surface sediments is much higher (core C = 0.80 ± 0.01 $\mu\text{mol/g}$ sed; core J = 1.12 ± 0.01 $\mu\text{mol/g}$ sediment) than in margin core A (0.24 ± 0.00 $\mu\text{mol/g}$ sediment). However, all three cores have a similar lipid P concentration at depth (0.05 ± 0.00 $\mu\text{mol/g}$ sediment in core A, compared with 0.08 ± 0.00 and 0.08 ± 0.00 $\mu\text{mol/g}$ in cores C and J, respectively). The lipid P concentration in both central basin cores decreases sharply with depth, with the most rapid decrease in the top 2 cm of sediments. In core A, the decrease in concentration occurs more gradually, over the top 5 centimeters. The differences and similarities in the water-soluble P profiles are much like those observed for lipid P. The core-top P concentration and the decrease with depth are greater in core J, intermediate in core C and lowest in core A.

Table 4-5. Total P in extracts from margin core A. Depths indicate the mid-point of a homogenized sediment interval. Reported errors represent the range of concentrations measured in duplicate analyses.

Depth (cm)	Lipid $\mu\text{mol P/g sed}$	Water-soluble $\mu\text{mol P/g sed}$	CDB-extractable $\mu\text{mol P/g sed}$	Acid-extractable $\mu\text{mol P/g sed}$	Base-extractable $\mu\text{mol P/g sed}$
0.18	0.24 \pm 0.00	0.41 \pm 0.01	24.75 \pm 0.12	17.58 \pm 0.21	7.17 \pm 0.07
0.53	0.16 \pm 0.02	0.40 \pm 0.00	17.92 \pm 0.29	16.92 \pm 0.23	7.25 \pm 0.11
0.88	0.19 \pm 0.01	0.29 \pm 0.01	18.60 \pm 0.21	18.59 \pm 0.10	7.12 \pm 0.08
1.23	0.19 \pm 0.00	0.23 \pm 0.00	16.43 \pm 0.04	18.01 \pm 0.14	7.49 \pm 0.14
1.58	0.16 \pm 0.01	0.08 \pm 0.00	12.64 \pm 0.14	18.96 \pm 0.09	8.22 \pm 0.16
1.93	0.19 \pm 0.01	0.22 \pm 0.03	14.47 \pm 0.10	10.43 \pm 0.10	8.32 \pm 0.13
3.34	0.12 \pm 0.01	0.10 \pm 0.00	9.84 \pm 0.06	20.24 \pm 0.05	4.21 \pm 0.06
6.26	0.08 \pm 0.01	0.05 \pm 0.00	8.79 \pm 0.09	20.33 \pm 0.17	4.52 \pm 0.03
9.32	0.09 \pm 0.00	0.05 \pm 0.00	6.73 \pm 0.04	21.02 \pm 0.09	- - -
13.00	0.07 \pm 0.00	0.03 \pm 0.00	8.06 \pm 0.06	20.66 \pm 0.10	4.08 \pm 0.03
19.22	0.06 \pm 0.00	0.03 \pm 0.00	7.03 \pm 0.14	21.90 \pm 0.10	5.63 \pm 0.05
22.03	0.07 \pm 0.00	0.01 \pm 0.00	6.49 \pm 0.11	21.92 \pm 0.16	6.30 \pm 0.03
24.83	0.05 \pm 0.00	0.02 \pm 0.00	5.03 \pm 0.04	20.66 \pm 0.11	5.51 \pm 0.08

Table 4-6. Total P in extracts from central basin core C. Depths indicate the mid-point of a homogenized sediment interval. Reported errors represent the range of concentrations measured in duplicate analyses.

Depth (cm)	Lipid $\mu\text{mol P/g sed}$	Water-soluble $\mu\text{mol P/g sed}$	CDB-extractable $\mu\text{mol P/g sed}$	Acid-extractable $\mu\text{mol P/g sed}$	Base-extractable $\mu\text{mol P/g sed}$
0.18	0.80 \pm 0.01	0.70 \pm 0.02	35.09 \pm 0.18	16.02 \pm 0.50	9.50 \pm 0.08
0.53	0.52 \pm 0.02	0.66 \pm 0.00	18.21 \pm 0.27	16.78 \pm 0.17	9.70 \pm 0.15
1.05	0.45 \pm 0.02	0.20 \pm 0.00	9.76 \pm 0.01	16.40 \pm 0.17	11.38 \pm 0.02
1.58	0.27 \pm 0.01	0.12 \pm 0.01	9.94 \pm 0.07	12.87 \pm 0.02	11.05 \pm 0.27
1.93	0.28 \pm 0.02	0.16 \pm 0.00	10.26 \pm 0.07	15.04 \pm 0.08	7.30 \pm 0.08
3.34	0.28 \pm 0.01	0.20 \pm 0.06	8.30 \pm 0.01	14.09 \pm 0.11	8.37 \pm 0.05
9.32	0.16 \pm 0.01	0.07 \pm 0.00	6.13 \pm 0.10	18.71 \pm 0.10	7.40 \pm 0.05
18.61	0.13 \pm 0.01	0.06 \pm 0.00	6.06 \pm 0.04	19.29 \pm 0.17	7.57 \pm 0.19
28.25	0.08 \pm 0.00	0.02 \pm 0.00	5.65 \pm 0.03	19.51 \pm 0.27	6.99 \pm 0.06

4.4.3.2 Other Soluble P Reservoirs

The comparable methodology used to extract lipid and aqueous P reservoirs from the three Santa Barbara Basin cores allows a comparison of the two central basin cores (core C and core J) to be used as an estimate of temporal and spatial variability in P chemistry. However, the base extraction procedure used for core J was deemed sub-optimal (see explanation in Appendix B-1), and was modified for extraction of cores A and C. Therefore, the base extract data from core J are not comparable to cores A and C, and are not discussed in this chapter. Instead, the modified procedures for core J and the data from acid- and base-extracted and insoluble P reservoirs for this core are presented in Appendix B-1. Because core J was extracted to full optimization of methods, examination of P reservoirs in the Santa Barbara Basin will focus almost entirely on the results from cores A and C.

4.4.3.3 Citrate Dithionite Bicarboxylate (CDB)

The concentrations of P in CDB extracts from cores A and C are shown in Figure 4-6. CDB solubilizes P associated with reactive iron species, such as iron oxyhydroxides and some oxides (Ruttenberg, 1992). In both cores, CDB-P is high at the surface, accounting for nearly half of total P. The amount of P extracted in CDB decreases downcore, both in terms of absolute concentration and as a fraction of total sediment P. In both cores, there is little change in CDB-P concentration below 10 cm, and approximately 20% of total P at depth is extractable in CDB. The decrease of CDB-P in core C is much more rapid than in core A. From a core-top concentration of 35 $\mu\text{mol P/g}$ in core C, CDB-P decreases within the top two sediment intervals (<2 cm) to 10 $\mu\text{mol/g}$. In core A, the core-top CDB-P concentration is somewhat lower (25 $\mu\text{mol P/g}$) than in core C, and decreases more gradually over the top 10 cm to a concentration of 5-10 $\mu\text{mol/g}$ at depth.

4.4.3.4 Acid Pre-extract

Figure 4-7 shows the concentration of P extracted from cores A and C in the acid treatment that immediately precedes base extraction. P in this fraction is derived from carbonate, authigenic and detrital apatite, and clay-bound P (after Ruttenberg, 1992). In both cores, the amount of P extractable in acid increases with depth. The depth trend of this increase is coincident with the decrease in iron-bound P inferred from the CDB-P profiles. However, in core C, there is a surface maximum which is not reflected by an opposite trend in CDB-P or observed in core A. Below 5-10 cm, there is little change in acid-P concentration in either core.

4.4.3.5 Base Extract

The concentration of base-extractable P in cores A and C is shown in Figure 4-8. P in this fraction is associated with humic compounds. There is an increase in base-extractable P within the top few centimeters of both cores, followed by a decrease. Deeper in core C (below 5-10 cm), P concentration is relatively constant. In core A, the concentration increases again slightly near the bottom of the core. Since the accumulation rate of core C is considerably higher (see ^{210}Pb results), it is possible that base-extractable P in core C also increases deeper in the sediments, below our sampling horizon.

4.4.4 Insoluble Residue

Figure 4-9 shows depth profiles of total P in the insoluble sediment residue after sequential extraction of cores A and C. In core A, the absolute concentration of P and the fraction of P that is insoluble remains roughly constant with depth. In core C, insoluble P increases sharply just below the sediment-water interface, but then decreases gradually to core-top values near the bottom of the core. The fraction of total P in the insoluble residue is between 5 and 10 percent in the deepest intervals of both cores.

The depth profiles of total organic P concentration in the insoluble sediment residue (Figure 4-10) are similar to those observed for total P. However, the percent of TOP in the insoluble residue of core C increases with depth for the entire length of the sediment core, while no such trend is observed for total P. Although the concentration data are more variable, the percent of TOP in the insoluble residue of core A also increases with depth. The percentage of total sedimentary organic P measured at depth in the insoluble fraction of cores A and C is between 30 and 50%.

4.4.5 ^{31}P -NMR Analysis Of Sediment Base Extracts

^{31}P -NMR spectra of base extracts for the three Santa Barbara Basin cores are shown in Figures 4-11, 4-12, and 4-13. For core J, only surface sediments (0-0.3 cm) and sediments at depth (38-40 cm) were analyzed by ^{31}P -NMR (Figure 4-13), and these two sediment samples were extracted using procedures identical to those used for cores A and C. The concentration of P functional groups for this core are given in Table 4-9, but no depth profiles are presented since only two intervals were analyzed. Visually, spectra from all three cores are similar and share a number of prominent features. As in base extracts of terrestrial soils (e.g., Tate & Newman, 1982; Adams & Byrne, 1989; Bedrock *et al.*, 1994), the most abundant components in these marine sediments are orthophosphate and monoester P. The orthophosphate peak in all spectra has been truncated to allow the other peaks to be visible in more detail. A number of small peaks are visible in the phosphonate region, and an end-group polyphosphate signal is visible in all spectra. In addition, a middle-group polyphosphate peak is visible in the surface spectra for core J (Figure 4-13). Each of these chemical shift regions is discussed in more detail below. As indicated in Chapter 2, there are several peaks that cannot be uniquely identified. The discussion will focus mainly on the functional groups that can be confidently assigned. However, these unidentified “other peaks” are quantified and

discussed briefly. In the tables, they are identified by their chemical shifts rather than by a structural name.

For orthophosphate and polyphosphate (the inorganic P functional groups resolved in these spectra), depth profiles are presented as total P concentration per gram sediment, and as a percent of total base-extractable P. For the remaining chemical shift regions (the organic fractions), results are presented as depth profiles of P concentration and as a percent of total organic P concentration, determined as the sum of the concentration of all organic fractions.

Table 4-7. Concentration of P functional groups (reported in $\mu\text{mol P}$ per gram sediment) in margin core A determined by ^{31}P -NMR. Peaks identified in the table by chemical shift cannot be confidently assigned to a particular functional group.

<u>Depth (cm)</u>	<u>25 – 30 ppm</u>	<u>Phos- phonate</u>	<u>6 to 15 ppm</u>	<u>Ortho- phosphate</u>	<u>Monoester</u>	<u>3 ppm</u>	<u>Diester</u>	<u>Poly- phosphate</u>	<u>ΣP_{org}</u>
0-0.7	0.09	0.09	0.07	5.30	1.17	0.06	0.21	0.23	1.68
0.7-1.4	0.09	0.06	0.04	5.56	1.10	0.05	0.23	0.18	1.57
1.4-2.1	0.03	0.12	0.06	6.20	1.49	0.09	0.15	0.11	1.95
3.2-3.5	0.04	0.08	0.02	3.33	0.67	0.01	0.02	0.03	0.85
6.0-6.6	0.10	0.07	0.01	3.30	0.69	0.06	0.23	0.06	1.16
9.0-9.6	0.02	0.02	0.00	1.54	0.29	0.01	0.06	0.01	0.41
18.9-19.5	0.05	0.02	0.00	4.45	0.84	0.03	0.18	0.05	1.13
24.5-25.1	0.06	0.04	0.00	4.36	0.83	0.05	0.14	0.03	1.12

Table 4-8. Concentration of P functional groups (reported in $\mu\text{mol P}$ per gram sediment) in central basin core C determined by ^{31}P -NMR. Peaks identified in the table by chemical shift cannot be confidently assigned to a particular functional group.

<u>Depth (cm)</u>	<u>25 – 30 ppm</u>	<u>Phos- phonate</u>	<u>6 to 15 ppm</u>	<u>Ortho- phosphate</u>	<u>Monoester</u>	<u>3 ppm</u>	<u>Diester</u>	<u>Poly- phosphate</u>	<u>ΣP_{org}</u>
0-0.7	0.31	0.29	0.08	6.27	2.02	0.11	0.40	0.16	3.20
0.7-1.4	0.44	0.18	0.08	8.29	1.67	0.08	0.47	0.17	2.92
1.4-2.1	0.18	0.29	0.16	6.18	1.78	0.17	0.31	0.06	2.89
3.2-3.5	0.36	0.25	0.00	5.48	1.88	0.14	0.23	0.03	2.86
9.0-9.6	0.13	0.10	0.00	5.04	1.52	0.12	0.35	0.12	2.24
18.3-18.9	0.16	0.09	0.03	5.48	1.38	0.12	0.26	0.05	2.04
25.7-30.7	0.09	0.10	0.08	5.07	1.28	0.08	0.25	0.04	1.88

Table 4-9. Concentration of P functional groups (reported in $\mu\text{mol P}$ per gram sediment) in central basin core J determined by ^{31}P -NMR. Peaks identified in the table by chemical shift cannot be confidently assigned to a particular functional group.

<u>Depth (cm)</u>	<u>25 – 30 ppm</u>	<u>Phos- phonate</u>	<u>6 to 15 ppm</u>	<u>Ortho- phosphate</u>	<u>Monoester</u>	<u>3 ppm</u>	<u>Diester</u>	<u>Poly- phosphate</u>	<u>ΣP_{org}</u>
0-0.3	1.12	0.62	0.00	29.12	9.57	0.55	2.00	3.03	13.86
38-40	0.00	0.15	0.00	6.02	1.26	0.07	0.43	0.06	1.91

4.4.5.1 Phosphonate

Phosphonates are compounds that contain a direct linkage between carbon and phosphorus, rather than the C-O-P linkage found in most P-bearing biochemicals.

Chemical shifts between 15 and 40 ppm have been reported for phosphonate compounds. However, thiophosphates (compounds with a P-S bond) can also have chemical shifts between 25 and 40 ppm. To quantify changes in phosphonates alone, only the peak area

in the chemical shift region between 15 and 25 ppm was used to calculate phosphonate abundance. Changes with depth in the abundance of compounds with chemical shifts between 25 and 30 ppm (no peaks were observed between 30 and 40 ppm) will be considered separately. This approach eliminates the possibility that depth trends actually driven by other (potentially labile) compounds could be erroneously attributed to phosphonates. Since the defined peak area range is consistent with depth, this means that potentially only a subset of phosphonates is being used to characterize the reactivity of all phosphonates.

Within central basin core J, phosphonates decrease both in quantity and diversity (based on peak shapes) with depth (Figure 4-13). In cores A and C, the phosphonate concentration decreases immediately below the sediment surface, increases again in the sub-surface sediments, and finally decreases to a fairly constant value by about 10 cm depth (Figure 4-14). Phosphonate concentrations are generally higher in core C, although in both cores phosphonates account for less than 10% of total base-extractable organic P.

4.4.5.2 Orthophosphate

Depth profiles of base-extractable orthophosphate for cores A and C are shown in Figure 4-15. Orthophosphate accounts for between 72 and 79% of base-extractable P in core A and between 65 and 73% in core C. In both cores, orthophosphate concentration is highest just below the sediment-water interface, then decreases within the upper few centimeters to reach fairly constant value with depth. However, while the orthophosphate concentration at depth in core C is only slightly less than surface values, the concentration at depth in core A is significantly lower than in surface sediments.

4.4.5.3 Monoester

Figure 4-16 shows depth profiles of monoester P in base extracts from cores A and C. Monoesters, which include phosphosugars, phosphoproteins, nucleotides, and inositol P, are by far the most abundant organic P fraction in these extract (55-80% of total organic P). The concentration of monoester P is higher in core C than in core A, consistent with the higher concentration of total P_{org} in the central basin core, and in core C the decrease in concentration with depth is less pronounced, as well.

4.4.5.4 Diester

Depth profiles of diester P abundance in base extracts from cores A and C are shown in Figure 4-17. Expressed as a percent of total organic P, the depth profiles for cores A and C are similar, with pronounced sub-surface minima, and a fractional abundance at depth that is very similar to that in surface sediments. However, the absolute diester P concentration is roughly ten times higher in central basin core C than in margin core A. Diesters present in the base-extractable reservoir may include phospholipids and DNA that were not accessible to the preceding solvent extraction (e.g., sequestered by the humic matrix), and/or diester linkages to the macromolecular humic matrix. RNA does not persist under the basic extraction conditions that generated these samples (see Chapter 2), but degrades into its constituent nucleotides. Therefore, RNA does not form any part of the diester pool detected by NMR, but would be detected in the monoester region.

4.4.5.5 Polyphosphates

Depth profiles of polyphosphate abundance in core A and C base extracts are shown in Figure 4-18. The signal at -3.4 ppm represents the end groups of the polyphosphate chain, while the signal at -17 ppm (seen only in the surface sample from

core J , Figure 4-13) represents middle groups from a longer polyphosphate chain ($n > 2$). In all cores, the polyphosphate signal is diminished at depth, with only the pyrophosphate, or end group, signal detectable in deeper intervals.

The fraction of total base-extractable P as polyphosphates and the absolute concentration show nearly identical patterns. Within core A, there is a clear decrease in concentration with depth, with the most precipitous drop in the upper 4 cm. Below 4 cm, concentration increases slightly to a fairly constant value of less than $0.05 \mu\text{mol P/g}$ sediment. In core C, there is also a sharp decrease in the top few centimeters, but the increase in polyphosphate concentration deeper in the core is more marked than in core A, returning nearly to surface values. At depth (18-30 cm), the concentration again returns to low values similar to those observed in core A.

The concentration of polyphosphates observed in the two intervals analyzed from core J shows that although the concentration at depth is similar to the other two cores, the surface concentration ($3 \mu\text{mol/g}$) is considerably higher. In addition the percentage of total P accounted for by polyphosphates is much higher in core J (6.6% compared to 1.6% in core C). At depth, the percent of base-extractable P in the polyphosphate fraction is similar in the three cores.

4.4.6 Mineral Surface Area

The surface area measured for surficial sediments in all three cores was surprisingly low. Sediments in the Santa Barbara Basin are less than 5% sand, and are primarily composed of silts (Thornton, 1984). Clays and silts usually have surface areas greater than $30 \text{ m}^2/\text{g}$ (M. Goñi, personal communication), but surface areas measured for surface sediments in cores A and C were between 11 and $15 \text{ m}^2/\text{g}$ (Table 4-10). This reduced surface area is likely a result of organic matter covering small pores, resulting in an underestimation of surface area.

The decision to measure surface area without removing organic matter was made due to concerns about altering the sediments during the organic matter removal process. Particularly in sediments with sulfide minerals and other reduced inorganic species, treatment with strong oxidants or dry combustion at high temperature, methods commonly used to remove organic matter coatings from mineral grains, might be expected to alter the sediment fabric. Previous studies have suggested that similar surface area results are obtained with and without organic matter removal (Mayer, 1994b). However, for samples with high organic matter content, such as the surface sediments of these cores, organic matter removal may be necessary to understand the relationship between organic matter preservation and mineral surface area.

There is little difference in the surface area measured for the three cores, and variations within the upper centimeter of sediments equal or exceed the variability between cores. Based on these data, no direct relationship between sediment surface area and P_{org} preservation can be made for the Santa Barbara Basin. Additional data (surface areas determined after organic matter removal) may allow such a relationship to be explored. However, for these very organic-rich sediments, much of the surface interaction with sediment particles may include organic matter-organic matter interaction rather than direct interaction with mineral surfaces.

Table 4-10. Surface area determined for surface sediments of the three Santa Barbara Basin cores.

<u>Core</u>	<u>Depth</u>	<u>Surface Area (m²/g sediment)</u>
Core A	0 - 0.35 cm	12.8
	0.35-0.7 cm	11.2
Core C	0 - 0.35 cm	13.1
	0.7 – 1.05 cm	14.4
Core J	0-0.6 cm	11.2

4.5 Discussion

4.5.1 The Importance of Chemical Structure for P_{org} Preservation

Phosphonates, compounds with direct C-P bonds, are the only P_{org} compounds that have been suggested as candidates for preferential preservation on the basis of chemical structure (e.g., Ingall *et al.*, 1990; Berner *et al.*, 1993). Since this compound class has been singled out in the literature, it will be considered first in this discussion of structural control on P_{org} preservation. Phosphonates have been identified in bacteria, ciliates, and higher organisms (Alhadeff & Daves Jr., 1970), as well as in marine sediments (Ingall *et al.*, 1990). Preferential preservation of these compounds has been hypothesized based on their stability to acid hydrolysis (Aalbers & Bieber, 1968; Kittredge & Roberts, 1969) and resistance to phosphatases (Rosenberg & La Nauze, 1967; Rosenthal & Pousada, 1968; Rosenthal & Ham, 1970). An increase in the relative importance of these compounds with depth in sediments would indicate that chemical structure is an important control on the rate of organic P degradation in these sediments.

As described in Chapter 3, phosphonates account for a small fraction of organic solvent-extractable P in surficial sediments of core J, but decrease below detection limits at depth (Figure 3-4). These data indicated that phosphonolipids are degraded at the same or more rapid rates than diester phospholipids. Phosphonates in the base-extractable fraction also decrease with depth, both in absolute concentration and as a fraction of total P_{org} (Figure 4-14, Tables 4-7, 4-8, and 4-9), indicating their susceptibility to remineralization. The most prominent phosphonate peak in the base extracts from all three cores has a chemical shift consistent with 2-aminoethylphosphonic acid (2-AEP), a product of phosphonate catabolism (Hori & Nozawa, 1982). Thus, in both the lipid and base-extractable pools, phosphonates are not preferentially preserved but degrade at rates comparable to non-phosphonate P_{org} compounds.

The observed degradation of phosphonates is consistent with culture experiments demonstrating that many bacteria produce enzymes capable of breaking the C-P bond (Zeleznick *et al.*, 1963; Harkness, 1966). However, it has been previously assumed that utilization of phosphonates by bacteria is inhibited by the presence of orthophosphate (Rosenberg & La Nauze, 1967). In these sediments, phosphonate degradation is clearly occurring in the presence of high pore water phosphate concentrations (Figure 4-2).

These data stand in contrast to the results of Clark *et al.* (1998; 1999), which show preferential preservation of phosphonates relative to ester bonds during transformation from biomass to high molecular weight dissolved organic matter in the water column. It is intriguing to speculate that these contrasting results may reflect differences in the ability of water column and sedimentary microbial consortia to degrade specific classes of P_{org} compounds. Such a contrast has been observed in the microbial degradation of carbohydrates in seawater versus sediments (Arnosti, 2000). The efficient degradation of compounds that are expected to be structurally resistant suggests that the dominant mechanism controlling preservation of P_{org} compounds in these sediments is not structural. To further address this question, the abundance of P in different P_{org} reservoirs is considered next.

4.5.2 Simple Biochemicals: Lipid and Aqueous P Reservoirs

Simple biochemicals are expected to dominate the lipid P and aqueous-extractable P reservoirs. The decrease with depth of these P reservoirs reflects a combination of decreasing biomass and diagenetic degradation of these simple biochemicals (see Chapter 3 for a full discussion). The most active metabolism of sedimentary organic matter takes place in surface sediments. Therefore, the fact that lipid P and aqueous P account for such a small fraction of total P_{org} in the deepest sediments of these cores suggests that they are efficiently degraded. However, it is possible that some fraction of these labile P pools is not degraded, but transferred into another reservoir. For example, if a simple

phospholipid were either sorbed or chemically linked to a humic compound, it would not be accessible in the solvent extract, but would instead be quantified as base-soluble P. The sub-surface increase in the relative concentration of diester P observed in both cores (Figure 4-17) may indicate such incorporation into the humic fraction. This possibility will be considered next.

4.5.3 Mechanisms for Incorporation of Monoester and Diester P into the Humic Fraction

Before discussing the distribution of monoester and diester P compounds inferred from ^{31}P -NMR analyses of the base extracts, it is important to recognize the nature of the information obtained using this method. Identification of P functional groups by ^{31}P -NMR analysis can indicate the abundance of primary biochemical compounds such as phosphosugars, nucleic acids and phospholipids within the base extract. However, the spectra demonstrate only that the electronic environments of groups of P nuclei in the sample are equivalent to particular kinds of primary P compounds. Thus, in the absence of a macromolecular shielding effect, a phosphate group esterified to a humic acid would have a chemical shift indistinguishable from a simple monoester P compound. This means that NMR data alone cannot distinguish whether simple P biochemicals persist in the humic fraction, either through physical sequestration within the humic matrix or by metal bridging, or if P compounds are chemically altered to become a part of the organic structure of a larger molecule. Figures 4-19 and 4-20 show two models for P incorporation into the humic fraction. In Figure 4-19, a simple phosphomonoester (inositol-2-phosphate) is attached to a humic acid via a metal bridge. In Figure 4-20, a phosphate group is esterified to the carbon skeleton of a fulvic acid. These models have different implications for the mechanism of P incorporation into the humic fraction. However, the fact that each contains a monoester P linkage to a carbon chain means that both will be detected as monoesters when analyzed by ^{31}P -NMR. The chemical shifts

detected by ^{31}P -NMR could not resolve differences in the chemical environment of the P nucleus related to the size or nature of the attached carbon skeleton (e.g., a simple P biochemical versus a fulvic acid). Both mechanisms of P incorporation into the humic fraction would result in extraction of P in the humic (rather than lipid or aqueous) reservoir. Both mechanisms would favor incorporation of monoester P relative to other organic P compounds because of interaction with the changed phosphate end group. Monoesters are distinct from other P_{org} functional groups, because they are the only compound class with this charged end-group. However, if monoester P were to become covalently bound to the humic matrix through the phosphate group itself, a diester P linkage would result. The fact that abundant monoester P is detected in the humic fraction, as opposed to diester P, indicates that incorporation of monoesters into the humic matrix may occur either by metal bridging between monoester phosphate and the humic compound, or by covalent bonding between the humic matrix and some other part of an organic P compound, but not the phosphate group. The latter possibility might still rely on charge interaction with the phosphate group to enhance attraction to the organic matrix, promoting condensation reactions.

Perhaps the most revealing observation for understanding the mechanisms that control P_{org} preservation is that the concentration of monoester P is so much higher than any other base-extractable P_{org} fraction. It has been previously suggested (Hinedi *et al.*, 1988) that monoesters are more recalcitrant to degradation than other organic P compounds. Potentially, a mechanism for this preferential preservation lies in the association of organic P compounds with inorganic surfaces (discussed in Section 4.5.6) and large organic molecules. As explained above, monoesters are more likely than other P_{org} compounds to bond to positively charged metals associated with organic matter and to the positively charged ends of clays through the reactive phosphate end group. In contrast, sorption of diesters is controlled by the surrounding organic moieties rather than the P group (Stewart & Tiessen, 1987). The decrease in absolute monoester concentration

with depth clearly demonstrates that monoesters are susceptible to remineralization during diagenesis. However, monoesters in sediments are relatively much more abundant than in the starting material (i.e., biomass), as shown in Table 4-11. This increase in relative abundance of monoester P may indicate preferential preservation via a physical protection mechanism. The monoester signal in soil profiles is often attributed in large part to inositol P (Newman & Tate, 1980; Tate & Newman, 1982). A number of different inositol P compounds are found in natural systems, and are differentiated based on the number and position of phosphate groups substituted in the hexahydroxycyclohexane structure. While a number of inositol P compounds have been identified in plankton, inositol hexaphosphate (phytic acid) has been found only in terrestrial environments (Suzumura & Kamatani, 1995b).

Table 4-11. The abundance of P biochemicals in bacterial biomass, calculated based on data from Neidhardt (1987) compared to the distribution of functional groups in sediments from cores A and C. Sediment data represent the percentages of monoester and diester P in base extracts from all sediment depths analyzed in these cores. This data compilation does not include phosphosugars, phosphoproteins or polyphosphates.

	<u>% cell P *</u>	<u>% P_{org} in Margin Core A</u>	<u>% P_{org} in Central Basin Core C</u>
Monoester P (e.g., ATP)	6	72±6	64±4
Diester P (e.g., DNA Phospholipid)	94	12±5	13±3

* % cell P is calculated assuming that all cellular P is accounted for by these compounds. The total cellular P from each compound is calculated by dividing the total weight of the compound in a cell (from % cell dry weight) by the molecular weight of the compound, and multiplying by the number of P atoms per mole of compound.

.This is thought to reflect the fact that while aquatic organisms store excess P as polyphosphates, terrestrial plants store P as phytic acid (e.g. Miyata *et al.*, 1986). Based on the resistance of inositol P to acid and alkali hydrolysis (White & Miller, 1976), it has been speculated that inositol P might constitute an important fraction of marine organic P in sediments (Froelich *et al.*, 1982; Ingall *et al.*, 1990). Phytic acid is particularly likely to be sorbed to sediment particles because of its high charge density (Stewart & Tiessen, 1987). However, analysis of inositol phosphates in marine sediments has suggested that these compounds are minor constituents of total P_{org} in marine sediments that do not persist with depth (Suzumura & Kamatani, 1995a). One explanation for the observation of low phytic acid concentration is that inositol P is chemically linked to larger molecules (Anderson & Hance, 1963) and may be modified during humification such that it is undetected by inositol P quantification methods. Dialysis of base extracts from surface sediments and at depth in core J demonstrates that most of the base-extractable P is associated with the >500 Dalton fraction (Chapter 2). Some phospholipids have a molecular weight above this cutoff, but most water-soluble P compounds have molecular weights that are much lower. In solution, humic compounds are expected to be conformationally more flexible and any sequestration that protected compounds in sediments is unlikely to remain intact in the extract. Thus, the fact that these compounds remain attached to high molecular weight compounds in solution suggests that they are bound, either through metal bridging or through covalent bonds, to a larger macromolecule. Therefore, at least in the central basin (for which the dialysis experiment was done), it is likely that incorporation of P compounds into a humic matrix is an important mechanism for P_{org} preservation.

Some useful insights into the possible mechanisms for immobilization of P in the humic fraction can be derived from the distribution of inorganic P in this reservoir. Orthophosphate is the most abundant P species in all base extracts analyzed from these sediments. In Chapter 2, hydrolysis experiments demonstrated that orthophosphate

cannot be a product of hydrolysis of organic P compounds and dialysis of base extracts showed that most orthophosphate and organic P is associated with the greater than 500 Dalton size fraction. This information, combined with ^{31}P -NMR identification of a large quantity of orthophosphate places fairly stringent constraints on the form of orthophosphate in these extracts. To explain all of the data, any proposed mechanism for incorporation of orthophosphate into this fraction must meet the following criteria: (i) orthophosphate must be bound in some way to a larger molecule, preventing removal of orthophosphate from the high-molecular-weight (>500 Dalton) fraction during dialysis, and (ii) orthophosphate may not be covalently bound to any compounds, or it would be detected in a different chemical shift region. Based on these constraints, a plausible explanation for the high orthophosphate concentration in the base-extractable fraction is metal bridging between orthophosphate and large organic molecules. Metal bridging has been widely suggested as a mechanism for P incorporation into humic compounds in lakes and terrestrial soils (e.g., Levesque & Schnitzer, 1967; Koenings & Hooper, 1976; Francko & Heath, 1982; Gerke, 1992; Jones *et al.*, 1993; Frossard *et al.*, 1995). The fact that the observed peaks in the NMR spectrum are so sharp indicates that no significant quantities of paramagnetic metals (such as Fe^{3+}) are likely to be present. Fe^{2+} and Al^{3+} are examples of non-paramagnetic metals that may link orthophosphate to humic compounds.

It is possible that extraction of the sediments with CDB to remove paramagnetic metals may result in secondary adsorption of orthophosphate liberated from mineral phases onto humic compounds. This possibility was not tested explicitly here, although there are a number of indirect lines of evidence that suggest this is not an important source of orthophosphate in the humic fraction. The most compelling evidence that re-adsorption did not contribute a significant quantity of orthophosphate to the humic fraction is that humic acids in the surface sediments of core J contained no measurable orthophosphate, but at depth the orthophosphate peak represented a substantial fraction of

total P. If re-adsorption were responsible for an important fraction of the orthophosphate measured in these extracts, this analytical artifact should be observed at all sediment depths.

The concentration of monoester P is higher in central basin core C than in margin core A (Figure 4-16), consistent with the higher concentration of total P_{org} in the central basin core. The decrease in concentration with depth in core C is less pronounced, suggesting that monoesters may be less efficiently degraded in the central basin core. None of the extracts from margin core A have been dialyzed. However, if a larger fraction of the organic matter in the core A base extracts is contained in the low molecular weight (<500 Dalton) fraction, this would indicate that incorporation of P into larger organic complexes is less efficient than in the central basin, explaining the decreased P_{org} concentration. The high abundance of monoester P compared to the P distribution in biomass (which is mainly diester P; Table 4-11) may be a result of preferential preservation of monoesters due to sorption or metal-bridging effects (discussed above). It is not clear if the high monoester abundance is due to concentration of a fraction of directly biomass-derived monoesters or if biomass diesters are degraded to monoesters, and then some fraction of these secondary monoesters is preserved. The latter suggestion seems more plausible, given the quantitative importance of diesters in the starting material. The fact that diester P is abundant even in the >500 Dalton fraction of dialyzed base extracts (Chapter 2) indicates that diesters are also incorporated into the humic matrix. Covalent bonding between humic compounds and monoesters would result in diester P in this fraction. Alternatively, condensation reactions between humic compounds and simple diester compounds like DNA could result in transfer of diester P into this fraction. Nucleic acid derivatives have been identified in hydrolysates of humic acids (Adams *et al.*, 1954; Anderson, 1958; Anderson, 1961), suggesting that even though DNA and other water-soluble P compounds do not persist in sediments in

unbound form (Figure 4-5), they may not be completely remineralized, either, due perhaps to sequestration within the humic matrix.

The decrease in base-extractable P with depth indicates that P in the humic fraction is susceptible to remineralization (Figure 4-8). However, the rate of this decrease is slower than that observed for the P biochemical fractions (Figure 4-5). Quantitatively, only a small fraction of the total P biochemical pool may be transferred into the humic fraction. However, this transfer may be an important mechanism for the ultimate preservation of this simple, reactive biochemical P_{org} fraction. Large geopolymers are expected to have lower susceptibility to microbial degradation (e.g., Henrichs & Doyle, 1986). For organic P compounds, one mechanism for enhanced preservation is steric hindrance of phospholipases by the bulky humic molecule (Brannon & Sommers, 1985).

If organic P is effectively remineralized during the formation of humic compounds, one would expect the amount of P to decrease in the progression from primary biochemicals to fulvic acids to humic acids and finally to kerogen. Consistent with this model, Nissenbaum (1979) measured higher P concentration in fulvic acids (FA) than in humic acids (HA) and used these results to argue for the progression from FA to HA during diagenetic alteration of organic matter. However, simple wet chemical analysis of these extracts cannot be used to prove this hypothesis because incorporation of metal-bound orthophosphate into the humic fraction, likely due to metal bridging, can result in an apparent increase in organic P (Section 4.5.4).

4.5.4 Metal-Bound P and Analytical Artifacts

A discrepancy between wet chemical measurements and ^{31}P -NMR data may in part address the paradox of organic P preservation: Given the lability of primary P_{org} compounds (White *et al.*, 1977; Paul *et al.*, 1987; Westheimer, 1987), why does any P_{org} persist in deeply buried sediments (Filippelli & Delaney, 1994; Delaney & Anderson, 1997) and ancient shales (Ingall *et al.*, 1993)? In all studies to date, the amount of

preserved organic P has been determined exclusively by wet chemical techniques. The use of such techniques may result in erroneously high estimates of P_{org} concentration in sediments and sedimentary rocks.

As demonstrated in Chapter 2, orthophosphate in base extracts is unlikely to originate from hydrolysis of organic P compounds. The fact that most orthophosphate measured in Core J was associated with compounds larger than 500 Daltons suggests that orthophosphate is somehow bound to macromolecular humic compounds, likely through metal bridging. Additional inorganic P data from cores A and C, again determined both by ^{31}P -NMR and wet chemical methods, show that the total amount of inorganic P determined by NMR is consistently higher than that determined by wet chemical measurement (Figure 4-21). As a result, organic P (calculated by difference) is overestimated using wet chemical measurements alone. These additional data, along with the data from core J (previously shown in Chapter 2), are presented in Table 4-12.

Based on the surface sediment results, these data suggest that there may be an oxygen effect on the magnitude of the P_{org} overestimation artifact, although more data are required to further evaluate this possibility. It is intriguing to speculate that the discrepancy between wet chemical and spectroscopic determinations of inorganic P is more severe in the core characterized by suboxic/anoxic sediments (core A). If there is a redox dependence to the magnitude of this analytical artifact, this mechanism for P immobilization may in part explain the low C:P ratios reported by Ingall and Jahnke (1994) in bioturbated shales compared to laminated shales. Metal binding of P may result in an artificially high organic P estimate, particularly in the bioturbated (suboxic/anoxic) case.

The mechanism of metal bridging to high molecular weight organic matter for orthophosphate immobilization has important implications for nutrient cycling. It has long been recognized that metals are efficient scavengers of phosphate (e.g., from sediment pore waters). However, scavenging of P by inorganic metals such as iron

Table 4-12. A comparison of inorganic and organic P in base extracts from central basin cores J and C, and margin core A, determined by ^{31}P -NMR and wet chemical analyses. The NMR inorganic and organic values represent, respectively, the sum of orthophosphate and polyphosphate peaks, and the sum of the phosphonate, monoester, and diester peaks. Errors reported for wet chemical analysis indicate the range of concentrations determined in duplicate analyses. Errors reported for ^{31}P -NMR indicate the 15% estimated uncertainty in functional group quantification by this method (Section 2.2.5). No deep interval comparison was made for Core C.

	Inorganic P ($\mu\text{mol /g sediment}$)	Organic P ($\mu\text{mol /g sediment}$)
<u>SBB9610 Core J</u>		
Surface (0-0.3 cm)		
^{31}P -NMR	32.9 \pm 4.9 (70%)	14.0 \pm 2.1 (30%)
Wet Chemical Analysis	34.0 \pm 0.1 (72%)	12.9 \pm 0.4 (28%)
Deep (38-40 cm)		
^{31}P -NMR	4.9 \pm 0.7 (75%)	1.6 \pm 0.24 (25%)
Wet Chemical Analysis	2.6 \pm 0.2 (40%)	3.9 \pm 1.15 (60%)
<u>SB 11/95 Core C</u>		
Surface (0-0.7 cm)		
^{31}P -NMR	4.9 \pm 0.4 (67%)	2.4 \pm 0.4 (33%)
Wet Chemical Analysis	4.2 \pm 0.0 (58%)	3.1 \pm 0.2 (42%)
<u>SB 11/95 Core A</u>		
Surface (0-0.7 cm)		
^{31}P -NMR	5.5 \pm 0.8 (77%)	1.68 \pm 0.1 (23%)
Wet Chemical Analysis	3.7 \pm 0.0 (51%)	3.52 \pm 0.2 (49%)
Deep (24.5-25.1 cm)		
^{31}P -NMR	4.4 \pm 0.7 (80%)	1.1 \pm 0.1 (20%)
Wet Chemical Analysis	3.3 \pm 0.0 (59%)	2.3 \pm 0.2 (41%)

oxyhydroxides is intimately linked with the redox conditions of the sediments, and P is remobilized under reducing conditions. Depending on the metals linking P to humic compounds, metal bridging between P and humic compounds may not be subject to redox dependence, and thus these complexes may ultimately be more stable in the sedimentary environment. For example, aluminum, calcium and magnesium are metals found in humic compounds that are not redox-dependent. These metallohumic complexes could constitute an important sedimentary sink for orthophosphate. It has been widely recognized that metallohumics can form an important intermediate in the cycling of P in soils (Schnitzer, 1969). Based on the data and arguments presented above, binding of orthophosphate to humic compounds by metal bridges can result in a substantial overestimation of sedimentary organic P, and could significantly impact its potential for remobilization.

The P_{org} overestimation artifact just described may result in overestimation of the burial flux of organic P in marine sediments. If this mechanism for immobilization of P by metals is widespread, it may be that most of the organic P concentrations determined for marine sediments are overestimates. The suggestion that this discrepancy may be most severe in the suboxic core (margin core A) suggests that metal-bound P constitutes a more important fraction of the total measured “organic P” in oxic or suboxic sediments, representing most of sediments buried in the open-ocean.

The inferred analytical artifact is large within the base fraction (in core A, P_{org} estimated by the wet chemical technique is nearly twice that estimated by ^{31}P -NMR). It is not clear if any other P reservoirs separated in this study would have a similar artifact. A minimum estimate of the impact of this analytical artifact on the estimate of total sedimentary organic P can be calculated by assuming conservatively that only base-extractable organic matter contains P that is analytically inaccessible to the wet chemical technique. For core A, this calculation indicates that of the 10.9 $\mu\text{mol/g}$ total “organic P” in surface sediments and 6.3 $\mu\text{mol/g}$ at depth, approximately 1.8 $\mu\text{mol/g}$ (17% of the

total) and 1.2 $\mu\text{mol/g}$ (19% of the total), respectively, can be attributed to analytically mis-identified orthophosphate. Note that these may be minimum estimates of the artifact in bulk sediment organic P determinations, because if metal-bound P is incorporated into the insoluble fraction, an additional portion of total measured "organic P" may also be orthophosphate.

4.5.5 Transfer of P Into the Insoluble Sediment Residue

Given the strong evidence that P from simple biochemicals is incorporated into the humic fraction, it is important to determine the amount of transfer from the humic fraction into the insoluble fraction. Quantifying this transfer is problematic. Artificially high P_{org} concentrations may be measured by wet chemical analysis of base extracts (Section 4.5.4). If this analytically inaccessible inorganic P persists through the transformation of humic compounds into kerogen, the analytical artifact may constitute a considerable fraction of the total P_{org} measured in the insoluble sediment residue by wet chemical techniques. The only method that has proven capable of unequivocally distinguishing organic from inorganic P is solution ^{31}P -NMR. It is possible to detect P using solid state ^{31}P -NMR. However, the resolution of this technique is considerably less than solution NMR, allowing only a distinction between phosphonates and phosphates (both organic and inorganic, see Figure 4-22).

We examined the possibility that phosphonates are not degraded, but instead are transferred into the insoluble reservoir, by analyzing the insoluble residue using solid-state ^{31}P -NMR. Phosphonates were below our detection limit in sub-surface sediments (Figure 4-22). Based on the estimated detection limit, this indicates that, at most, 3% of the total P in the insoluble residue (or 0.6 $\mu\text{mol P}$ per gram sediment) could be present as phosphonate compounds. Using a simple mass balance, the NMR data could be consistent with transfer into the insoluble reservoir of as much as 40% of the 1.6 $\mu\text{mol/g}$ phosphonate lost from the soluble fractions (Table 4-9). This amount of transfer seems

unlikely, however, because the total concentration of P_{org} in the insoluble fraction does not increase with depth. To shift this quantity of phosphonates into the insoluble residue, while maintaining an invariant P_{org} concentration, would require degradation of an amount of ester-linked P_{org} compounds exactly coincident with the quantity of phosphonates incorporated into the insoluble reservoir. A simpler, and more plausible, explanation is that phosphonate transfer is not quantitatively important.

If sorption or metal binding of P compounds is an important mechanism for transfer of P into more insoluble, and thus more resistant, organic reservoirs, the transfer of monoester P may be much more important than the amount we have calculated for phosphonate P. While monoesters have a reactive charged phosphate group, phosphonates have no such reactive group. Thus, the conclusion that relatively little soluble phosphonate is transferred into the insoluble residue cannot be extended to other P compounds. In particular, if charge interaction is an important mechanism for P incorporation into the humic fraction, it is possible that formation of kerogen from humic compounds includes transfer of substantial quantities of monoester P into the insoluble organic matter reservoir.

4.5.6 Sorption to Mineral Surfaces

Most of the discussion of physical protection mechanisms thus far has focussed on interaction with large organic molecules such as humic acids. Difficulties interpreting the sediment surface area data collected thus far prevent an extensive analysis of the importance of interaction between P_{org} compounds and mineral surfaces. However, many of the arguments presented above with respect to the preferential sorption of monoesters could easily apply to interaction with mineral surfaces as well. As discussed in Chapter 3, the fact that a significant fraction of lipid P persists at depth in central basin core J suggests some physical protection mechanism may result in lipid P preservation. Further examination of the relationship between P_{org} concentration and the surface area

determined on naked mineral surfaces may provide more insight, allowing the relative importance of sorption to organic matter and mineral surfaces to be distinguished.

4.5.7 Depositional Conditions: The Importance of Bottom Water Oxygen Concentration

There are several major differences in P_{org} distribution between cores A and C that may be attributed to the effects of bottom water oxygen concentration. The contrast in total organic P (TOP) concentration determined by traditional wet chemical methods, with twice as much TOP in the central basin core as in the margin core (Figure 4-4), seems consistent with previous observations of high organic matter accumulation in regions of low bottom water oxygen. Further, the concentrations of total base-extractable P (including orthophosphate) in central basin core C are higher than in margin core A (Figure 4-8). However, the amount of organic P in the base-extractable fraction of cores A and C is similar (Figure 4-21), indicating that most of the difference in base-extractable P concentration between these two cores is related to the distribution of inorganic, and not organic, P. This distinction is important, because while the TOP data suggest differences in the efficiency of P_{org} remineralization related to bottom water oxygen concentrations, the additional insights provided by this study demonstrate that much of this redox-dependency may be related to changes in the efficiency of orthophosphate sequestration in the high molecular weight organic fraction, rather than differences in the efficiency of P_{org} degradation. Thus, while TOP concentration profiles are consistent with the idea that bottom-water oxygen concentration affects P_{org} preservation, the molecular-level information obtained in this study reveal that the mechanisms traditionally invoked to explain such differences may be incorrect.

Both cores show a rapid decrease in P concentration in the lipid P and aqueous P fractions, providing evidence that simple P biochemicals are remineralized regardless of oxygen conditions. It has been asserted that the contrast in degradation rates between oxic

and anoxic sediments is not generally observed for labile compounds, but only for the more refractory organic fractions (e.g., Henrichs & Reeburgh, 1987; Pederson *et al.*, 1992; Canfield, 1993). However, organic P concentrations in the base-extractable fraction of the two cores indicate that, even in high molecular weight organic matter, no redox-dependent difference in the efficiency of P_{org} degradation is observed.

Another important depositional condition that is expected to strongly influence the abundance and quality of sedimentary organic matter is the organic matter source. In the central Santa Barbara Basin, it is likely that the P_{org} composition of individual layers within the varves is quite different. Logistically, analyzing P_{org} composition requires a large amount of material. Thus, for this study, it was not possible to sample on the depth scales necessary to distinguish P_{org} composition within varves. Even at the surface of the core (before compaction), a single varve sediment couplet is approximately 0.4 cm, while the sampling interval for P_{org} reservoir extraction was between 0.35 and 0.6 cm. For ^{31}P -NMR analyses, it was necessary to pool extracts near the top of the core, so depth resolution for these results was 0.7 cm. In future, it would be interesting to try to acquire varve-scale structural information, perhaps by sampling whole box cores so that more material could be pooled without sacrificing depth resolution. It is expected that terrestrially-dominated sediment layers would tend to have lower total organic P and fractionally less lipid and aqueous-extractable P. Within the base extract, the relative importance of monoesters may be even more prominent in sediment intervals where less fresh organic matter is input in surface sediments.

4.5.8 Polyphosphates: Indicators of Luxury P Consumption

Polyphosphates, while not organic compounds, are of biogenic origin. The occurrence of polyphosphates in these sediments indicates P storage by algae and/or bacteria under conditions of excess phosphate, a phenomenon referred to as "luxury consumption" (Dawes & Senior, 1973; Kulaev, 1979; Preiss, 1989). Intracellular

polyphosphate accumulation can be large, accounting for up to 20% of cell dry weight (Deinema *et al.*, 1980). The similarity between the depth profiles of polyphosphate (Figure 4-18) and the simple P biochemicals measured in the lipid and aqueous P reservoirs (Figure 4-5) suggests that much of the polyphosphate measured in these sediments may originate from polyphosphates contained within intact biomass at the time of collection. Since polyphosphates are very polar and therefore would tend to sorb to ferric iron minerals, they are probably not extracted in the aqueous P reservoir. Hupfer *et al.* (1995b) suggested that polyphosphates may be present in surface sediments, but not deeper. In Santa Barbara Basin sediments, a small fraction of polyphosphates is found even in the deepest intervals of each core.

The polyphosphate concentration in core J is much higher than that observed in the other central basin core. Abundance of this compound indicates that the sediment biota and/or the plankton contributing organic matter to these sediments are living under nutrient-enriched conditions. Relatively higher polyphosphate concentration could indicate a combination of higher biomass concentration and an increase in the polyphosphate content of cells. Certainly, there is a reasonable chance that the sediment-water interface may contain more biomass in core J, since it was collected in the prime season for development of the bacterial mat. The large difference between the two central basin cores indicates that this is true and serves as a reminder that the temporal (and perhaps spatial) variability of P components can be large.

It is generally thought that polyphosphates act as a redox-dependent P sink in sediments (Davelaar, 1993), with P storage under anaerobic conditions and P release under aerobic conditions (Comeau *et al.*, 1986; Wentzel *et al.*, 1991). The data from Core J support that hypothesis. The fluctuating redox conditions in the basin which result from intermittent flushing of bottom waters perfectly describe the ideal condition for polyphosphate metabolism. Further, the observation that bacteria store polyphosphate mainly under anaerobic conditions may explain the extremely high polyphosphate

concentration observed in core J. This core was collected in October, when the bacterial mat is at its peak. At the time of collection, a well developed interfacial mat was visually discernible. The low-oxygen conditions that favor development of the bacterial mat also favor storage of P as polyphosphates.

4.6 Conclusions

The novel approach described here, using a sequential extraction scheme in tandem with molecular-level information from ^{31}P -NMR, provides a unique avenue for resolving structural controls on the evolution of the sedimentary P_{org} pool during diagenesis. These data allow diagenetic remineralization of specific P_{org} compound classes in marine sediments to be quantified for the first time. The results of this study refute the hypothesis that phosphonates (compounds with direct C-P linkage) are inherently more resistant to degradation than other P_{org} compounds. Rather, they are degraded at the same rate, or possibly even faster, than other P_{org} compounds. The rapid decrease with depth in the lipid P and aqueous P reservoirs indicates that unbound P_{org} biochemicals are not a quantitatively important reservoir of preserved P_{org} .

Incorporation of simple P_{org} compounds into a humic matrix, either by sequestration, chemical bonding during humification, or metal bridging, is likely to be the primary mechanism for P_{org} preservation in these sediments. In addition, metal bridging to organic matter or mineral surfaces may serve another important role in determining P_{org} depth distributions in marine sediments. Interaction with metals can result in immobilization of orthophosphate, leading to a P fraction that behaves analytically like P_{org} , but is not organic at all.

Combining the information from soluble and insoluble P_{org} fractions, it is apparent that little transfer of phosphonates into the insoluble sediment fraction is likely. However, this conclusion cannot be extended to other organic P compound classes, and monoesters

in particular might be expected to persist in the insoluble organic fraction. While these data provide no evidence for direct structural control on remineralization of P_{org} , they suggest that sorption of particular P_{org} compound classes may play an important role in enhancing their preservation.

Finally, the P_{org} overestimation artifact identified by contrasting P_{org} quantified by ^{31}P -NMR versus traditional wet chemical means suggests that P_{org} concentrations used to date in global marine P budgets may be in error. Specifically, overestimates of sedimentary P_{org} concentration that exist in all budgets constructed to date result in attribution of an erroneously high portion of the P burial flux to organic P. This finding goes some way to addressing the paradox of P_{org} preservation articulated in this and other chapters of this thesis. That is, given the inherently reactive nature of P biochemicals, why do they persist in marine sediments and ancient sedimentary rocks? The magnitude of this paradox needs to be re-visited in light of the P_{org} overestimation artifact identified by this work.

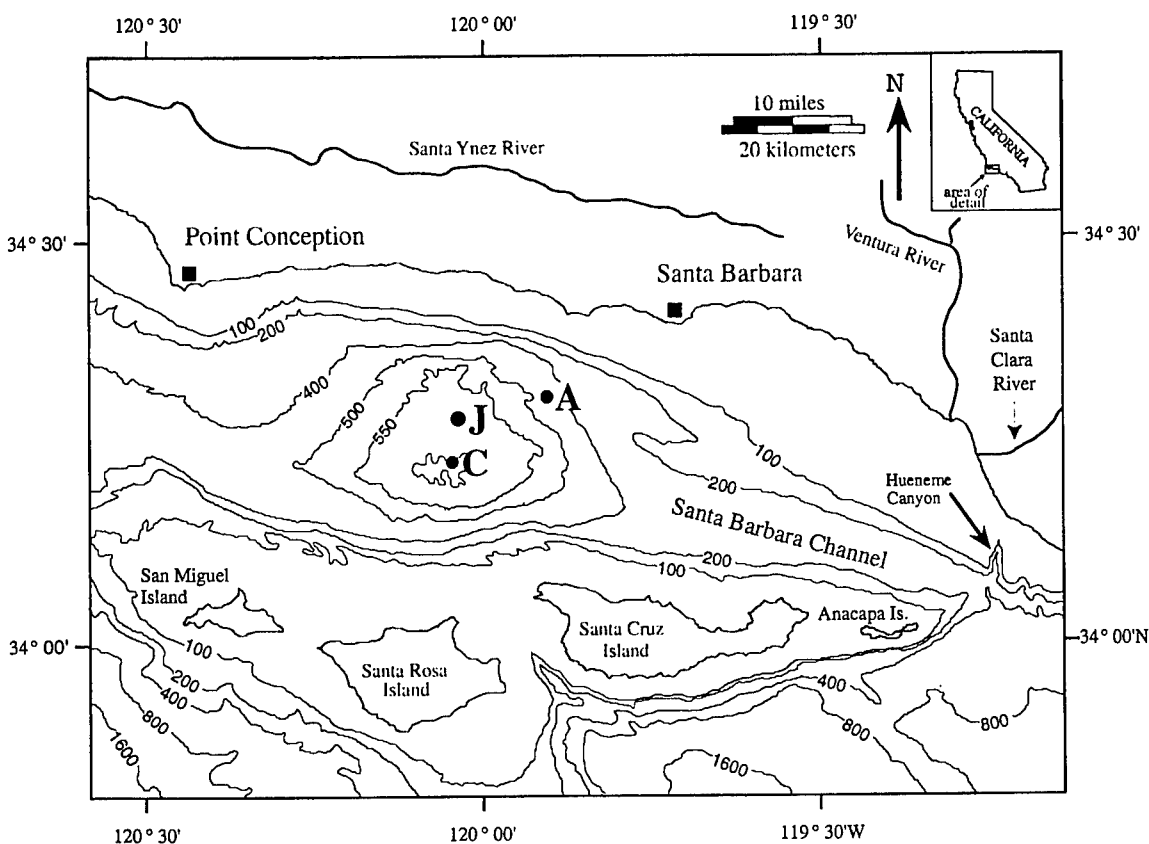


Figure 4-1. Map of the Santa Barbara Basin (after Kennett *et al.*, 1994), showing the location of the three cores used in this study. Water depths are given in meters. In the deep basin, where core C and core J were collected, bottom waters have little or no oxygen, and a bacterial mat dominates sediments at the sediment-water interface. On the margin of the basin (core A), bottom waters are oxygenated and sediments are bioturbated to a depth of 5-10 centimeters.

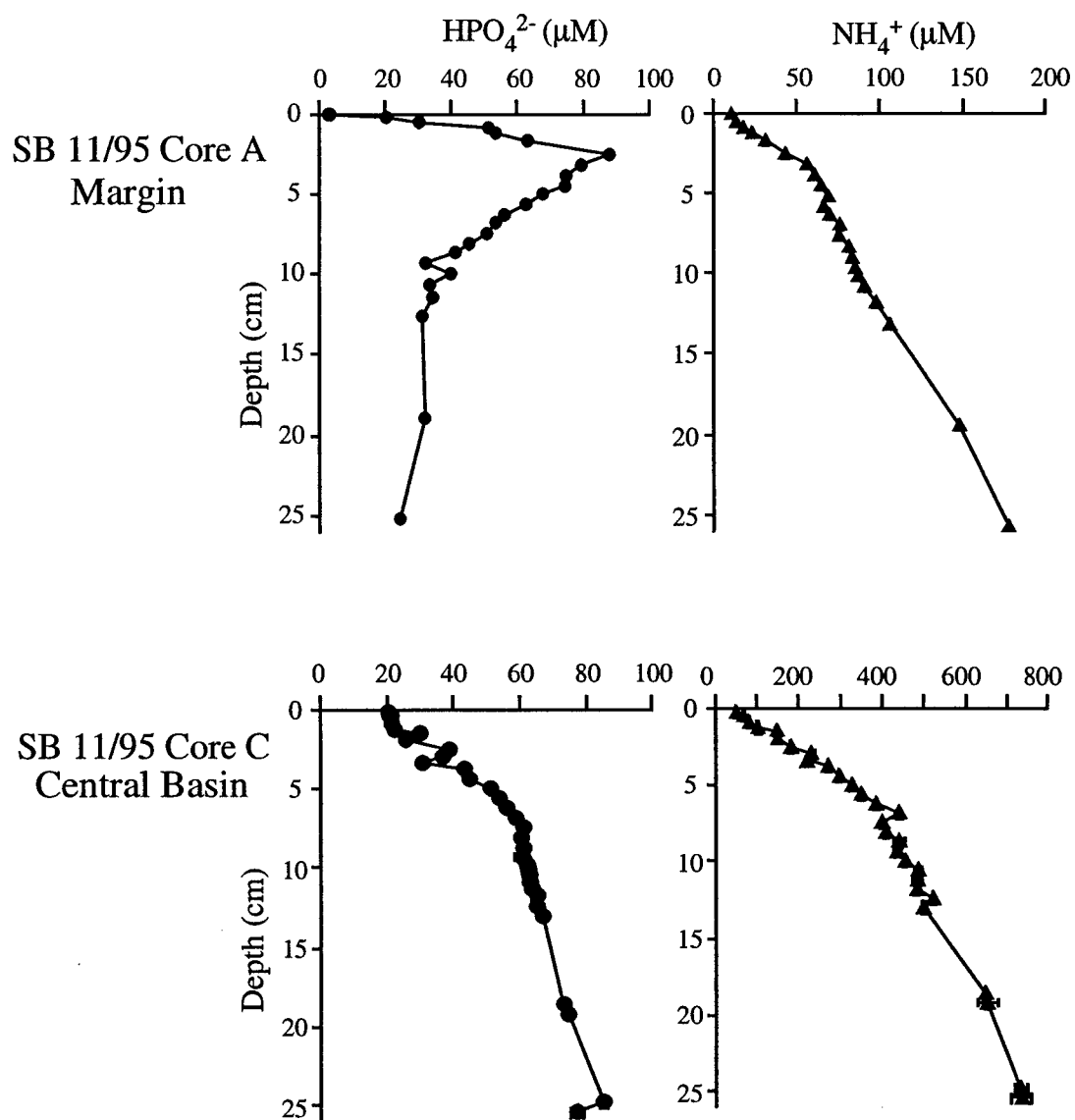


Figure 4-2. Pore water profiles of soluble reactive P (e.g., orthophosphate) and ammonia in cores A and C (Ruttenberg, unpublished data). P accumulates in pore waters over the full depth scale of core C, but in core A is removed by some process at depth, causing a decrease in concentration below 4 cm. In both cores, ammonia accumulates in pore waters throughout the core, reflecting the ongoing degradation of sedimentary organic matter.

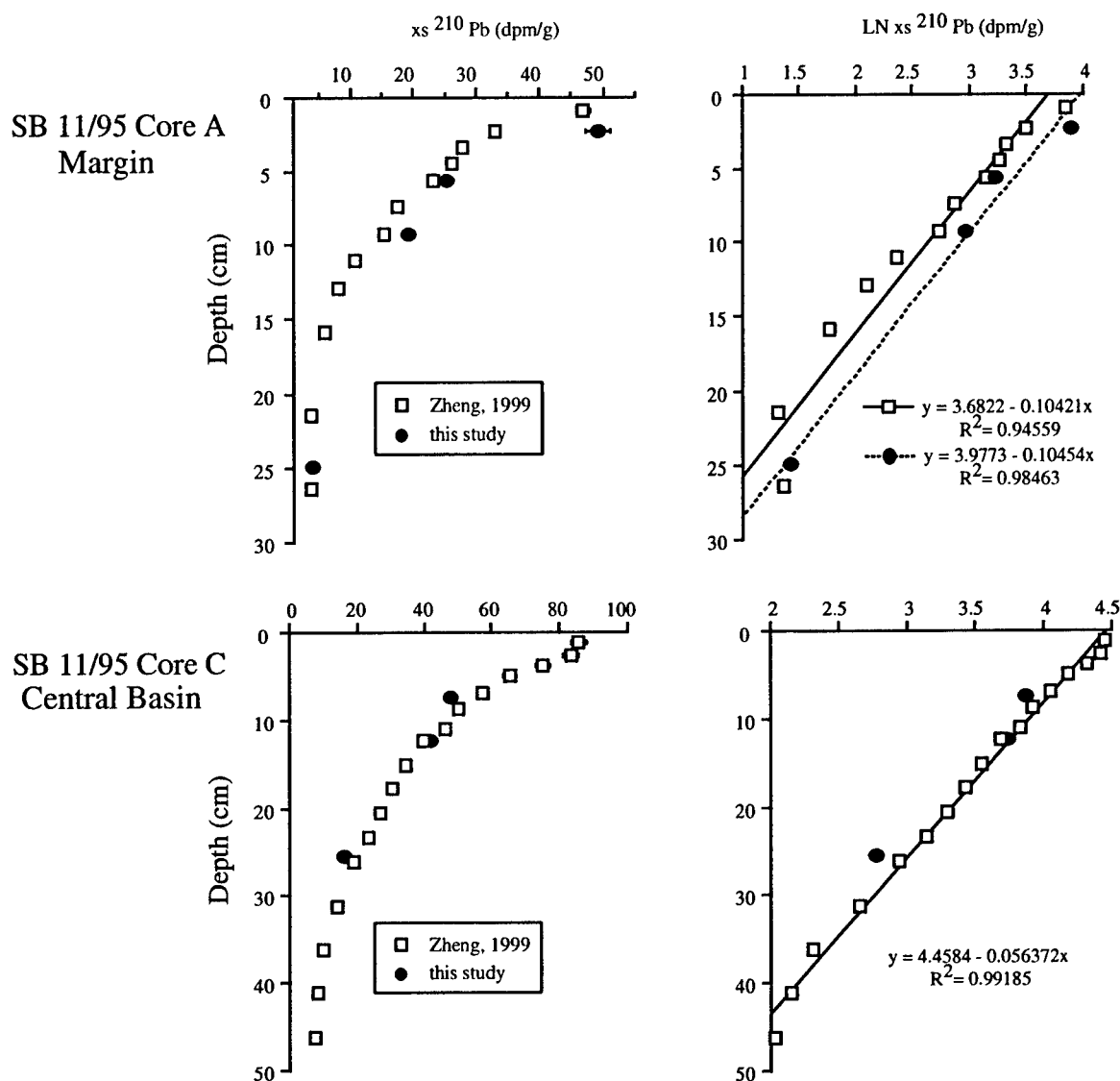


Figure 4-3. Comparison of excess ^{210}Pb measured in cores A and C with depth profiles of ^{210}Pb from parallel cores collected in the same multi-core deployments (Zheng, 1999). Measured values in core C agree well with the previously-collected data. Excess ^{210}Pb concentrations measured in core A are slightly higher than in the parallel core, but the slope of natural log [$x\text{s-}^{210}\text{Pb}$] vs. depth (used to calculate sedimentation rate) for both data sets are in excellent agreement.

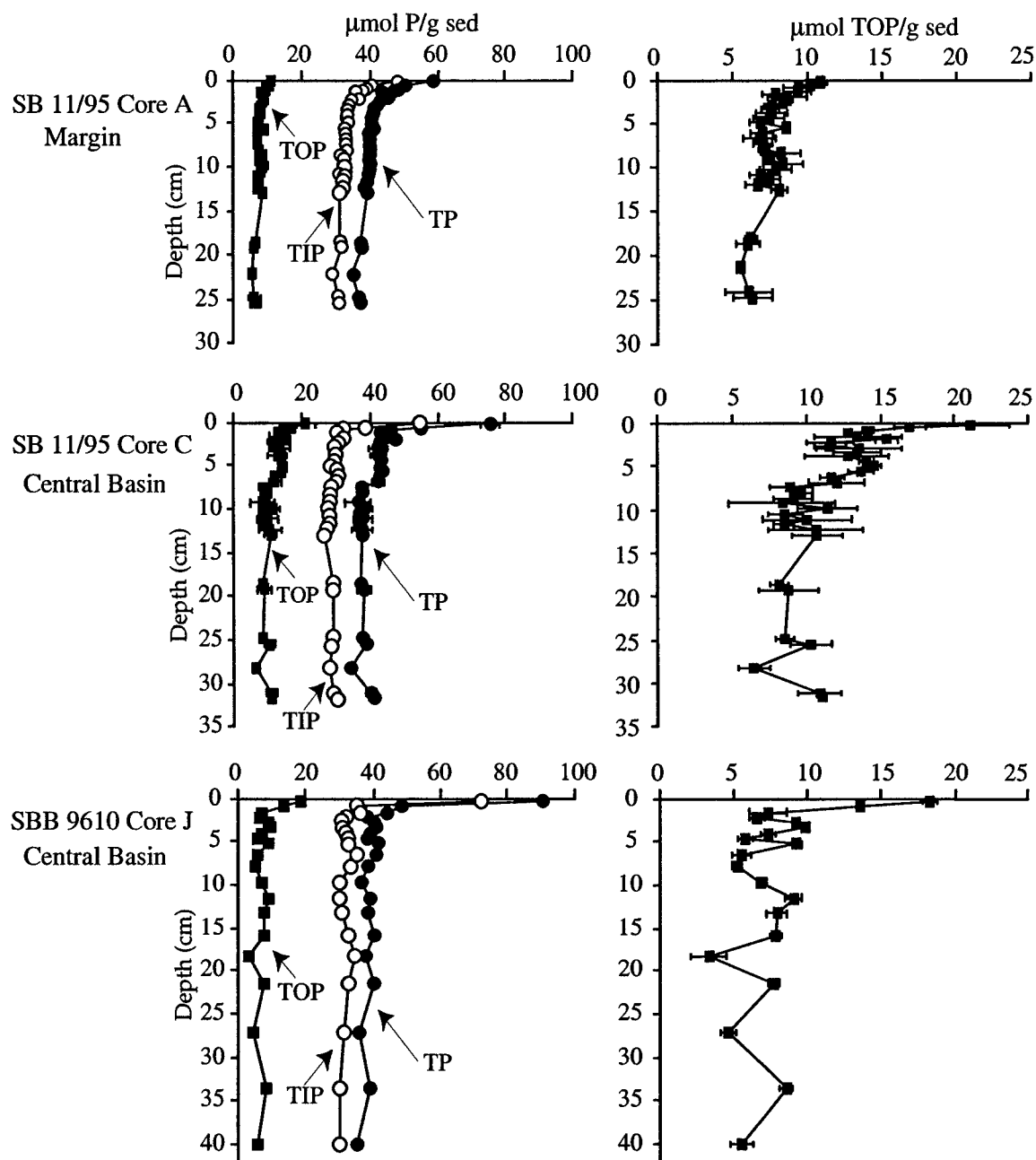


Figure 4-4. Total P (TP), total inorganic P (TIP), and total organic P (TOP) concentrations determined for the three Santa Barbara Basin cores using the Aspila *et al.* (1976) method. Panels on the right show only total organic P concentration, with the concentration scale magnified to show the depth profiles in more detail. Error bars indicate the full range of concentrations determined by duplicate analyses.

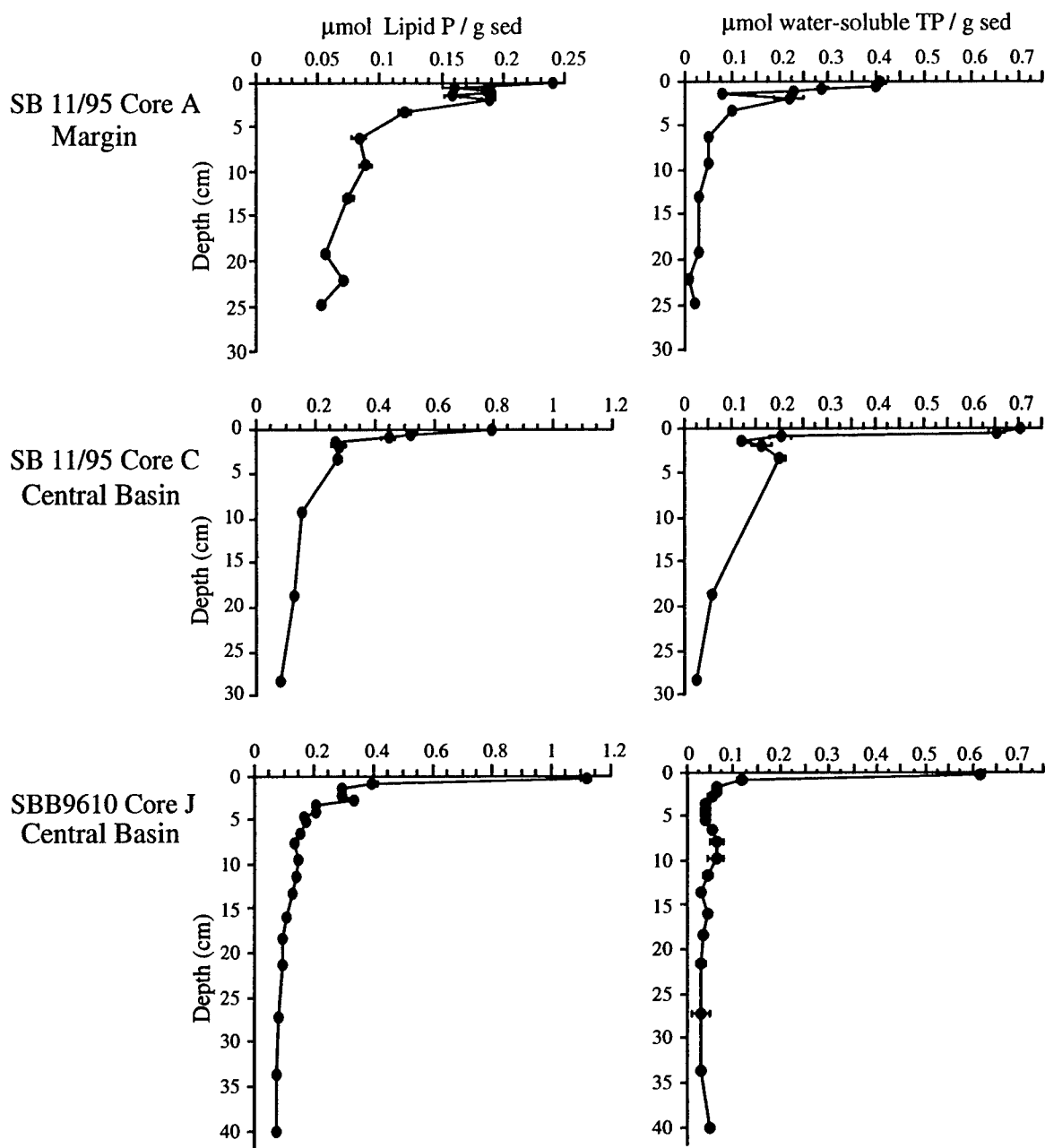


Figure 4-5. Total dissolved P concentration in lipid (left) and aqueous (right) reservoirs extracted from the three Santa Barbara Basin cores. In all 3 cores, these P reservoirs decrease rapidly with depth, reflecting a combination of decreasing biomass and remineralization during diagenesis. Error bars indicate the range of concentrations determined for duplicate analyses. Where error bars are not visible, they are smaller than the symbol size. Lipid P concentrations in core A are much lower than in the other two cores, and data are presented with an expanded x-axis.

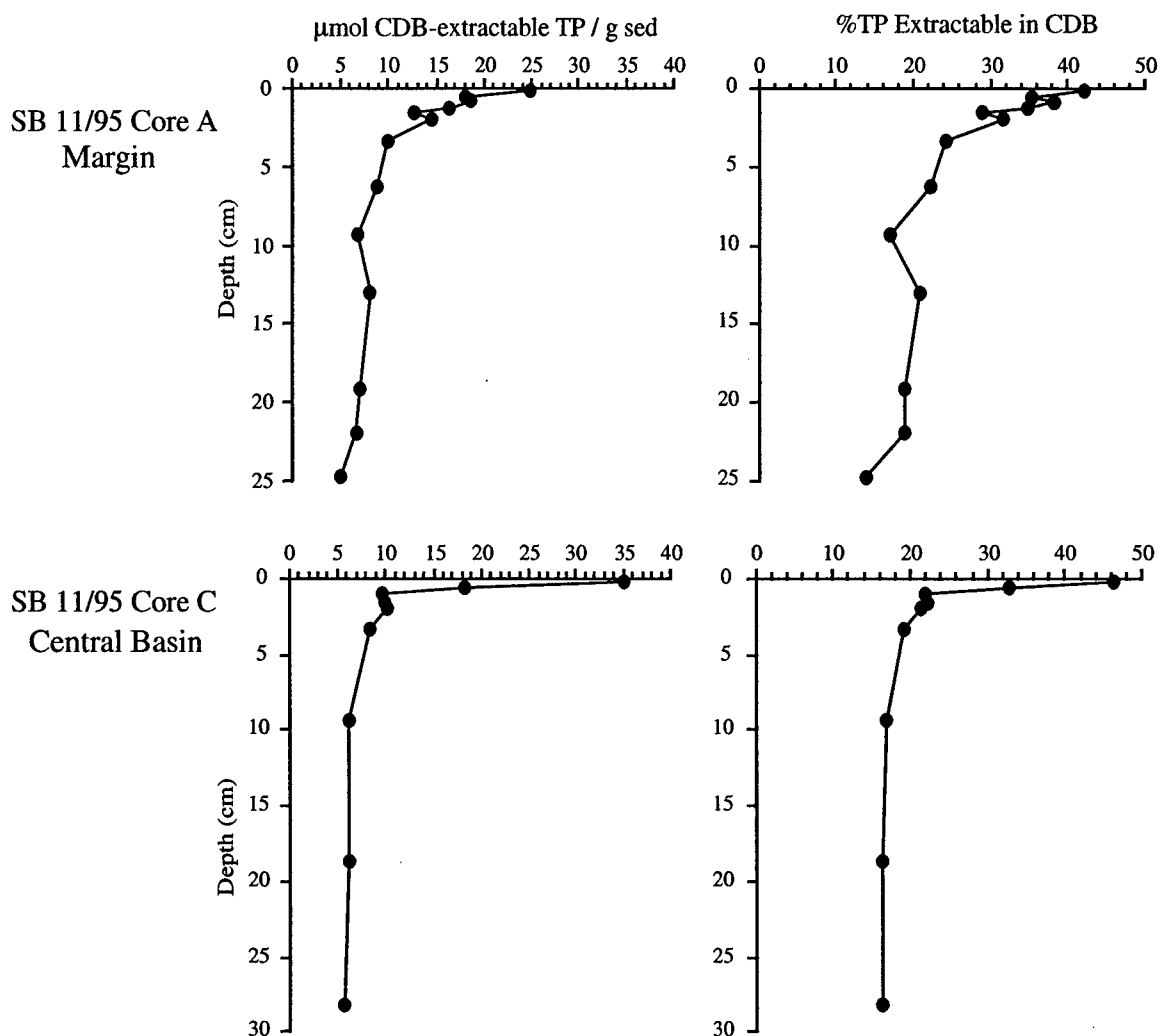


Figure 4-6. Depth profiles of total P extracted from sediments in cores A and C with citrate dithionite bicarbonate (CDB). CDB-P concentration (left) and the percent of total sediment P in the CDB extract (right) are shown. Error bars indicate the range of concentrations determined for duplicate analyses. Where error bars are not visible, they are smaller than the symbol size. CDB-P is high at the surface, accounting for nearly half of total P. The decrease in CDB-P with depth in core A is more gradual than in core C, where CDB-P decreases strikingly in the top two centimeters. The decrease with depth reflects release of P from reactive iron phases such as iron oxyhydroxides.

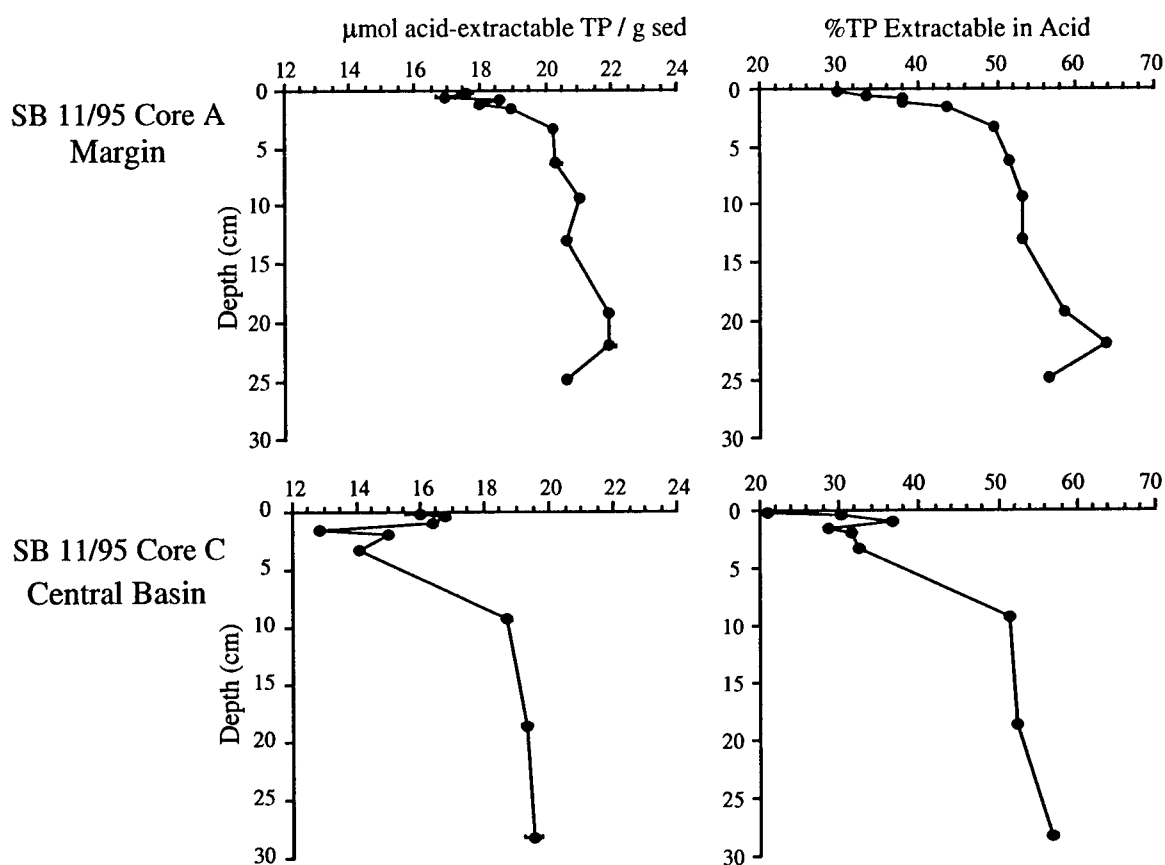


Figure 4-7. Depth profiles of total P extracted in 0.1 M HCl. Acid-P concentration (left) and the percent of total sediment P in the acid extract (right) are shown. Error bars indicate the range of concentrations determined by duplicate analyses. Where error bars are not visible, they are smaller than the symbol size. The increase in acid-P in these two cores suggests incorporation of P into clays and authigenic minerals during diagenesis.

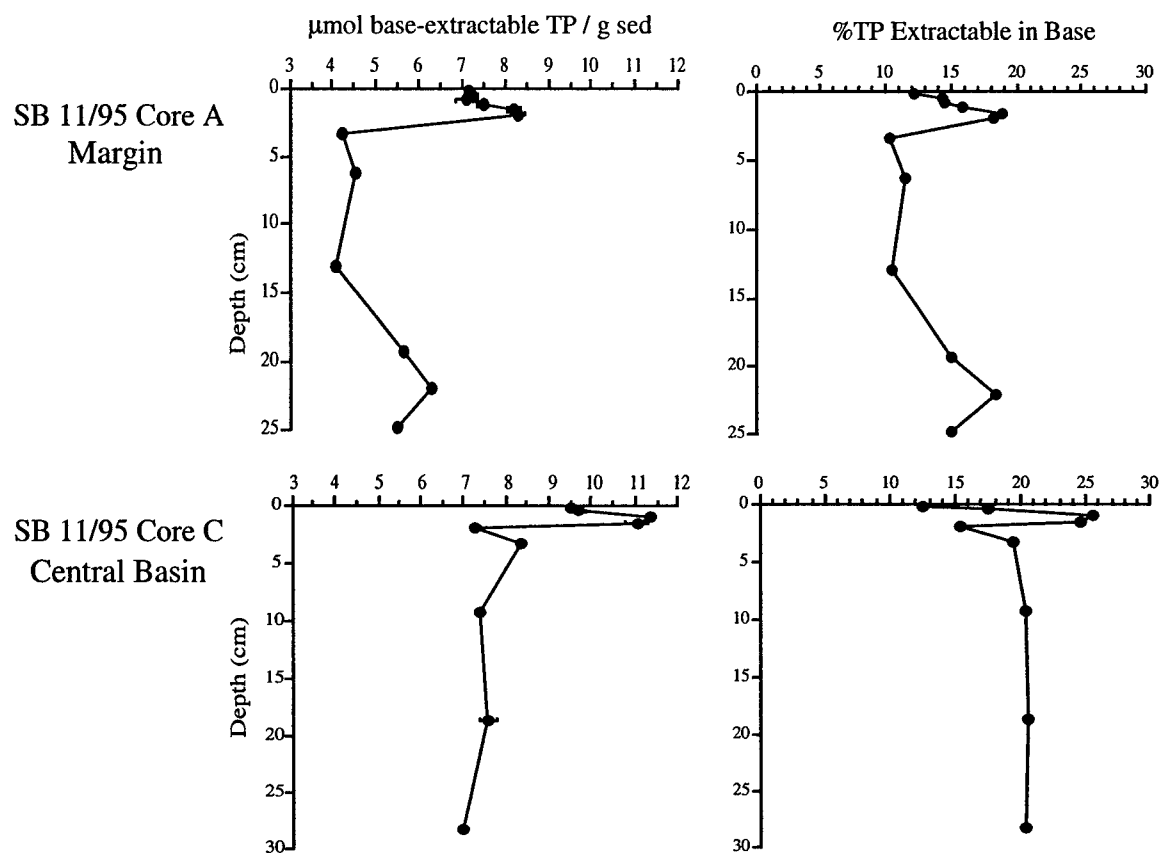


Figure 4-8. Depth profiles of total P extracted in 0.5 M NaOH for cores SB 11/95 A and C. Base-P concentration (left) and the percent of total sediment P in the base extract (right) are shown. Error bars indicate the range of concentrations determined for duplicate analyses. Where error bars are not visible, they are smaller than the symbol size. P in this fraction is associated with humic compounds.

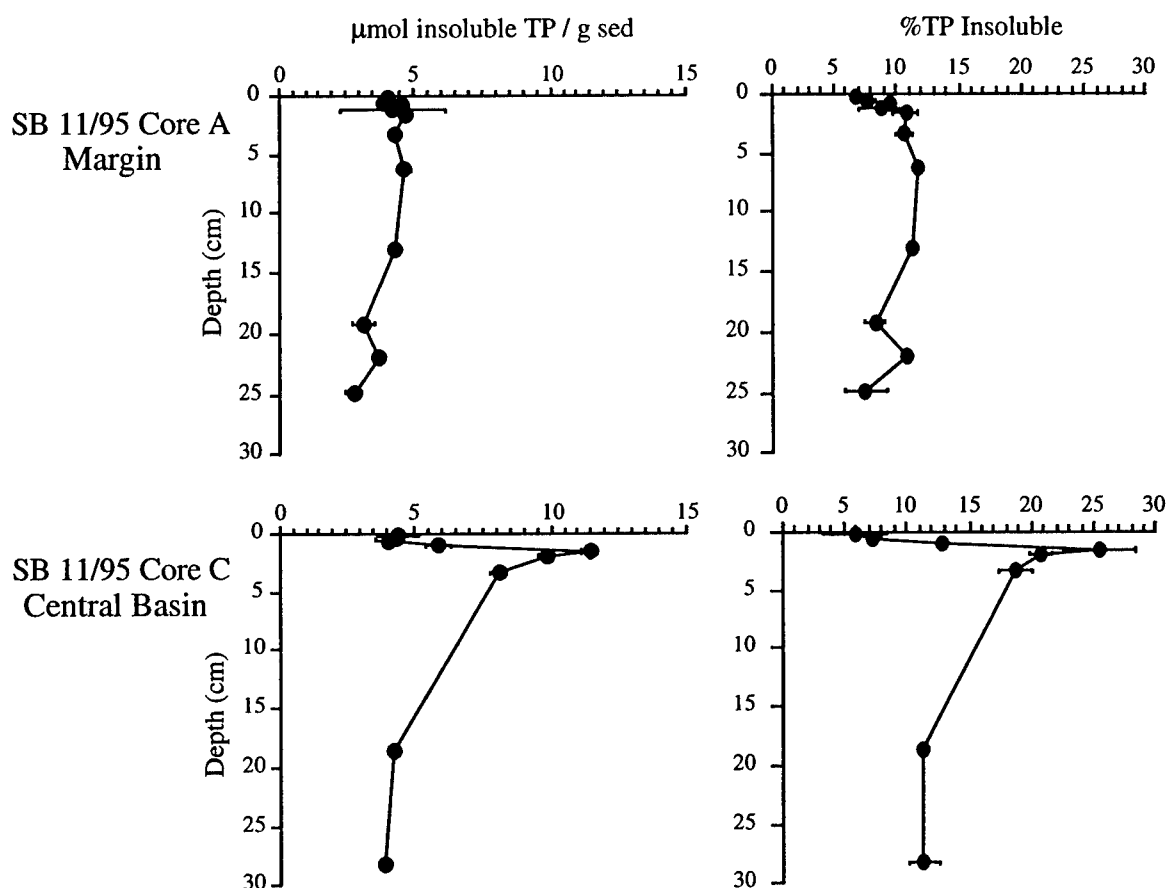


Figure 4-9. Total P in the insoluble sediment residue after sequential extraction of cores A and C. Error bars indicate the range of concentrations determined for duplicate analyses. Where error bars are not visible, they are smaller than the symbol size. In core A, the absolute concentration of P and the fraction of P that is insoluble remains roughly constant with depth. In core C, insoluble P increases sharply below the surface, but decreases gradually to core-top values. Total P in the insoluble residue is between 5 and 15 percent of total sediment P in the deepest intervals of both cores.

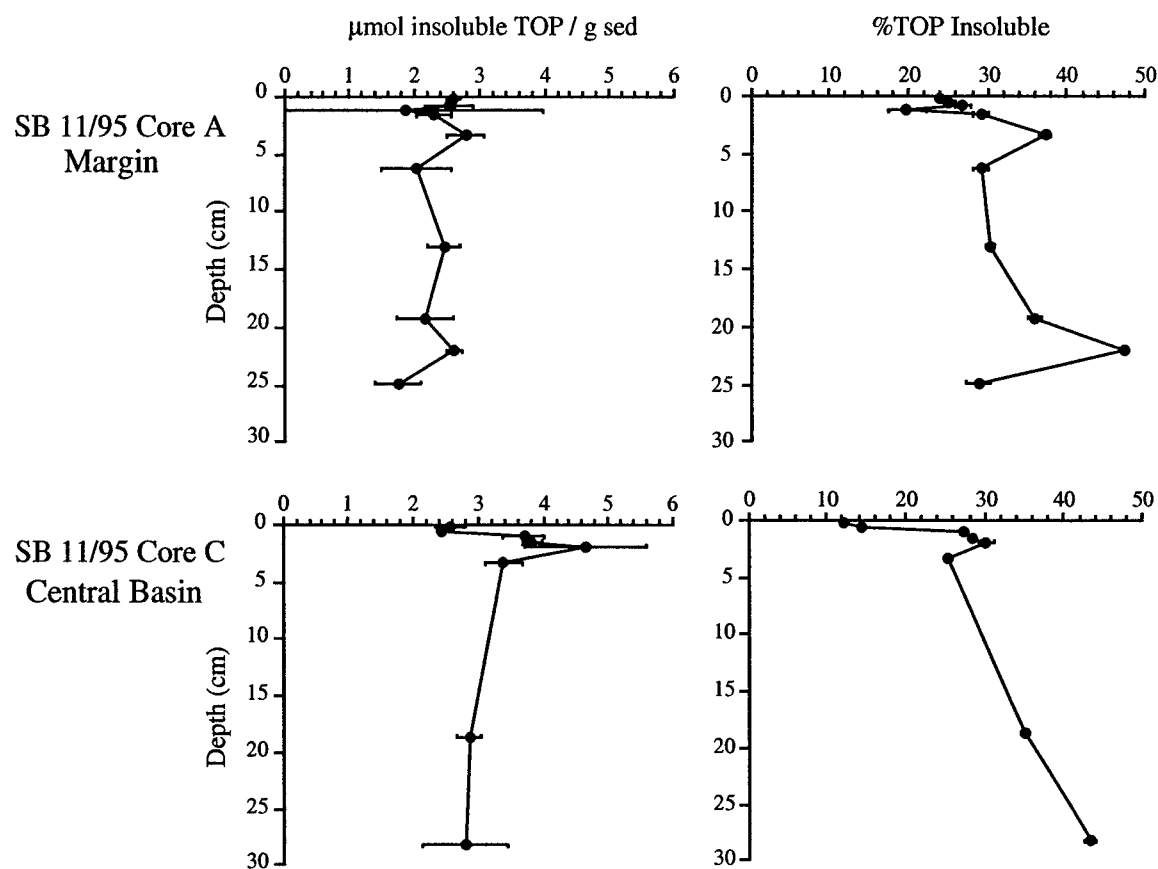


Figure 4-10. Organic P in the insoluble sediment residue after sequential extraction of cores A and C. Error bars indicate the range of concentrations determined for duplicate analyses. Where error bars are not visible, they are smaller than the symbol size. The changes in each profile with depth are similar to those observed for total P. At depth in these cores, between 30 and 50% of total sediment organic P is measured in the insoluble fraction.

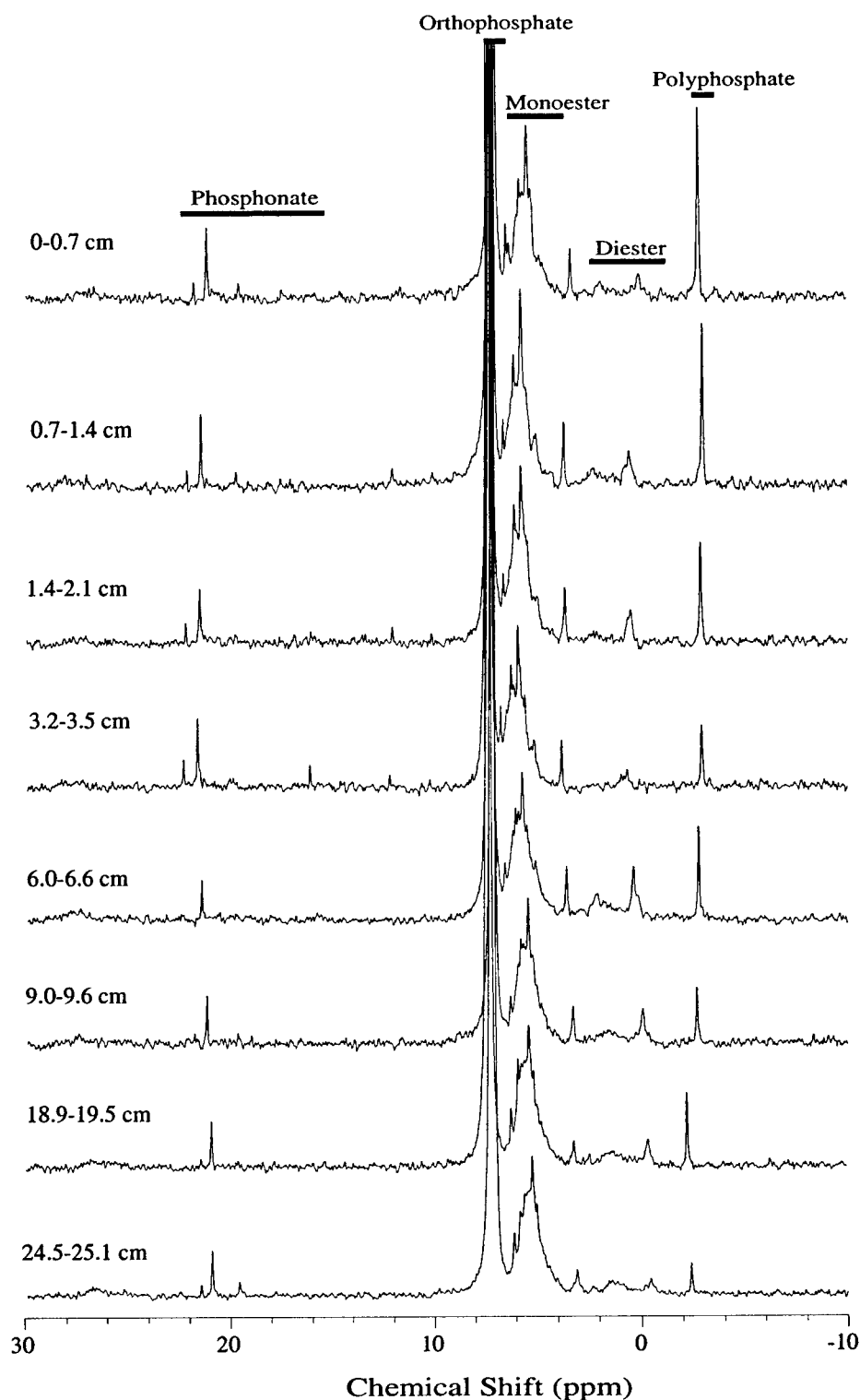


Figure 4-11. ^{31}P -NMR spectra of base extracts from margin core SB11/95 A. Spectra were acquired with a 100 ppm spectral window centered at 0 ppm, using a 45° flip angle, 0.6 second acquisition time and a delay of 1.5 seconds. 10 Hz line-broadening was applied to all spectra. In all spectra, the orthophosphate peak (which represents 70-80% of the total signal) has been truncated to make the other peaks visible in more detail.

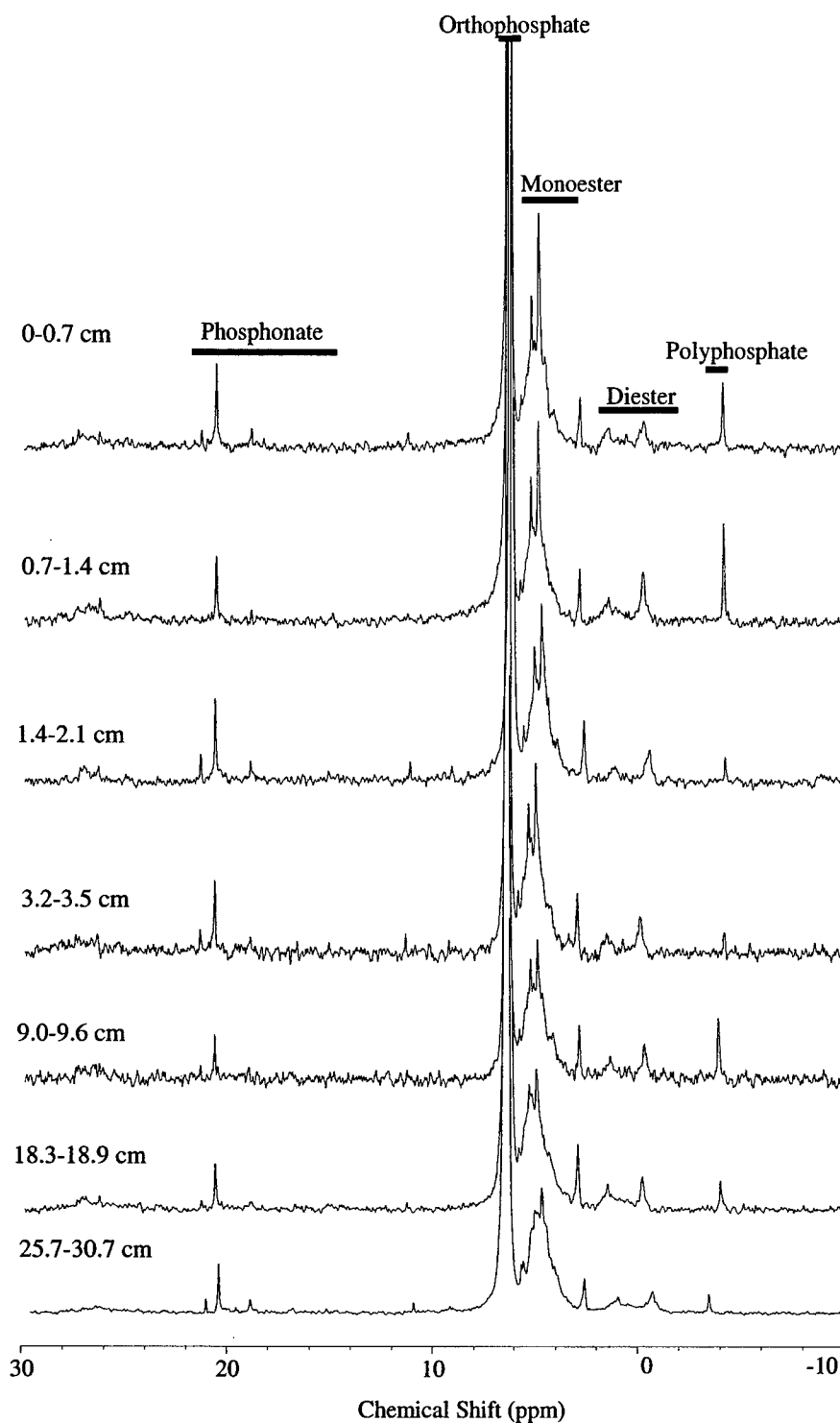


Figure 4-12. ^{31}P -NMR spectra of base extracts from central basin core SB11/95 C. Spectra were acquired with a 100 ppm spectral window centered at 0 ppm, using a 45° flip angle, 0.6 second acquisition time and a delay of 1.5 seconds. 10 Hz line-broadening was applied to all spectra. In all spectra, the orthophosphate peak (which represents 65-75% of the total signal) has been truncated to make the other peaks visible in more detail.

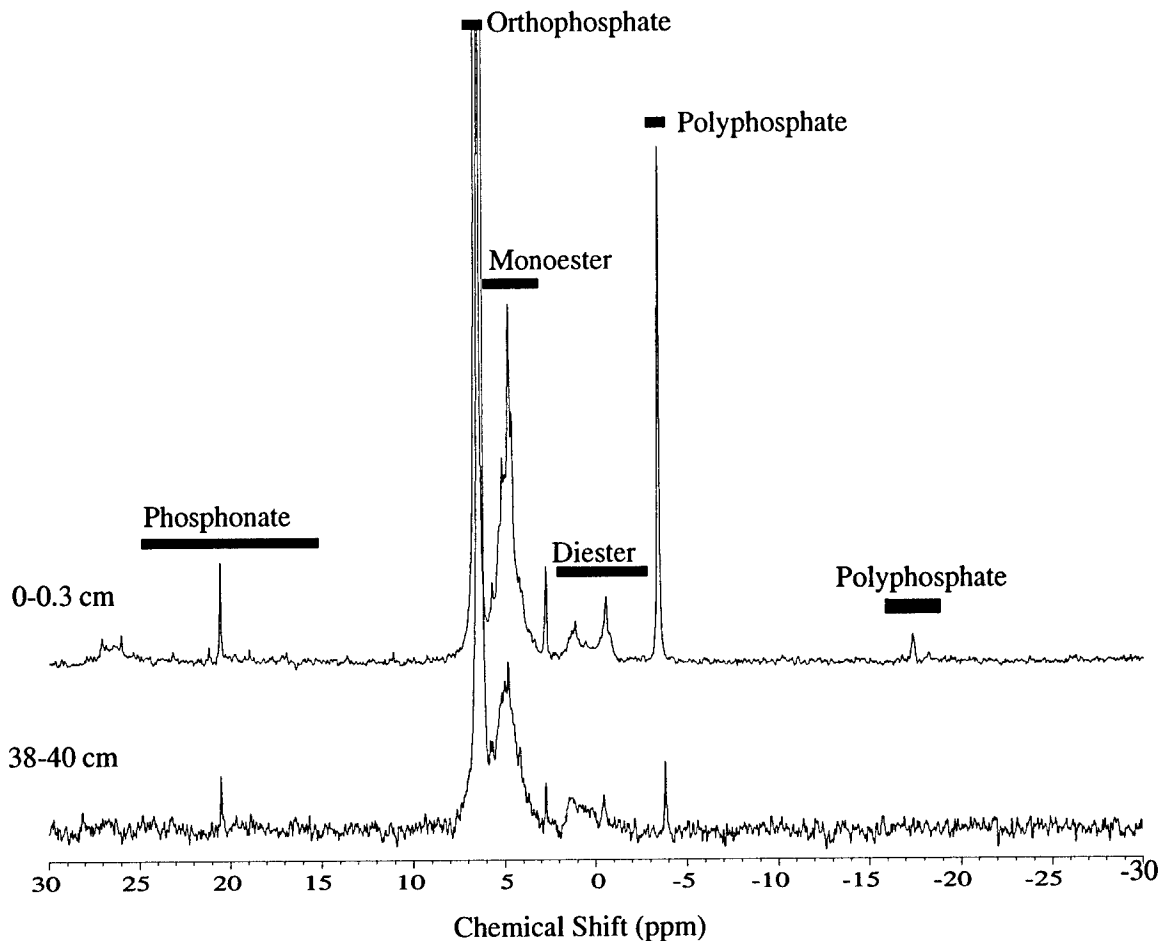


Figure 4-13. ^{31}P -NMR spectra of base extracts from central basin core J. Spectra were acquired with a 100 ppm spectral window centered at 0 ppm, using a 45° flip angle, 0.6 second acquisition time and a delay of 1.5 seconds. 10 Hz line-broadening was applied to both spectra. In both spectra, the orthophosphate peak (which represents 65-75% of the total signal) has been truncated to make the other peaks visible in more detail. Only two intervals from this core were analyzed by ^{31}P -NMR, and these two sediment samples were prepared identically to sediments from cores SB11/95 A and C.

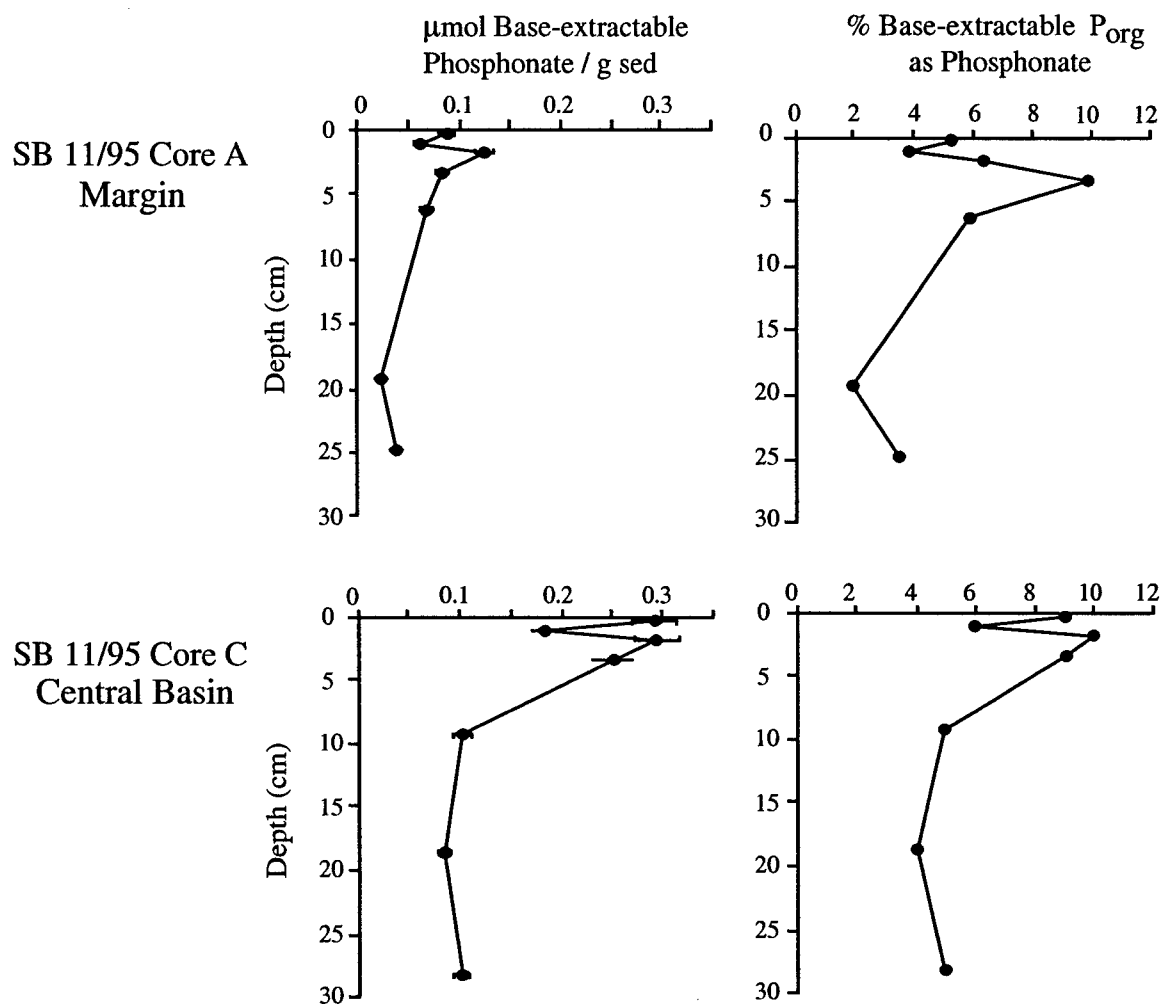


Figure 4-14. Concentration of base-extractable phosphonates in cores A and C. Functional group concentrations (left panel) are calculated by multiplying total P in the base extract by the fraction of total peak area in the phosphonate ^{31}P -NMR chemical shift region. Error bars indicate the estimated 15% variation in peak area response for functional group abundance measured by ^{31}P -NMR (see Chapter 2). Also shown is the percent of base-extracted organic P in the phosphonate fraction (right panel). Phosphonates account for less than 10% of total organic P in these extracts.

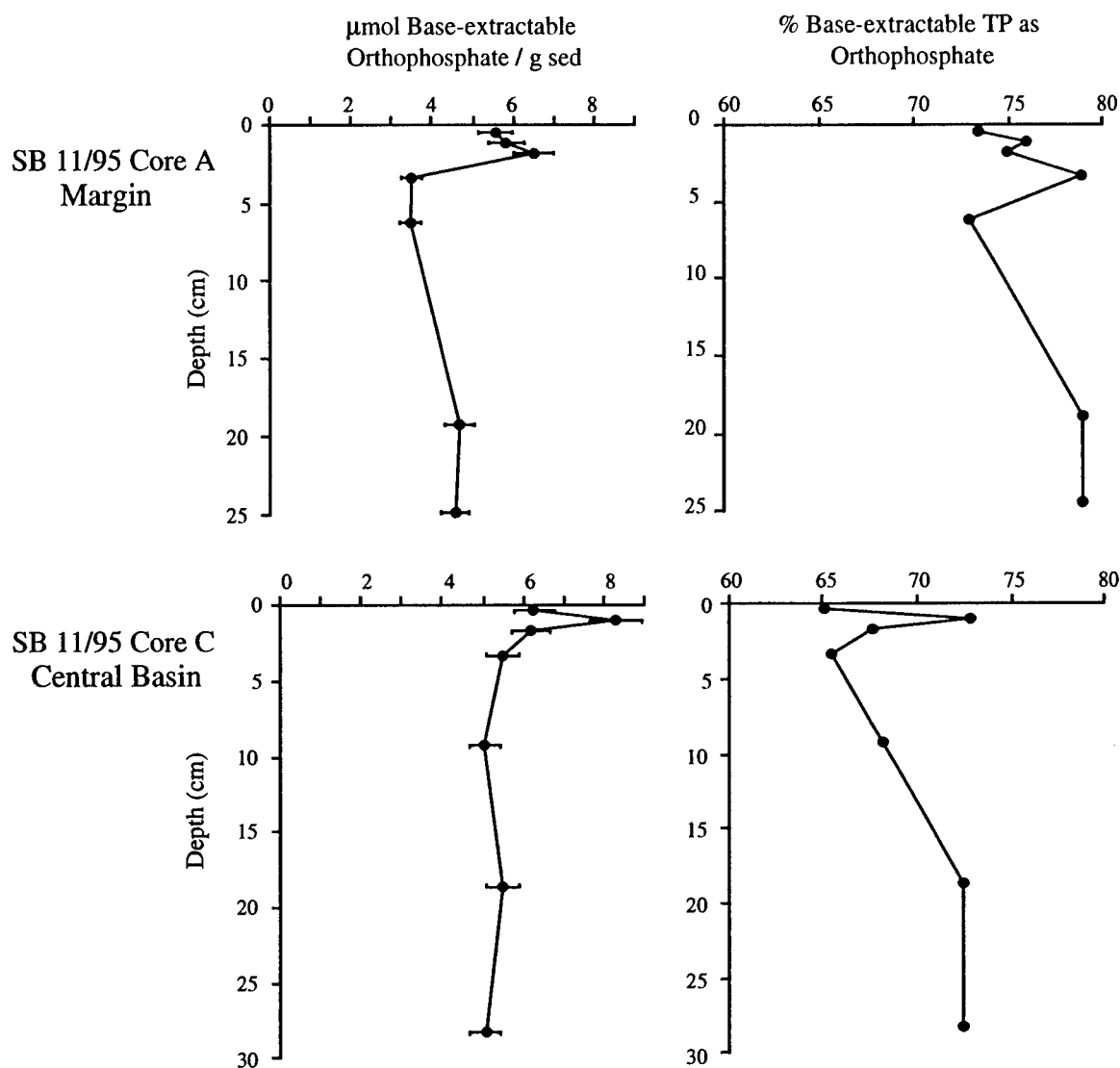


Figure 4-15. Concentration of base-extractable orthophosphate in cores A and C. Functional group concentrations (left panel) are calculated by multiplying total P in the base extract by the fraction of total peak area in the orthophosphate ^{31}P -NMR chemical shift region. Error bars indicate the estimated 15% variation in peak area response for functional group abundance measured by ^{31}P -NMR see Chapter 2). Also shown is the percent of total base-extracted P in the orthophosphate fraction (right panel). Orthophosphate accounts for 65 to 80% of total P in these extracts.

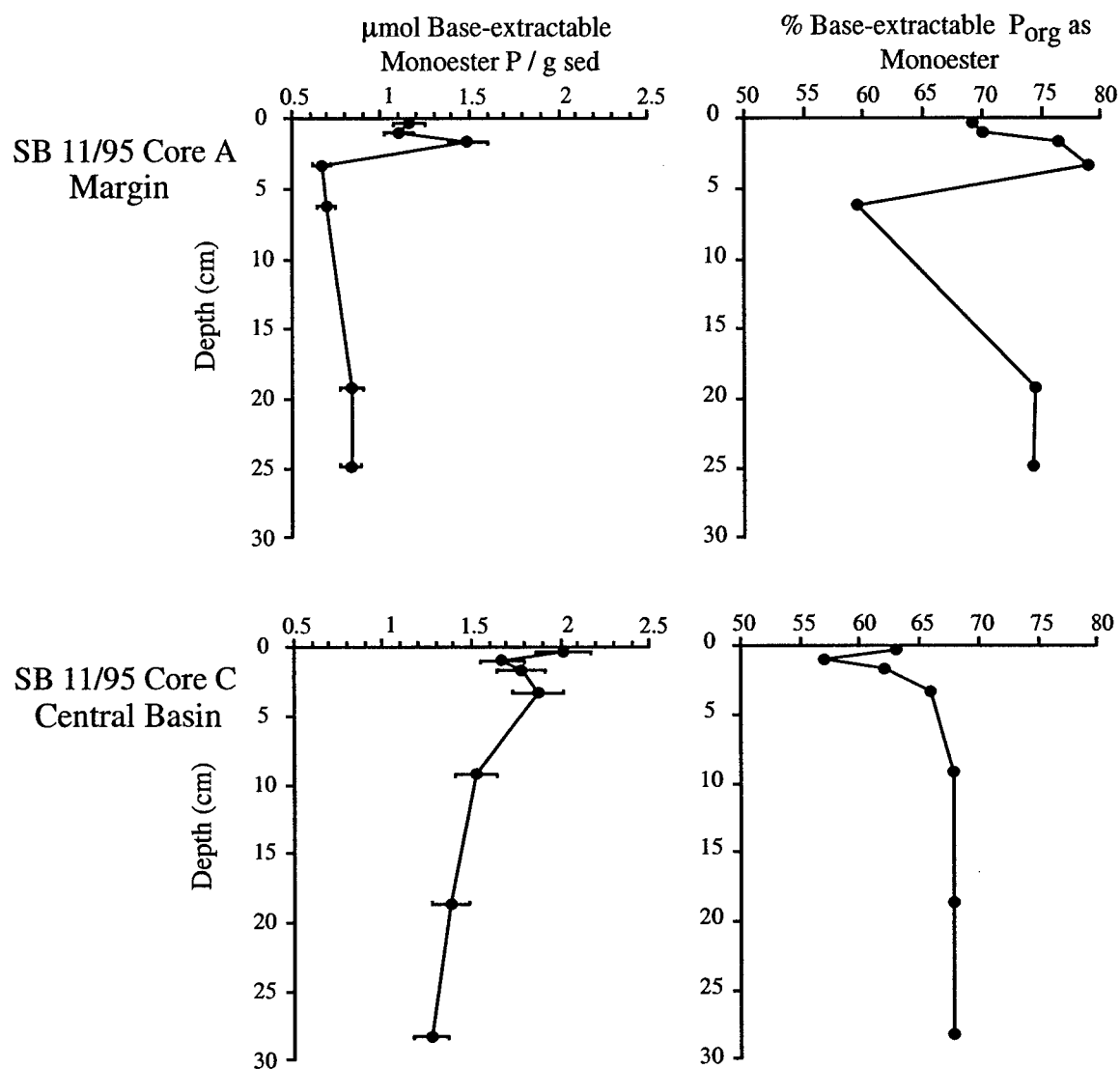


Figure 4-16. Concentration of base-extractable monoester P in cores A and C. Functional group concentrations (left panel) are calculated by multiplying total P in the base extract by the fraction of total peak area in the monoester ^{31}P -NMR chemical shift region. Error bars indicate the estimated 15% variation in peak area response for functional group abundance measured by ^{31}P -NMR (see Chapter 2). Also shown is the percent of base-extracted organic P in the monoester fraction (right panel). Monoesters are by far the most abundant organic P fraction in these extract (55-80% of total organic P), but they decrease with depth in both cores, indicating their susceptibility to remineralization.

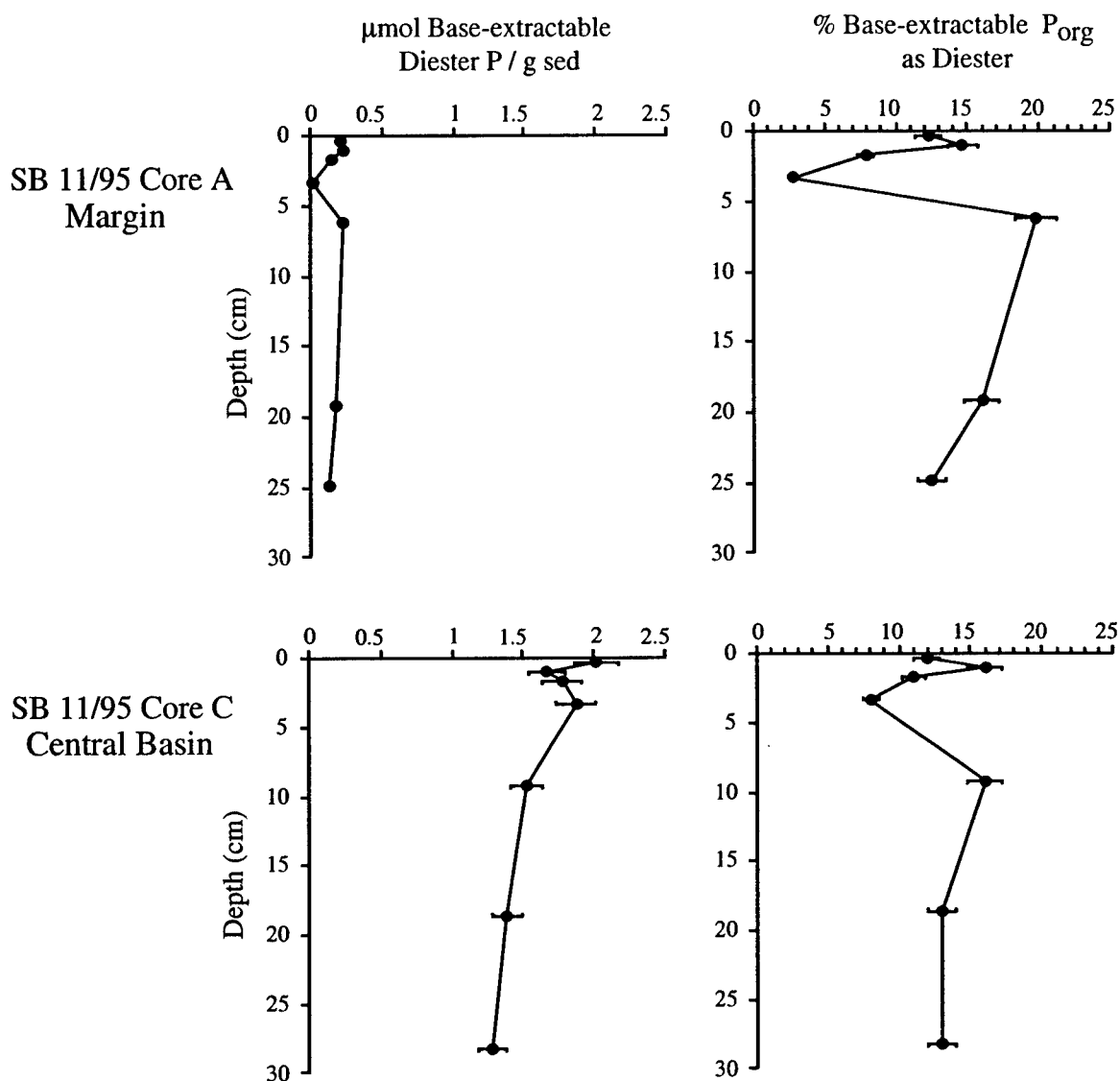


Figure 4-17. Concentration of base-extractable diester P in cores A and C. Functional group concentrations (left panel) are calculated by multiplying total P in the base extract by the fraction of total peak area in the diester ^{31}P -NMR chemical shift region. Error bars indicate the estimated 15% variation in peak area response for functional group abundance measured by ^{31}P -NMR (see Chapter 2). Also shown is the percent of base-extracted organic P in the diester fraction (right panel). The increase in diesters as a percent of organic P below ~5 cm in both cores suggests incorporation of diesters into humic compounds during diagenesis.

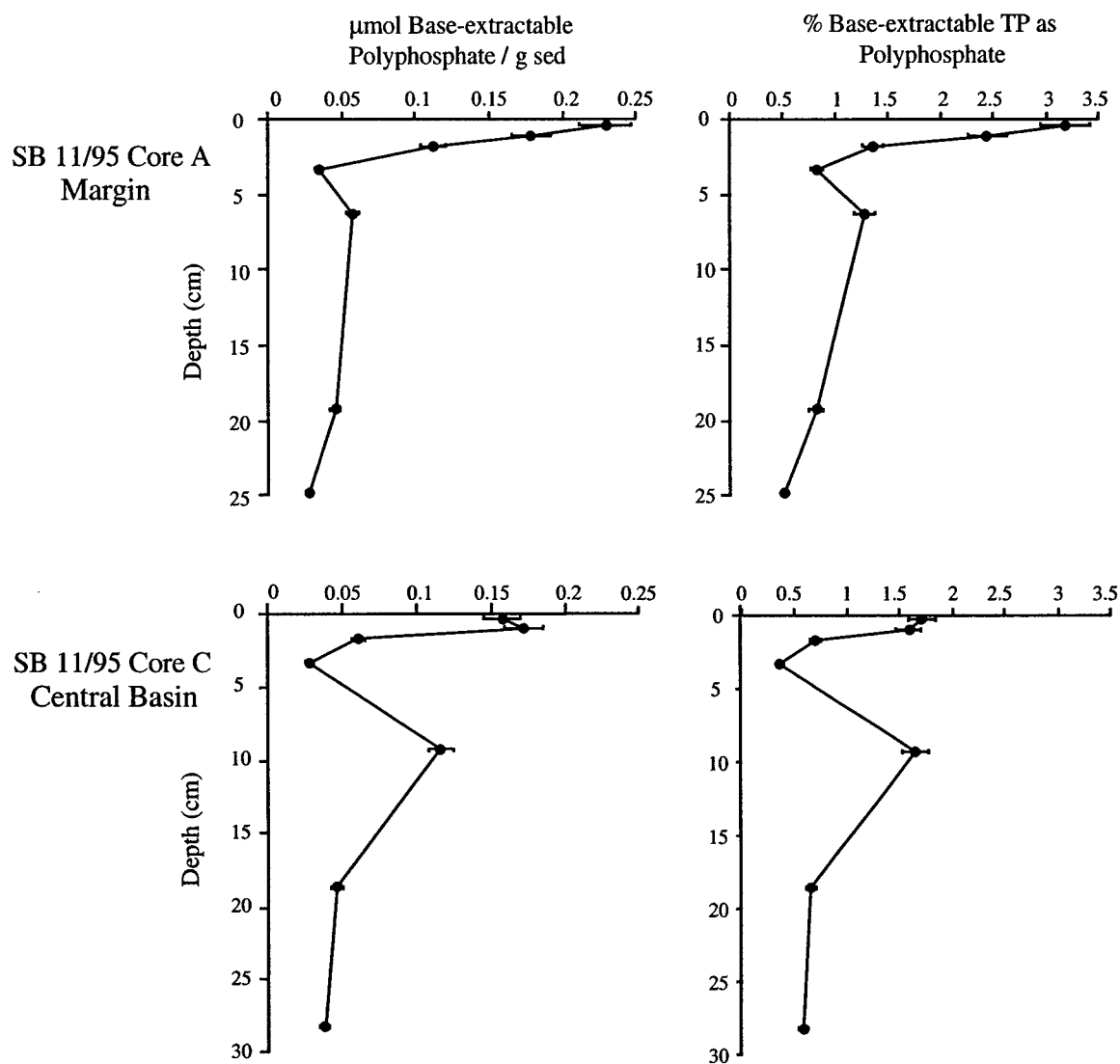


Figure 4-18. Concentration of base-extractable polyphosphates in cores A and C. Functional group concentrations (left panel) are calculated by multiplying total P in the base extract by the fraction of total peak area in the polyphosphate ^{31}P -NMR chemical shift region. Error bars indicate the estimated 15% variation in peak area response for functional group abundance measured by ^{31}P -NMR (see Chapter 2). Also shown is the percent of total base-extracted P in the polyphosphate fraction (right panel). Polyphosphates account for only a small fraction of total base-extractable P.

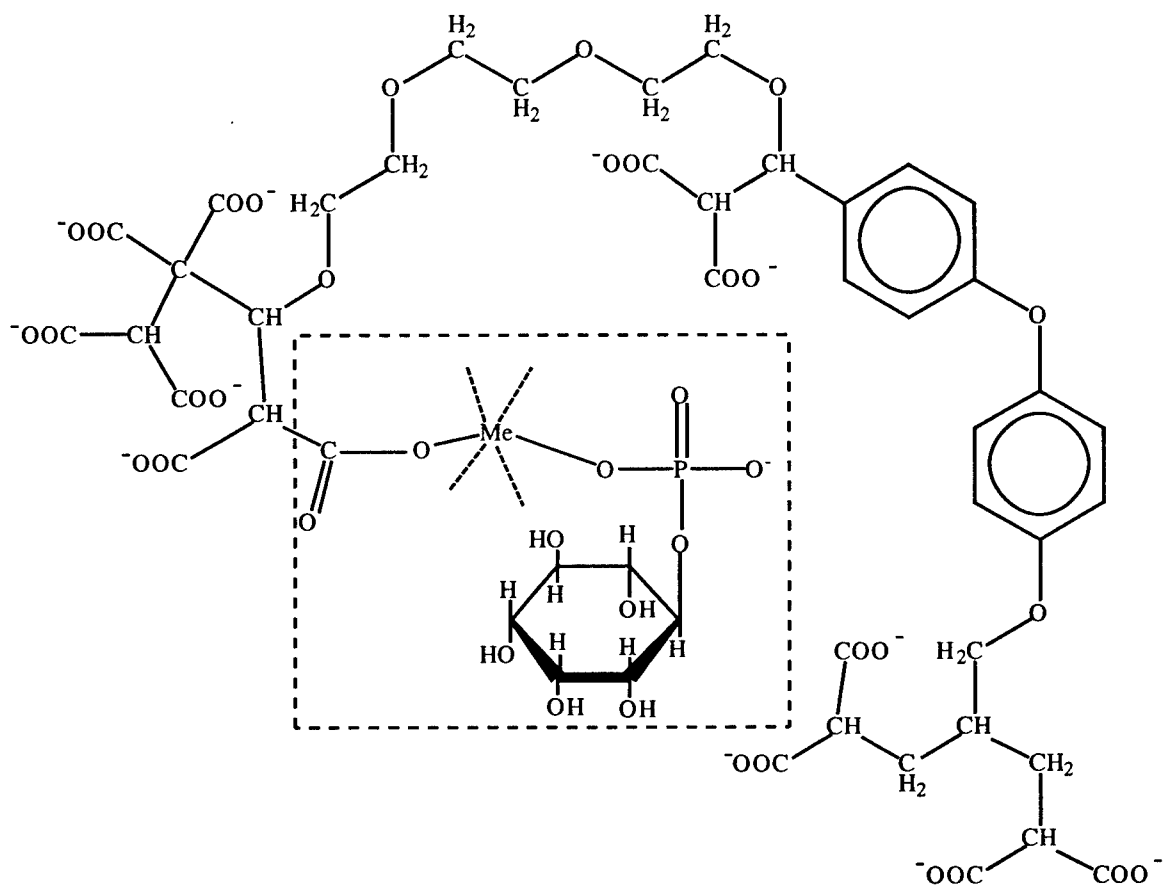


Figure 4-19. A model for binding of P into the humic fraction of sedimentary organic matter via a metal bridge. A negatively charged carboxylic acid group in the fulvic acid (after Buffle, 1977) is linked to a phosphomonoester (inositol-2-phosphate) through a metal cation (Me).

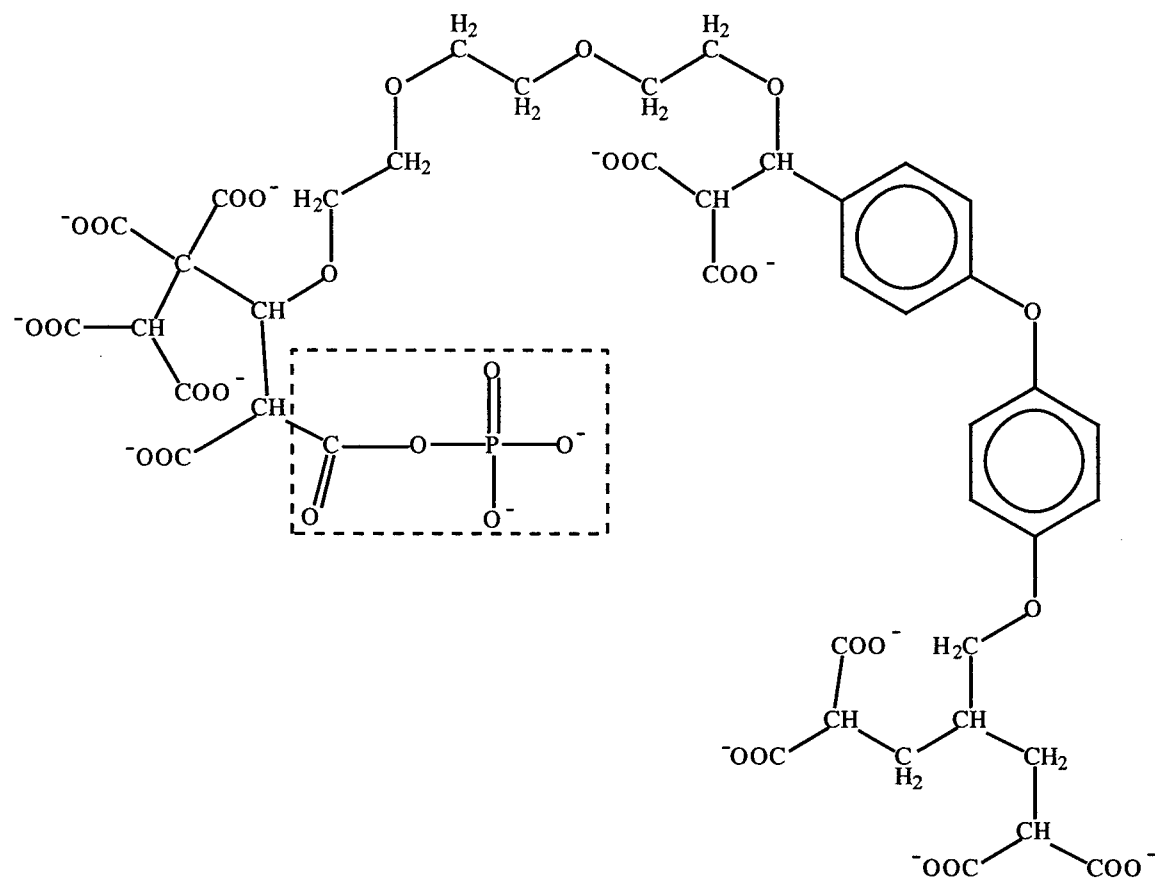


Figure 4-20. A model for binding of P into the humic fraction of sedimentary organic matter via covalent bonding to the humic matrix. An ester linkage connects the fulvic acid (after Buffle, 1977) to a phosphate group, forming a phosphomonoester.

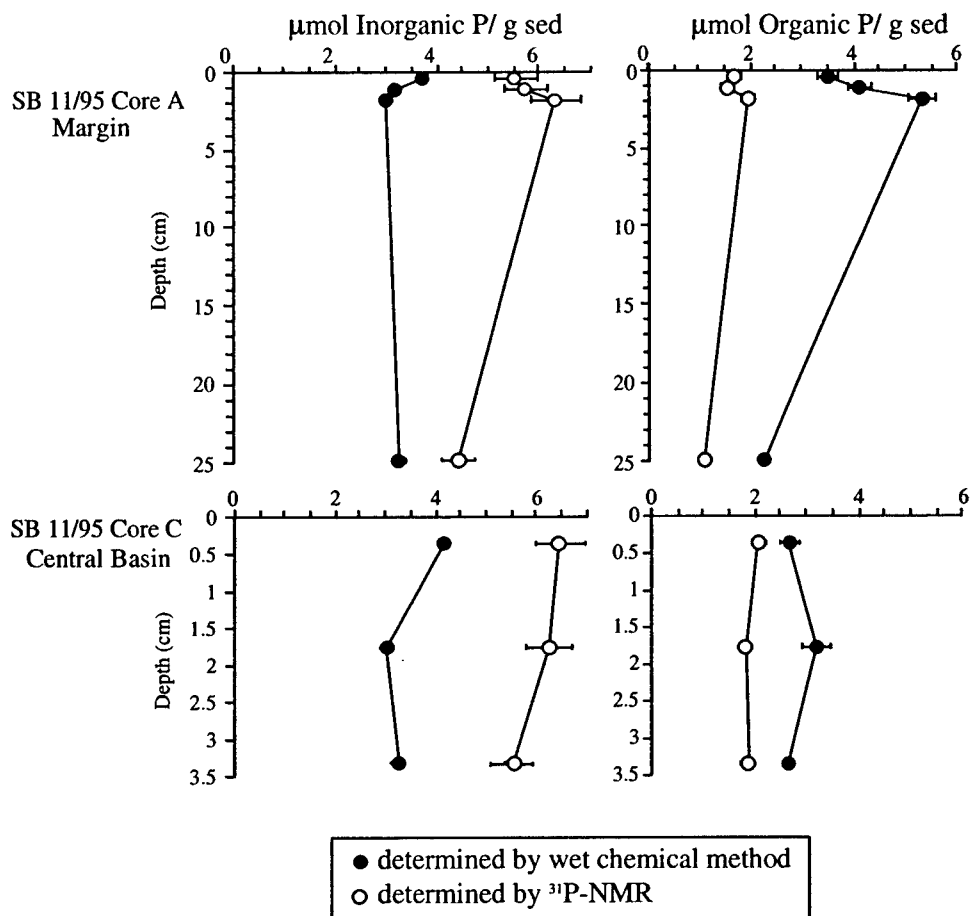


Figure 4-21. Comparison of base-extractable inorganic P (left) and organic P (right) in cores A and C, determined by NMR and wet chemical methods. The amount of inorganic P determined by NMR is consistently higher than that determined by wet chemical measurement of SRP. As a result, organic P (calculated by difference) is overestimated.

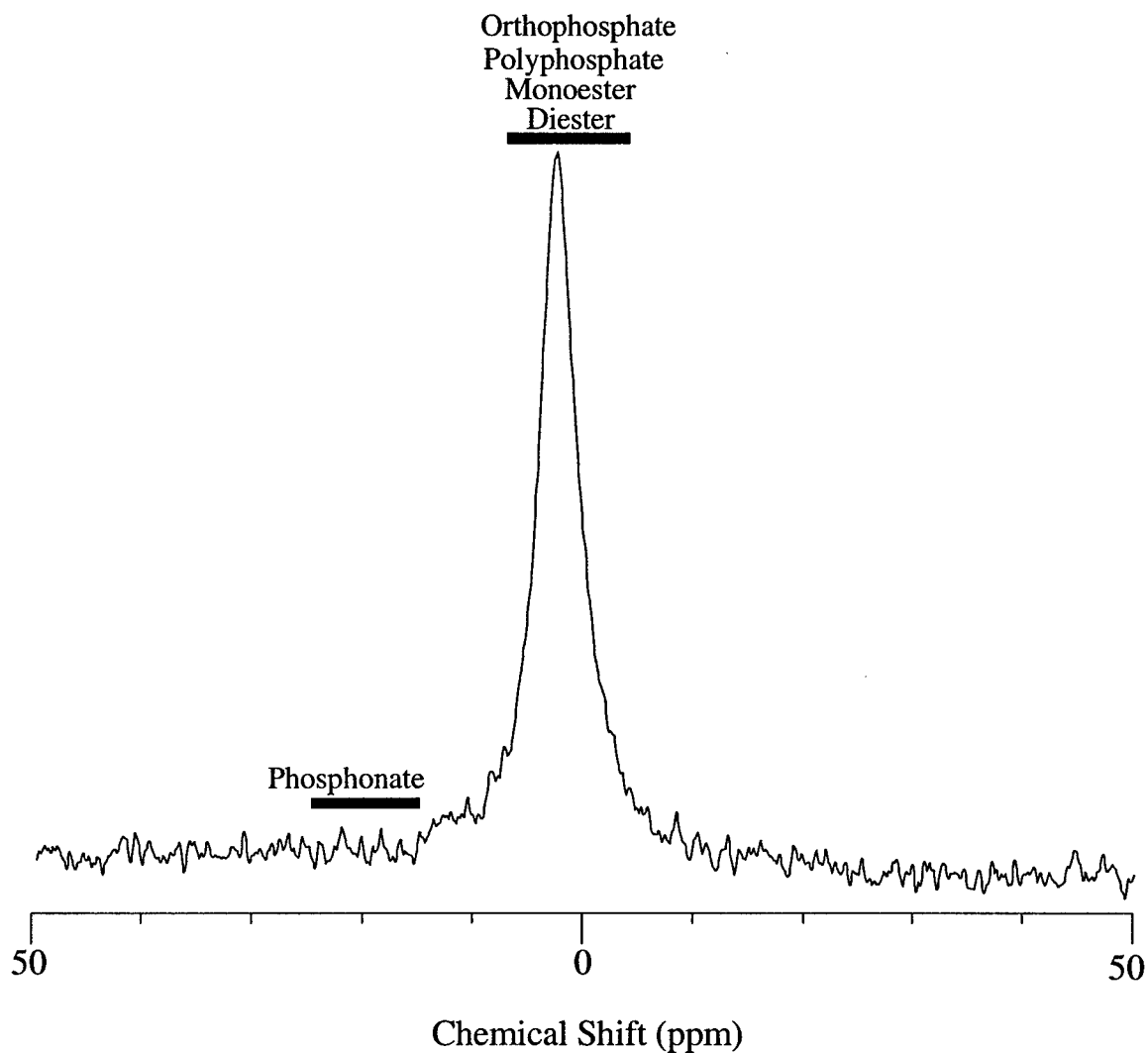


Figure 4-22. Solid state ^{31}P -NMR spectrum of the insoluble sediment residue at depth (33 cm) in core J. Broadening of the spectral lines makes it impossible to distinguish orthophosphate, phosphate esters and polyphosphates from one another. Only phosphonates give a distinct chemical shift. The absence of peaks above background suggests phosphonates are not accumulating in the insoluble residue during diagenesis. Note that the absolute values of chemical shifts for solid state spectra may be slightly different than in solution NMR data.

Chapter 5

Conclusions

Great is the art of beginning, but greater is the art of ending.

- Henry Wadsworth Longfellow

5.1 Results of This Study

This thesis was undertaken with two main goals in mind: to characterize the chemical structure of P_{org} in marine sediments, and to assess the mechanisms that result in persistence of P_{org} at depth in marine sediments and in the sedimentary rock record. The development of new analytical tools for characterizing P_{org} concentration and chemical structure is a challenge, because P_{org} compounds are not amenable to many traditional organic geochemical techniques. The analytical approach of this thesis was developed to improve our current understanding of the structure and diagenetic modification of sedimentary P_{org} . The results of this study address the paradox of organic P preservation: given the labile nature of organic P biochemicals, why is any organic P preserved in marine sediments and sedimentary rocks? The relative importance of chemical structure, physical protection mechanisms and sediment biomass in shaping observed organic P profiles was considered.

The sequential extraction presented in Chapter 2, used in tandem with structural information from ^{31}P -NMR, allows new insights into the mechanisms that control P_{org} preservation in marine sediments. An exhaustive series of tests was used to optimize the sequential extraction. The extraction procedures were adjusted to maximize P solubility, and to minimize structural alteration and degradation. Tests with standard compounds were used to demonstrate that quantitative information about P_{org} structure can be obtained using ^{31}P -NMR. Together, these methods were used to generate downcore

profiles of specific P_{org} functional groups, allowing the hypothesis of structural control on organic P degradation to be directly tested.

Examination of depth trends to assess diagenetic vulnerability of different reservoirs of P_{org} requires that P associated with living biomass does not substantially drive P_{org} depth trends. With the exception of the surface sediment interval, where bacterial biomass contributes an important fraction of total organic matter, the contribution of biomass to the total sedimentary P_{org} pool determined by ATP analysis is small (<10%), indicating that the observed depth trends in P_{org} are not substantially affected by biomass. Measurements of the sediment concentrations of ATP and lipid P indicate that a significant fraction of lipid P is not associated with living biomass, and that biomass estimated using lipid P concentrations at this site is likely to be too high. The results of this study indicate that instantaneous degradation of all simple P_{org} compounds after cell death cannot be assumed, and concurs with other studies that suggest intact cells cannot explain the entire pool of sedimentary lipid P.

Applying the methods developed in Chapter 2 to three cores from the Santa Barbara Basin, it was possible for the first time to quantify diagenetic remineralization of specific P_{org} compound classes in marine sediments. The results presented in Chapter 4 indicate that monoester P is abundant in sediments, particularly when compared to the low monoester P concentration in cellular biomass, the presumed source of sedimentary organic matter. Despite predictions that phosphonates (compounds with direct C-P linkage) would constitute a relatively stable class of marine sediment P_{org} , depth profiles of phosphonate concentration in both the solvent- and base-extractable P reservoirs indicate that phosphonates degrade at rates equal to or greater than more typical C-O-P bonded P biochemicals.

In the absence of a mechanism for preservation due to inherent chemical structure, it is likely that some physical protection mechanism (e.g., association with mineral surfaces or a macromolecular organic matrix) is responsible for the persistence

of lipid P in sediments after cell death. Distinguishing P_{org} interaction with mineral surfaces from incorporation into high molecular weight organic compounds, such as humic materials, is not straight-forward. Incorporation of simple P_{org} compounds into a humic matrix, either by physical sequestration, chemical bonding during humification, or metal bridging, is likely to be an important mechanism for P_{org} preservation in these sediments.

Interaction with metals can result in immobilization of orthophosphate, leading to a P fraction that behaves analytically like P_{org} , but is not organic at all. Organic and inorganic P are defined according to the operationally-defined conventions in the literature (e.g., Aspila *et al.*, 1976; Ruttenberg, 1992). The results of an acid hydrolysis experiment (Chapter 2) support the robustness of these definitions. However, a comparison of inorganic P estimated by wet chemical and ^{31}P -NMR techniques indicate that there is a pool of orthophosphate that is not quantified as inorganic P when the traditional operational definition is used. This non-reactive orthophosphate, detected by ^{31}P -NMR in all three core analyzed for this study (Chapters 2, 4), may be bound to humic compounds via metal bridges. The magnitude of this P_{org} overestimation artifact suggests that at least 15-20% of the total organic P determined by wet chemical techniques is actually orthophosphate.

Transfer of phosphonates into the insoluble sediment fraction is not quantitatively important. However, if it is assumed that formation of humic compounds is an intermediate step in the formation of insoluble organic matter from primary biochemicals, the high abundance of monoester P in the humic fraction may result in a significant transfer of monoester P into the insoluble organic matter pool. While these data provide no evidence for direct structural control on remineralization of P_{org} , they suggest that sorption of particular P_{org} compound classes may play an important role in enhancing their preservation. Thus, chemical structure may play an important, but secondary, role in P_{org} preservation.

P_{org} concentration and molecular structure were compared in sediment cores from environments characterized by different bottom water oxygen concentrations. These data reveal that although sediments deposited under anoxic bottom waters have higher total organic P concentrations, much of the observed difference between the two cores can be attributed to differences in sequestration of orthophosphate within high molecular weight organic matter, rather than differences in the efficiency of P_{org} remineralization.

5.2 Directions for Future Research

The results obtained by this study open a number of interesting avenues for further research. The comparison of P_{org} structure in Santa Barbara Basin sediment cores with contrasting bottom water oxygen concentrations could be expanded to include a wider suite of cores in more varied depositional settings. Sediment profiles obtained from depositional environments characterized by differences in bulk organic matter concentration, dominance of terrestrial vs. marine organic matter input, and sediment surface area, could be used to evaluate environmental controls on P_{org} composition, distribution, and preservation.

The additional data (e.g., NMR of lipid spectra) obtained for the larger surface sample collected for core SBB9610 J demonstrate the advantage of collecting samples at high depth resolution. This is particularly true when there is independent evidence of high-resolution depth changes in sediments such as, for example, varves and bacterial mats. Whole-box core sampling may be necessary to acquire sufficient material for P_{org} structural analysis, particularly in sediments with organic P concentrations lower than those measured in the Santa Barbara Basin.

Additional analyses, such as measurements of metal concentrations in base extracts, may be used to further investigate the importance of metal bridging as a mechanism for immobilization of organic and inorganic P. The P_{org} -overestimation

artifact identified here by comparison of NMR data and wet chemical analyses indicates that new methods to quantify total organic P in sediments and sedimentary rocks are needed.

The nature of the association of P_{org} with humic compounds may be investigated by expanding the NMR tools developed in this study to include other techniques such as 2-D NMR. Correlation of ^{13}C and ^{31}P chemical shift regions in base extracts can be used to understand the remineralization of P_{org} in the context of structural changes in total sedimentary organic matter (e.g., Gressel *et al.*, 1996). Development of additional analytical techniques such as those described above, and their application to a broad suite of samples, can be used to vastly increase our knowledge of the form and fate of organic P in marine sediments.

Summary of Appendices

Appendix A: Laboratory Procedures for Sediment Extraction

A-1: Solvent Extraction Protocol

A-2: Base Extraction Protocol

Appendix B: Additional Sediment Extraction Data

B-1: Base Extraction Data for Santa Barbara Basin Core SBB9610 J

B-2: Data from Peru Margin Cores

Appendix C: Alternative Methods for Analysis of P_{org}

C-1: Quantification of Phosphonates by Differential Hydrolysis

C-2: Structural Characterization of Phospholipids by High-Performance Liquid Chromatography (HPLC)

C-3: Kerogen Isolation from the Insoluble Sediment Residue

C-4: Analysis of P_{org} Structure using Pyrolysis-Gas Chromatography with a Flame Photometric Detector (Py-GC-FPD)

Appendix A

Laboratory Procedures for Sediment Extraction

Appendix A-1: Solvent Extraction Protocol

SUMMARY OF METHOD:

Extraction of unbound lipids from sediments into organic solvents based on the Bligh and Dyer (1957) procedure, an accepted method for extraction of lipid and other cellular materials from biochemical preparations.

The solvent phase is designed to efficiently extract polar lipids, including phospholipids, and is therefore more suitable to this study than a less polar solvent system. The solvent extract is partitioned against water to remove non-lipid compounds.

CHEMICALS:

1. Chloroform, Optima grade (CHCl_3 , Fisher cat. # C297-4)
2. Methanol, GC Resolv grade (MeOH , Fisher cat. # A457-4)
3. 2- Propanol, Optima grade (2- PrOH , Fisher cat. # A464-4)
4. Hexane
5. Dichloromethane

REAGENTS:

Bligh and Dyer extraction mixture = water: methanol: chloroform (0.8:2:1)

Using a graduated cylinder, measure 600 mL MeOH , 300 mL CHCl_3 , and 240 mL milli-Q H_2O . Combine the solvents in a 2L volumetric flask (the mixture is not diluted to 2L, the flask is just for easier mixing of the volatile solvents). Do not put in the stopper, but shake gently until the solvents are thoroughly mixed. It is best to make up fresh solvent before each set of extractions. Any extra solvent mixture can be stored in an amber reagent bottle.

EQUIPMENT:

*glassware and plasticware are acid-cleaned in 10% HCl, and glassware is muffled @ 500°C for 2 hours

*volumetric glassware is acid-cleaned in NoChromix™ cleaner + concentrated H₂SO₄

1. Analytical balance
2. 50 ml Kimax glass centrifuge tubes + caps, 1 per sample + 1 extra for cleaning probe (Fisher cat. # 05-558-12B)
3. Semi-micro spatula, 1 per sample (Fisher cat. # 14-374)
4. 500 ml round bottom flasks, 2 per sample (Fisher cat. # 10-067-2F)
5. Size 24/40 ground glass stoppers, 2 per sample (Fisher cat. # 14-640J)
6. 500 ml separatory funnels with PTFE stopcock, 1 per sample (Fisher cat. # 10-437-10D)
7. 50 ml pear shaped flasks, 1 per sample (Fisher cat. # 10-060-9C)
8. Size 19/22 ground glass stoppers, 1 per sample (Fisher cat. # 14-640-2D)
9. 250 ml polypropylene bottles, 1 per sample (Fisher cat. # 02-925D)
10. 10 ml volumetric flasks, 1 per sample (Fisher cat. # 10-212AA)
11. Freeze Drier
12. Crystallizing dish, 190x100 mm (Fisher cat. # 08-762-2)
13. Lab jack
14. Tekmar sonic disrupter probe
15. Centrifuge w/ 50 ml centrifuge tube holders
16. 100 ml glass graduated cylinder (Fisher cat. # 08-548D)
17. Rotary evaporator
18. Borosilicate Glass Pasteur Pipettes (Fisher cat. # 13-678-20D)
19. 5 ml glass syringe with luer tip (Fisher cat. # 14-823-15B)
20. 25 mm PTFE 0.45 µm syringe filters (Fisher cat. # 09-730-142)
21. 20 cc plastic syringes with luer tips, 1 per sample (Fisher cat. # 14-823-2B)
22. 0.45 µm polycarbonate membrane filters, 25mm diam. (Millipore cat. #HAWP-025-00)
23. Plastic Swinnex filter holders for luer syringe tip (Millipore cat. # SX0002500)
24. 22 cc HDPE scintillation vials, 1 per sample (Wheaton cat. # 986704)
25. Prepared solvent-rinsed foil squares (Thomas Sci. cat. # 1086J26)
26. 50 mm Plastic petrie dishes, 1 per sample (Fisher cat. # 09-753-53A)
27. Clamps
28. Glass dish for solvent waste, 100x80 mm (Fisher cat. # 08-782)
29. Ring stands
30. Cork rings
31. Tape/pens for labeling
32. Kimwipes
33. Paper towels
34. Ice

PROCEDURE

Preparation

Before extraction, sediments are freeze dried, ground, and sieved to $<125\ \mu\text{m}$. Generally, four samples are processed at one time. The day before extraction, sediments should be weighed into 50 mL centrifuge tubes. For each sample, label 2-500 mL round-bottom flasks (label 1 AQ, 1 SOLV), one separatory funnel, one pear-shaped flask, one 250 mL bottle, two 10 mL volumetric flasks (label 1 AQ, 1 SOLV), and one plastic petrie dish. Attach the separatory funnels to ring stands in the hood.

Just before beginning extraction, prepare an ice bath by filling a crystallizing dish with ice and cold tap water. Place the dish on the lab jack inside the sonicator cabinet. The sonic probe is cleaned according to the directions below before beginning extractions, and between all samples.

Cleaning the Probe

1. rinse the probe with a MeOH squirt bottle, then wipe with a kimwipe
use a glass dish to catch the solvent waste
2. using solvent squirt bottles, rinse the probe successively with: MeOH - DCM – hexane, washing down all sides of the probe
3. fill a 50 ml tube with the Bligh and Dyer solvent mixture (no sediment in the tube, this step is just to clean the probe), then clamp it into sample arm
 - top of clamp should be at the shoulder of the tube, and the tube immersed in the ice bath
 - move clamp/ice water bath setup so that probe is lined up with the tube
 - crank the lab jack up until top of tube nears the point where the probe "flares out"
 - the probe should be immersed in solvent
 - wobble the tube until the probe is not touching glass on any side
4. wet a paper towel and fold into a "collar", wrap around sample tube
 - drape the ends of the collar in the ice bath
 - this step is not crucial for the cleaning step, but keeps samples from heating up during sonication
5. sonicate for 1 minute (pulsed mode, %duty cycle =70; output control = 7)

Extraction

1. add 2-PrOH to each sample, stirring with a spatula until all sediment is suspended
2. use a squirt bottle to add more PrOH, rinsing the spatula and the sides of the extraction tube, until a total of 40 mL has been added
3. clamp the sample into the sonic probe (see above), position sample and wrap paper towel "collar" around the tube
4. sonicate for 10 minutes (pulsed mode, %duty cycle =70; output control = 7)
5. lower the lab jack until the probe is no longer immersed in the solvent, and use a squirt bottle of 2-PrOH to rinse any particles on the probe back into the sample
6. put the cap on the tube, and centrifuge for 10 minutes at 2500 rpm
 - counter-weight the tube in the centrifuge with a tube full of milli-Q H₂O (weight difference <0.1 g)
 - after centrifuging, sediment should have formed a plug so that no particles are visible in the supernatant
7. decant the supernatant into a 500 mL separatory funnel
8. add Bligh and Dyer solvent mixture to the sample, and resuspend the sediment with a spatula
9. rinsing the spatula and walls of the tube as above, fill the tube to 40mL with Bligh and Dyer solvent mixture
10. sonicate 10 minutes, then centrifuge 10 minutes, as above (steps #3-6)
11. combine the supernatant with the PrOH extract from step #7
12. repeat steps 8-11 for a total of 4-7 extraction steps with the Bligh and Dyer extraction mixture, until the extract is pale yellow in color
13. freeze the solvent-extracted sediments, then freeze-dry, and record the weight after extraction

Partitioning:

1. after all extracts have been combined in the separatory funnel, calculate the volume of water and CHCl₃ needed for a final ratio of water: propanol/methanol: chloroform of 1.8:2:2.
2. add the calculated amounts of chloroform and mQ-H₂O to the separatory funnel
3. gently invert the separatory funnel and then turn it upright, opening the stopper to allow the funnel to "breathe"
4. shake the separatory funnel vigorously, then allow the extract to separate into chloroform (SOLV) and methanol-milli-Q H₂O (AQ) phases (for the initial separation, samples are left to settle overnight)

5. when the two layers have separated, open the stopcock and allow the SOLV (bottom) layer to drain into a labeled round-bottom flask
6. add 50 mL of chloroform to the AQ layer remaining in separatory funnel
7. shake the separatory funnel and allow the 2 layers to separate (for a minimum of 1 hour)
8. drain the SOLV layer into the flask from step 5
9. repeat steps 6-8 twice more, for a total of 3 chloroform rinses of the AQ layer
10. open the stopcock and drain the separatory funnel completely (it should contain only the AQ layer) into a second round-bottom flask, labeled AQ
11. CLOSE the stopcock on the separatory funnel!
12. pour the SOLV extract from the round-bottom flask into the separatory funnel
13. add 50 mL of milli-Q H₂O to the SOLV extract
14. shake the separatory funnel and allow the layers to separate (for a minimum of 1 hour)
15. drain the SOLV layer into one round-bottom flask, and drain the AQ layer into the second round bottom flask
16. repeat steps 11-15 twice, for a total of 3 water rinses of the SOLV layer

Reduce and Filter the Extracts:

SOLV:

1. reduced the SOLV extract volume to < 25 mL on a rotary evaporator (vacuum = 27 psi ;water bath@20°C)
2. transfer the extract to a 50 mL pear-shaped flask using a glass Pasteur pipette, using additional chloroform to rinse the walls of the flask until the solvent is colorless
3. in the pear-shaped flask, reduce the extract almost to dryness
4. filter the sample using a glass syringe with a luer tip and a Teflon (PTFE) 0.45µm syringe filter
 - rinse the syringe 7 times with methanol and 7 times with chloroform
 - attach the filter to the syringe barrel, then filter a few mL of chloroform through the filter into waste
 - transfer the sample from the pear-shaped flask into the barrel of the syringe with a Pasteur pipette
 - rinse the flask with additional chloroform, adding the rinse to the syringe barrel
5. filter the extract into a 10 mL volumetric flask

6. after the sample has been completely filtered, fill the syringe barrel with additional chloroform to rinse the syringe and filter
7. add chloroform to the fill line of the volumetric flask
8. the extract is now ready for CHN and P analysis (see Chapter 2), and is stored frozen (-30°C) in the volumetric flask until analyses are completed

AQ:

1. reduce the AQ extract for two hours on the rotovap (vacuum = 27 psi ;water bath@ 25°C)
2. once most of the methanol has been removed, transfer ~100 mL of the extract to a 250 mL bottle for lyophilization
3. freeze the ~100 mL split of the extract overnight in a -30°C freezer
4. place the remaining AQ extract (in the flask) in a -30°C freezer.
5. cover the bottle with solvent-rinsed foil perforated with holes
6. attach the sample (in freeze-drying flask) to the freeze drier and reduce the extract
 - when the sample has been almost totally reduced, the remaining sample from the round-bottom flask can be transferred into the bottle
 - the flask should be rinsed completely with milli-Q H_2O for quantitative transfer and then the bottle is frozen overnight in -30°C freezer.
 - reduce the extract to dryness.
7. re-hydrate the extract in a few mL of milli-Q H_2O .
 - after adding water to the bottle, agitate the bottle for a few seconds to wet all of the sample.
8. attach a filter (polycarbonate membrane filter in a Swinnex holder) to a 20 cc plastic syringe
9. filter a few mL of milli-Q H_2O to rinse the filter (discard the water)
10. filter the extract into a 10 mL volumetric flask
11. after the sample has been completely filtered, fill the syringe barrel with additional milli-Q H_2O to rinse the syringe and filter
12. add milli-Q H_2O to the fill line of the volumetric flask
13. the extracts are now ready for CHN and P analysis (see Chapter 2), and are transferred into 22 cc HDPE vials and stored frozen (-30°C) until analyses are completed
14. the filter (and material collected on it) are stored refrigerated in a plastic petrie dish for use in the base extraction protocol (see Appendix A-2)
 - base extraction is generally done within a few days of solvent extraction, and it takes several days for the aqueous extract to be completely reduced on the freeze-drier. Therefore, little storage time is necessary for the filters, and they are refrigerated (rather than frozen) for convenient short-term storage

Appendix A-2: Base Extraction Protocol

SUMMARY OF METHOD:

Extraction of humic substances, defined in the soil science literature as any organic matter soluble in aqueous alkaline solution.

The full extraction procedure consists of 4 steps: (i) extraction of sediments with citrate dithionite bicarbonate (CDB) to remove reactive iron phases, (ii) extraction with MgCl_2 as a rinse, to remove residual CDB and re-adsorbed P from the preceding step, (iii) extraction with dilute acid to break up humic compound salt complexes and enhance the extractability of humic compounds in alkaline solution, and (iv) extraction in 0.5 N NaOH to solubilize humic substances. Steps (i) and (ii) follow procedures from Ruttenberg (1990, 1992). All extracts, and the sediment residue after extraction, are analyzed for P concentration.

During NaOH extraction, precautions are taken to minimize exposure of samples to oxygen, which can form peroxides that attack organic matter. The volume of the extracts decreases by more than an order of magnitude from the CDB extraction (100 mL/g sediment) to the base extraction (6.7 mL/g sediment), and the sample is transferred several times to accommodate these different volumes. Therefore, it is crucial to be quantitative about sediment transfer. In addition, a lot of particulate material is trapped on the filters, even after centrifuging the extracts. Therefore, for each sample, the same filters are re-used for the entire procedure to avoid loss of material on filters. Details of sediment transfer steps are given where appropriate.

Note: The procedure detailed below is for a 7 g sample, a typical sample size for the base extractions in this study. The sample size can be changed as long as the reagent volumes are adjusted to maintain a constant solid:solution ratio. This procedure has been used on samples ranging from 0.5 to 15 g of sediment. Any sediment size outside of this range may require further standardization or modifications to the method.

CHEMICALS:

1. Tri-sodium citrate ($\text{Na}_3\text{C}_6\text{H}_5\text{O}_7 \cdot 2\text{H}_2\text{O}$ FW=294.10; Fisher cat. #S279-500)
2. Sodium bicarbonate (NaHCO_3 FW=84.01; Fisher cat. #S233-3)
3. Sodium dithionite ($\text{Na}_2\text{S}_2\text{O}_4$ FW=174.10; Fisher cat. #S310-500)
4. Magnesium chloride ($\text{MgCl}_2 \cdot 6\text{H}_2\text{O}$ FW=203.30; Fisher cat. #BP214-500)
5. Concentrated (12 M) HCl (Fisher cat. #A144C-212)
6. Sodium hydroxide (NaOH FW=40.00 ; Sigma cat. #S-5881)

REAGENTS:

1. Citrate-Bicarbonate Solution (3 L)
Measure 3 L of milli-Q H_2O using a graduated cylinder
Pour milli-Q into a 4 L beaker
While stirring, add 265.25 g of tri-sodium citrate and 252.98 g of sodium bicarbonate
Slowly (to minimize effervescence) add 60 mL of concentrated HCl (salts will not dissolve until the pH is brought down)
Immediately before use, check the pH and add NaOH to bring the solution to pH 7.6
(a pH 7 phosphate buffer is used to standardize the pH probe. To prevent contamination, soak the probe in a small split of the CDB solution before use).
2. 1 M MgCl_2 (3 L)
Measure 3 L of milli-Q H_2O using a graduated cylinder
Pour milli-Q into a 4 L beaker
While stirring, add 610.49 g of magnesium chloride
Continue stirring for 30 minutes
Filter the solution through a 0.45 μm polycarbonate filter
Adjust to pH 8.0 using NaOH (as above, soak the pH probe in a small split of the solution to avoid contamination)
3. 0.1 M HCl (1 L)
Measure 1 L of milli-Q H_2O using a volumetric flask
Pour the milli-Q H_2O into a 1 L bottle, add 8.4 mL concentrated HCl with a 5 mL pipette, and shake thoroughly
4. 0.5 M NaOH (1 L)
Measure 1 L of milli-Q H_2O using a volumetric flask
Weigh out 40 g NaOH
Add the NaOH and milli-Q H_2O to a 1L polypropylene bottle and shake until all pellets are completely dissolved
Sparge with N_2 for 8 hours before use in extraction

EQUIPMENT (all glass & plasticware acid-cleaned in 10% HCl):

1. pH meter
2. Freeze drier
3. Analytical balance
4. Shaker table
5. Benchtop sonicator bath
6. Vortex mixer
7. Centrifuge w/ 50 ml centrifuge tube holders and 250 mL centrifuge bottle holders
8. 1 L HDPE bottles, 2 per sample (Fisher cat. # 02-923F)
9. 250 mL polypropylene centrifuge bottles, 1 per sample (Fisher cat. # 05-433A)
10. 250 mL polysulfone filtration units, 1 per sample (Fisher cat. # 09-740-23A)
11. 0.45 μ m GH Polypro membrane filters, 47 mm (Gelman P/N 66548)
12. 10 μ m polypropylene membrane filters, 47 mm (Gelman P/N 61757)
13. 500 ml HDPE bottles, 1 per sample (Fisher cat. # 02-923E)
14. 100 ml HDPE bottles, 2 per sample (Fisher cat. # 02-923C)
15. 50 ml polypropylene centrifuge tubes, 5 per sample (Fisher cat. # 05-538-60)
16. 22 cc HDPE scintillation vials, 1 per sample (Wheaton cat. # 986704)
17. 50 mL plastic beaker, 1 per sample
18. Spatulas for weighing samples (metal), dithionite (ceramic), and for scraping sediment from extraction vessels and filters (plastic)
19. Plastic forceps
20. 1000 ml glass graduated cylinder
21. 100 ml glass graduated cylinder
22. 100 ml glass volumetric flasks, 1 per sample
23. 50 ml glass volumetric flasks, 1 per sample
24. 20 cc borosilicate glass vials, 1 per sample (Fisher cat. # 03-339-21G)
25. Parafilm
26. Tape/pens for labeling
27. Sparger for NaOH solution
28. Electrical tape
29. Crew-wipes
30. Kimwipes
31. Weigh boats
32. N₂ tank and regulator
33. Glass watchglasses

PREPARATION

Sediments have been solvent-extracted (see lipid protocol), freeze-dried and crushed lightly with a mortar and pestle. Generally, six sample are processed at one time. For each sample, label: 1 filtration unit, 2-1L bottles (1 for extraction, 1 for CDB filtered extract), 1-500 mL bottle (for MgCl_2 filtered extract), 1-250 mL centrifuge bottle, 2-100 mL bottles (for filtered acid extract and filtered base extract #1), 5-50 mL centrifuge tubes (1 for sediment extraction and 4 for base extracts #2-5), a 20 cc plastic vial (for a split of base extract #1), and a small plastic beaker. Assemble the filtration units with 2 stacked membrane filters so that the sample passes first through a 10 μm polypropylene and then through a 0.45 μm GH Polypro filter. For each sample, weigh sediments into a 1 L bottle. The CDB extraction takes 8 hours, so the procedure should be started either very early or very late in the day.

EXTRACTION PROCEDURE:

CDB:

1. Adjust the citrate-bicarbonate (CB) solution to pH 7.6 using NaOH (generally requires a few mL of 12M NaOH)
2. For each sample, weigh out 17.5 g Na-dithionite (2.5 g dithionite/g sediment) in a weigh boat
3. Transfer the dithionite to the 1L bottle containing the sediment sample
4. Slowly add 700 mL (100 mL solution/g sediment) of CB solution, to prevent excessive effervescence
5. Shake manually to suspend the sediment, opening the cap once or twice to permit gas to escape before sealing the cap tightly for the last time, just before placing the bottle on a shaker table
6. Shake samples for 8 hours @250 rpm on the shaker table (Note start and stop times)
7. Pour 200 mL of each solution into pre-labeled 250 mL centrifuge bottles
8. Centrifuge 10 minutes at 3500 rpm
9. Decant the supernatants into the labeled filtration units and filter at 12 psi
10. Pour the filtered extracts into pre-labeled 1 L bottles
11. Repeat steps 6-8 until the entire extract is filtered (typically, this takes ~ 1.5 hours for a set of six 7 g sediment samples)
12. Store the extract refrigerated (4°C) for P analysis

MgCl₂:

1. Adjust the MgCl₂ solution to pH 8 using NaOH (generally requires < 1mL of 0.1 M NaOH)
2. Take apart the filtration units, and transfer the each set of filters to a small labeled plastic beaker. Also place the 25 mm polycarbonate filter from each aqueous extract (Appendix A-1) in the beaker for that sample
3. For each sample, measure out 350 mL of MgCl₂
4. Add a few mL of MgCl₂ to each beaker, and gently scrape the filters to remove particles
5. Rinse the filters with an additional squirt of MgCl₂, and re-assemble the filtration units, using the same filters
 - At this point, the filtration units are not cleaned or rinsed. The extract volumes are large and thus sample carry-over from the small amount of residual liquid in the filtration units will be small. In addition, since the MgCl₂ extraction is intended as a rinse, sample carryover is not a concern for this step.
6. Use the remaining volume (for a total of 350 mL) for each sample to transfer the sediment quantitatively from the beaker and the 250 mL centrifuge bottle back into the 1L bottle
7. Manually shake the sample until all sediment is resuspended
8. Shake samples for 2 hours @250 rpm on the shaker table (Note start and stop times)
9. Pour 200 mL of each solution into the 250 mL centrifuge bottles
10. Centrifuge 10 minutes at 3500 rpm
11. Decant the supernatants into the labeled filtration units and filter at 12 psi
12. Pour the filtered extracts into pre-labeled 500 mL bottles
13. Repeat steps 9-11 with the remaining extract (this generally takes less than an hour for a set of six 7g sediment samples)
 - after centrifuging the last split of each extract, use the supernatant to rinse all sediment from the 1L bottle into the 250 mL centrifuge bottle. Centrifuge the remaining extract and filter as above.
14. Store the extract refrigerated (4°C) for P analysis

HCl:

1. Take apart the filtration units, and transfer the filters into the plastic beakers
2. For each sample, measure out 93 mL of 0.1 M HCl (13.33 mL/g sediment)
3. Add a few mL of the 0.1 M HCl to each beaker, and gently scrape the filters to remove particles
4. Rinse filters with an additional squirt of 0.1 M HCl and re-assemble filtration units, using the same filters
 - At this point, the filtration units are not cleaned or rinsed. The MgCl_2 extract has very low P concentration (generally $< 20 \mu\text{M}$), whereas the HCl extract has very high P concentration (500-2000 μM), so P contamination from sample carry-over is not a concern.
5. Use the remaining volume (for a total of 93 mL) for each sample to transfer the sediment quantitatively from the beaker into the 250 mL centrifuge bottle.
6. Manually shake the sample until all sediment is resuspended
7. Shake samples for 1 hour @250 rpm on the shaker table (Note start and stop times)
8. Pour 50 mL of each solution into pre-labeled 50 mL centrifuge tubes
 - This is the last sample transfer in the extraction procedure. To calculate total sample weight loss during the full base extraction procedure (all steps discussed here), the final dry weight is determined after freeze-drying the sediment residue. Therefore, the weight of the empty 50 mL tubes should be recorded before transferring samples. The final weight for each sediment residue will be determined by weighing the dried residue in the 50 mL tube and subtracting the empty tube weight.
9. Centrifuge 10 minutes at 3500 rpm
10. Decant the supernatants into the labeled filtration units and filter at 12 psi
11. Add the remainder of the extract to the 50 mL centrifuge tubes
12. Centrifuge 10 minutes at 3500 rpm
13. Use the centrifuged supernatant to rinse the 250 mL centrifuge bottle, transferring all sediment into the 50 mL centrifuge tube. Centrifuge and repeat the rinsing if necessary. The transfer must be quantitative, so carefully rinse the walls and cap of the 250 mL centrifuge bottle
14. After the entire extract has been filtered, decant into a 100 mL volumetric flask and fill to the volume line with 0.1 M HCl.
15. Pour the extract into a labeled 100 mL bottle, and store the extract refrigerated (4°C) for P analysis.
16. Take apart the filtration units, and transfer the filters to the plastic beakers
17. Rinse the filtration units with milli-Q H_2O , place crew-wipes and large Kimwipes on the bench, and after shaking off excess water, leave the filtration units upside-down overnight to dry. Cover with a kimwipe to keep dust off. The filtration units need not be completely dry before using the next day.

NaOH:

1. For each sample, measure out 47 mL of 0.5 M NaOH (6.67 mL/g sediment) that has been sparged with N₂ for 8 hours to remove oxygen
2. Add a few mL of 0.5 M NaOH to each beaker, and gently scrape the filters to remove particles
3. Rinse filters with an additional few mL of 0.5 M NaOH
4. Use the remaining volume (for a total of 47 mL) for each sample to transfer the sediment quantitatively from the beaker into the 50 mL centrifuge tube
5. Just before capping, blow a stream of N₂ into the tube to evacuate oxygen from the headspace
6. Cap tightly, and wrap around the seal, first with parafilm and then with electrical tape to make sure it does not leak
7. Manually shake the tube, and vortex until all sediment is resuspended
8. Shake samples for 12 hours @250 rpm on the shaker table (Note start and stop times)
9. Centrifuge the tubes for 10 minutes at 3500 rpm
10. Re-assemble filtration units, using the same filters
11. Decant the supernatants into the labeled filtration units and filter at 12 psi
12. After the entire extract has been filtered, decant into a 50 mL volumetric flask and fill to the volume line with milli-Q H₂O
13. Pour the extract into a labeled 100 mL bottle, and remove a 5 mL split for elemental analysis. Store this split refrigerated (4°C) until analysis.
14. The remaining sample, in the 100 mL bottle, should be frozen in a -30°C freezer, then lyophilized. When the extract is dry, it can be prepared for NMR analysis by transferring it to a 7 mL vial with 1 mL D₂O, 1 mL 2M NaOH, and 2 mL milli-Q H₂O. This volume should be used to rinse *ALL* of the sample from the bottle!
15. Take apart the filtration units, place the filters in plastic beakers with a few mL of NaOH, and cover with a watchglass for overnight storage. Rinse the filtration units and 50 mL volumetric flasks with milli-Q H₂O, place crew-wipes and large kimwipes on the bench, and after shaking off excess water, leave the filtration units and volumetrics upside-down overnight to dry. Cover with a kimwipe to keep dust off.
16. Add 47 mL of 0.5 M NaOH to each sample
17. Repeat steps 5-12
18. When all extracts are filtered and brought to 50 mL volume in volumetric flasks, pour the extracts into 50 mL centrifuge tubes and store refrigerated (4°C) for P analysis
19. Repeat steps 16-18 for each sample until each sediment sample has been extracted with base a total of 5 times.
20. When all extractions are completed, take apart the filtration units and return the filters to the small plastic beakers
21. Add a few mL of milli-Q H₂O to each beaker and scrape the filters (vigorously this time, to remove as much particulate material as possible).

22. After scraping, the water and suspended particles are added to the centrifuge tube with the sediment residue. Add ~10 mL of milli-Q H₂O to the beaker, and sonicate for 5 minutes in a benchtop sonicator bath. Again, add the milli-Q rinse and any particles into the tube with the sediment residue.
23. Freeze the sediment residue (-30°C) and lyophilize, then record the dry weight. Final dry weight of the sediment is calculated by subtracting the weight of the centrifuge tube (see HCl step#8). The final sediment weight is compared with the initial weight (sediment weighed into the 1L bottle in the Preparation section) to determine the loss due to removal of CDB-, MgCl₂-, HCl- and NaOH-soluble material as well as any sediment particles lost during extraction and sample transfer.
24. Place the filters (all 3: polycarbonate, GH Polypro, polypropylene) in a 20 cc borosilicate glass scintillation vial for combustion and total P analysis to determine P loss during the full extraction procedure

Appendix B

Additional Sediment Extraction Data

Appendix B-1:

Base Extraction Data for Santa Barbara Basin Core J

Summary

These data are presented separately from the data for Santa Barbara Basin cores SB 11/95 A and C, because the extraction method used for this core was different than the method described in Chapters 2 and 4, and in Appendix A-2. This core (SBB9610 J) was extracted during the time that the sequential extraction method was being optimized. Based on the results obtained for this core, it was decided that a different procedure would be more appropriate for obtaining P concentration data and preparing base extracts for ^{31}P -NMR analysis. The location and sampling information for core SBB9610 J, hereafter referred to as core J, are described in Chapter 4.

The two major methodological differences that distinguish this data set from that presented in Chapter 4 are: (i) no citrate dithionite bicarbonate (CDB) and MgCl_2 extractions were performed, and (ii) sediments were extracted with a mixed solution of aqueous base and ethylenediaminetetraacetic acid (EDTA). Because of these differences in extraction protocol, the data presented here are not directly comparable with the data presented in Chapter 4.

Extraction Procedure

As noted above, the extraction procedure for this core differed from that presented in Appendix A-2 on only two major points. Unless otherwise noted, all extraction details were identical to those described in Appendix A-2. After solvent extraction, sediments were freeze-dried and lightly crushed. Sediments were then extracted for 1 hour in 0.1 M

HCl. Following this extraction, sediments were extracted with a solution of 0.5 M NaOH + 0.01 M EDTA. The NaOH/EDTA solution was sparged of oxygen prior to the extraction, as described in Appendix A-2. The method used here followed the suggestion of Hupfer et al. (1995b) and others that EDTA, by chelating paramagnetic cations, suppresses their undesirable effect on NMR spectra. In this study (see Chapter 2), the amount of P solubilized in base was also enhanced by adding EDTA to the extractant, with maximum P recovery obtained using 0.01 M EDTA (Figure 2-7).

P Concentration Data

Figure B-1 shows the amount of P solubilized in 0.1 M HCl. Because no CDB extraction was performed prior to acid extraction, this reservoir is likely to contain P associated with reactive iron phases as well as carbonate, authigenic and detrital apatite, and clay-bound P (after Ruttenberg, 1992). However, it is likely that these phases were not completely solubilized, since the solid:solution ratio was quite high (1 g sediment:13 mL extract compared to 1 g sediment:100 mL used in the SEDEX method, see Chapter 2) and because the extraction time was very short (1 hour). In the SB11/95 cores (Chapter 4), the amount of P extractable in acid increases with depth. Core J shows a more jagged pattern, but an overall decrease is apparent (both the minima and maxima trend toward decreasing concentration with depth). Interpreting this profile is difficult, because, as mentioned above, it is likely to incorporate a number of different P phases. However, it is interesting to note that the concentration of P in CDB extracts from cores A and C (Chapter 4) decreases with depth, while the concentration of acid-P increases with depth. In core J, the acid extract is likely to include P that would be extracted either by CDB or by acid in the modified extraction protocol used for cores A and C. Therefore, the observed zigzag pattern may reflect the competing effects of these two opposing trends.

As shown in Figure B-2, the jagged pattern observed in the acid extracts is seen again in the base extracts. The zigzag pattern is almost perfectly anti-correlated with the

acid-P concentration data. It is likely that some of the P accessible to acid is also accessible to base, because the base extract for core J contains EDTA and would therefore solubilize metals. Thus, the complimentary patterns may indicate that when the acid did not efficiently solubilize iron-bound P, the base extract was able to access this P.

Figures B-3 and B-4 show the total P and total organic P, respectively, in the insoluble sediment residue. The percent of TOP in the insoluble fraction of core J is very high, and in one interval exceeds total measured sediment TOP. Combined with the total organic P concentration determined for soluble P extracts from this core, these data indicate a combined total of organic P that exceeds the total organic P measured on bulk sediments. The percent of total organic P in the insoluble residue increases with depth, while the soluble organic P reservoirs decrease with depth. This is consistent with data from the other data Santa Barbara Basin cores (Chapter 4), which indicates soluble reservoirs are more vulnerable to diagenetic degradation.

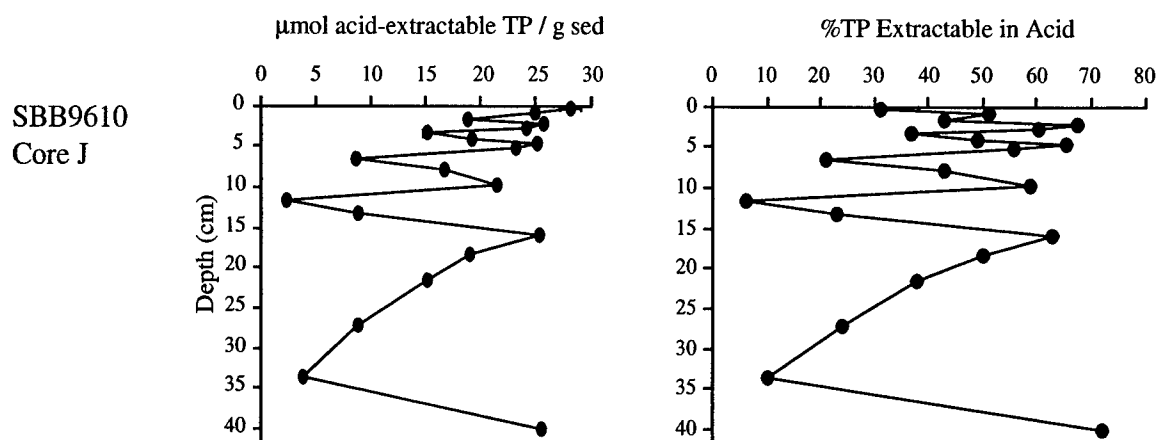


Figure B-1. Depth profiles of total P extracted in 0.1 M HCl. Acid-P concentration (left) and the percent of total sediment P in the acid extract (right) are shown. Error bars indicate the range of concentrations determined by duplicate analyses. Where error bars are not visible, they are smaller than the symbol size.

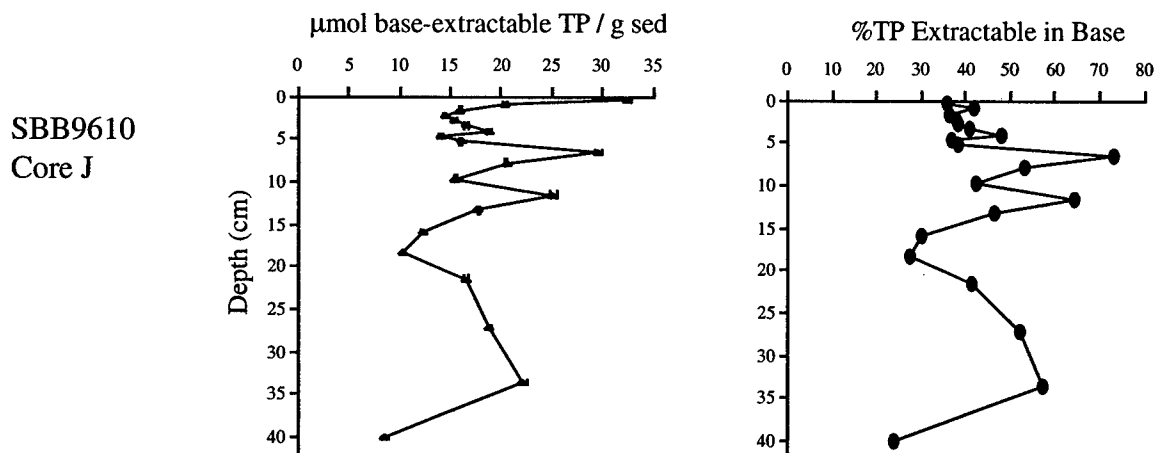


Figure B-2. Depth profiles of total P extracted in 0.5 M NaOH + 0.01 M EDTA. Base-P concentration (left) and the percent of total sediment P in the base extract (right) are shown. Error bars indicate the range of concentrations determined for duplicate analyses. Where error bars are not visible, they are smaller than the symbol size.

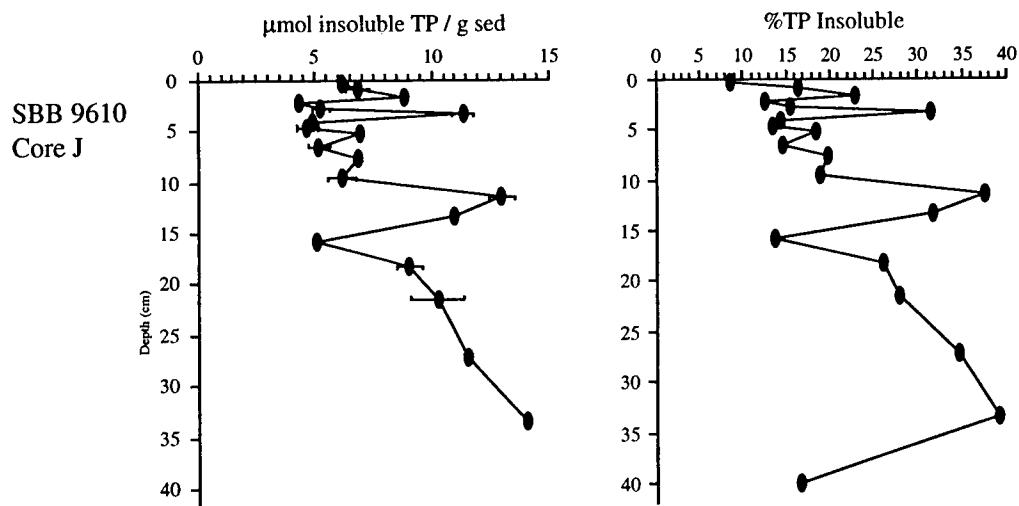


Figure B-3. Total P in the insoluble sediment residue after sequential extraction of core J. Error bars indicate the range of concentrations determined for duplicate analyses. Where error bars are not visible, they are smaller than the symbol size.

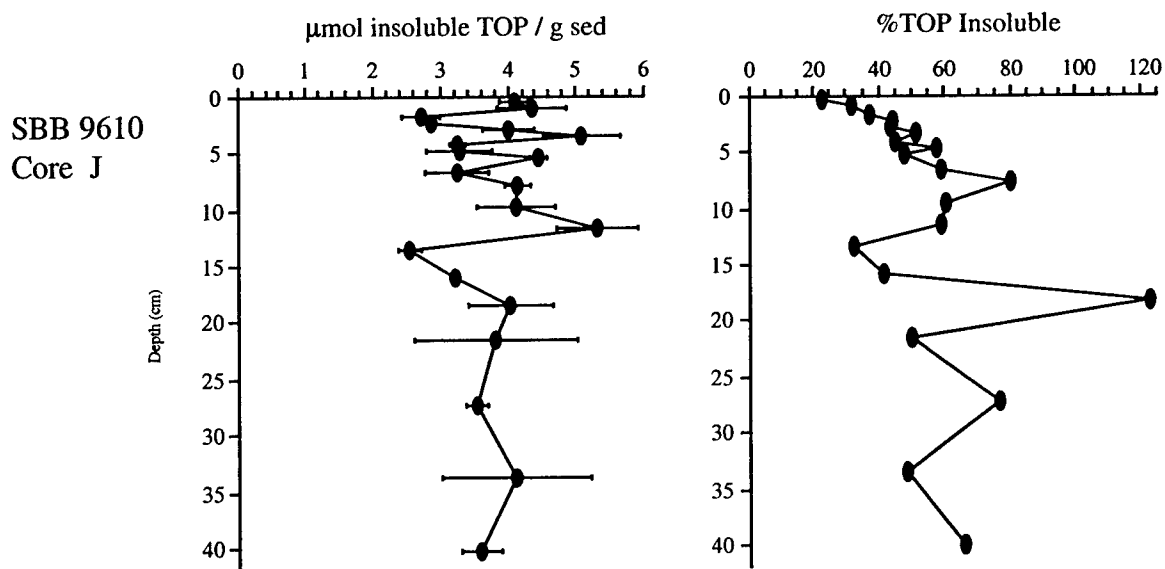


Figure B-4. Organic P in the insoluble sediment residue after sequential extraction of core J. Error bars indicate the range of concentrations determined for duplicate analyses. Where error bars are not visible, they are smaller than the symbol size.

Conclusions

The extraction method used to collect these data was ultimately abandoned in favor of the procedures outlined in Appendix A-2. The two main objectives in using EDTA in the base extractant were: (i) to chelate paramagnetic metals, improving the quality of ^{31}P -NMR spectra, and (ii) to maximize the amount of P solubilized for molecular-level structural analysis. In practice, the disadvantages of this EDTA addition far outweigh its advantages. When compared with base extracts from sediment samples pre-treated with citrate dithionite bicarbonate (CDB), the ^{31}P -NMR spectra of samples prepared using EDTA in the base extractant were far inferior. NMR spectra of the base extracts with EDTA had a much lower signal-to-noise ratio and more peak-broadening. Additional problems that arise when EDTA is added to the base extractant are:

- The considerable amounts of added C and N preclude determination of C:N:P ratios in the base extractable reservoir.
- Precipitation of EDTA during SRP analyses, presumably due to its lower solubility in acidic solution, resulted in erroneous measured phosphate concentrations (described in Chapter 2).
- The separation of P associated with reactive iron phases, authigenic and detrital minerals, and humic compounds is maximized by the preferred method of CDB extraction followed by acid and then base extractions.

Based on the results of this study, addition of EDTA to base extracts, either during extraction or before NMR analysis, is not recommended.

Appendix B-2: Data from Peru Margin Cores

Summary

Sediments from the Peru Margin were used in the initial tests for development of the sequential extraction presented in Chapter 2 (final extraction protocols in Appendix A). Three sediment intervals in each of two cores were analyzed for total and inorganic P by the Aspila (1976) method, and organic solvents and an aqueous alkaline solution were used to isolate organic P reservoirs. Based on these tests, and those of Santa Barbara Basin Core J (see Appendix B-1), the extraction methods were optimized. Therefore, the data presented here are not directly comparable with data presented for the Santa Barbara Basin cores. However, these data demonstrate that changes in the P_{org} pool are taking place with depth in Peru Margin sediments and that there are clear, discernible differences between sites with different depositional conditions.

Peru Margin Study Sites

The Peru Margin was chosen for this study because of the high sedimentary organic matter content, allowing the collection of enough P_{org} for detailed analysis, and because of the importance of this site in understanding P dynamics in a modern P-rich sedimentary environment. Surface sediments along the transect where samples were taken for this study show a great deal of variability (Arthur *et al.*, 1998). Sediments from two contrasting depositional environments were chosen (see Figure B-1), with an effort to minimize differences between the sites other than deep water oxygen concentration. Both cores were taken from the shallow shelf (BC091 at 309 m water depth; GGC143 at 100 m) and were overlain by bacterial mats at the time of collection (T. Eglinton, personal communication, 1996). Note that while the sediments in both locations are fully anoxic, core BC091 is located well within the oxygen minimum zone (OMZ), whereas

site GGC143 is at the edge of the OMZ. Thus, GGC143 has experienced intermittently oxic conditions. Hereafter, the sites are referred to as “oxic” and “suboxic” for simplicity.

Extraction Procedure

Freeze-dried, ground ($<125\ \mu\text{m}$) sediments were weighed into 50 mL glass centrifuge tubes, then lipids were extracted by sonicating the sediments consecutively with 40 mL aliquots of the following sequence of solvents : (i) 100% methanol, (ii) 3 x 20:80 (dichloromethane: methanol), (iii) 2 x 100% hexane. All extracts were combined and concentrated by rotary evaporation before P concentration was determined. All of the remaining samples used in this study (all Santa Barbara Basin sediments) were extracted using a modified Bligh and Dyer (1959) solvent extraction (see Appendix A-1), rather than the extraction scheme described here. The Bligh and Dyer extraction uses more polar solvents than those listed above, and therefore is able to more efficiently extract even very polar lipids (including phospholipids) from sediments.

Solvent-extracted sediments were freeze dried and crushed lightly with a mortar and pestle, then transferred to 50 mL polypropylene centrifuge tubes. Sample weights ranged from 3 to 9 grams of sediment. Each sample was extracted for 1 hour with 40 mL of 0.1 M HCl. The samples were centrifuged (10 minutes, 4000 rpm) and the supernatant was decanted, then 40 mL of 0.5 M NaOH was added to each sample. The samples were extracted in the base solution for 16 hours, then filtered through GF/F filters (nominal pore size $0.7\ \mu\text{m}$) and polycarbonate filters (pore size = $0.4\ \mu\text{m}$). Filtering of these extracts was extremely problematic. The filters tended to clog quickly, and were replaced with new filters, resulting in a large loss of particulate material. In addition, the GF/F filters did not stand up to long-term exposure to the alkaline solution. These were two of the major factors that contributed to the changes in filtration protocol described in Chapter 2. The base extraction and filtration of the extracts was repeated for a total of seven extraction steps. The samples were then transferred to 250 mL centrifuge bottles

and the base extraction was continued for sixteen more extraction steps at a volume of 100 mL per extraction step. The pooled base extracts were then acidified to pH 1 to separate fulvic acids (soluble under acidic as well as basic conditions) from humic acids (which precipitate under acidic conditions).

P Concentration Data

Data from the Peru Margin clearly show differences in the size of the P_{org} reservoir between two sites with different bottom water oxygen concentrations (Figure B-2). Soluble P reservoir data from the Peru Margin (Figure B-3) indicate that while there is a decrease in lipid and fulvic acid reservoirs of P, these changes alone do not account for the rapid drop in total P_{org} with depth observed both in the “anoxic” and the “suboxic” site. This suggests that remineralization of insoluble (previously uncharacterized) P_{org} compounds contributes significantly to the total P_{org} remineralization in sediments.

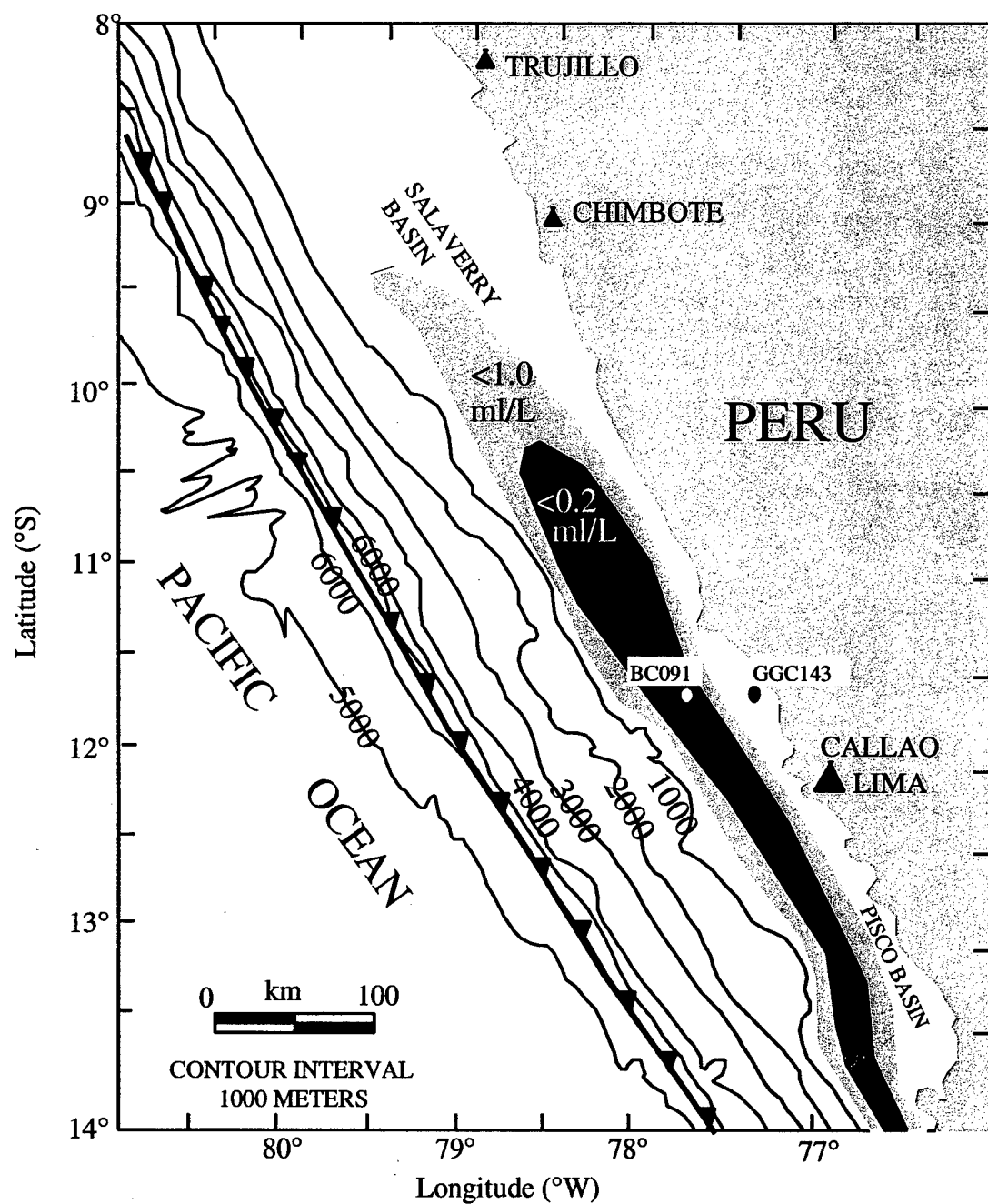


Figure B-6. Map of the Peru Margin, showing the locations of cores BC091 (“anoxic”) and GGC143 (“suboxic”).

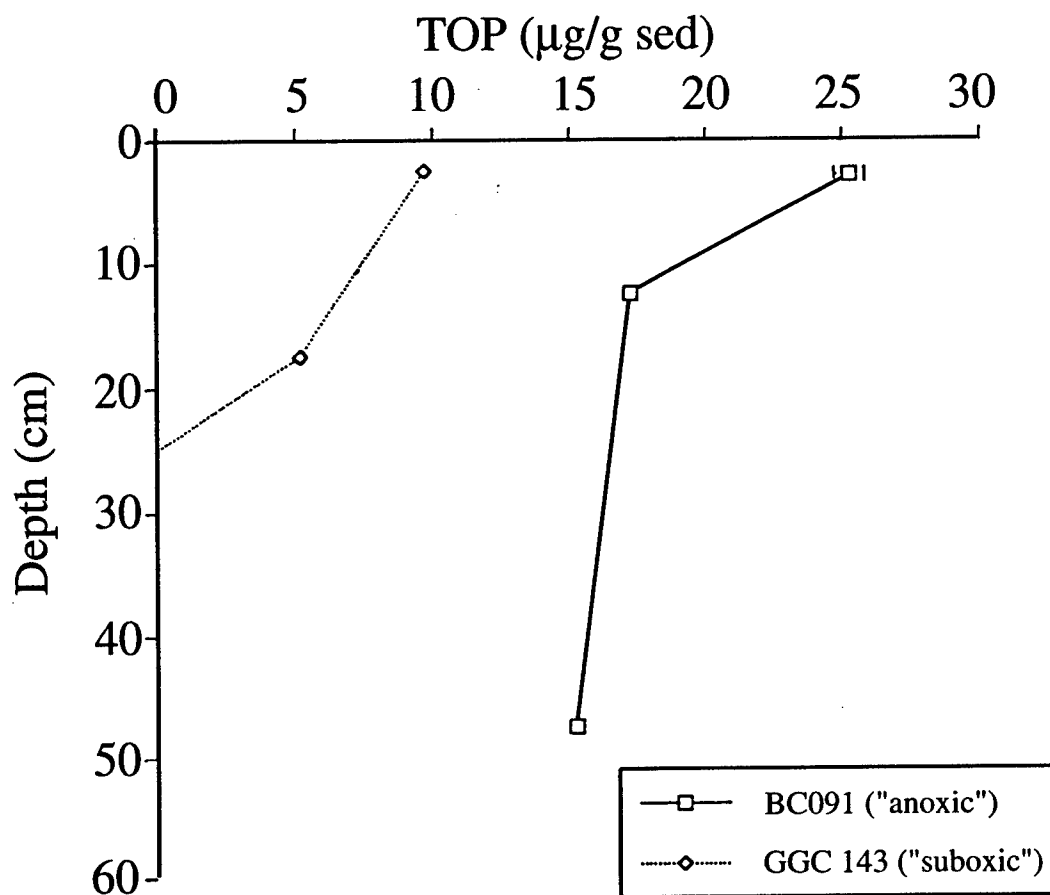
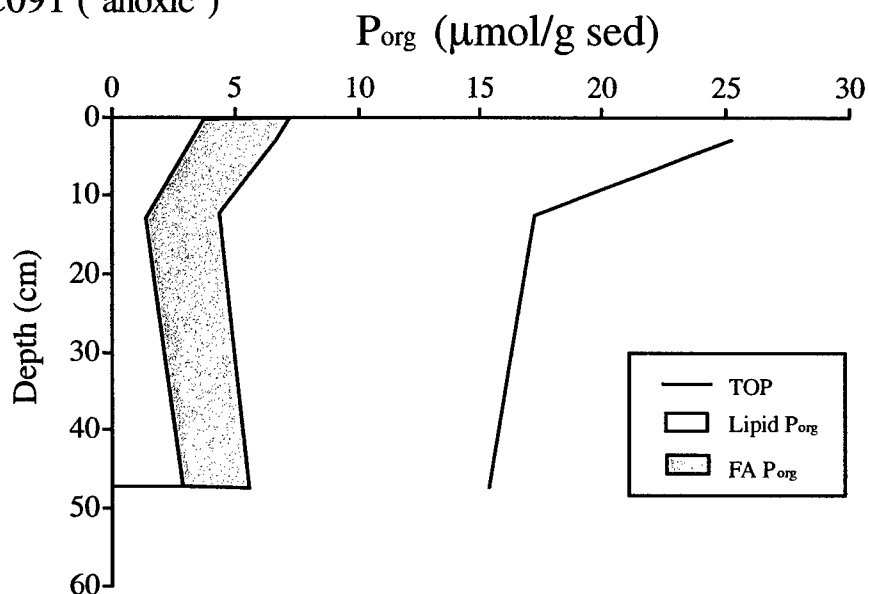


Figure B-7. Depth profiles of TOP in sediments from two sites on the Peru Margin. TOP content is higher in the core which has experienced fully anoxic conditions and decreases with depth in both cores. Error bars ($\pm 1\sigma$) for each data point are shown. The calculated TOP value for the deepest point in core GGC 143 was negative, had large error bars.

BC091 ("anoxic")



GGC143 ("suboxic")

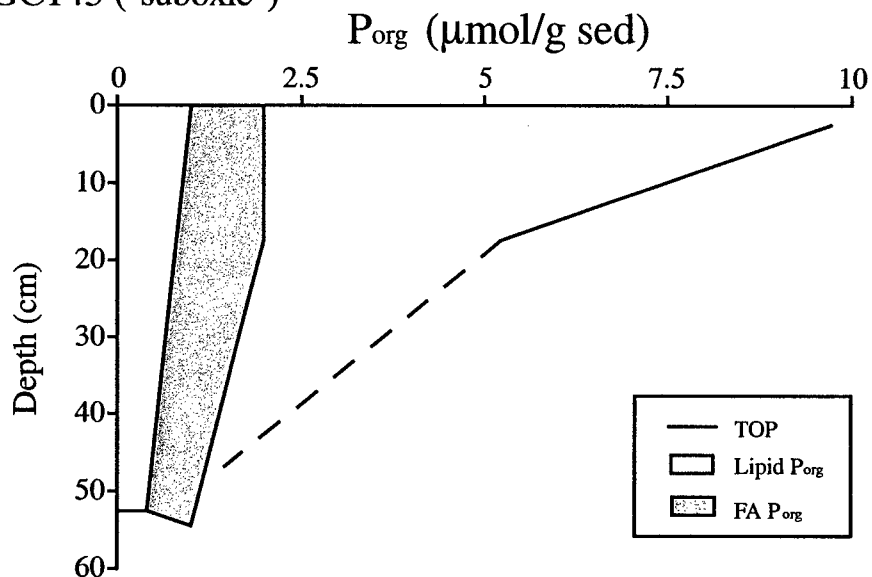


Figure B-8. Partitioning of P_{org} in different organic compound classes vs. depth in cores BC091 ("anoxic") and GGC143 ("suboxic"). Note the difference in scale of the x-axis in the two plots. There is a sharp decrease in total P_{org} the upper 50 cm of each core. This change cannot be fully accounted for by regeneration of P from lipids and fulvic acids, suggesting that remineralization of more insoluble macromolecular compounds is important in total P_{org} removal.

Appendix C: Alternative Methods for Analysis of P_{org}

*When ideas fail, words come in very handy.
- Goethe*

Appendix C-1: Quantification of Phosphonates by Differential Hydrolysis

Summary

The objective of these tests was to determine if the concentration of phosphonates in lipid extracts of marine sediments could be quantified using a differential hydrolysis method. Aalbers and Bieber (1968) presented such a method, which takes advantage of the fact that the C-P bonds of phosphonolipids are not as easily hydrolyzed as the C-O-P bonds of phospholipids. Using the approach of Aalbers and Bieber (1968), phosphonates are quantified by the following three steps: (i) compounds with C-O-P bonds are quantified using the hydrolysis procedure of Bartlett (1959), (ii) total P is quantified using an ashing method similar to that described in Chapter 2, and (iii) phosphonate concentration is calculated by subtracting C-O-P from total P.

The major problems encountered when applying this method to pure organic P standard solutions and to Santa Barbara Basin sediment extracts were: (i) Bartlett's method, as published, was inefficient at hydrolyzing all C-O-P bonds and oxidizing all of the lipid material in natural samples, and (ii) the "phosphonate by difference" method of Aalbers and Bieber was not sensitive enough to accurately quantify the concentrations of phosphonates in natural samples. Bartlett's method was optimized for accurate and precise measurement of P concentration, effectiveness of hydrolysis, and complete oxidation of lipid samples, as described below. These modifications are discussed in the

first sections of this appendix. In the last section, problems with application of the Aalbers and Bieber method to sediment extracts are discussed.

Modified Procedure

Aalbers and Bieber (1968) used the hydrolysis procedure of Bartlett (1959) to hydrolyze C-O-P bonds by heating samples in 10 N H_2SO_4 , and reacting the liberated orthophosphate with color development reagents to quantify the concentration of C-O-P bonds spectrophotometrically. For this study, lipid extracts in chloroform were evaporated to dryness in a stream of nitrogen, 0.450 ml of 20 N H_2SO_4 was added, and samples were heated for 3 hours in a 160°C oven. To ensure complete decomposition of organic compounds and release of P into solution, samples were oxidized by addition of 0.200 ml of 30% H_2O_2 and heated for two hours at 160°C. The additional heating time is required to fully decompose the peroxide, which can interfere with colorimetric measurements. For color development, 4.150 ml of H_2O , 0.2 ml of 5% ammonium molybdate, and 0.2 ml of Fiske and Subba-Rowe reagent (3 g sodium bisulfite, 0.5 g 4-amino-3-hydroxy-1-naphthalenesulfonic acid, 1 g sodium sulfite in 200 ml H_2O) were added to the sample and heated for 30 minutes at 160°C. A blue color proportional to orthophosphate concentration (absorbance measured at 830 nm) develops during this time. The major modifications made to the Bartlett method were: (i) increased heating time for color development (30 to 40 minutes, instead of 7 to 10 minutes), (ii) increased H_2SO_4 concentration (20 N instead of 10 N), and (iii) increased H_2O_2 volume (0.2 mL instead of 0.04 mL). The rationale for each of these modifications is discussed below.

Measurement of Phosphate Concentration

Color development is very pH sensitive and involves a precise balance of reagents. The Bartlett method suggests heating samples in a hot water bath for 7 to 10 minutes for maximum color development. Samples for these tests were heated in a 160°C

oven to allow processing of a large number of samples. Color development did not peak at 7 to 10 minutes and was still increasing at 90 minutes. Although linear standard curves were obtained for each set of standards, the percent error between replicate standards was often greater than 10%. We believe that the high percent error reflected incomplete color development, such that absorbance increased between replicate standards. To determine the heating time that would minimize percent error between replicate samples, 15 μ M standards were analyzed after allowing color development to proceed for times ranging from 15 to 60 minutes. Figure C-8 shows the relative percent error between duplicate standards as a function of heating time, where percent error is described by the equation:

$$\text{Relative \% error} = \frac{[\text{SRP}]_1 - [\text{SRP}]_2}{\text{mean } [\text{SRP}]} \times 100 \quad (\text{C-1})$$

Percent error decreased from 15 to 40 minutes, and increased again at 50 minutes (Figure C-8). Color development was not complete even after 60 minutes, and absorbance continued to increase. However, samples heated for an hour or longer could not be analyzed because their absorbances were too high to measure accurately on the spectrophotometer. The minimum relative percent error was achieved with a heating time of 30-40 minutes. The increase in relative percent error in samples heated longer than 50 minutes reflects the difficulty in measuring high absorbance values that are outside of the linear measurement range on the spectrophotometer. If this method for P concentration measurement were pursued in the future, diluting the sample P concentration is suggested. With diluted samples, color development could go to completion and absorbances would still be in the linear range for measurement.

Hydrolysis of organic P standards

The Bartlett method was modified to minimize hydrolysis of C-P bonds in phosphonate compounds (e.g., 2-AEP) and to maximize hydrolysis of P-O-P and C-O-P bonds in non-phosphonate organic P compounds (e.g., glycerophosphate,

tripolyphosphate, phytic acid, DNA, phosphatidyl ethanolamine). Hydrolysis for 3 hours in 10 N H_2SO_4 , as described by Bartlett, was ineffective in achieving 100% hydrolysis of the phosphoester and phosphoanhydride bonds. Using their procedure, phosphonate hydrolysis was less than 1%, but only 70-80% of C-O-P and P-O-P bonds were hydrolyzed. H_2SO_4 concentration was increased to 20 N, following the modification made by White et al. (1979c). As shown in Table C-1, heating for 3 hours in 0.450 ml of 20 N H_2SO_4 resulted in close to 100% hydrolysis of all C-O-P and P-O-P bonds and only $2.3 \pm 1.1\%$ hydrolysis of 2-AEP (less than the 6% hydrolysis of 2-AEP reported by Aalbers and Bieber using the Bartlett method).

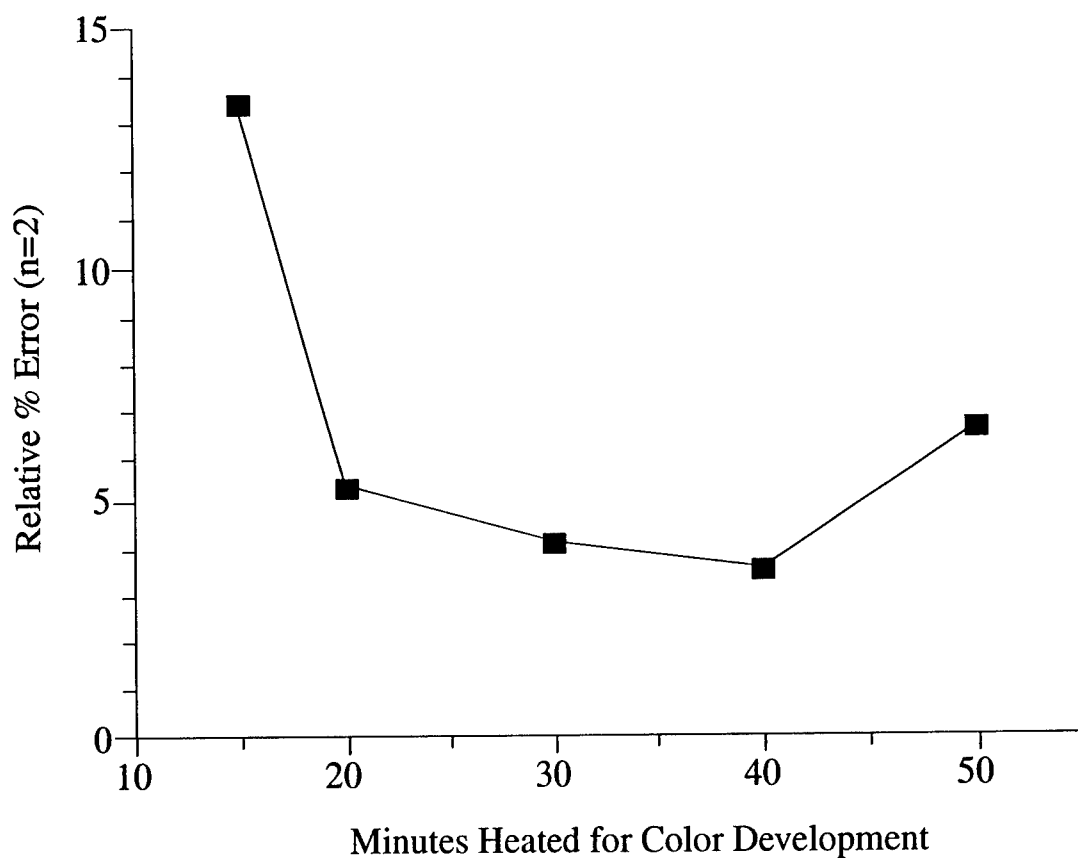


Figure C-1. Relative percent error for replicate standards as a function of heating time allowed for color development. Duplicate 15 μM orthophosphate standards were analyzed after color was allowed to develop over a range of times (15-50 minutes). According to this test, the optimal heating time for reproducible ($\pm 5\%$) color development is 30-40 minutes.

Table C-1. Hydrolysis (20 N H₂SO₄, 3 hours) of standard compounds using the modified Bartlett (1959) method described here.

Compound	% Hydrolyzed
<u>C-O-P and P-O-P Bonds</u>	
Glycerophosphate	100.6 ± 3.4
Tripolyphosphate	95.6 ± 4.4
Phytic Acid	102.4 ± 5.2
DNA	92.1 ± 4.6
<u>C-P Bonds</u>	
2-AEP	2.3 ± 1.1

Analysis of Sediment Lipid Extracts

Application of the Bartlett hydrolysis method to lipids extracted from Santa Barbara Basin sediments required further modification to account for the excess of oxidizable material in natural samples compared to pure standard compounds. For 0.1 mL of lipid extract from Santa Barbara Basin surface sediments (3% organic C, 0.03% organic P by weight), it was necessary to increase the H₂O₂ volume from 0.04 mL to 0.20 mL. Because the volume of H₂O₂ was modified, it was also necessary to increase the heating time allowed for its decomposition to 2 hours. When heated for less than 1.5 hours, excess H₂O₂ interfered with color development. The additional water volume resulting from decomposed H₂O₂ does not interfere with the color development step. In fact, the volume of water added with the molybdate and Fiske and Subba-Row reagents can be varied from 4.05 to 4.5 ml without affecting color development. Note that the adjustments to hydrogen peroxide volume and total heating time had not been made at the time when the percent hydrolysis of standard compounds (Table C-1) was tested. It is not known how the additional levels of H₂O₂ and the increased heating time affect hydrolysis of standard compounds. Certainly, increased heating time and more efficient oxidation should not reduce the efficiency of C-O-P and P-O-P bond hydrolysis. However, it is possible that phosphonate hydrolysis may be increased as a result of these modifications.

Application to Natural Samples

The most notable drawback of the Aalbers and Bieber “difference method” approach is that since the abundance of phosphonates is so small compared to the non-phosphonate abundance, the C-P concentration is calculated by taking the difference of two large numbers. The resulting (small) phosphonate concentration has a relatively large associated error. Due to this large error, the method lacks sufficient sensitivity to resolve the concentration of C-P vs. C-O-P bonds in natural samples. Even in the extreme case where the relative phosphonate concentration in sediments is as high as that in living cells, the phosphonate concentration is still too low to be accurately measured using the difference method. This sensitivity problem can be demonstrated by comparing the natural levels of phosphonate bonds in living tissues and in sediment extracts with the errors imposed by the difference method. As shown in Table C-2, the concentration of phosphonates in living cells is approximately 3% of total cellular P (Kittredge *et al.*, 1969). The percent of total P accounted for by phosphonates in lipid and base extracts of Santa Barbara Basin sediments (determined by ^{31}P -NMR) is in all cases less than 10% and is generally less than 3%. Here, the Aalbers and Bieber method was tested only for lipid extracts. The method would require further modification before it could be applied to base extracts, but the same sensitivity problems would be encountered. While the total P concentration in base extracts is much higher than in lipid extracts, the relative amount of phosphonate (determined by ^{31}P -NMR) is quite small and a large background concentration of orthophosphate would be quantified together with C-O-P value, magnifying the problem.

Table C-2. Comparison of the phosphonate concentration in living cells, lipid and base extracts of Santa Barbara Basin sediments, and the detection limits for the Aalbers and Bieber “difference method” approach.

	<u>C-P</u>	<u>C-O-P</u>
Living Cells ^a	3	97
Lipid P ^b	0 - 9	91-100
Base P ^c	0.5 - 3.5	96.5-99.5
% Hydrolyzed by Bartlett method ^d	2.3 ± 1.1	98±10

^a (Kittredge *et al.*, 1969)

^b Percent of total P as phosphonate determined by ³¹P-NMR (Chapter 3)

^c Percent of total P as phosphonate determined by ³¹P-NMR (Chapter 4)

^d represents the full range of variability listed in Table C-1.

Conclusions

Although the Bartlett hydrolysis method was optimized here to maximize C-O-P hydrolysis and to minimize phosphonate hydrolysis, the range of variation routinely observed in measurements of standard compounds was nevertheless comparable to natural levels of phosphonates in our samples. Since phosphonate concentration is calculated as the small difference between two large numbers, there is a large relative error associated with the difference method. Based on these tests, incomplete hydrolysis of C-O-P and P-O-P bonds, combined with a small amount of hydrolysis of C-P bonds would result in errors greater than 5%, exceeding the natural phosphonate abundance. On the basis of the tests described above, we have determined that use of a differential hydrolysis method to quantify phosphonate concentration in these sediments is infeasible due to its lack of sensitivity.

Appendix C-2:

Structural Characterization of Phospholipids by High-Performance Liquid Chromatography (HPLC)

Summary

Intact phospholipids can be analyzed using only a limited number of standard organic geochemical techniques. Phospholipids are too large and too polar to be directly injected onto a GC column. Pyrolysis and derivatization, two approaches to making large, polar compounds more amenable to GC analysis, result in degradation of simple P standard compounds (See Appendix C-4). Using other standard geochemical techniques such as saponification is problematic because it cannot be determined which fragments originated in P-bearing compounds.

HPLC is a promising technique to examine the structure of free phospholipids, although it does not provide any information about the lipid material associated with (e.g., bound to) higher molecular weight compounds. Authentic phospholipid standards representing the most abundant membrane phospholipids were separated successfully using an HPLC method modified from that of Guichardant and Lagarde (1983). A series of tests was used to establish procedural blanks, compound retention times, and the reproducibility of results obtained by this method. However, the detection limit was too low to apply this method to analyze natural levels of phospholipids in sediments.

Separation and Detection of Lipids by HPLC

The structures of most phospholipids found in cell membranes are similar (Figure C-2). Two of the three carbons in a glycerol molecule are ester-linked to fatty acid chains and a phosphate group is esterified to the third carbon, to form phosphatidic acid. Additional functional groups are attached to the phosphate group of phosphatidic acid to form different phospholipid compound classes. Differences between phospholipids arise

from the additional functional groups linked to the phosphate unit (referred to as the phosphate “head group”) and from changes in the length and degree of saturation of the fatty acid “tails”. In normal-phase HPLC, employed here, compounds are injected onto a polar stationary phase and eluted with relatively non-polar solvents.

Separation of phospholipids by normal-phase HPLC is based on differences in the polarity of each compound, which is a function of the phosphate head group and the fatty acid tails. It is also possible to separate phospholipids by reverse-phase column chromatography, in which compounds are injected onto a non-polar stationary phase (such as a C₁₈ column) and eluted with polar solvents. However, such separations tend to group phospholipids based primarily on their fatty acid chain lengths, rather than their phosphate head groups. To examine the distribution of phospholipid compound classes such as those shown in Figure C-2, it is necessary to use normal phase HPLC.

Most normal phase separations of phospholipids described in the literature use a silica gel column as a stationary phase. Ultra-violet (UV) detectors are a standard method of detection for most HPLC systems because they are versatile and non-destructive. Phospholipids do not have specific UV absorption peaks, but display strong absorption in the 203-214 nm region, reflecting a combination of unsaturated carbons, carbonyl, carboxyl, phosphate, amino and quaternary ammonium groups (Hax & Geurts van Kessel, 1977).

The solvent system used for these separations varies, but is somewhat limited based on solubility and detection concerns. However, chloroform, which is a solvent frequently used to solubilize phospholipids, absorbs in the UV range used to detect phospholipids and therefore cannot be used in methods utilizing UV detection.

Method Development and Testing

The method described by Guichardant and Lagarde(1983) is based on a binary solvent system. Mobile phase A is composed of 60:120:10 (hexane:2-isopropanol:acetate

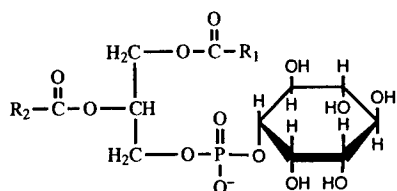
buffer (pH 7)) and mobile phase B is 60:120:21 (hexane:2-isopropanol:acetate buffer (pH 7)). The solvent gradient program suggested by Guichardant and Lagarde is: 5 minutes of 100% A, gradient to 100% B for 25 minutes, then 100% B for 60 minutes. The stationary phase is a silica gel column (Alltech Econosphere 5 μ m; I.D. 4.6 mm; Length 250 mm).

The gradient program prescribed by Guichardant and Lagarde was modified slightly to optimize the separation of phospholipid compound classes. The gradient program used for these tests was: 5 minutes of 100%A, gradient to 70% B for 12 minutes, gradient to 100%B for 13 minutes, then 100%B for 60 minutes. Before use, all solvents were degassed by sonication under vacuum. The separation of phospholipids using this method is shown in Figure C-3. Phospholipids were quantified using UV detection at a wavelength of 206 nm.

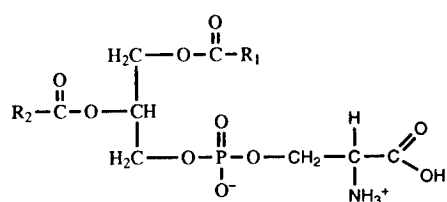
Detection Limit and Use for Natural Samples

Intact phospholipids have not been previously characterized in marine sediments due to insufficient sensitivity of analytical methods (Chen & Kou, 1982; Gillan & Sandstrom, 1985). Similar sensitivity problems were encountered in this study. UV detection is limiting in sensitivity and results in large baseline drift (see Figure C-3). While the calculated detection limit for individual phospholipid groups varied from 500-7000 μ M P, the concentration of total P in most lipid extracts from sediments in this study was less than 100 μ M P. Modification of this method to include detection with an evaporative light scattering detector (ELSD) would improve the problems with sensitivity and baseline drift. Reported detection limits for the ELSD indicate that sample sizes consistent with natural levels can be easily detected (Becart *et al.*, 1990; Letter, 1992; Nordbäck *et al.*, 1998). However, since lipid P represents only a small fraction of total sediment P, no further modifications of the HPLC method were attempted for this study.

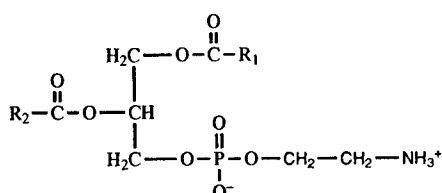
Phosphatidyl Inositol



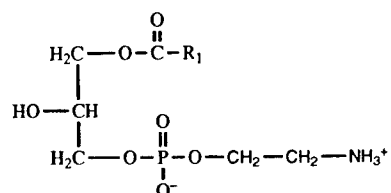
Phosphatidyl Serine



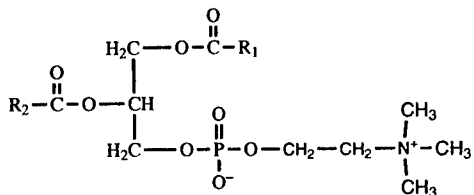
Phosphatidyl Ethanolamine



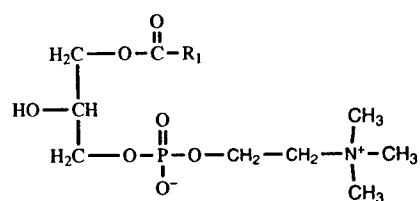
Lyso- Phosphatidyl Ethanolamine



Phosphatidyl Choline



Lyso- Phosphatidyl Choline



Cardiolipin

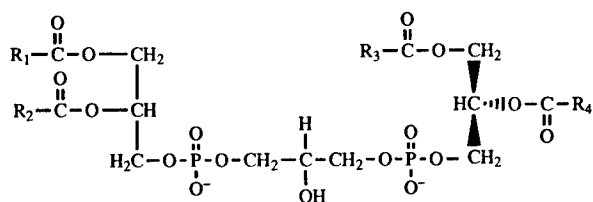


Figure C-2. Major classes of phospholipids separated by the described HPLC method.

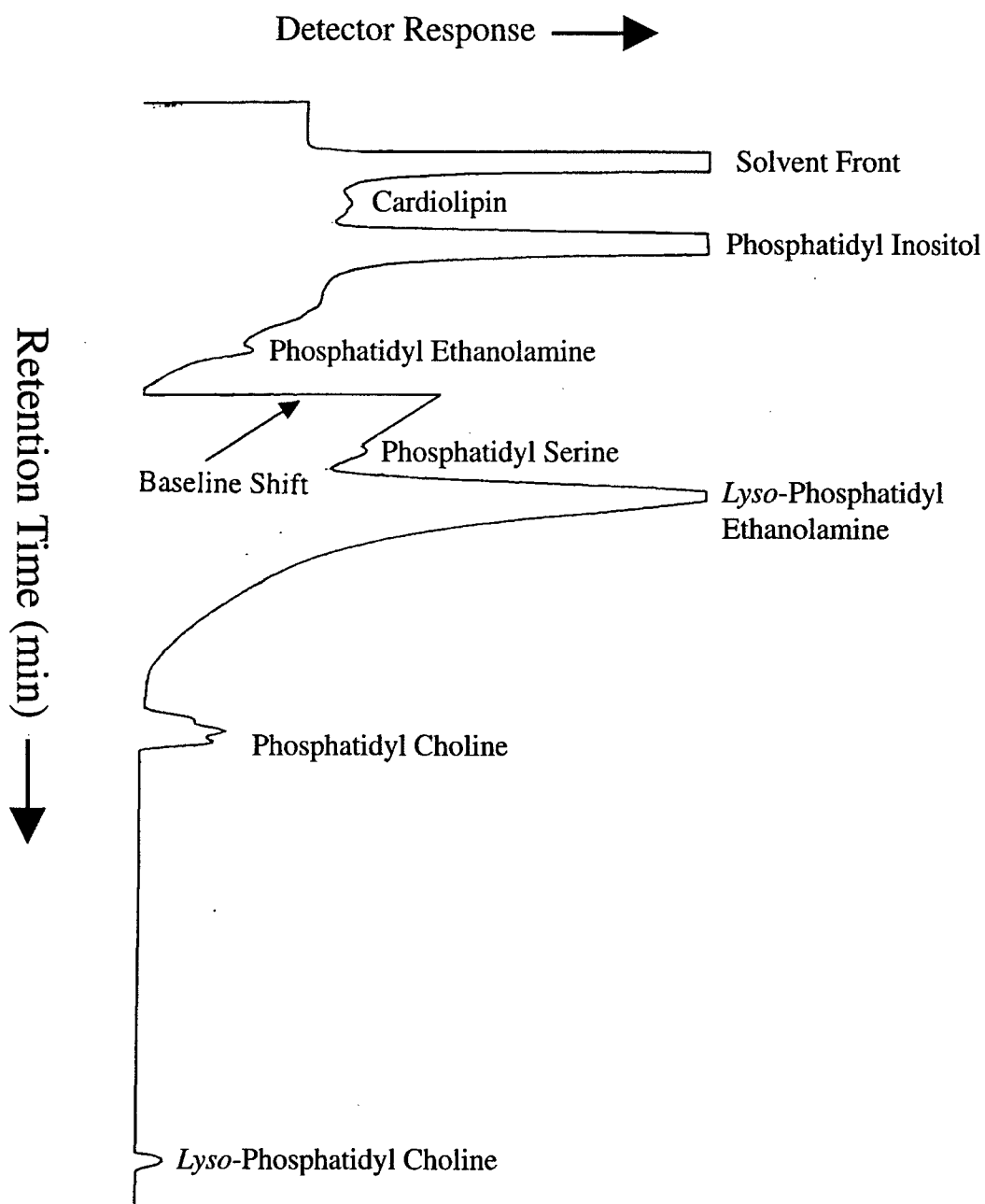


Figure C-3 HPLC separation of major membrane phospholipids. The large baseline drift requires an imposed shift (marked) to keep absorbance readings on-scale. Peak broadening or splitting (particularly apparent in phosphatidyl choline) reflects variations in fatty acid chain length.

Appendix C-3: Kerogen Isolation from the Insoluble Sediment Residue

Summary

Kerogen, the insoluble organic matter in sedimentary rocks, is routinely isolated by dissolving the mineral matrix in cold inorganic acids. Applying a broader definition of kerogen to include the insoluble organic matter in recent, unconsolidated sediments, this procedure was applied to the sediment residue after sequential extraction of Santa Barbara Basin sediments according to the methods outlined in Chapter 2 and Appendix A.

The goal of isolating the kerogen fraction from these sediments was to concentrate organic matter for analysis by solid state ^{31}P -NMR. By removing the mineral matrix, we hoped to increase the amount of kerogen-associated P that could be analyzed in the limited volume of the solid-state magic-angle-spinning (MAS) rotor. However, the procedure used for isolating kerogens resulted in extensive loss of P, and the resulting kerogen-P concentration was actually lower than the estimated P_{org} in the insoluble sediment residue. Based on this result, we concluded that kerogen isolation is not an effective method for concentrating insoluble P_{org} in unconsolidated sediments. The procedure used for kerogen isolation, problems encountered with the method, and the possible sources of P loss are discussed below.

Procedure for Kerogen Isolation

A standard organic geochemical method (T. Eglinton, personal communication) of treatment with HCl and HF was used to dissolve the mineral matrix of the solid sediment residue left after solvent and base extractions. Samples were weighed into 50 mL teflon centrifuge tubes, and 40 mL of 20% HCl was added. Samples were loosely capped and left to digest overnight, thus removing reactive mineral phases such as

carbonates, which would cause violent reaction during treatment with HF. The samples were centrifuged (10 minutes, 3000 rpm) and the supernatant was decanted into a 100 mL HDPE bottle. Sediments were then rinsed with 40 mL of milli-Q H₂O, resuspended, centrifuged and the supernatant was combined with the 20% HCl extract. The pooled acid extract and water rinse were filtered through a 0.4 µm GH Polypro syringe filter and soluble reactive P and total P were measured.

A few mL of 20% HCl were added to each centrifuge tube, then 48% HF was added dropwise, with constant stirring of sediments with a teflon spatula. Tubes were filled approximately two-thirds full with HF, and left to digest overnight. HF was neutralized with a saturated solution of boric acid in milli-Q H₂O and then centrifuged (15 minutes, 3000 rpm). For safety reasons, the supernatant was discarded and no P analyses were performed. A second HF digestion, following the steps given above, was required for complete removal of mineral matrix. After the second HF extraction, the supernatant was neutralized with boric acid, samples were centrifuged and the HF supernatant was discarded. Sediments were then rinsed three times with milli-Q H₂O. After each rinse, the samples were centrifuged (15 minutes, 3000 rpm) and the water rinse was discarded.

Demineralized organic matter was extracted consecutively with organic solvents: (i) MeOH:DCM (4:1), (ii) MeOH:hexane (4:1), (iii) hexane:DCM (4:1), to remove organic matter that was rendered “lipid-like” by the acid treatment. For each solvent treatment, the sample was sonicated for 15 minutes, then centrifuged (15 minutes, 3000 rpm) and the solvent was removed with a Pasteur pipette. These solvent rinses, referred to collectively as total lipid extract II (TLE II), were pooled and analyzed for total P content. The remaining solid residue is referred to here as kerogen, although the insoluble organic matter isolated from recent sediments is more rigorously defined as “proto-kerogen”. The isolated kerogen was lyophilized, and analyzed for P content.

P Concentration Results

By definition, the material isolated by this procedure is organic. Therefore, only total P was measured for the kerogen fraction. Based on the P concentration in samples analyzed by Clark et al. (1998; 1999), it was estimated that a total of 100 $\mu\text{mol P}_{\text{org}}$ was needed to achieve comparable solid state NMR results. As shown in Figure C-4, the procedure did not successfully concentrate organic P. In fact, approximately 90% of the total P_{org} in the base extracted residue (determined by the Aspila method) was lost during kerogen isolation.

Explanations for the Apparent P Loss

The loss of P_{org} observed in these samples can be explained by one or more of the following possibilities: (i) P_{org} solubilized in 20% HCl, (ii) P_{org} solubilized in 48% HF, (iii) P_{org} associated with fine sediments is lost during either of the acid extractions, (iii) P_{org} solubilized in TLE II. The objective of the kerogen isolation was to concentrate organic P. Therefore, solubilization of inorganic P in this extracts is not problematic. As shown in Figure C-5, the P solubilized in the 20% HCl extract was dominantly inorganic. However, it is possible that some organic P was hydrolyzed to orthophosphate by this relatively strong acid treatment. Based on the results of the acid hydrolysis

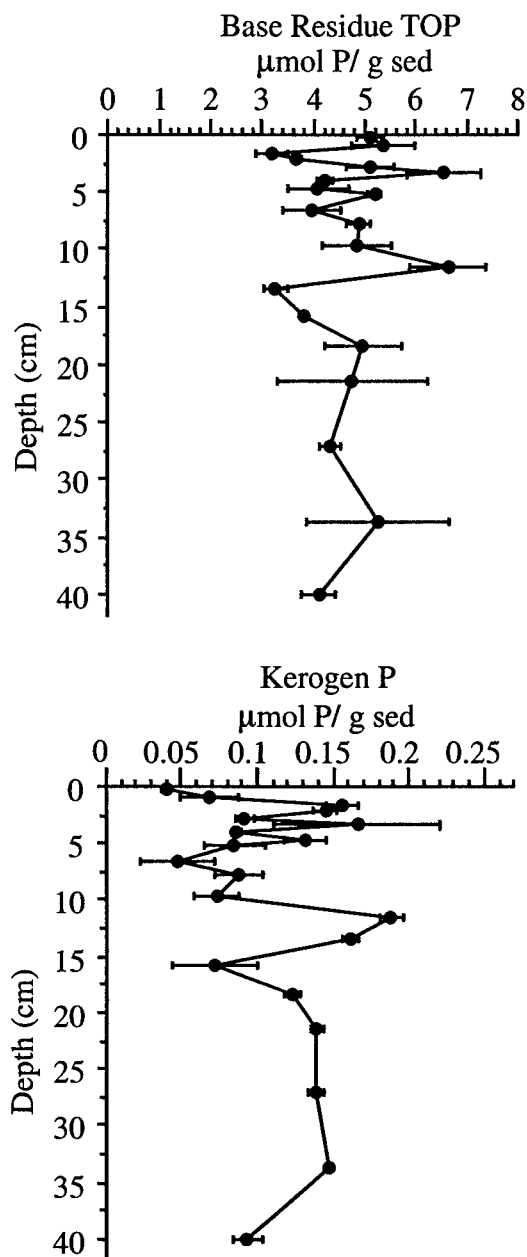


Figure C-4. Profiles of insoluble organic P in sediments and organic P isolated by the kerogen isolation procedure. Error bars indicate the range of concentrations determined for duplicate analyses. Where error bars are not visible, they are smaller than the symbol size. Most of the P in the insoluble residue is lost during the kerogen isolation procedure. Note the difference in the scale for the x-axis (P concentration) in the two panels.

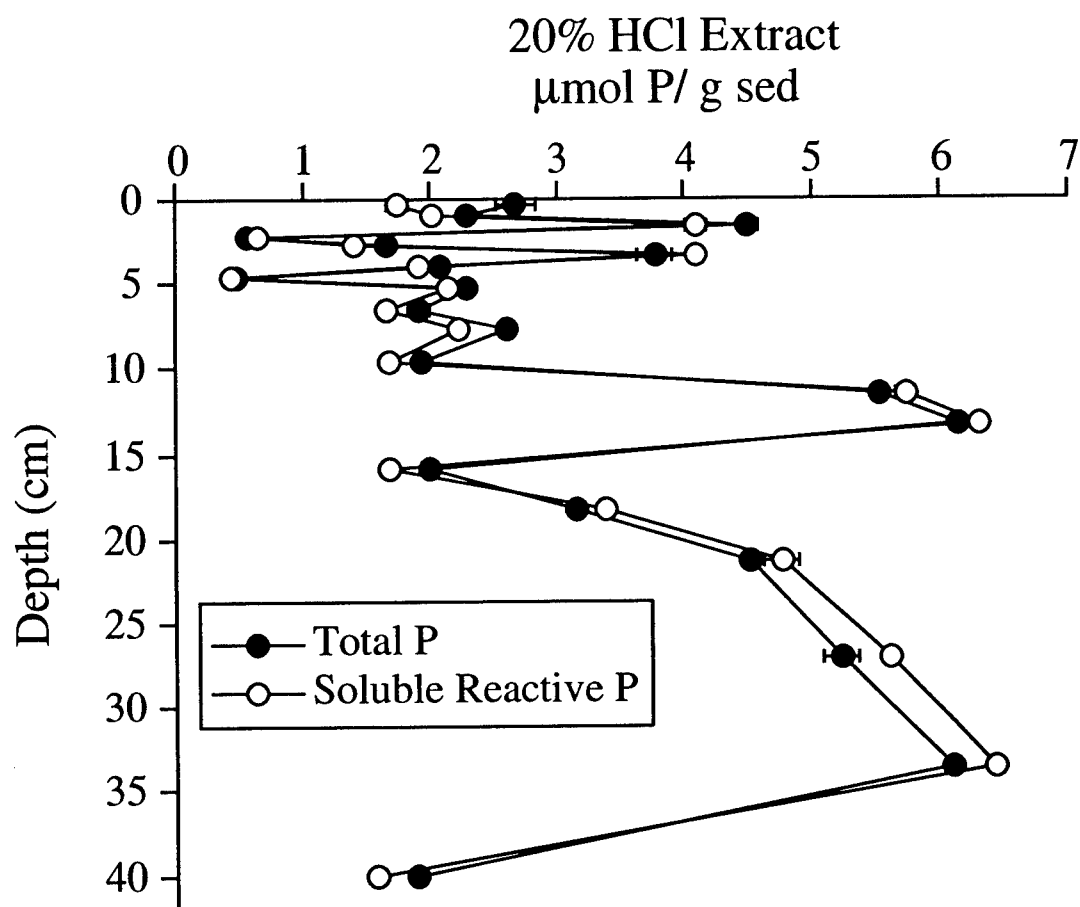


Figure C-5. P extracted in 20% HCl treatment used for kerogen isolation. Error bars indicate the range of concentrations determined for duplicate analyses. Where error bars are not visible, they are smaller than the symbol size.

experiment presented in Chapter 2, a small amount of organic P hydrolysis may occur during the 20% HCl extraction. Taking an extreme case where all of the P in the 20% HCl was from the organic pool, this still can only account for less than 50% of the “missing” P_{org} in most intervals. Since a number of inorganic P phases are likely to be solubilized in this step, such a scenario is extremely unlikely. By simple mass balance, this implies that the missing P was in the HF extract, either hydrolyzed to orthophosphate or simply solubilized, or washed away in the form of fine sediments (the HF extract was not filtered). Due to safety concerns, this measurement was not made directly. Therefore, solubilization and/or hydrolysis of organic P in 48% HF could not be directly evaluated using these results. Total P in TLE II was below our detection limit for all samples used in this study. Thus, of the above-mentioned possibilities, the only feasible explanations for the loss of organic P from these samples are hydrolysis during HCl treatment, or solubilization and/or hydrolysis during HF treatment.

An alternative explanation is that the P solubilized during the acid treatments is dominantly inorganic. In Chapters 2 and 4, a potential analytical artifact in the Aspila method was discussed. A fraction of inorganic P detected by ^{31}P -NMR was incorrectly characterized as organic P using the operational definitions applied for the Aspila method. It is believed that this P is bound to the humic matrix (perhaps by metal bridges) and therefore inaccessible to acid extraction. If organic P in the insoluble sediment residues was over-estimated, it may explain a large fraction of the apparent organic P loss during the kerogen isolation procedure.

The results of this study contrast with the successful concentration of organic P for solid state NMR reported by Ingall *et al.* (1990). In that study, HCl and HF were also used to isolate organic matter. However, the sediments used in their study were not subjected to the sequential extraction used here. Consequently, they may have isolated organic matter in their “kerogen isolate” that was extracted and defined here as humic material. Based on the limited resolution of solid state ^{31}P -NMR spectra, it is not possible

to distinguish between organic and inorganic P in the sediment residues. Therefore, NMR analysis of these samples at present can only be used to distinguish phosphonates from the sum of inorganic and ester-linked P.

Conclusions

Isolation of insoluble organic matter, or kerogen, from the sediment residue remaining after sequential extraction was tested. Extensive loss of P during the HCl and HF acid treatments prevented further analysis of the kerogen isolate by solid state NMR. The apparent loss of organic P can be explained by: (i) hydrolysis of P in 20% HCl, (ii) hydrolysis and/or solubilization of P in 48% HF, or (iii) over-estimation of organic P in the sediment residue prior to kerogen isolation. Although loss of P in the HF extract cannot be ruled out, it is likely that a substantial fraction of the organic P quantified by the Aspila method is actually inorganic P. Based on these results, no additional kerogen isolations were performed. Solid state NMR results from this sample set are therefore limited to distinguishing phosphonate and non-phosphonate compounds.

Appendix C-4:

Analysis of P_{org} Structure using Pyrolysis-Gas Chromatography with a Flame Photometric Detector (Py-GC-FPD)

Summary

In this study, pyrolysis- gas chromatography was tested as a method for structural analysis of the composition of P_{org} in marine sediments. Due to their polarity and high-molecular-weight, direct injection of intact P_{org} compounds onto a GC column is generally not possible. Only polar stationary phases can achieve separation of polar compounds such as organophosphates. However, such columns are not stable at the high temperatures needed to volatilize the high molecular weight compounds that constitute much of the sedimentary P_{org} reservoir. Samples were prepared for GC injection by on-line with tetrabutyl ammonium hydroxide, which renders even polar P compounds amenable to GC analysis. The method of analysis was curie-point pyrolysis with direct injection onto a GC and P detection by a flame photometric detector (Py-GC-FPD).

Based on preliminary Py-GC-FPD chromatograms of kerogens isolated (with no sequential extraction) from Mississippi Delta and Peru Margin sediments (Figure C-6), it is clear that a variety of P_{org} compounds give rise to well-resolved peaks with distinctive retention times. The differences in the chromatograms from the two sites indicate that P_{org} composition is distinct, and may reflect the role of depositional environment in determining the nature of buried sedimentary P_{org} . To identify the P fragments observed in these samples, and to evaluate the potential to distinguish different P_{org} compounds using this method, standard compounds were analyzed by this method. Analysis of individual P_{org} standards revealed that simple P compounds were consistently degraded to orthophosphate. This degradation may have taken place during , pyrolysis, or both. Thus, while the distinct peaks observed in natural samples suggests the Py-GC-FPD is

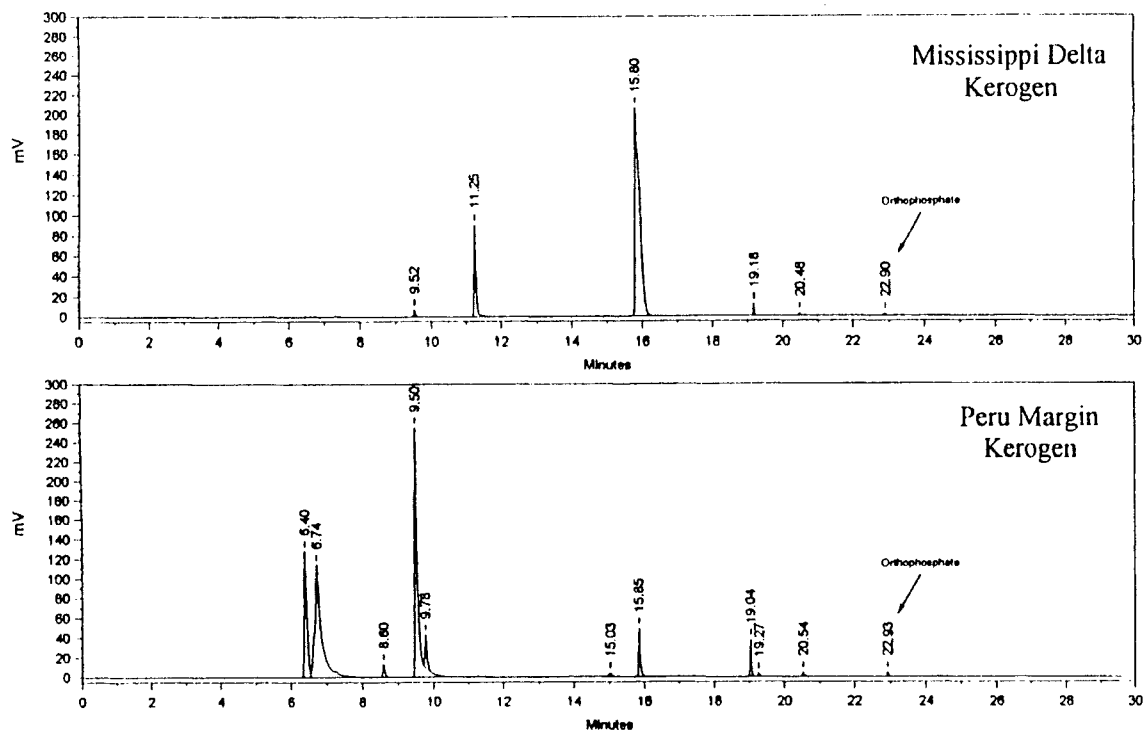


Figure C-6. Chromatograms obtained by Py-GC-FPD analysis, showing P peaks in kerogen samples from the Mississippi Delta and the Peru Margin. The position of the peak representing orthophosphate (determined from standard runs) is indicated on each trace. The differences in peak distribution indicate contrasting P_{org} composition in the two samples, which may reflect the different depositional conditions at the two sites.

potentially a promising technique for analysis of the complex sediment P_{org} reservoir, at present, the results cannot be standardized and peaks cannot be identified.

The Flame Photometric Detector: Theory of Operation

The flame photometric detector is based on the emission of light in characteristic band spectra by P compounds when they are degraded in a flame and then excited. A schematic of the detector is shown in Figure C-7. As the carrier gas elutes compounds from the GC column, they mix with oxygen and burn in a hydrogen flame, decomposing P compounds into the heteroatom species HPO, which is then excited to a higher electronic state. As the excited molecules return to ground state, they emit light in a characteristic band spectrum, with a maximum around 526 nm:



The full spectrum of this emission is shown in Figure C-8a. An optical filter in the detector screens out all wavelengths except 526 nm, so that only this wavelength reaches the photomultiplier tube (PMT). The detector can also be run in sulfur mode, by using an optical filter with a wavelength of 394 nm. The emission spectrum for sulfur compounds is shown in Figure C-8b. The transmitted light stimulates current generation in the PMT, the current is amplified, and the signal is processed into a corresponding peak on the chromatogram (Rood, 1991).

Quenching

The response of the FPD is reduced if non-P, non-S compounds co-elute (even partially) with a species of interest. This is referred to as quenching (Rood, 1991). In particular, hydrocarbons may reduce response, because light is absorbed by the CO_2 species they produce (Rood, 1991). However, the co-eluting compound must be present at 10-50 times the concentration of the species of interest to significantly reduce response

(Rood, 1991). “Self-quenching” is also possible if there are high concentrations of the heteroatom species of interest (Rood, 1991).

Selectivity for phosphorus compounds

The FPD is not considered a specific, but rather a selective detector (Dressler, 1986). Due to an overlap in wavelength emissions, the selectivity of P over hydrocarbons is 10^4 - 10^5 , while the selectivity of P over S is 5-10 (Poole & Schuette, 1984; Dressler, 1986; Rood, 1991). As a result, high concentrations of S compounds may be detected in P mode (Rood, 1991). However, several approaches can be used to eliminate ambiguity in sediments with high organic S content. The detector is much more selective for S in sulfur mode, so that interference of P compounds is minimal. By running the sample in both S- and P-mode, the detection of S compounds can be used to determine where true P peaks are located on the chromatogram. There are two ways in which the detector response differs for S and P compounds. By changing the conditions of the run, the interference of S compounds can be detected. The FPD response to S compounds decreases with increasing detector temperature, while the FPD response to P increases with increasing detector temperature. Therefore, duplicate analyses at different detector temperatures can be used to distinguish P from S because the peak heights at elevated temperature will be smaller for S, but larger for P compounds. The response of the detector to S compounds increases exponentially with increased compound concentration, while the response to P compounds increases linearly with increased concentration. Therefore, repetitive analyses of the same sample injected at different volumes can be used to distinguish P and S compounds, based on the difference in peak heights (Dressler, 1986).

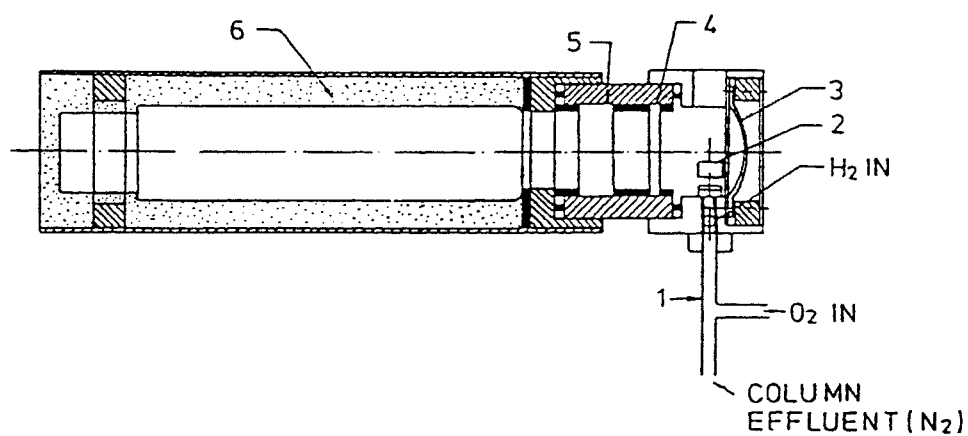


Figure C-7. Schematic diagram of a flame photometric detector (FPD). 1=flame-ionization burner tip; 2=burner; 3=mirror; 4=glass window; 5=optical filter; 6=photomultiplier tube (Dressler, 1986).

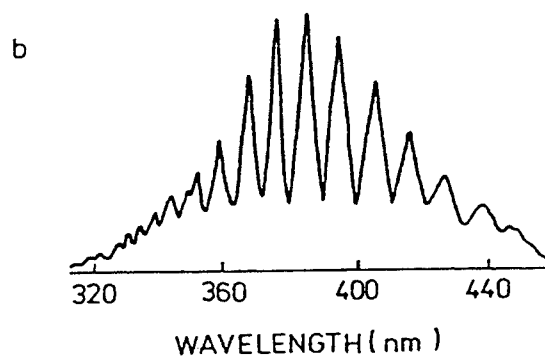
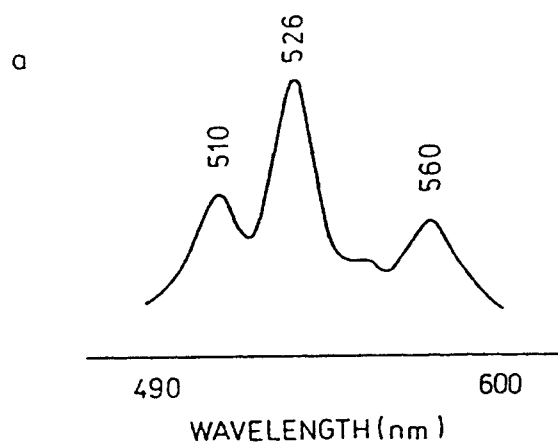


Figure C-8. Emission spectra of (a) HPO species, and (b) S₂ species (Dressler, 1986).

Sensitivity of the Detector

The minimum detectable quantity for P compounds is 1-10 pg (Rood, 1991), with maximum sensitivity at lower detector temperature (Rood, 1991). There is a linear relationship between concentration and detector response in P mode (Poole & Schuette, 1984). The response of the FPD is also affected by gas flow rates (Dressler, 1986; Rood, 1991) and the structure of the particular compound (Sass & Parker, 1980). The structural dependence is the result of differences in the efficiency of production of HPO* species (Dressler, 1986). As a result, quantitative information from Py-GC-FPD analyses would require calibration using individual analyses of specific compounds. Such a calibration was attempted, with results discussed in the next section.

Application to Natural Samples

Before this method can be applied to natural samples, it will be necessary to find an effective means of identifying the P-containing fragments responsible for peaks on the chromatograms. Based on tests with standard compounds, it is clear that the combination of *and* pyrolysis resulted in degradation of all tested standards (DNA, inositol hexaphosphoric acid (phytic acid), glycerophosphate) to orthophosphate.

References

- Aalbers, J.A. & Bieber, L.T. (1968) A method for the quantitative determination of phosphonate phosphorus in the presence of organic and inorganic phosphate. *Anal. Biochem.*, 24, 443-447.
- Adams, A.P., Bartholemew, W.V. & Clark, F.E. (1954) Measurement of nucleic acid components in soil. *Soil. Sci. Soc. Amer. Proc.*, 18, 40-46.
- Adams, M.A. & Byrne, L.T. (1989) ^{31}P -NMR analysis of phosphorus compounds in extracts of surface soils from selected Karri (*Eucalyptus diversicolor* F. Muell.) forests. *Soil Biol. Biochem.*, 21, 523-528.
- Alhadeff, J.A. & Daves Jr., G.D. (1970) Occurrence of 2-aminoethylphosphonic acid in human brain. *Biochemistry*, 9, 4866-4869.
- Anderson, G. (1958) Identification of derivatives of deoxyribonucleic acid in humic acid. *Soil Science*, 86, 169-174.
- Anderson, G. (1961) Estimation of purines and pyrimidines in soil humic acid. *Soil Science*, 91, 156-161.
- Anderson, G. & Hance, R.J. (1963) Investigation of an organic phosphorus component of fulvic acid. *Plant and Soil*, 19, 296-303.
- Arnosti, C. (2000) Substrate specificity in polysaccharide hydrolysis: Contrasts between bottom water and sediments. *Limnology and Oceanography*, 45(5), 1112-1119.
- Arthur, M.A., Dean, W.E. & Laarkamp, K. (1998) Organic carbon accumulation and preservation in surface sediments on the Peru Margin. *Chemical Geology*, 152(3-4), 273-286.
- Aspila, K.I., Agemian, H. & Chau, A.S.Y. (1976) A semi-automatic method for the determination of inorganic, organic and total phosphate in sediments. *Analyst*, 101, 187-197.
- Baird, B.H. & Thistle, D. (1986) Uptake of bacterial extracellular polymer by a deposit-feeding holothurian (*Isostichopus badiotus*). *Marine Biology*, 92(2), 183-187.
- Baird, B.H. & White, D.C. (1985) Biomass and community structure of the abyssal microbiota determined from the ester-linked phospholipids recovered from Venezuela Basin and Puerto Rico Trench sediments. *Marine Geology*, 68(1-4), 217-231.

- Baker, R.T. (1977) Humic acid-associated organic phosphate. *New Zealand Journal of Science*, 20, 439-441.
- Balkwill, D.L., Leach, F.R., Wilson, J.T., McNabb, J.F. & White, D.C. (1988) Equivalence of microbial biomass measures based on membrane lipid and cell wall components, adenosine triphosphate, and direct counts in subsurface aquifer sediments. *Microb. Ecol.*, 16, 73-84.
- Bartlett, G.L. (1959) Phosphorus assay in column chromatography. *J. Biol. Chem.*, 234, 466-468.
- Becart, J., Chevalier, C. & Biesse, J.P. (1990) Quantitative analysis of phospholipids by HPLC with a light scattering evaporating detector - Application to raw material for cosmetic use. *Journal of High Resolution Chromatography*, 13, 126-129.
- Bedrock, C.N., Cheshire, M.V., Chudek, J.A., Fraser, A.R., Goodman, B.A. & Shand, C.A. (1995) Effect of pH on precipitation of humic acid from peat and mineral soils on the distribution of phosphorus forms in humic and fulvic acid fractions. *Communications in Soil Science and Plant Analysis*, 26, 1411-1425.
- Bedrock, C.N., Cheshire, M.V., Chudek, J.A., Goodman, B.A. & Shand, C.A. (1994) Use of ^{31}P -NMR to study the forms of phosphorus in peat soils. *The Science of the Total Environment*, 152, 1-8.
- Berner, R.A. (1982) Burial of organic carbon and pyrite sulfur in the modern ocean: Its geochemical and environmental significance. *American Journal of Science*, 282, 451-473.
- Berner, R.A. (1989) Biogeochemical cycles of carbon and sulfur and their effect on atmospheric oxygen over Phanerozoic time. *Palaeogeography, Palaeoclimatology, Palaeoecology*, 73, 97-122.
- Berner, R.A., Ruttenberg, K.C., Ingall, E.D. & Rao, J.-L. (1993) The nature of phosphorus burial in modern marine sediments. In: *Interactions of C, N, P and S Biogeochemical Cycles and Global Change, 14, NATO ASI Series* (Ed. by R. Wollast, F. T. Mackenzie & L. Chou), pp. 365-378. Springer-Verlag, Berlin Heidelberg.
- Bernhard, J.M., Buck, K.R., Farmer, M.A. & Bowser, S.S. (2000) The Santa Barbara Basin is a symbiosis oasis. *Nature*, 403, 77-80.
- Bernhard, J.M. & Reimers, C.E. (1991) Benthic foraminiferal population fluctuations related to anoxia: Santa Barbara Basin. *Biogeochemistry*, 15, 127-149.

- Bishop, M.L., Chang, A.C. & Lee, R.W.K. (1994) Enzymatic mineralization of organic phosphorus in a volcanic soil in Chile. *Soil Science*, 157, 238-243.
- Bligh, E.G. & Dyer, W.J. (1959) A rapid method of total lipid extraction and purification. *Canadian Journal of Biochemistry and Physiology*, 37, 911-917.
- Bobbie, R.J., Morrison, S.J. & White, D.C. (1978) Effects of substrate biodegradability on the mass and activity of the associated estuarine microbiota. *Applied and Environmental Microbiology*, 35, 179-184.
- Bossard, P. & Karl, D.M. (1986) The direct measurement of ATP and adenine nucleotide pool turnover in microorganisms: a new method for environmental assessment of metabolism, energy flux and phosphorus dynamics. *Journal of Plankton Research*, 8(1), 1-13.
- Bostrom, B. & Pettersson, K. (1982) Different patterns of phosphorus release from lake sediments in laboratory experiments. *Hydrobiologia*, 92, 415-429.
- Brannon, C.A. & Sommers, L.E. (1985) Stability and mineralization of organic phosphorus incorporated into model humic polymers. *Soil Biol. Biochem.*, 17, 221-227.
- Broecker, W.S. (1982) Glacial to interglacial changes in ocean chemistry. *Prog. Oceanogr.*, 11, 151-197.
- Broecker, W.S. & Peng, T.-H. (1982) *Tracers in the Sea*. Eldigio Press, New York.
- Buffle, J.A.E. (1977) Les substances humiques et leurs interactions avec les ions minéraux. In: *Commission d'Hydrologie Appliquée de A.G.H.T.M.*, pp. 3-10, l'Université d'Orsay.
- Burnett, B.R. (1977) Quantitative sampling of nanobiota (microbiota) of the deep-sea benthos III. The bathyl San Diego Trough. *Deep-Sea Research*, 28, 649-664.
- Callender, E. & Hammond, D.E. (1982) Nutrient exchange across the sediment-water interface in the Potomac River estuary. *Estuarine, Coastal and Shelf Science*, 15(4), 395-413.
- Canfield, D.E. (1993) Organic matter oxidation in marine sediments. In: *Interactions of C, N, P and S Biogeochemical Cycles and Global Change, 14, NATO ASI Series* (Ed. by R. Wollast, F. T. Mackenzie & L. Chou), pp. 333-363. Springer-Verlag, Berlin Heidelberg.

- Carman, R. & Jonsson, P. (1991) The distribution pattern of different forms of phosphorus in some surficial sediment types of the Baltic Sea. *Chemical Geology*, 90, 91-106.
- Chapman, A.G. & Atkinson, D.E. (1977) Adenine nucleotide concentrations and turnover rates. Their correlation with biological activity in bacteria and yeast. *Adv. Microb. Physiol.*, 15, 253-306.
- Chen, S.S. & Kou, A.Y. (1982) Improved procedure for the separation of phospholipids by high-performance liquid chromatography. *Journal of Chromatography*, 227, 25-31.
- Clark, L.L., Ingall, E.D. & Benner, R. (1998) Marine phosphorus is selectively remineralized. *Nature*, 393, 426.
- Clark, L.L., Ingall, E.D. & Benner, R. (1999) Marine organic phosphorus cycling: Novel insights from nuclear magnetic resonance. *American Journal of Science*, 299, 724-737.
- Codispoti, L.A. (1989) Phosphorus vs. nitrogen limitation of new and export production. In: *Productivity of the Ocean: Present and Past* (Ed. by W. H. Berger, V. S. Smetacek & G. Wefer), pp. 377-394. John Wiley & Sons.
- Colman, A.S. & Holland, H.D. (2000) The Global Diagenetic Flux of Phosphorus from Marine Sediments to the Oceans: Redox Sensitivity and the Control of Atmospheric Oxygen Levels. In: *Marine Authigenesis: From Global to Microbial*, 66, *SEPM Special Publication* (Ed. by C. R. Glenn, L. Prévôt-Lucas & J. Lucas). Society for Sedimentary Geology.
- Comeau, Y., Hall, K.J., Hanrock, R.E.W. & Oldman, W.K. (1986) Biogeochemical model for enhanced biological phosphorus removal. *Water*, 20, 1511-1521.
- Condon, L.M., Frossard, E., Tiessen, H., Newman, R.H. & Stewart, J.W.B. (1990) Chemical nature of organic phosphorus in cultivated and uncultivated soils under different environmental conditions. *Journal of Soil Science*, 41, 41-50.
- Condon, L.M., Goh, K.M. & Newman, R.H. (1985) Nature and distribution of soil phosphorus as revealed by a sequential extraction method followed by ^{31}P nuclear magnetic resonance analysis. *Journal of Soil Science*, 36, 199-207.
- Cotner, J., Ammerman, J., Peele, E. & Bentzen, E. (1997) Phosphorus-limited bacterioplankton growth in the Sargasso Sea. *Aquatic Microbial Ecology*, 13, 141-149.

- Cragg, B.A., Harvey, S.M., Fry, J.C., Herbert, R.A. & Parkes, R.J. (1992) Bacterial biomass and activity in the deep sediment layers of the Japan Sea, Hole 798B. *Proceedings of the Ocean Drilling Program, Scientific Results*, 127/128, 761-776.
- Cragg, B.A., Parkes, R.J., Fry, J.C., Herbert, R.A., Wimpenny, J.W.L. & Getliff, J.M. (1990) Bacterial biomass and activity profiles within deep sediment layers. In: *Proceedings of the Ocean Drilling Program, Scientific Results*, 112 (Ed. by E. Suess, R. von Huene, K.-C. Emeis & J. Bourgois), pp. 607-619. Ocean Drilling Program, College Station, TX.
- Cragg, B.A., Parkes, R.J., Fry, J.C., Weightman, A.J., Maxwell, J.R., Kastner, M., Hovland, M., Whiticar, M.J., Sample, J.C. & Stein, R. (1995) Bacterial profiles in deep sediments of the Santa Barbara Basin, Site 893. In: *Proceedings of the Ocean Drilling Program, Scientific Results*, 146 (Ed. by J. P. Kennett, J. G. Baldauf, R. Behl, W. R. Bryant & M. Fuller), pp. 139-144. Ocean Drilling Program, College Station, TX.
- Cranwell, P.A. (1984) Lipid geochemistry of sediments from Upton Broad, a small productive lake. *Organic Geochemistry*, 7, 25-37.
- Craven, D.B., Jahnke, R.A. & Carlucci, A.F. (1986) Fine-scale vertical distributions of microbial biomass and activity in California Borderland sediments. *Deep-Sea Research*, 33, 379-390.
- Craven, D.B. & Karl, D.M. (1984) Microbial RNA and DNA synthesis in marine sediments. *Marine Biology*, 83(2), 129-139.
- Dale, N.G. (1974) Bacteria in intertidal sediments: Factors related to their distribution. *Limnology and Oceanography*, 19, 509-518.
- Davelaar, D. (1993) Ecological significance of bacterial polyphosphate metabolism in sediments. *Hydrobiologia*, 253, 179-192.
- Davis, W.M. & White, D.C. (1980) Fluorometric determination of adenosine nucleotide derivatives as measures of the microfouling, detrital and sedimentary microbial biomass and physiological status. *Applied and Environmental Microbiology*, 40, 539-548.
- Dawes, E.A. & Senior, P.J. (1973) Energy reserve polymers in microorganisms. *Adv. Microbiol. Physiol.*, 10, 135-266.
- De Leeuw, J.W. & Largeau, C. (1993) A review of macromolecular organic compounds that comprise living organisms and their role in kerogen, coal, and petroleum formation. In: *Organic Geochemistry* (Ed. by M. H. Engel & S. A. Macko), pp. 23-72. Plenum Press, New York.

- DeBoer, P.L. (1981) Mechanical effects of micro-organisms on intertidal bedform migration. *Sedimentology*, 28, 129-132.
- Deinema, M.H., Habets, L.H.A., Scholten, J., Turkstra, E. & Webers, H.A.A.M. (1980) The accumulation of polyphosphate in *Acinetobacter* spp. *FEMS Microbiol. Letters*, 9, 275-279.
- Delaney, M.L. (1998) Phosphorus accumulation in marine sediments and the ocean phosphorus cycle. *Global Biogeochemical Cycles*, 12(4), 563-572.
- Delaney, M.L. & Anderson, L.D. (1997) Phosphorus geochemistry in Ceara Rise sediments. In: *Proc. ODP, Sci. Results, 154* (Ed. by N. J. Shackleton, W. B. Curry, C. Richter & T. J. Bralower), pp. 475-482. Ocean Drilling Program, College Station, TX.
- Demaison, G.J. & Moore, G.T. (1980) Anoxic environments and oil source bed genesis. *The American Association of Petroleum Geologists Bulletin*, 64(8), 1179-1209.
- Deming, J.W. & Baross, J.A. (1993) The early diagenesis of organic matter: Bacterial activity. In: *Organic Geochemistry* (Ed. by M. H. Engel & S. A. Macko), pp. 119-144. Plenum Press, New York.
- Deming, J.W. & Colwell, R.R. (1982) Barophilic bacteria associated with digestive tracts of abyssal holothurions. *Applied and Environmental Microbiology*, 44, 1222-1230.
- Doi, Y., Kawaguchi, Y., Nakamura, Y. & Konioka, M. (1989) Nuclear magnetic resonance studies of poly (3-hydroxy-butylate) and polyphosphate metabolism in *Alcaligenes eutrophus*. *Applied and Environmental Microbiology*, 47, 519-525.
- Doremus, C. & Clesceri, L.S. (1982) Microbial metabolism in surface sediments and its role in the immobilization of phosphorus in oligotrophic lake sediments. *Hydrobiologia*, 91, 261-268.
- Dressler, M. (1986) *Selective Gas Chromatographic Detectors*. Elsevier, New York.
- Emerson, S. & Hedges, J.I. (1988) Processes controlling the organic carbon content of open ocean sediments. *Paleoceanography*, 3(5), 621-634.
- Emery, K.O. & Hulsemann, J. (1962) The relationships of sediments, life and water in a marine basin. *Deep-Sea Research*, 8, 165-180.
- Eto, M. (1974) *Organophosphorus Pesticides: Organic and Biological Chemistry*. CRC Press, Ohio.

- Feuillade, J., Bielicki, G. & Renou, J.-P. (1995) ^{31}P -NMR study of natural phytoplankton samples. *Hydrobiologia*, 300, 391-398.
- Filipek, L.H. & Owen, R.M. (1981) Diagenetic controls of phosphorus in outer continental-shelf sediments from the Gulf of Mexico. *Chemical Geology*, 33(3-4), 181-204.
- Filippelli, G.M. & Delaney, M.L. (1994) Phosphorus geochemistry of Equatorial Pacific sediments. *Geochimica et Cosmochimica Acta*, 60(9), 1479-1495.
- Findlay, R.H. & Dobbs, F.C. (1993) Quantitative description of microbial communities using lipid analysis. In: *Aquatic Microbial Ecology* (Ed. by Kemp, Sherr, Sherr & Cole). Lewis Publishers.
- Fisher, T.R., Peele, E.R., Ammerman, J.W. & Harding, L.W. (1992) Nutrient limitation of phytoplankton in Cheseapeake Bay. *Marine Ecology Progress Series*, 82, 51-63.
- Folch, J., Lees, M. & Stanley, G.H. (1957) A simple method for the isolation and purification of total lipids from animal tissues. *Journal of Biological Chemistry*, 226, 497-509.
- Francko, D.A. & Heath, R.T. (1982) UV-sensitive complex phosphorus: Association with dissolved humic material and iron in a bog lake. *Limnology and Oceanography*, 27(3), 564-569.
- Froelich, P.N. (1988) Kinetic control of dissolved phosphate in natural rivers and estuaries: A primer on the phosphate buffer mechanism. *Limnology and Oceanography*, 33, 649-668.
- Froelich, P.N., Bender, M.L., Luedtke, N.A., Heath, G.R. & DeVries, T. (1982) The marine phosphorus cycle. *American Journal of Science*, 282, 474-511.
- Frossard, E., Brossard, M., Hedley, M.J. & Metherell, A. (1995) Reactions controlling the cycling of P in soils. In: *Phosphorus in the Global Environment, Scope* (Ed. by H. Tiessen). John Wiley & Sons Ltd.
- Gächter, R. & Meyer, J.S. (1993) The role of microorganisms in mobilization and fixation of phosphorus in sediments. *Hydrobiologia*, 253, 103-121.
- Gächter, R., Meyer, J.S. & Mares, A. (1988) Contribution of bacteria to release and fixation of phosphorus in lake sediments. *Limnology and Oceanography*, 33(6), 1542-1558.

- Gard, J.K., Burquin, J.C., Wise, W.B. & Herman, B.S. (1992a) Automated ^{31}P NMR: A complete assay of oligophosphates and their mixtures using a robotic sample manager. *Spectroscopy*, 7(6), 28-31.
- Gard, J.K., Gard, D.R. & Callis, C.F. (1992b) Quantitative analysis of inorganic phosphates using ^{31}P NMR spectroscopy. In: *Phosphorus Chemistry: Developments in American Science* (Ed. by E. N. Walsh, E. J. Griffith, L. D. Quin & R. W. Parry). American Chemical Society.
- Gehron, M.J. & White, D.C. (1983) Sensitive assay of phospholipid glycerol in environmental samples. *J. Microbial Methods*, 1, 23-32.
- Gerke, J. (1992) Orthophosphate and organic phosphate in the soil solution of four sandy soils in relation to pH-evidence for humic-Fe-(Al)-phosphate complexes. *Commun. Soil Sci. Plant Anal.*, 23, 601-612.
- Getliff, J.M., Fry, J.C., Cragg, B.A. & Parkes, R.J. (1992) The potential for bacteria growth in deep sediment layers of the Japan Sea, Hole 798B- Leg 128. *Proceedings of the Ocean Drilling Program, Scientific Results*, 127/128, 755-760.
- Gillan, F.T. & Sandstrom, M.W. (1985) Microbial lipids from a nearshore sediment from Bowling Green Bay, North Queensland: The fatty acid composition of intact lipid fractions. *Organic Geochemistry*, 8(5), 321-328.
- Glonek, T., Henderson, T.O., Hildebrand, R.L. & Myers, T.C. (1970) Biological phosphonates: Determination by phosphorus-31 nuclear magnetic resonance. *Science*, 169, 192-194.
- Goldenbaum, P.E., Keyser, P.D. & White, D.C. (1975) Role of vitamin K₂ in the organization and function of *Staphylococcus aureus* membranes. *J. Bacteriol.*, 121, 442-449.
- Gressel, N., McColl, J.G., Preston, C.M., Newman, R.H. & Powers, R.F. (1996) Linkages between phosphorus transformations and carbon decomposition in a forest soil. *Biogeochemistry*, 33(2), 97-123.
- Guichardant, M. & Lagarde, M. (1983) Phospholipid analysis and fatty acid content in platelets by the combination of high-performance liquid chromatography and glass capillary gas-liquid chromatography. *Journal of Chromatography*, 275, 400-406.
- Hamilton, R.D. & Holm-Hansen, O. (1967) Adenosine triphosphate content of marine bacteria. *Limnology and Oceanography*, 12, 319-324.
- Harkness, R.D. (1966) Bacterial growth on aminoalkylphosphonic acids. *J. Bacteriol.*, 92, 623-627.

- Hartmann, M., Muller, P., Suess, E. & van der Weijden, C.H. (1976) Chemistry of Late Quaternary sediments and their interstitial waters from the NW African continental margin. *Meteor Forsch.-Ergebnisse*, C 24, 1-67.
- Harvey, H.R., Fallon, R.D. & Patton, J.S. (1986) The effect of organic matter and oxygen on the degradation of bacterial membrane lipids in marine sediments. *Geochimica et Cosmochimica Acta*, 50, 795-804.
- Harvey, H.R., Richardson, M.D. & Patton, J.S. (1984) Lipid composition and vertical distribution of bacteria in aerobic sediments of the Venezuela Basin. *Deep-Sea Research*, 31(4), 403-413.
- Hawkes, G.E., Powlson, D.S., Randall, E.W. & Tate, K.R. (1984) A ^{31}P nuclear magnetic resonance study of the phosphorus species in alkali extracts of soils from long-term field experiments. *Journal of Soil Science*, 35, 35-45.
- Hawthorne, J.N. & Ansell, G.B. (1982) *Phospholipids*. Elsevier Biomedical, Amsterdam.
- Hax, W.M.A. & Geurts van Kessel, W.S.M. (1977) High-performance liquid chromatographic separation and direct ultraviolet detection of phospholipids. *Journal of Chromatography*, 142, 735-741.
- Hayes, M.H.B., MacCarthy, P., Malcolm, R.L. & Swift, R.S. (1989) *Humic Substances II: In Search of Structure*. John Wiley & Sons, New York.
- Hedges, J.I. (1988) Polymerization of humic substances in natural environments. In: *Humic Substances and their Role in the Environment* (Ed. by F. H. Frimmel & R. F. Christman), pp. 45-58. Wiley, New York.
- Henrichs, S.M. & Doyle, A.P. (1986) Decomposition of ^{14}C -labeled organic substances in marine sediments. *Limnology and Oceanography*, 31, 765-778.
- Henrichs, S.M. & Reeburgh, W.S. (1987) Anaerobic mineralization of marine sediment organic matter: Rates and the role of anaerobic processes in the oceanic carbon economy. *Geomicrobiological Journal*, 5(3/4), 191-236.
- Hinedi, Z.R., Chang, A.C. & Lee, R.W.K. (1988) Mineralization of phosphorus in sludge-amended soils monitored by phosphorus-31-nuclear magnetic resonance spectroscopy. *Soil Science Society of America Journal*, 52, 1593-1596.
- Hinedi, Z.R., Chang, A.C. & Lee, R.W.K. (1989) Characterization of phosphorus in sludge extracts using phosphorus-31-nuclear magnetic resonance spectroscopy. *Journal of Environmental Quality*, 18, 323-329.

- Hodson, R.E., Holm-Hansen, O. & Azam, F. (1976) Improved methodology for ATP determination in marine environments. *Marine Biology*, 34, 143-149.
- Holland, H.D. (1978) *The chemistry of the atmosphere and oceans*. Wiley-Interscience, New York.
- Holm-Hansen, O. (1969) Determination of microbial biomass in ocean profiles. *Limnology and Oceanography*, 14, 740-747.
- Holm-Hansen, O. (1970) ATP levels in algal cells as influenced by environmental conditions. *Plant and Cell Physiology*, 11, 689-700.
- Holm-Hansen, O. (1973) The use of ATP determination in ecological studies. *Bull. Ecol. Res. Comm.*, 17, 215-222.
- Holm-Hansen, O. & Booth, C.R. (1966) The measurement of adenosine triphosphate in the ocean and its ecological significance. *Limnology and Oceanography*, 11, 510-519.
- Hori, T. & Nozawa, Y. (1982) Phosphonolipids. In: *Phospholipids*, 4 (Ed. by J. N. Hawthorne & G. B. Ansell), pp. 95-128. Elsevier Biomedical, Amsterdam.
- Huc, A.Y. & Durand, B.M. (1977) Occurrence and significance of humic acids in ancient sediments. *Fuel*, 56, 73-80.
- Huh, C.-A., Zahnle, D.L., Small, L.F. & Noshkin, V.E. (1987) Budgets and behaviors of uranium and thorium series isotopes in Santa Monica Basin sediments. *Geochimica et Cosmochimica Acta*, 51, 1743-1754.
- Hulsemann, J. & Emery, K.O. (1961) Stratification in recent sediments of Santa Barbara Basin as controlled by organisms and water character. *Journal of Geology*, 69, 279-290.
- Hupfer, M., Gachter, R. & Giovanoli, R. (1995a) Transformation of phosphorus in settling seston and during early sediment diagenesis. *Aquatic Sciences*, 57(4), 305-324.
- Hupfer, M., Gachter, R. & Ruegger, H. (1995b) Polyphosphate in lake sediments: ³¹P NMR spectroscopy as a tool for its identification. *Limnology and Oceanography*, 40, 610-617.
- Hupfer, M. & Uhlmann, D. (1991) Microbially mediated phosphorus exchange across the mud-water interface. *Verh. Internat. Verein. Limnol.*, 24, 2999-3003.

- Hutson, S.M., Williams, G.D., Berkich, D.A., LaNoue, K.F. & Briggs, R.W. (1992) A ^{31}P NMR study of mitochondrial inorganic phosphate visibility: Effects of Ca^{2+} , Mn^{2+} , and the pH gradient. *Biochemistry*, 31, 1322-1330.
- Ingall, E. & Jahnke, R. (1994) Evidence for enhanced phosphorus regeneration from marine sediments overlain by oxygen depleted waters. *Geochimica et Cosmochimica Acta*, 58(11), 2571-2575.
- Ingall, E.D. (1991) Geochemistry of organic phosphorus in marine sediments. Ph.D. Thesis 136 pp. Yale University, New Haven, CT.
- Ingall, E.D., Bustin, R.M. & Van Cappellen, P. (1993) Influence of water column anoxia on the burial and preservation of carbon and phosphorus in marine shales. *Geochimica et Cosmochimica Acta*, 57, 303-316.
- Ingall, E.D., Schroeder, P.A. & Berner, R.A. (1990) The nature of organic phosphorus in marine sediments: New insights from ^{31}P NMR. *Geochimica et Cosmochimica Acta*, 54, 2617-2620.
- Ingall, E.D. & Van Cappellen, P. (1990) Relation between sedimentation rate and burial of organic phosphorus and organic carbon in marine sediments. *Geochimica et Cosmochimica Acta*, 54(7), 373-386.
- Jensen, H.S. & Thamdrup, B. (1993) Iron-bound phosphorus in marine sediments as measured by bicarbonate-dithionite extraction. *Hydrobiologia*, 253, 47-59.
- Jones, R.I., Shaw, P.J. & De Haan, H. (1993) Effects of dissolved humic substances on the speciation of iron and phosphate at different pH and ionic strength. *Environmental Science and Technology*, 27(6), 1052-1059.
- Karl, D.M. (1980) Cellular nucleotide measurements and applications in microbial ecology. *Microbiol. Rev.*, 44, 739-796.
- Karl, D.M. (1993) Total microbial biomass estimation derived from the measurement of particulate adenosine-5'-triphosphate. In: *Aquatic Microbial Ecology* (Ed. by Kemp, Sherr, Sherr & Cole), pp. 359-368. Lewis Publishers.
- Karl, D.M. & Holm-Hansen, O. (1976) Effects of luciferin concentration on the quantitative assay of ATP using crude luciferase preparations. *Analyt. Biochem.*, 75, 100-112.
- Karl, D.M. & Holm-Hansen, O. (1978) Methodology and measurement of adenylate energy charge ratios in environmental samples. *Marine Biology*, 48(2), 185-197.

- Karl, D.M. & Tien, G. (1997) Temporal variability in dissolved phosphorus concentrations in the subtropical North Pacific Ocean. *Marine Chemistry*, 56, 77-96.
- Kates, M. (1964) Bacterial lipids. In: *Advances in Lipid Research*, 2 (Ed. by R. Paoletti & D. Kritchevsky), pp. 17-90. Academic Press, New York.
- Keil, R.G., Montlucon, D.B., Prahl, F.G. & Hedges, J.I. (1994a) Sorptive preservation of labile organic matter in marine sediments. *Nature*, 370, 549-552.
- Keil, R.G., Tsamakis, E., Fuh, C.B., Giddings, J.C. & Hedges, J.I. (1994b) Mineralogical and textural controls on the organic composition of coastal marine sediments: Hydrodynamic separation using SPLITT-fractionation. *Geochimica et Cosmochimica Acta*, 58(2), 879-893.
- Kemp, P.F. (1987) Potential impact on bacteria of grazing by a macrofaunal deposit-feeder and the fate of bacterial production. *Marine Ecology Progress Series*, 36, 151-161.
- Kennett, J.P., Baldauf, J.G. & Party, S.S. (1994) *Proceedings of the Ocean Drilling Program: Initial Reports*. Ocean Drilling Program, College Station, Texas.
- King, J.D. & White, D.C. (1977) Muramic acid as a measure of microbial biomass in estuarine and marine samples. *Applied and Environmental Microbiology*, 33, 777-783.
- King, J.D., White, D.C. & Taylor, C.W. (1977) Use of lipid composition and metabolism to examine structure and activity of estuarine detrital microflora. *Applied and Environmental Microbiology*, 33, 1177-1183.
- Kittredge, J.S., Horiguchi, M. & Williams, P.M. (1969) Aminophosphonic acids: Biosynthesis by marine phytoplankton. *Comp. Biochem. Physiol.*, 29(2), 859-863.
- Kittredge, J.S. & Roberts, E. (1969) A carbon-phosphorus bond in nature. *Science*, 164, 37-42.
- Koenings, J.P. & Hooper, F.F. (1976) The influence of colloidal organic matter on iron and iron-phosphorus cycling in an acid bog lake. *Limnology and Oceanography*, 21(5), 684-696.
- Koide, M., Soutar, A. & Goldberg, E.D. (1972) Marine geochronology with ^{210}Pb . *Earth and Planetary Science Letters*, 14, 424-446.
- Koroleff, F. (1976) Determination of nutrients. In: *Methods of Seawater Analysis* (Ed. by K. Grasshoff, M. Ehrhardt & K. Kremling), pp. 117-156. Verlag-Chimie, New York.

- Krom, M.D. & Berner, R.A. (1981) The diagenesis of phosphorus in a nearshore marine sediment. *Geochimica et Cosmochimica Acta*, 45, 207-216.
- Kulaev, I.S. (1979) *The Biochemistry of Inorganic Polyphosphates*. Wiley, New York.
- Kuwabara, J.S., van Geen, A., McCorkle, D.C. & Bernhard, J.M. (1999) Dissolved sulfide distributions in the water column and sediment porewaters of the Santa Barbara Basin. *Geochimica et Cosmochimica Acta*, 63(15), 2199-2209.
- Larter, S.R. & Douglas, A.G. (1980) Melanoidins-kerogen precursors and geochemical lipid sinks: a study using pyrolysis gas chromatography (PGC). *Geochimica et Cosmochimica Acta*, 44, 2087-2095.
- Lee, C. (1992) Controls on organic carbon preservation: The use of stratified water bodies to compare intrinsic rates of decomposition in oxic and anoxic systems. *Geochimica et Cosmochimica Acta*, 56, 3323-3335.
- Lee, S. & Fuhrman, J.A. (1987) Relationships between biovolume and biomass of naturally derived marine bacterioplankton. *Applied and Environmental Microbiology*, 53, 1298-1303.
- Letter, W.S. (1992) A rapid method for phospholipid separation by HPLC using a light-scattering detector. *Journal of Liquid Chromatography*, 15(2), 253-266.
- Levesque, M. & Schnitzer, M. (1967) Organo-metallic interactions in soils: 6. Preparation and properties of fulvic acid-metal phosphates. *Soil Science*, 103(3), 183-190.
- Mach, D.L., Ramirez, A. & Holland, H.D. (1987) Organic phosphorus and carbon in marine sediments. *American Journal of Science*, 287(5), 429-441.
- Maher, W.A. & DeVries, M. (1994) The release of phosphorus from oxygenated estuarine sediments. *Chemical Geology*, 112(1-2), 91-104.
- Mancuso, C.A., Franzmann, P.D., Burton, H.R. & Nichols, P.D. (1990) Microbial community structure and biomass estimates of a methanogenic Antarctic Lake ecosystem as determined by phospholipid analyses. *Microbial Ecology*, 19, 73-95.
- Martens, C.S. & Klump, J.V. (1984) Biogeochemical cycling in an organic coastal marine basin 4: An organic carbon budget for sediment dominated by sulfate reduction and methanogenesis. *Geochimica et Cosmochimica Acta*, 48, 1987-2004.
- Mayer, L.M. (1994a) Relationship between mineral surfaces and organic carbon concentrations in soils and sediments. *Chemical Geology*, 114, 347-363.

- Mayer, L.M. (1994b) Surface area control of organic carbon accumulation in continental shelf sediments. *Geochimica et Cosmochimica Acta*, 58(4), 1271-1284.
- Mayer, L.M. (1999) Extent of coverage of mineral surfaces by organic matter in marine sediments. *Geochimica et Cosmochimica Acta*, 63(2), 207-215.
- McElroy, M.B. (1983) Marine biological controls on atmospheric CO₂ and climate. *Nature*, 302, 328-329.
- Meyer-Reil, L.-A. (1984) Bacterial biomass and heterotrophic activity in sediments and overlying waters. In: *Heterotrophic Activity in the Sea, 15, NATO Conference Series IV. Marine Sciences* (Ed. by J. E. Hobbie & P. J. B. Williams), pp. 523-546. Plenum Press, New York.
- Miyata, K., Hattori, A. & Otsuki, A. (1986) Variation of cellular phosphorus composition of *Skeletonema costatum* and *Heterosigma akashiwo* grown in chemostats. *Marine Biology*, 93, 291-297.
- Monaghan, E.J. & Ruttenberg, K.C. (1999) Dissolved organic phosphorus in the coastal ocean: Reassessment of available methods and seasonal phosphorus profiles from the Eel River Shelf. *Limnology and Oceanography*, 44(7), 1702-1714.
- Morrison, S.J., King, J.D., Bobbie, R.J., Bechtold, R.E. & White, D.C. (1977) Evidence for microbial succession on allochthonous plant litter in Apalachicola Bay, Florida, U.S.A. *Marine Biology*, 41, 229-240.
- Morse, J.W. & Cook, N. (1978) The distribution and form of phosphorus in North Atlantic Ocean deep-sea and continental slope sediments. *Limnology and Oceanography*, 23, 825-830.
- Mortimer, C.H. (1941) The exchange of dissolved substances between mud and water in lakes, I. *Journal of Ecology*, 29, 280-329.
- Neidhardt, F.C. (1987) Chemical composition of *Escherichia coli*. In: *Escherichia coli and Salmonella Typhimurium: Cellular and Molecular Biology, 1* (Ed. by F. C. Neidhardt, J. L. Ingraham, K. B. Low, B. Magasanik, M. Schaechter & H. E. Umbarger), pp. 3-6. American Society for Microbiology, Washington, D.C.
- Newman, R.H. & Tate, K.R. (1980) Soil phosphorus characterization by ³¹P nuclear magnetic resonance. *Commun. Soil Sci. Plant Anal.*, 11, 835-842.
- Nichols, P.D., Mancuso, C.A. & White, D.C. (1987) Measurement of methanotroph and methanogen signature phospholipids for use in assessment of biomass and community structure in model ecosystems. *Organic Geochemistry*, 11, 4512-461.

- Nissenbaum, A. (1974) The organic geochemistry of marine and terrestrial humic substances: implications of carbon and hydrogen isotope studies. *Organic Geochemistry*, 39-52.
- Nissenbaum, A. (1979) Phosphorus in marine and non-marine humic substances. *Geochimica et Cosmochimica Acta*, 43, 1973-1978.
- Nissenbaum, A. & Kaplan, I.R. (1972) Chemical and isotopic evidence for the *in situ* origin of marine humic substances. *Limnology and Oceanography*, 17(4), 570-582.
- Nissenbaum, A. & Swaine, D.J. (1976) Organic matter- metal interactions in Recent sediments: the role of humic substances. *Geochimica et Cosmochimica Acta*, 40, 809-816.
- Nordbäck, J., Lundberg, E. & Christie, W.W. (1998) Separation of lipid classes from marine particulate material by HPLC on a polyvinyl alcohol-bonded stationary phase using dual-channel evaporative light-scattering detection. *Marine Chemistry*, 60, 165-175.
- Ogner, G. (1983) ³¹P-NMR spectra of humic acids: A comparison of four different raw humus types in Norway. *Geoderma*, 29, 215-219.
- Osborne, M.J., Rick, P.D., Lehmann, V., Rupprecht, E. & Singh, M. (1974) Structure and biogenesis of the cell envelope of Gram negative bacteria. *Annals of the New York Academy of Science*, 235, 52-65.
- Parkes, R.J., Cragg, B.A., Bale, S.J., Getliff, J.M., Goodman, K., Rochelle, P.A., Fry, J.C., Weightman, A.J. & Harvey, S.M. (1994) Deep bacterial biomass in Pacific Ocean sediments. *Nature*, 371, 410-413.
- Paul, J.H., Jeffrey, W.H. & DeFlaun, M.F. (1987) Dynamics of extracellular DNA in the marine environment. *Applied and Environmental Microbiology*, 53, 170-179.
- Pederson, T.F., Shimmiel, G.B. & Price, N.B. (1992) Lack of enhanced preservation of organic matter in sediments under the oxygen minimum on the Oman Margin. *Geochimica et Cosmochimica Acta*, 56, 545-551.
- Poole, C.F. & Schuette, S.A. (1984) *Contemporary practice of chromatography*. Elsevier, New York.
- Preiss, J. (1989) Chemistry and metabolism of intracellular reserves. In: *Bacteria in Nature: Structure, Physiology, and Genetic Adaptability*, 3 (Ed. by J. S. Poindexter & E. R. Leadbetter), pp. 224-258. Plenum Press, New York.

- Preston, C.M. (1996) Applications of NMR to soil organic matter analysis: History and prospects. *Soil Science*, 161(3), 144-166.
- Preston, C.M., Ripmeester, J.A., Mathur, S.P. & Levesque, M. (1986) Application of solution and solid-state multinuclear NMR to a peat-based composting system for fish and crab scrap. *Can. J. Spectrosc.*, 31, 63-69.
- Quin, L.D. & Shelburne, F.A. (1969) An examination of marine animals for the presence of carbon-bound phosphorus. *Journal of Marine Research*, 27(1), 73-84.
- Reimers, C.E., Lange, C.B., Tabak, M. & Bernhard, J.M. (1990) Seasonal spillover and varve formation in the Santa Barbara Basin, California. *Limnology and Oceanography*, 35(7), 1577-1585.
- Reimers, C.E., Ruttenberg, K.C., Canfield, D.E., Christiansen, M.B. & Martin, J.B. (1996) Pore water pH and authigenic phases formed in the uppermost sediments of the Santa Barbara Basin. *Geochimica et Cosmochimica Acta*, 60(21), 4037-4057.
- Rittenberg, S.C. (1940) Bacteriological analysis of some long cores of marine sediments. *Journal of Marine Research*, 3, 191-201.
- Rood, D. (1991) *A practical guide to the care, maintenance, and troubleshooting of capillary gas chromatographic systems*. Huthig, Heidelberg.
- Rosenberg, H. & La Nauze, J.M. (1967) The metabolism of phosphonates by microorganisms. The transport of aminoethylphosphonic acid in *Bacillus cereus*. *Biochimica et Biophysica Acta*, 141, 79-90.
- Rosenthal, A.F. & Ham, S.C.-H. (1970) A study of phospholipase A inhibition by glycerophosphatide analogs in various systems. *Biochimica et Biophysica Acta*, 218, 213-220.
- Rosenthal, A.F. & Pousada, M. (1968) Inhibition of phospholipase C by phosphonate analogs of glycerophosphatides. *Biochimica et Biophysica Acta*, 164, 226-237.
- Ruttenberg, K.C. (1990) Diagenesis and burial of phosphorus in marine sediments: Implications for the marine phosphorus budget. Ph.D. Thesis 375 pp. Yale University, New Haven, CT.
- Ruttenberg, K.C. (1992) Development of a sequential extraction method for different forms of phosphorus in marine sediments. *Limnology and Oceanography*, 37(7), 1460-1482.
- Ruttenberg, K.C. (1993) Reassessment of the oceanic residence time of phosphorus. *Chemical Geology*, 107, 405-409.

- Ruttenberg, K.C. (2000) The Global Biogeochemical Cycle of Phosphorus. In: *Encyclopedia of Global Change*. Oxford University Press.
- Ruttenberg, K.C. & Berner, R.A. (1993) Authigenic apatite formation and burial in sediments from non-upwelling, continental margin environments. *Geochimica et Cosmochimica Acta*, 57(5), 991-1007.
- Ruttenberg, K.C. & Goñi, M.A. (1997) Phosphorus distribution, (C:N:P) ratios, and $\delta^{13}\text{C}$ in arctic, temperate, and tropical coastal sediments: Tools for characterizing bulk sedimentary organic matter. *Marine Geology*, 139(1/4), 123-146.
- Rzepa, H. (1994) NMR Spectroscopy. Principles and Application, 1999.
- Sanders, J.K.M. & Hunter, B.K. (1993) *Modern NMR Spectroscopy: A Guide for Chemists*. Oxford University Press, New York.
- Sandstrom, M.W. (1982) Diagenesis of organic phosphorus in marine sediments: implications for the global carbon and phosphorus cycles. In: *Cycling of Carbon, Nitrogen, Sulfur and Phosphorus in Terrestrial and Aquatic Ecosystems* (Ed. by J. R. Freney & I. E. Galbally), pp. 133-141. Springer-Verlag.
- Sass, S. & Parker, G.A. (1980) Structure- response relationship of gas chromatography-flame photometric detection to some organophosphorus compounds. *Journal of Chromatography*, 189, 331-349.
- Schimmelmann, A. & Lange, C.B. (1996) Tales of 1001 varves: a review of Santa Barbara Basin sediment studies. In: *Palaeoclimatology and Palaeoceanography from Laminated Sediments*, 116 (Ed. by A. E. S. Kemp), pp. 121-141. Geological Society Special Publication.
- Schimmelmann, A. & Tegner, M.J. (1991) Historical oceanographic events reflected in the $^{13}\text{C}/^{12}\text{C}$ ratio of total organic carbon in laminated Santa Barbara Basin sediments. *Global Biogeochemical Cycles*, 5(2), 173-188.
- Schmidt, H. & Reimers, C. (1991) The recent history of trace metal accumulation in the Santa Barbara Basin, Southern California Borderland. *Estuarine, Coastal and Shelf Science*, 33, 485-500.
- Schnitzer, M. (1969) Interactions between fulvic acid, a soil humic compound, and inorganic soil constituents. *Soil Sci.Soc. Am. Proc.*, 33, 75-81.
- Shaka, A.J., Keeler, J. & Freeman, R. (1983) *Progress in Nuclear Magnetic Resonance Spectroscopy*, 19, 47-129.

- Sholkovitz, E. & Gieskes, J.M. (1971) A physical-chemical study of the flushing of the Santa Barbara Basin. *Limnology and Oceanography*, 16, 479-489.
- Sholkovitz, E. & Soutar, A. (1975) Changes in the composition of the bottom water of the Santa Barbara Basin: effect of turbidity currents. *Deep-Sea Research*, 22, 13-21.
- Sianoudis, J.A., Kuesel, C., Mayer, A., Grimme, L.H. & Leibfritz. (1986) Distribution of polyphosphates in cell-compartments of *Chlorella fusca* as measured by ^{31}P -NMR spectroscopy. *Arch. Microbiol.*, 144, 48-54.
- Smith, S.M. & Hitchcock, G.L. (1994) Nutrient enrichments and phytoplankton growth in the surface waters of the Louisiana Bight. *Estuaries*, 17(4), 740-753.
- Smith, S.V. (1984) Phosphorus versus nitrogen limitation in the marine environment. *Limnology and Oceanography*, 29, 1149-1160.
- Solórzano, L. & Sharp, J.H. (1980) Determination of total dissolved phosphorus and particulate phosphorus in natural waters. *Limnology and Oceanography*, 25(4), 754-758.
- Soutar, A. & Crill, P.A. (1977) Sedimentation and climate patterns in the Santa Barbara Basin during the 19th and 20th centuries. *Geol. Soc. Amer. Bull.*, 88, 1161-1172.
- Stein, J.L. (1984) Subtidal gastropods consume sulfur-oxidizing bacteria: Evidence from coastal hydrothermal vents. *Science*, 223, 696-698.
- Stevenson, F.J. (1994) *Humus Chemistry: Genesis, Composition, Reactions*. John Wiley and Sons, New York.
- Stewart, J.W.B. & Tiessen, H. (1987) Dynamics of soil organic phosphorus. *Biogeochemistry*, 4, 41-60.
- Strickland, J.D.H. & Parsons, T.R. (1972) Determination of total phosphorus. In: *A Practical Handbook of Seawater Analysis*. Fisheries Research Board of Canada, Ottawa.
- Suzumura, M. & Kamatani, A. (1995a) Mineralization of inositol hexaphosphate in aerobic and anaerobic marine sediments: Implications for the phosphorus cycle. *Geochimica et Cosmochimica Acta*, 59(5), 1021-1026.
- Suzumura, M. & Kamatani, A. (1995b) Origin and distribution of inositol hexaphosphate in estuarine and coastal sediments. *Limnology and Oceanography*, 40(7), 1254-1261.
- Tate, K.R. & Newman, R.H. (1982) Phosphorus fractions of a climosequence of soils in New Zealand tussock grassland. *Soil Biology and Biochemistry*, 14, 191-196.

- Tegelaar, E.W., DeLeeuw, J.W., Derenne, S. & Largeau, C. (1989) A reappraisal of kerogen formation. *Geochimica et Cosmochimica Acta*, 53, 3103-3106.
- Theng, B.K.G. (1979) *Formation and Properties of Clay-Polymer Complexes*. Elsevier, New York.
- Thornton, S.E. (1984) Basin model for hemipelagic sedimentation in a tectonically active continental margin: Santa Barbara Basin, California Continental Borderland. In: *Fine-Grained Sediments: Deep-Water Processes and Facies* (Ed. by D. A. V. Stow & D. J. W. Piper), pp. 377-394. Blackwell Scientific Publications, Oxford.
- Thunell, R.C., Tappa, E. & Anderson, D.M. (1995) Sediment fluxes and varve formation in Santa Barbara Basin. *Geology*, 23(12), 1083-1086.
- Tissot, B.P. & Welte, D.H. (1984) *Petroleum Formation and Occurrence*. Springer-Verlag, Berlin Heidelberg.
- Tyson, R.V. (1987) The genesis and palynofacies characteristics of marine petroleum source rocks. In: *Marine Petroleum Source Rocks*, 26 (Ed. by J. Brooks & A. J. Fleet), pp. 47-67, Geol. Soc. Spec. Pub.
- Uhlmann, D. & Bauer, D. (1988) A remark on microorganisms in lake sediments with emphasis on polyphosphate accumulating bacteria. *Int. Rev. Gesamten Hydrobiol.*, 73, 703-708.
- van Wazer, J.R. & Ditchfield, R. (1987) Phosphorus compounds and their ^{31}P chemical shifts. In: *Phosphorus NMR in Biology* (Ed. by C. T. Burt). CRC.
- Vassallo, A.M., Wilson, M.A., Collins, P.J., Oades, J.M., Waters, A.G. & Malcolm, R.L. (1987) Structural analysis of geochemical samples by solid-state nuclear magnetic resonance spectrometry. Role of paramagnetic material. *Anal. Chem.*, 59, 558-562.
- Vogel, H.J. (1984) ^{31}P -NMR studies of phosphoproteins. In: *Phosphorus-31 NMR: Principles and Applications* (Ed. by D. G. Gorenstein), pp. 105-154. Academic Press, Orlando, FL.
- Webster, J.J., Hampton, G.J. & Leach, R.F. (1984) ATP in soil: a new extractant and extraction procedure. *Soil Biol. Biochem.*, 16, 335-342.
- Webster, J.J., Hampton, G.J., Wilson, J.T., Ghiorse, W.C. & Leach, R.F. (1985) Determination of microbial cell numbers in subsurface samples. *Ground Water*, 23, 17-25.

- Welte, D.H. (1974) Recent advances in organic geochemistry of humic substances and kerogen- A review. In: *Advances in Organic Geochemistry* (Ed. by B. Tissot & F. Bienner), pp. 3-13.
- Wentzel, M.C., Lotter, L.H., Ekama, G.A., Loewenthal, R.E. & Marais, G.v.R. (1991) Evaluation of biogeochemical models for biological excess phosphorus removal. *Water Sci. Technol.*, 23, 567-574.
- Westheimer, F.H. (1987) Why nature chose phosphates. *Science*, 235, 1173-1178.
- Whelan, J.K. & Thompson-Rizer, C.L. (1993) Chemical methods for assessing kerogen and protokerogen types and maturity. In: *Organic Geochemistry* (Ed. by M. H. Engel & S. A. Macko), pp. 289-353. Plenum Press, New York.
- White, D.C. (1993) *In situ* measurement of microbial biomass, community structure and nutritional status. *Philosophical Transactions of the Royal Society of London*, A 344, 59-67.
- White, D.C., Bobbie, R.J., Herron, J.S., King, J.D. & Morrison, S.J. (1979a) Biochemical measurements of microbial mass and activity from environmental samples. In: *Native Aquatic Bacteria: Enumeration, Activity and Ecology*, ASTM STP (Ed. by J. W. Costerton & R. R. Colwell), pp. 69-81. American Society for Testing and Materials, Philadelphia.
- White, D.C., Bobbie, R.J., King, J.D., Nickels, J.S. & Amoe, P. (1979b) Lipid analysis of sediments for microbial biomass and community structure. In: *Methodology for Biomass Determination and Microbial Activity in Sediments*, 673, ASTM STP (Ed. by C. D. Litchfield & P. L. Seyfried), pp. 87-103. American Society for Testing and Materials, Philadelphia.
- White, D.C., Bobbie, R.J., Morrison, S.J., Oosterhof, D.K., Taylor, C.W. & Meeter, D.A. (1977) Determination of microbial activity of estuarine detritus by relative rates of lipid biosynthesis. *Limnology and Oceanography*, 22, 1089-1099.
- White, D.C., Davis, W.M., Nickels, J.S., King, J.D. & Bobbie, R.J. (1979c) Determination of the sedimentary microbial biomass by extractable lipid phosphate. *Oecologia*, 40, 51-62.
- White, R.H. & Miller, S.L. (1976) Inositol isomers: Occurrence in marine sediments. *Science*, 193, 885-886.
- Wilson, M.A. (1987) *NMR Techniques and applications in geochemistry and soil chemistry*. Pergamon Press, Oxford, U.K.

- Wilson, M.A. (1991) Analysis of functional groups in soil by nuclear magnetic resonance spectroscopy. In: *Soil Analysis: Modern Analytical Techniques* (Ed. by K. A. Smith), pp. 601-645. Marcel Dekker Inc., New York.
- Zeleznick, L.D., Myers, T.C. & Titchner, E.B. (1963) Growth of *Escherichia coli* on methyl- and ethylphosphonic acids. *Biochimica et Biophysica Acta*, 78, 564-567.
- Zheng, Y. (1999) The Marine Geochemistry of Germanium, Molybdenum and Uranium: The Sinks. PhD Thesis 336 pp. Columbia University, New York, NY.

Document Library

Distribution List for Technical Report Exchange—November 1999

University of California, San Diego
SIO Library 0175C
9500 Gilman Drive
La Jolla, CA 92093-0175

Hancock Library of Biology & Oceanography
Alan Hancock Laboratory
University of Southern California
University Park
Los Angeles, CA 90089-0371

Gifts & Exchanges
Library
Bedford Institute of Oceanography
P.O. Box 1006
Dartmouth, NS B2Y 4 A2
CANADA

NOAA/EDIS Miami Library Center
4301 Rickenbacker Causeway
Miami, FL 33149

Research Library
U.S. Army Corps of Engineers
Waterways Experiment Station
3909 Halls Ferry Road
Vicksburg, MS 39180-6199

Institute of Geophysics
University of Hawaii
Library Room 252
2525 Correa Road
Honolulu, HI 96822

Marine Resources Information Center
Building E38-320
MIT
Cambridge, MA 02139

Library
Lamont-Doherty Geological Observatory
Columbia University
Palisades, NY 10964

Library
Serials Department
Oregon State University
Corvallis, OR 97331

Pell Marine Science Library
University of Rhode Island
Narragansett Bay Campus
Narragansett, RI 02882

Working Collection
Texas A&M University
Dept. of Oceanography
College Station, TX 77843

Fisheries-Oceanography Library
151 Oceanography Teaching Bldg.
University of Washington
Seattle, WA 98195

Library
R.S.M.A.S.
University of Miami
4600 Rickenbacker Causeway
Miami, FL 33149

Maury Oceanographic Library
Naval Oceanographic Office
Building 1003 South
1002 Balch Blvd.
Stennis Space Center, MS 39522-5001

Library
Institute of Ocean Sciences
P.O. Box 6000
Sidney, B.C. V8L 4B2
CANADA

National Oceanographic Library
Southampton Oceanography Centre
European Way
Southampton SO14 3ZH
UK

The Librarian
CSIRO Marine Laboratories
G.P.O. Box 1538
Hobart, Tasmania
AUSTRALIA 7001

Library
Proudman Oceanographic Laboratory
Bidston Observatory
Birkenhead
Merseyside L43 7 RA
UK

IFREMER
Centre de Brest
Service Documentation—Publications
BP 70 29280 PLOUZANE
FRANCE

REPORT DOCUMENTATION PAGE	1. REPORT NO. MIT/WHOI 00-24	2.	3. Recipient's Accession No.
4. Title and Subtitle Organic Phosphorus in Marine Sediments: Chemical Structure, Diagenetic Alteration, and Mechanisms of Preservation			5. Report Date September 2000
7. Author(s) Kirsten Lynn Laarkamp			6.
9. Performing Organization Name and Address MIT/WHOI Joint Program in Oceanography/Applied Ocean Science & Engineering			8. Performing Organization Rept. No.
12. Sponsoring Organization Name and Address National Science Foundation Office of Naval Research American Chemical Society Petroleum Research Fund			10. Project/Task/Work Unit No. MIT/WHOI 00-24
			11. Contract(C) or Grant(G) No. OCE-9216553 (C) N00014-95-1-0478 (G) 32186-G2 35930-AC2
			13. Type of Report & Period Covered Ph.D. Thesis
14.			
15. Supplementary Notes This thesis should be cited as: Kirsten Lynn Laarkamp, 2000. Organic Phosphorus in Marine Sediments: Chemical Structure, Diagenetic Alteration, and Mechanisms of Preservation. Ph.D. Thesis. MIT/WHOI, 00-24.			
16. Abstract (Limit: 200 words) Phosphorus, an essential nutrient, is removed from the oceans only through burial with marine sediments. Organic phosphorus (P_{org}) constitutes an important fraction (<i>ca.</i> 25%) of total-P in marine sediments. However, given the inherent lability of primary P_{org} biochemicals, it is a puzzle that any P_{org} is preserved in marine sediments. The goal of this thesis was to address this apparent paradox by linking bulk and molecular-level P_{org} information. A newly-developed sequential extraction method, which isolates sedimentary P_{org} reservoirs based on solubility, was used in concert with ^{31}P nuclear magnetic resonance spectroscopy (^{31}P -NMR) to quantify P_{org} functional group concentrations. The coupled extraction/ ^{31}P -NMR method was applied to three sediment cores from the Santa Barbara Basin, and the first-ever high-resolution depth profiles of molecular-level P_{org} distribution during diagenesis were generated. These depth profiles were used to consider regulation of P_{org} distribution by biomass abundance, chemical structure, and physical protection mechanisms. Biomass cannot account for more than a few percent of sedimentary P_{org} . No evidence for direct structural control on remineralization of P_{org} was found. Instead, sorptive protection appears to be an important mechanism for P_{org} preservation, and structure may act as a secondary control due to preferential sorption of specific P_{org} compound classes.			
17. Document Analysis a. Descriptors Santa Barbara Basin nutrient chemistry nuclear magnetic resonance spectroscopy b. Identifiers/Open-Ended Terms c. COSATI Field/Group			
18. Availability Statement Approved for publication; distribution unlimited.		19. Security Class (This Report) UNCLASSIFIED	21. No. of Pages 286
		20. Security Class (This Page)	22. Price